PAGES 1517—1628

ISSN 0003—2654

The Analyst

A monthly international journal dealing with all branches of analytical chemistry

Vol. 109 No. 12
December
1984

ROYAL SOCIETY OF CHEMISTRY

The Analyst

The Analytical Journal of The Royal Society of Chemistry

Editorial Office: The Royal Society of Chemistry, Burlington House, Piccadilly, London, W1V 0BN. Telephone 01-734 9864. Telex No. 268001

Advertisements: Advertisement Department, The Royal Society of Chemistry, Burlington House, Piccadilly, London, W1V 0BN. Telephone 01-734 9864. Telex No. 268001

The Analyst (ISSN 0003–2654) is published monthly by The Royal Society of Chemistry, Burlington House, London W1V 0BN, England. All orders accompanied with payment should be sent directly to The Royal Society of Chemistry, The Distribution Centre, Blackhorse Road, Letchworth, Herts. SG6 1HN, England. 1984 Annual subscription rate UK £112.00, Rest of World £118.00, USA $223.00. Purchased with *Analytical Abstracts* UK £257.50, Rest of World £270.00, USA $514.00. Purchased with *Analytical Abstracts* plus *Analytical Proceedings* UK £287.50, Rest of World £302.00, USA $574.00. Purchased with *Analytical Proceedings* UK £141.00, Rest of World £148.00, USA $281.00. Air freight and mailing in the USA by Publications Expediting Inc., 200 Meacham Avenue, Elmont, NY 11003.
USA Postmaster: Send address changes to: *The Analyst,* Publications Expediting Inc., 200 Meacham Avenue, Elmont, NY 11003. Second class postage paid at Jamaica, NY 11431. All other despatches outside the UK by Bulk Airmail within Europe, Accelerated Surface Post outside Europe. PRINTED IN THE UK.

Information for Authors

Full details of how to submit material for publication in *The Analyst* are given in the Instructions to Authors in the January issue. Separate copies are available on request.

The Analyst publishes papers on all aspects of the theory and practice of analytical chemistry, fundamental and applied, inorganic and organic, including chemical, physical and biological methods. There is no page charge.

The following types of papers will be considered:

Full papers, describing original work.

Short papers, also describing original work, but shorter and of limited breadth of subject matter; there will be no difference in the quality of the work described in full and short papers.

Communications, which must be on an urgent matter and be of obvious scientific importance. Rapidity of publication is enhanced if diagrams are omitted, but tables and formulae can be included. Communications should not be simple claims for priority: this facility for rapid publication is intended for brief descriptions of work that has progressed to a stage at which it is likely to be valuable to workers faced with similar problems. A fuller paper may be offered subsequently, if justified by later work.

Reviews, which must be a critical evaluation of the existing state of knowledge on a particular facet of analytical chemistry.

Every paper (except Communications) will be submitted to at least two referees, by whose advice the Editorial Board of *The Analyst* will be guided as to its acceptance or rejection. Papers that are accepted must not be published elsewhere except by permission. Submission of a manuscript will be regarded as an undertaking that the same material is not being considered for publication by another journal.

Regional Advisory Editors. For the benefit of potential contributors outside the United Kingdom, a Panel of Regional Advisory Editors exists. Requests for help or advice on any matter related to the preparation of papers and their submission for publication in *The Analyst* can be sent to the nearest member of the Panel. Currently serving Regional Advisory Editors are listed in each issue of *The Analyst*.

Manuscripts (three copies typed in double spacing) should be addressed to:
The Editor, *The Analyst,*
Royal Society of Chemistry,
Burlington House,
Piccadilly,
LONDON W1V 0BN, UK

Particular attention should be paid to the use of standard methods of literature citation, including the journal abbreviations defined in Chemical Abstracts Service Source Index. Wherever possible, the nomenclature employed should follow IUPAC recommendations, and units and symbols should be those associated with SI.

All queries relating to the presentation and submission of papers, and any correspondence regarding accepted papers and proofs, should be directed to the Editor, *The Analyst* (address as above). Members of the Analytical Editorial Board (who may be contacted directly or via the Editorial Office) would welcome comments, suggestions and advice on general policy matters concerning *The Analyst.*

Fifty reprints of each published contribution are supplied free of charge, and further copies can be purchased.

The companies appearing on this page are able to offer scientific support to users of laboratory instrumentation. THE ANALYST will regularly publish specific Application Notes provided by their applications chemists.

Determination of Lindane Vapour in Air by Passive Sampling

Part I. Development of the Passive Sampling Device and Measurement of the Diffusion Coefficient of Lindane in Air

Marjory A. Bland, Stephen Crisp, Peter R. Houlgate and Jeffery W. Llewellyn
Laboratory of the Government Chemist, Cornwall House, Stamford Street, London SE1 9NQ, UK

The development of a passive sampling device for the determination of low concentrations of lindane (γ-hexachlorocyclohexane) vapour in air is described. The sampler consists of an open glass tube mounted in a Perspex base that contains Chromosorb 102 sorbent and collects lindane vapour by diffusion according to Fick's law. The diffusion coefficient of lindane in air is determined by exposing tubes to standard atmospheres of lindane vapour generated in the laboratory. Good agreement with the theoretical value was obtained.

Keywords: *Lindane determination; passive sampling; diffusion coefficient; air*

The insecticidal properties of lindane (1α,2α,3β,4α,5α,6α-hexachlorocyclohexane) were first reported in the mid 1940s[1] and it has been used extensively as a pesticide since then. The acute LD_{50} for male rats[2] is 88 mg kg^{-1} and, although its toxic effect in man is not well established, a threshold limit value (TLV) of 0.5 mg m^{-3} has been imposed by the American Conference of Governmental Industrial Hygienists (ACGIH)[3] based on evidence of EEG disturbance following prolonged exposure. Prolonged exposure to lindane is also reported to be associated with high polymorphonuclear leukocyte and reticulocyte counts, low lymphocyte counts, prothrombin level and blood concentrations of creatinine and uric acid,[4] and abnormalities in sex hormone regulation.[5] Rats fed on diets containing 100 p.p.m. of lindane suffered tissue damage[3] and mice fed on diets containing 250–500 p.p.m. of lindane developed liver hepatomas.[3]

At 20 °C lindane is solid and has a vapour pressure of 9.4×10^{-6} Torr (1.25 mPa). It can be present in air both as a dust and a vapour, the latter being the predominant phase at lower concentrations. Existing methods of sampling airborne lindane vapour include collection in ethylene glycol[6] or dimethylformamide[7] and collection on solid sorbents such as Chromosorb 102,[6] polyurethane foam,[8–10] silica gel[11] and activated charcoal.[11]

All of these methods require air to be drawn through the collection medium by a pump. These are often inconvenient to transport, as they mostly require a mains electrical supply that restricts the locations at which sampling may be performed. Battery-operated pumps may be used for sampling at remote sites where access may be difficult[9,10] but the duration of their period of continuous operation is usually only of the order of 8 h. These techniques permit the monitoring of lindane concentration for a limited period of time only. If it is necessary to monitor low concentrations over an extended period then frequent changes of pump and collection medium are required, which is labour intensive and hence expensive.

These problems may be alleviated by the use of "passive" sampling methods. Such methods utilise light-weight sampling devices that are, in essence, tubes of known dimensions, closed at one end, which contain an appropriate sorbent. The open devices are placed, for a measured period, in the atmosphere containing the analyte to be determined. This is subsequently collected on the sorption medium following diffusion down the tube according to Fick's law:

$$dm = -D\frac{dc}{dx}dt \quad \ldots \quad (1)$$

where dm is the mass of analyte diffusing across a plane of unit area in a time of dt; $-dc/dx$ is the concentration gradient of the analyte across the plane of diffusion; and D is the diffusion coefficient. The concentration of analyte in the layer of air at the surface of the sorbent may be assumed to be zero. Thus, for a concentration C of the analyte in the atmosphere, the concentration gradient down the tube will be C/l, where l is the length of the tube. If the area of cross-section of the diffusion tube is A then equation (1) can be rewritten in the integrated form:

$$M = \frac{-DCAt}{l} \quad \ldots \quad (2)$$

where M is the total mass of analyte collected in time t. It follows from equation (2) that if A, l, t and D are known then measurement of M enables the concentration of the analyte, C, to be determined.

Samplers based on this principle have found widespread use in workplace atmosphere monitoring[12] as they are inexpensive, do not require the use of pumps and do not restrict the choice of sampling site. Further, they enable a time-weighted average concentration of the analyte to be determined, which is often more relevant than a series of spot values obtained over the same period.

There have been few reports of the use of passive sampling devices for monitoring ambient concentrations of pollutants in the field. They have, however, been used to determine nitrogen dioxide concentrations in homes,[13–16] in textile factories[17] and rural atmospheres.[17] A laboratory evaluation of three commercially available samplers for the determination of "ambient" concentrations of benzene, chlorobenzene and six chlorinated hydrocarbons has been carried out.[18] It was found that contaminants within the adsorbent impaired the detection limit of the devices and only a relatively small number of compounds could be detected at representative ambient levels using a 24-h exposure period.

This paper describes the development of a passive sampling device for the determination of ambient concentrations of lindane vapour in air, and the subsequent use of the device to determine the diffusion coefficient of lindane in air.

Experimental

Calculation of the Diffusion Coefficient of Lindane in Air

The diffusion coefficient of lindane in air was calculated using the two following theoretical equations:

Hirschfelder, Bird and Spotz (HBS) equation[19]:

$$D_{LA} = \frac{1.858 \times 10^{-3} T^{1.5}[(M_A + M_L)/M_A M_L]^{0.5}}{P\sigma_{LA}^2 \Omega_D} \quad (3)$$

where T = temperature (K); P = pressure (atmospheres); M_A = relative molecular mass of air = 28.96; M_L = relative molecular mass of lindane = 290.86; σ_{LA} = collision diameter of lindane in air = 5.493 Å ; and Ω_D = collision integral of lindane for diffusion = 1.1204. In order to avoid recalculating numerical constants in equations (3) and (4), the units used in the original references are retained. Greater details of the calculation of σ_{LA} and Ω_D are given in the Appendix.

Fuller, Schettler and Giddings (FSG) equation[21]:

$$D_{LA} = \frac{1.00 \times 10^{-3} T^{1.75} (1/M_A + 1/M_L)^{0.5}}{P(V_A^{1/3} + V_L^{1/3})^2} \quad .. \quad (4)$$

where D_{LA}, P, T, M_A and M_L are as given above and V_A and $V_L = \Sigma V_i$, where V_i are atomic volume increments with values of C = 16.5, H = 1.98, O = 5.48, Cl = 19.5 and air = 20.1. Hence V_L = 227.88.

The calculated values of D_{LA} obtained by each equation are presented in Table 1.

Design and Construction of Passive Sampling Tubes

The passive sampling tubes were constructed to the dimensions shown in Fig. 1. They consisted of a precision-bore glass tube fitted tightly into an annular groove cut into a circular Perspex base. The central part of the base was milled out to form an inverted cone. This was filled with cleaned Chromosorb 102 such that the level of the sorbent was just level with the top of the Perspex base.

Preparation of Chromosorb 102 Adsorbent

A Whatman Soxhlet thimble, 80 mm long × 25 mm i.d., was approximately three-quarters filled with fresh Chromosorb 102 and plugged with silanised glass-wool. It was extracted in a Soxhlet apparatus for 3 h using 5% *V/V* acetone in methanol solution (100 ml). The solvent was then replaced with hexane (100 ml) and the Chromosorb 102 was re-extracted for a further 3 h, after which it was dried in air at room temperature.

Preparation of Atmospheres of Lindane Vapour in Air

Atmospheres of lindane vapour in air were generated in the laboratory using the apparatus shown in Fig. 2. Air, cleaned by passage through charcoal tower T_1, was passed at a measured flow-rate (rotameter R_1) through a glass tube (S) (150 × 4 mm i.d.), in a thermostated water-bath (W) controlled to ±0.5 °C that contained a mixture of equal parts of lindane powder and Celite retained between two plugs of glass-wool to form a short column approximately 60 mm long. The lindane vapour passed into a mixing chamber (M) where it was diluted with a second stream of clean air at a flow-rate indicated by rotameter R_2. The diluted vapour stream was then split; the larger fraction was led through charcoal tower T_3 to waste. The smaller stream was drawn into the bottom of a large closed desiccator (D) (of approximate diameter 200 mm and volume 4 l) that served as an exposure chamber for the passive sampling tubes. The concentration of lindane was kept uniform within the desiccator by stirring with a magnetic follower (MS) (25 mm). Lindane vapour was withdrawn from the top of the chamber at a flow-rate indicated by rotameter R_3, through charcoal tower T_3 to exhaust.

For the determination of lindane concentration, two-way tap A was opened to divert the flow through two sintered-glass bubblers fitted with No. 2 sinters, connected in series, each of which contained a 5% *V/V* solution of acetone in hexane (40 ml). The concentration of lindane in the atmosphere generated could be controlled by variation of the source flow-rate (typically within the range 40–200 ml min^{-1}), the diluting air flow-rate (1–4 l min^{-1}) and the temperature of the thermostated bath (15–35 °C). All rotameters were calibrated in line using a soap bubble flow meter. The homogeneity of the atmosphere was tested by disconnecting the lindane source and introducing smoke from an air current detector tube (Draeger Ltd.) into the vapour stream and connecting the vapour line directly to the outlet of rotameter R_1. The smoke became evenly distributed in the desiccator chamber but it was necessary to stir the atmosphere in the chamber to avoid streaming between the inlet and outlet.

In order that sampling tubes could be placed in the chamber easily, the entire desiccator could be disconnected from the system by releasing the clips on the inlet and outlet lines. The lid could then be removed with care in the usual way. The apparatus was run for 72 h prior to loading with sampling tubes to allow the concentration of lindane in the atmosphere to stabilise.

Determination of Lindane in Generated Atmospheres

Lindane vapour emerging from the exposure chamber was drawn through the sintered-glass bubblers as described in the preceding section. The rate of flow and time of passage of the atmosphere (usually between 30 min and 1 h) were noted and the volume sampled was calculated. Each bubbler was emptied, rinsed and the contents made up to a standard volume of 50 ml with 5% *V/V* acetone in hexane solution. The concentration of lindane in each solution was determined by gas chromatography on a Pye 104 chromatograph. Aliquots (5 µl) of the solution were injected directly on to a 2 m × 4 mm i.d. column of 6% OV-210 on Chromosorb W HP

Table 1. Calculated values of D_{LA} at 1 atm (101 308 N m^{-2}) pressure

	D_{LA}/mm^2 s^{-1}	
Temperature/ °C	HBS equation	FSG equation
25	5.508	5.344
22	5.418	5.250
20	5.370	5.210
15	5.180	5.033
5	4.844	4.732

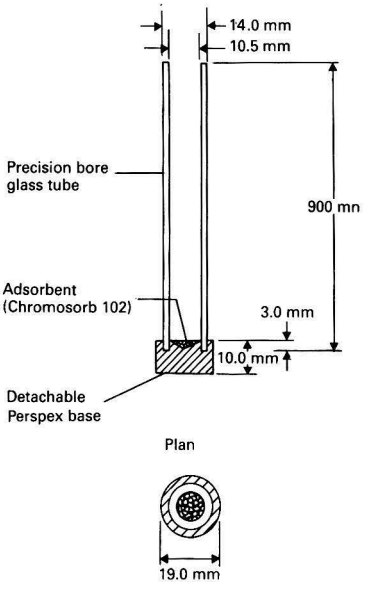

Fig. 1 Passive sampling device

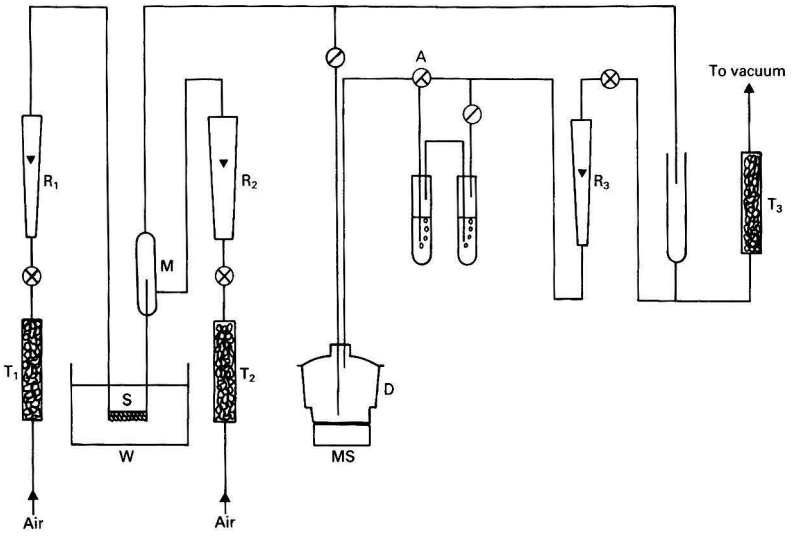

Fig. 2. Apparatus for generation of atmospheres of lindane. D, Desiccator; M, mixing chamber; MS, magnetic stirrer; R_1, rotameter (0–250 ml min^{-1}); R_2 rotameter (0–5 l min^{-1}); R_3, rotameter (0–1.2 l min^{-1}); S, lindane source; T_1, T_2 and T_3, charcoal towers; W, water-bath; ⊗, needle valve; and ∅, tap

(80–100 mesh) at 165 °C. The carrier gas (nitrogen) flow-rate was 30 ml min^{-1}. Peaks were detected by electron capture at 275 °C. The detector response was calibrated using a series of standard solutions of lindane in acetone - hexane (5% *V/V* solution) (2.5, 5 and 10 ng ml^{-1}). The concentration of lindane in the generated atmosphere was calculated from the expression

$$C = \frac{1000 M_1^2}{V(M_1 - M_2)} \quad \ldots \quad (5)$$

where C is the concentration of lindane in the atmosphere (μg m^{-3}); V is the volume of the atmosphere sampled (l); M_1 is the total mass of lindane collected in the first bubbler (μg); and M_2 is the total mass of lindane collected in the second bubbler (μg).

Stability of Generated Atmospheres

The generator was set up with a source flow-rate of 200 ml min^{-1}, diluting air flow-rate of 2350 ml min^{-1} and a flow-rate through the chamber of 397 ml min^{-1}. The water-bath (source) temperature was maintained at 19–19.5 °C. The generator was run for 1 week to stabilise and then samples of the generated atmosphere were collected on five consecutive days using the sintered-glass bubbler system. Samples were collected for 1 h at a flow-rate of 397 ml min^{-1} and their lindane contents were determined by gas chromatography (Table 2).

Effect of Chamber Flow-rate

Eleven or twelve unsilanised passive sampling tubes were placed in the generator chamber and exposed to lindane atmospheres for a period of 24 h exactly. The source was maintained at 20 ± 0.5 °C and the flow-rate at 40 ml min^{-1} with a diluting air flow-rate of 800 ml min^{-1}. Three sets of duplicate experiments were performed at chamber flow-rates of 100, 250 and 500 ml min^{-1}, respectively. The atmosphere concentration was determined immediately before, during (approximately 6 h after the start) and immediately after each experiment and the average value used to calculate the average diffusion coefficient for each experiment (Table 3). The generator was left to stabilise for at least 1 d between experiments.

Silanisation of Passive Sampling Tube Walls

The inside walls of the glass tubes were silanised before use. The tubes were rinsed three times with acetone and allowed to dry in air. A 2% *V/V* solution of dimethyldichlorosilane in 1,1,1-trichloroethane (Repelcote; BDH Chemicals) (2 ml) was drawn into a Pasteur pipette and then run gently down the inside walls of the tube, which was rotated slowly to ensure that all parts of the walls were coated. This was repeated four times. The tube walls were rinsed with de-mineralised water and dried in an air oven for 45 min at 85 °C.

Effect of Silanisation of Tube Walls

Six silanised and six unsilanised tubes were placed in the generator for a period of 24 h 10 min, with a chamber flow-rate of 100 ml min^{-1}. The average concentration of lindane vapour during the exposure period was 17 μg m^{-3}. On removal from the generator chamber the tube walls were rinsed twice with a 5% *V/V* solution of acetone in hexane (5 ml) and the rinsings were transferred into a 10-ml calibrated flask and made up to volume. Lindane was determined by GC as described above.

Determination of the Diffusion Coefficient of Lindane in Air

The generator was set up with a source flow-rate of 40 ml min^{-1} and a diluting air flow-rate of 800 ml min^{-1}. The chamber flow-rate was set at 100 ml min^{-1} (runs 1 and 2) or 200 ml min^{-1} (runs 3–5). The water-bath temperature was maintained at 20 ± 0.5 °C. The generator was allowed to stabilise and for each determination six silanised sampling tubes were placed in the chamber. The period of exposure (approximately 24 h) was measured to the nearest minute. The concentration of the atmosphere was measured, as described above, immediately before, approximately 6 h after the start

and immediately prior to termination of the exposure period, using a sampling flow-rate through the bubblers of 92.5 ml min^{-1} (runs 1 and 2) and 185 ml min^{-1} (runs 3–5). After exposure the tubes were removed, the adsorbent emptied into glass vials and eluted (twice) by suspension in 5% *V/V* acetone in hexane solution (4 ml). The eluates were transferred into 10-ml calibrated flasks and made up to volume. Lindane was determined by GC as described above. Five determinations were carried out and the generator was allowed to stabilise for at least 24 h between determinations. Room temperature was within the range 22–24 °C during the period of the five determintions (Table 4).

Results

Stability of Generated Atmospheres

The concentration of lindane vapour in an atmosphere generated continuously over a period 5 d is presented in Table 2.

Effect of Chamber Flow-rate

The diffusion coefficients of lindane in air calculated using equation (2) for different flow-rates of lindane vapour through the exposure chamber are presented in Table 3. The values reported are the averages of the values calculated for each individual sampling tube. An analysis of variance showed that the effect of flow-rate through the exposure chamber was not significant.

Effect of Silanisation of Tube Walls

The mean masses of lindane recovered from the walls of six unsilanised and six silanised tubes were found to be 10.5 ng (standard deviation 6.7 ng) and 2.1 ng (standard deviation 1.0 ng), respectively.

Determination of the Diffusion Coefficient, D_{LA}, of Lindane in Air

The results of five experiments to determine the diffusion coefficient of lindane in air are presented in Table 4.

An *F*-test and Student's *t*-test showed that there was no significant difference between any of these results and that they could be combined. The over-all mean value of D_{LA} was therefore 5.4 $mm^2 s^{-1}$ (standard deviation 1.7 $mm^2 s^{-1}$) at 22–24 °C.

Table 2. Stability of a lindane atmosphere over a period of 5 d

Day No.	1	2	3	4	5	Mean ± s.d.
Concentration/μg m^{-3}	28.7	24.2	22.7	23.6	23.5	24.5 ± 2.4

Table 3. Effect of chamber flow-rate

Flow-rate/ ml min^{-1}	Average diffusion coefficient/ $mm^2 s^{-1}$	S.d./ $mm^2 s^{-1}$	No. of tubes exposed
100	5.1	1.9	12
100	6.0	1.4	11
250	4.6	1.2	11
250	5.6	2.8	12
500	4.7	3.1	5
500	5.6	2.1	12

Table 4. Determination of the diffusion coefficient (D_{LA}) of lindane in air

Experiment No.	Average diffusion coefficient/ $mm^2 s^{-1}$	S.d./ $mm^2 s^{-1}$	No. of tubes
1	5.8	1.5	6
2	3.7	1.0	6
3	5.6	2.2	5
4	6.2	1.4	5
5	5.9	1.7	5

Discussion

The diffusion coefficient of lindane in air, determined by exposure of the passive sampling devices to atmospheres of known concentration of lindane, was 5.4 $mm^2 s^{-1}$, which was in excellent agreement with the values calculated empirically by two independent means (5.418 and 5.250 $mm^2 s^{-1}$ at 22 °C). Further, it is interesting that the two empirical methods of calculation agreed so closely, thereby entirely justifying the use in the Hirschfelder, Bird and Spotz equation of the assumed values (based on analogy with published values for similar compounds) of 7.276 Å for the collision diameter of the lindane molecule (σ_L) and 350 for the force constant of lindane (ε_L/k.)

The standard deviation of the experimentally determined mean value of the diffusion coefficient of lindane in air was 1.7 $mm^2 s^{-1}$ (coefficient of variation 31.5%). The error of a single determination of D_{LA} (*i.e.*, for an individual sampling tube) consists of errors in the chromatographic determination of the mass of lindane adsorbed, estimated to be approximately ±5%, error in the measurement of the adsorption tube dimensions, error in the measurement of the time of exposure, error in the determination of the concentration of the generated atmosphere (which may be assumed to be approximately ±10%) and an error arising from the fluctuation in concentration of the generated atmosphere during the period of exposure. The errors in measurement of the time of exposure and of diffusion tube length were both less than 1% and can be discounted. An error of ±0.25 mm in the measurement of the tube diameter, however, gives rise to an error in D_{LA} of ±5%. The standard deviation of the mean concentration of the generated atmosphere in the stability experiment (24.5 μg m^{-3}) was 2.4 μg m^{-3} (coefficient of variation 10%). (The effect of change of flow-rate through the generator chamber was shown to be not significant.) Hence the total error of the value of D_{LA} determined for each individual diffusion tube (expressed as the r.m.s. value) that can be accounted for is ±16%. The higher standard deviation of the experimentally determined value is indicative of other unspecified sources of error. These may be due to turbulence at the tube mouth with consequent reduction of the effective diffusion path length, variable retention of lindane on the sorbent or variable elution from it or due to sorption of lindane on the tube walls.

It was apparent from early studies that substantial adsorption of lindane vapour occurred on the tube walls, and silanisation of the glass walls effectively reduced it. However, as can be seen from Table 3, the mean value of the diffusion coefficient of lindane in air determined using unsilanised tubes (in the experiments to establish the effect of flow-rate through the exposure chamber) was 5.3 $mm^2 s^{-1}$, which was not significantly different to the result using silanised tubes (*t*-test, *F*-test). However, it was felt that silanisation afforded a more precise result (*i.e.*, lower standard deviation) and, therefore, the procedure was adopted as standard. At the very low concentrations of lindane studied, the precision of these devices is sufficient to assess the concentration of lindane.

The passive sampling tubes were designed to be inexpensive to construct and very simple to use. The length to area of cross-section ratio of 10 : 1 was considered to be the minimum necessary to reduce the effect of turbulence at the tube mouth on the diffusion process. Although the device has been developed to sample lindane vapour it should, in theory, be suitable for the determination of time-weighted average values of low concentrations of any volatile compound and should be of much wider utility.

The authors thank the Parliamentry Works Officer, Department of the Environment, Property Services Agency, for permission to publish this paper.

Appendix

Collision Diameter of Lindane in Air

σ_{LA} was calculated from the equation

$$\sigma_{LA} = 0.5(\sigma_L + \sigma_A) \quad .. \quad .. \quad .. \quad (6)$$

where σ_A is the collision diameter of air = 3.711 Å[19]; σ_L is the collision diameter of lindane, which was calculated empirically:

$$\sigma_L = \sigma_{cyclohexane} + 0.5(\sigma_{CCl_4} - \sigma_{CH_4}) \quad .. \quad (7)$$

in which $\sigma_{cyclohexane}$ = 6.182 Å, σ_{CCl_4} = 5.947 Å and σ_{CH_4} = 3.758 Å.[20] Hence by substituting these values in equation (7), σ_L = 7.276 Å and thus from equation (6), σ_{LA} = 5.493 Å.

Collision Integral for Ω_D Lindane for Diffusion

Ω_D was calculated using the expression

$$\Omega_D = \frac{1.06036}{T^{*\,0.15610}} + \frac{0.19300}{e^{0.47635T^*}} + \frac{1.03587}{e^{1.52996T^*}} + \frac{1.76474}{e^{3.89411T^*}} \quad (8)$$

where

$$T^* = kT/(\varepsilon_A \times \varepsilon_B)^{0.5} \quad .. \quad .. \quad .. \quad (9)$$

in which k is Boltzmann's constant (J K^{-1}) and ε_A/k, ε_L/k are the force constants for air (78.6 K) and for lindane (assumed to be 350 K[20]), respectively.

Substituting these values in equation (9) gives T^* = 1.7967 hence from equation (8) Ω_D = 1.1204.

References

1. Slade, R. E., *Chem Ind. (London)*, 1945, 314.
2. Worthing, C. R., *Editor*, "Pesticide Manual," Seventh Edition, British Crop Protection Council, Bath, 1983, p. 300.
3. "Documentation of the Threshold Limit Values," Fourth Edition, American Conference of Governmental Hygienists Inc., 1980, p. 246.
4. Brasslow, H.-L., Baumann, K., and Lehnert, G., *Int. Arch. Occup. Environ. Health*, 1981, **48**, 81.
5. Tomczak, S., Baumann, K., and Lehnert, G., *Int. Arch. Occup. Environ. Health*, 1981, **48**, 283.
6. Thomas, T. C., and Seiber, J. N., *Bull. Environ. Contam. Toxicol.*, 1974, **12**, 17.
7. Abbott, D. C., Harrison, R. B., Tatton, J. O'G., and Thomson, J., *Nature (London)*, 1966, **211**, 259.
8. Oehme, M., and Stray, H., *Fresenius Z. Anal. Chem.*, 1982, **311**, 665.
9. Lewis, R. G., and Macleod, K. E., *Anal. Chem.*, 1982, **54**, 310.
10. Lewis, R. G., and Jackson, M. D., *Anal. Chem.*, 1982, **54**, 592.
11. Dangwal, S. K., *Am. Ind. Hyg. Assoc. J.*, 1982, **43**, 912.
12. Rose, V. E., and Perkins, J. L., *Am. Ind. Hyg. Assoc. J.*, 1982, **43**, 605.
13. Palmes, E. D., Tomczyk, C., and DiMattio, J., *Atmos. Environ.*, 1977, **11**, 869.
14. Apling, A. J., Stevenson, K. J., Goldstein, B. D., Melia, R. J. W., and Atkins, D. H. F., "Air Pollution in Homes. 2: Validation of Diffusion Tube Measurements of Nitrogen Dioxide," WSL Report LR311 (AP), Warren Spring Laboratory, Stevenage, 1979.
15. Stevenson, K. J., Apling, A. J., and Sullivan, E. J. "Air Pollution in Homes. 3: Measurements of Carbon Monoxide and Nitrogen Oxides in Two Living Rooms," WSL Report LR332 (AP), Warren Spring Laboratory, Stevenage, 1979.
16. Atkins, D. H. F., Healy, C., and Tarrant, J. B.," The Use of Simple Diffusion Tubes for the Measurement of Nitrogen Dioxide Levels in Homes using Gas and Electricity for Cooking," Report No. R9184, AERE, Harwell, 1978.
17. Ward, C. D., *HATRA Knitting Ind. Tech. Rev.*, 1981, **1**, 60.
18. Coutant, R. W., and Scott, D. R., *Environ. Sci. Technol.*, 1982, **16**, 410.
19. Hirschfelder, J. O., Bird, R. B., and Spotz, E. L., *J. Chem. Phys.*, 1948, **16**, 968.
20. Reid, R. C., Prausnitz, J. M., and Sherwood, T. K., "The Properties of Gases and Liquids," Third Edition, McGraw-Hill, New York, 1977, p. 548.
21. Fuller, E. N., and Gidding, J. C., *J. Gas Chromatogr.*, 1965, **3**, 222.

Paper A4/148
Received April 12th, 1984
Accepted June 22nd, 1984

Determination of Lindane Vapour in Air by Passive Sampling Part II.* Comparison of the Passive Sampling Method With a Dynamic Adsorption Technique

Marjory A. Bland, Stephen Crisp, Peter R. Houlgate and Jeffery W. Llewellyn
Laboratory of the Government Chemist, Cornwall House, Stamford Street, London SE1 9NQ, UK

The passive sampling device described in Part I has been compared with a dynamic adsorption technique for the determination of atmospheres of known concentration of lindane vapour generated in the laboratory, and for the determination of lindane vapour in the field. The agreement of results obtained using the two techniques was very good, although the passive sampling technique was less precise. The passive sampling technique is now used to monitor concentrations of lindane vapour in the Palace of Westminster on a routine basis over periods of one month.

Keywords: *Lindane determination; passive sampling; diffusion coefficient; air*

The diffusion coefficient of lindane in air, determined experimentally using a passive sampling technique, was in close agreement with the value calculated by two empirical means,[1] which suggests that the devices might be used successfully to determine lindane in air. Passive sampling devices offer significant advantages of cost and convenience over dynamic (pumped) sampling techniques, particularly for the determination of time-weighted average concentrations of airborne vapours and gases over extended periods. Passive sampling techniques have been widely adopted for monitoring in the workplace, but have not so far been used for ambient air monitoring to any great extent.

Prior to its use in the field, a passive sampling technique must be validated in the laboratory. Accordingly, the performance of the devices for the determination of the concentration of lindane in laboratory-generated standard atmospheres was assessed and was compared with a dynamic sampling technique based on that of Thomas and Seiber.[2]

The two techniques were also compared in parallel determinations of low concentrations of lindane vapour in the Westminster Hall of the Palace of Westminster. The roof timbers of the hall, which date from 1401 and which, at 69 feet in length, are the longest in Northern Europe, had been treated with lindane dust in an attempt to eradicate Death Watch beetles. As the building is open to the public it is necessary to monitor the levels of lindane vapour remaining in the atmosphere after treatment. The choice of sampling sites was very restricted and the use of the dynamic method was found to be highly inconvenient. An unobtrusive, simple and reliable method of sampling low levels of lindane vapour in air was thus required to enable the average concentration of lindane vapour to be determined over a period of many months. Since the completion of this work Brown *et al.*[3] have proposed an evaluation protocol for passive samplers.

Experimental

Atmospheres of known concentration of lindane vapour were generated in the laboratory using the apparatus described in Part I. The passive sampling tubes used were also as described in Part I.

Comparison of Passive Sampling and Dynamic Adsorption Techniques for the Determination of Lindane in Generated Atmospheres

Atmospheres of lindane vapour having concentrations in the range 0.5–36.0 μg m^{-3} (determined from samples collected in the bubbler system) were generated by setting the generator source flow-rate and diluting air flow-rate appropriately. To determine each atmosphere concentration, six sampling tubes were placed in the chamber and the period of exposure was measured to the nearest minute. For atmospheres in the concentration range 0.5–2.9 μg m^{-3} tubes were exposed for approximately 5 and 2 d, respectively. For all other concentrations tubes were exposed for approximately 24 h. For each concentration the atmosphere was sampled both by collection in hexane as described in Part I, and by dynamic adsorption, immediately before exposure of the sampling tubes, approximately half way through the period of exposure, and immedately prior to termination of the exposure. Lindane was determined in the bubbler samples and in the adsorption tube and passive sampling tube eluates by GC as described in Part I.

Throughout the series of experiments the water-bath temperature was maintained within the range 19–20 °C and the room (chamber) temperature was within the range 20–25 °C. The generator was allowed to stabilise for at least 24 h between generations of successive atmospheres.

Determination of the Concentration of Lindane in Generated Atmospheres by Dynamic Adsorption

The concentration of lindane in the generated atmospheres was determined by dynamic adsorption on Chromosorb 102 using a method based on that of Thomas and Seiber.[2]

The dynamic adsorption tubes, illustrated in Fig. 1, were made from glass (i.d. 10 mm, o.d. 13 mm) and were packed with cleaned Chromosorb 102 in two sections 40 and 20 mm in length, separated by a plug of glass-wool. Each section contained 1 and 0.5 g of adsorbent, respectively, which was retained with loosely packed glass-wool as shown. In later work shorter tubes (over-all length 135 mm) that contained only 1 g of adsorbent in a single section were used.

In order to sample the lindane atmosphere, the inlet of the adsorption tube was connected by a short length of flexible

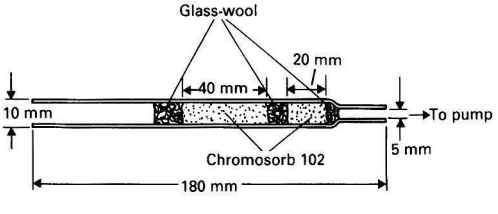

Fig. 1. Dynamic adsorption tube

* For Part I of this series, see p. 1517.

tubing to the generator at the outlet of the exposure chamber (after removal of the bubbler system). The tube outlet was connected to the generator at a point in the chamber exhaust line prior to the "exhaust flow" rotameter. The lindane vapour atmosphere was drawn through the adsorption tube at a flow-rate of 200 ml min^{-1} for a measured period of time (usually between 30 min and 1 h) after which the tubes were disconnected. Each section was emptied into a separate glass vial and extracted twice with 10 ml of 5% *V/V* acetone in hexane solution. For each section, the extracts were combined and made up to a standard volume of 25 ml. Lindane was determined by GC as described in Part I.

Field Determination of Lindane Vapour in Air Passive Sampling

Twelve silanised glass tubes and clean bases were selected. The tubes were taken to the sampling site in sealed plastic bags. Cleaned Chromosorb 102 was transported to the sampling site in a separate sealed container. At the sampling site ten bases were filled with adsorbent to give a level surface just flush with the top of the base and the glass tubes were inserted into the annular groove. The tubes were then placed carefully in a specially constructed rack that was then put inside an open Perspex box to minimise the effect of draughts, ensuring that the sampling tubes stood as near vertical as possible. Two blank sampling tubes (*i.e.*, tubes fitted to bases that did not contain any adsorbent) were also placed in the rack and a removable cover was placed over the tubes to prevent particulate matter dropping into them. The gap between the cover and the tops of the tubes was approximately 30 mm to allow free circulation of air. The time at which the tubes were placed in the rack was noted and the entire assembly was placed in a position such that it was shielded from strong draughts and was in a place of relative safety. The assembly of tubes was left at the site for a period of 4 weeks (in one instance tubes were exposed for a period of 5 weeks and 5 days), the exact period of exposure being measured to the nearest minute.

The tubes were then taken out of the rack and the bases removed very carefully. The Chromosorb 102 was tipped into a glass vial (5 ml) that had been cleaned previously by rinsing three times in acetone and drying in air. The vials were capped with a plastic cap, numbered and returned to the laboratory.

In the laboratory the adsorbents were each eluted twice with 5% *V/V* acetone in hexane solution (2 ml) and each eluate was made up to a standard volume of 10 ml. The blank bases were rinsed twice with the same solvent (2 ml) and made up to 10 ml. Lindane was determined by GC as described in Part I. The concentration of lindane in the atmosphere was calculated for each sampling tube and from these the average result was obtained.

Field Determination of Lindane Vapour in Air by Dynamic Adsorption

The procedure used was essentially that of Thomas and Seiber.[2] Air samples were drawn through adsorption tubes (described above) by an electrical pump. The flow-rate (2 l min^{-1}) was controlled by the insertion of a suitable critical orifice in the flexible tube between the pump and adsorption tube outlet, and the exact flow-rate was measured prior to sampling by means of a rotameter connected in line to the inlet of the adsorption tube. The sampling period was noted and lindane determined by GC as described previously. Samples were taken in duplicate on all occasions. The samples were taken a sufficient distance from the passive samplers so as not to disturb the air in the immediate vicinity.

Results

Determination of Lindane in Laboratory-generated Atmospheres

The results of the determination of the concentration of lindane vapour in laboratory-generated atmospheres by collection of samples in hexane, dynamic adsorption and by passive sampling are presented in Table 1.

Table 1. Comparison of passive, dynamic adsorption and bubbler sampling techniques for the determination of lindane in laboratory-generated atmospheres

Concentration of lindane/μg m^{-2}					
Collection in bubbler		Dynamic adsorption		Passive sampling	
Mean of 3 determinations	Standard error	Mean of 3 determinations	Standard error	Mean, 6 tubes exposed*	Standard error
0.5	0.09	0.5	0.07	0.5	0.11
0.8	0.03	0.5	0.03	1.1	0.29
1.5	0.12	1.4	0.09	2.0	0.43
2.2	0.18	2.1	0.20	3.4	0.99
2.9	0.38	2.7	0.22	3.8	0.64
9.7	0.78	9.9	1.85	17.1	2.45
12.1	0.66	10.7	0.47	15.1	2.05
12.4	0.80	12.7	0.59	11.7	1.82
12.8	0.52	9.5	0.63	8.8	0.67
13.8	1.59	14.7	1.87	14.1	2.71
14.7	—	14.4	—	13.9	3.04
15.9	0.62	13.4	0.28	12.3	2.67
19.3	2.54	16.0	2.37	18.0	2.33
29.2	1.13	27.3	13.40	30.7	2.75
31.3	2.75	20.8	4.48	29.1	6.04
36.0	1.80	38.4	0.12	33.7	4.14

* Calculated using the experimentally determined value of $D_{1,A}$ of 5.4 mm^2 s^{-1}.

Table 2. Determination of lindane in air in the Great Westminster Hall

Period	Temperature range (and average) during period/°C	No. of tubes exposed	Concentration of lindane/μg m^{-3}			
			Passive sampling*	Standard error	Dynamic adsorption†	Standard error
22.10.81–19.11.81	7–15 (9.0)	5	0.15	0.019	0.21	0.0
5.11.81–3.12.81	4–15 (8.9)	6	0.24	0.031	0.23	0.007
19.11.81–17.12.81	−1–15 (6.5)	3	0.23	0.040	0.20	0.016
3.12.81–7.1.82	−2–12 (3.5)	5	0.22	0.066	0.18	0.022
12.5.82–10.6.82	18–24 (21.0)	10	0.53	0.078	0.37	0.010
10.6.82–20.7.82	18–24 (20.6)	10	0.47	0.049	0.44	0.068‡

* Calculated using the experimentally determined value of D_{LA} of 5.4 mm^2 s^{-1}.
† Mean of five values taken at the beginning and end of the 1st, 2nd, 3rd and 4th weeks of exposure.
‡ Mean of seven values taken at the beginning and end of the 1st, 2nd, 3rd, 4th, 5th and 6th weeks of exposure.

Linear regression analysis of the results by dynamic adsorption (y) *versus* results by passive sampling (x) afforded a line having the equation

$$y = 0.937x - 0.413 \ (r = 0.951)$$

as the line of best fit. For comparison, linear regression analysis of the results by collection in a bubbler (y) *versus* results by dynamic sampling (x) afforded a line having the equation

$$y = 1.034x + 0.847 \ (r = 0.965)$$

as the line of best fit and linear regression analysis of the results by collection in a bubbler (y) *versus* results by passive sampling (x) gave a line having the equation

$$y = 1.021x - 0.264 \ (r = 0.969)$$

as the line of best fit.

Determination of Lindane in the Atmosphere in the Great Westminister Hall (Palace of Westminster)

The results of the determination of the concentration of lindane vapour in air in the Great Westminster Hall by passive sampling and by a dynamic adsorption technique over five periods of 4 weeks are presented in Table 2.

Linear regression analysis ot the results by passive sampling (x) *versus* those obtained by the dynamic technique (y) afforded as line of best fit a line having the equation

$$y = 0.633x + 0.077 \ (r = 0.914)$$

Discussion

In a comparison of the passive sampling method and the well established dynamic sorption technique, linear regression analysis showed the results of the determination of laboratory-generated atmospheres of lindane vapour to be in close agreement over a wide range of concentrations. Linear regression analysis also showed that results obtained by either technique were in better agreement with those obtained from samples of the generated atmosphere collected in a solvent (the bubbler method) than between themselves. Concentrations of lindane determined by the passive technique were in marginally closer agreement with results of the bubbler method than were those of the dynamic method, which is to be expected as the bubbler method served as the standard in the determination of the diffusion coefficient of lindane in air, used to calculate the unknown concentrations of lindane for the passive samplers. A t-test showed that there was no significant difference between the concentration of lindane determined using any of the three methods of sampling.

The laboratory comparison of the techniques showed that although the results obtained were comparable, the passive sampling method was less precise. The average values of the standard error (expressed as a percentage of the mean) for each technique were bubbler method 8.1%, dynamic technique 9.1% and passive sampling technique 17.8%.

The results of the field trials of the passive sampling tubes agreed less well with those obtained by the dynamic adsorption technique as demonstrated by linear regression analysis. However, a t-test confirmed that the difference in the concentration of lindane determined using the two sampling methods was not significant. It must be remembered, however, that the passive sampling devices afforded a time-weighted average value of the lindane concentration in the Westminster Hall, relating to the entire exposure period of 4 (or more) weeks. The dynamic adsorption techniques afforded a series of duplicate spot values taken throughout the exposure period, which did not reflect changes in lindane concentration arising from day-to-day changes in ambient temperature.

The average standard error (expressed as a percentage of the mean) of the results of the field determination of lindane by passive sampling and dynamic adsorption were 16.5 and 6.9%, respectively, and were in good agreement with the corresponding values for the laboratory comparison. The passive sampling technique was thus deemed suitable for monitoring lindane in air in the Great Westminster Hall and is now used routinely. Tubes are exposed for periods of 4 or 5 weeks.

Although the device was developed for monitoring lindane, this study confirms the statement made in Part I that the device should, in theory, be suitable for the determination of time-weighted average values of very low concentrations of a wide range of volatile compounds, and should, therefore, be of widespread use in ambient air monitoring.

The authors thank the Parliamentary Works Officer, Department of the Environment, Property Services Agency, for permission to publish this paper.

References

1. Bland, M. A., Crisp, S., Houlgate, P. R., and Llewellyn, J. W., *Analyst*, 1984, **109**, 1517.
2. Thomas, T. C., and Sieber, J. N., *Bull. Environ. Contam. Toxicol.*, 1974, **12**, 17.
3. Brown, R. H., Harvey, R. P., Purnell, C. J., and Saunders, K. J., *Am. Ind. Hyg. Assoc. J.*, 1984, **45**, 67.

Paper A4/149
Received April 12th, 1984
Accepted June 22nd, 1984

Determination of Organotin Compounds Contained in Aqueous Samples Using Capillary Gas Chromatography

Ann Woollins* and W. R. Cullen
Chemistry Department, University of British Columbia, Vancouver, BC, Canada

A method for the extraction of various organotin compounds [$(R_3Sn)_2O$ and R_nSnX_{4-n}; R = Me, Et, Bu, Ph; X = Cl, Br, OH, OMe; n = 2, 3] from aqueous solution and their subsequent determination is described. The compounds were initially converted into their corresponding hydrides, which were then obtained for analysis by a combination of helium purging and ether extraction of the aqueous solution. Separation of the hydrides was carried out using capillary column gas chromatography, which enabled nanogram amounts to be detected.

Keywords: *Organotin determination; capillary gas chromatography; aqueous samples*

Although organotin compounds are widely used for a variety of commercial applications, *e.g.*, as fungicides,[1] wood preservers[2] and stablisers in plastics,[3] very little is known about the final (*i.e.*, environmental) fate of these compounds. One area of obvious concern is the possible build-up of tin compounds in waterways and oceans. The determination of organotin species has been studied by a variety of techiques such as gas chromatography,[4,5] atomic-absorption spectrometry[6,7] and anodic stripping,[8] but in most previous studies the procedure adopted has been restricted to one type of organic group in each instance, *e.g.*, butyltin bromides[9] or phenyltin hydrides.[10] Clearly it would be advantageous to establish a method for the extraction and determination of a wide variety of organotin compounds from aqueous solutions and it was the purpose of this work to develop such a procedure.

Experimental

Reagents

Research-grade tin compounds (Alfa) were purified by recrystallisation or distillation according to standard methods. Lithium aluminium hydride (Alfa) and sodium tetrahydroborate(III) (Alfa) were used as supplied. Biphenyl (Aldrich) was recrystallised from ethanol. Solvents were of chromatography grade (Burdick and Jackson) with the exception of dibutyl ether (Eastman), where the reagent-grade material was freed of peroxides by shaking with a saturated aqueous solution of iron(II) sulphate and then distilled twice at 10 Torr. Water was purified by double distillation followed by passage through XAD-2 rectilinear resin. Zero-grade helium (Mattheson) was used for blowing out the volatile hydrides and for the chromatography. The glassware was cleaned by soaking in 2 M HCl and again in 1% EDTA - 2% NaOH.

Standards

Organotin hydrides were prepared by treatment of the appropriate chloride compound (10 mmol) in dry diethyl ethyl (50 ml) with a slurry of $LiAlH_4$ in diethyl ether (100 mmol in 50 ml). The mixture was stirred at room temperature under nitrogen in the dark for 1 h, after which time water was added dropwise to destroy any unreacted $LiAlH_4$. Filtration, followed by drying over Na_2SO_4 and subsequent removal of the ether under vacuum at room temperature, gave the desired product, which was purified by distillation under reduced pressure.

* To whom correspondence should be addressed at: Chemistry Department, Queen Mary College, University of London, London E1 4NS, UK.

The above procedure was not satisfactory for the preparation of low-boiling hydrides (*i.e.*, Me_2SnH_2, Me_3SnH and Et_2SnH_2), which distilled over with the ether. An alternative method for the preparation of these hydrides was to perform the reduction in dibutyl ether and then distil off the tin compounds, leaving the dibutyl ether behind.

Standards for the chromatographic analysis were obtained by dissolution of the hydrides in chromatography-grade hexane immediately after preparation as they are not very stable (particularly those containing methyl or phenyl groups). The solutions, in the concentration range 1×10^{-4}–1×10^{-2} p.p.m. of tin, were stable for over 6 months when stored under nitrogen at 6 °C in the dark.

Analysis of Aqueous Solutions

A 1-l sample of water spiked with organotin chlorides was acidified[4] with 10 ml of 1 M acetic acid and placed in a 2-l round-bottomed flask equipped with a fritted-disk gas inlet-tube, a PTFE outlet tube (connected to a hydride trap) and a PTFE-lined inlet septum. The stirred solution was purged with helium (70 ml min^{-1}) for 5 min while the hydride trap was being cooled to liquid nitrogen temperature. After this time, 1 ml of freshly prepared aqueous $NaBH_4$ (5%) was injected into the reaction vessel via the septum. The helium flow was continued for 1 h after which the hydride trap was closed off and removed (still at −196 °C) to the gas chromatograph for analysis. The hydrides that had not been blown out were extracted by shaking the aqueous solution with 200 ml of diethyl ether. The ether layer was dried over Na_2SO_4, filtered and reduced to 0.5 ml using a strong nitrogen flow. This solution was analysed by injection into the gas chromatograph.

Apparatus

The hydride trap was constructed (Fig. 1) from two PTFE three-way taps connected by 4-mm PTFE tubing. This inert material was chosen because it is known that metal surfaces and silicone grease greatly enhance the decomposition of organotin hydrides.[11] The U-tube was packed with Chromosorb W. PTFE tubing also connected the trap to the reaction vessel; however, glass-lines steel tubing (4 mm i.d.) was necessary to link with the gas chromatograph owing to the high temperature of the injection port. The latter was adapted to accommodate the steel tube. In order to permit quick change over from the standard injection technique to use of the trap, the helium line was modified as shown in Fig. 2. A T-piece was inserted between the flow meter and the injection port. The additional gas line was connected directly to the hydride trap or closed off at point B. If the trap was being used the inlet A was closed.

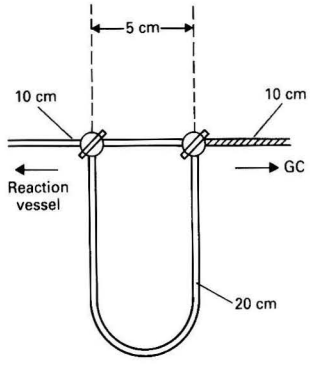

Fig. 1. Trap for volatile hydrides. All tubing is 4 mm i.d. PTFE, except that shaded, which is glass-lined steel, also 4 mm i.d.

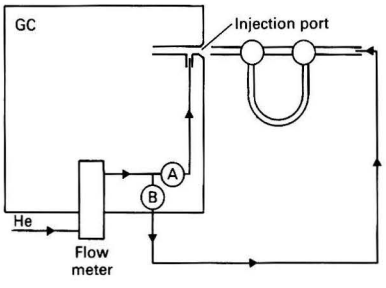

Fig. 2. Adaptation of the gas chromatograph for alternate use of the hydride trap or syringe. A and B are two-way valves

"Injection" of samples from the hydride trap into the gas chromatograph was achieved as follows. With the trap closed off, it was connected into the gas supply lines (Fig. 2). The three-way taps were opened across the bridge to enable the pressure to equilibrate, then the U-tube was opened to the instrument and the liquid nitrogen removed. At this stage a pressure increase across the column was often noted, varying from one experiment to the next. This resulted in a variation in retention times of up to 10% although the ordering was unaffected.

Gas chromatography was performed using a Varian 2700 instrument equipped with a flame-ionisation detector and a capillary column (flexible quartz, SE-30, 20 m × 0.2 mm i.d., 0.2 μm film). Both the carrier gas (zero-grade helium, 1 ml min^{-1}) and the make-up gas (N_2, 200 ml min^{-1}) were freed from volatile impurities by passage through a dry-ice trap. Low-bleed, high-temperature, Thermogreen septa (Supelco) were found to be the most satisfactory at the high injector temperatures used here. For syringe injections (0.01–0.1 μl) the injection port was at 275 °C, the detector at 300 °C and the oven at 50 °C for the first 5 min, after which the oven temperature was increased at 10 °C min^{-1} up to a final temperature of 200 °C. When the hydride trap was the sample source the injector and detector temperatures were as above, while the oven temperature was 40 °C for the first 10 min followed by a 10 °C min^{-1} increase up to a maximum of 200 °C. An internal reference, biphenyl, was used for quantitative analysis by comparison of peak areas.

Atomic-absorption measurements were carried out using a Varian AA4 instrument operating at 224.6 nm with a slit width of 100 μm and an air - hydrogen flame. Standard solutions, prepared from tin(II) chloride, gave a detection limit of 0.5 p.p.m. However, it was noted that much lower limits (by a factor of 50) were possible for the hydrides.

Results and Discussion

The purpose of this work was simultaneously to detect and quantify as many different types of organotin compounds as possible whilst retaining the organic moieties. We chose gas chromatography as the method for separating these very similar compounds with the view that very powerful and selective detectors are available (*e.g.*, flame photometric,[6] mass spectrophotometric[5]), even though we only had access to a flame-ionisation detector. Capillary columns were chosen in order to obtain the best separation; accordingly, the instrument was suitably adapted. In order to present the samples to the gas chromatograph in a volatile enough form, we decided to convert them into their corresponding hydrides. Unfortunately, the reported methods[12–17] used for this process vary widely. For instance butyltin chlorides have been reduced using $LiAlH_4$ in refluxing diethyl ether, butyltin oxides with a silicone polymer at room temperature under nitrogen and organotin methoxides with diborane. As seen above, both the reducing agent and the reaction temperature differ. We required one system only, one that was powerful enough to reduce butyltin oxides and yet mild enough not to decompose the phenyltin hydrides once prepared.[12] This was finally accomplished by stirring the aqueous sample with an approximately 100-fold excess of $NaBH_4$ at room temperature for 1 h.

To establish that this method gave 100% reduction and that the resultant hydrides were completely extracted from the water by the methods described above, we employed atomic-absorption spectrophotometry. Samples of 1 l of water were spiked with the appropriate chloride, or chlorides, (10 p.p.m.) and treated with $NaBH_4$ in 100-fold excess as in the final procedure; 10-ml aliquots of the solution were removed by syringe and measured using atomic-absorption spectrophotometry. The readings obtained at zero time (immediately the $NaBH_4$ was added) were compared with aliquots removed after 15, 30 and 60 min. The flow-rate of the purging helium was adjusted to observe its effect on the extraction process. When the flow-rate equalled 70 ml min^{-1} the methyl derivatives were completely removed from the water after 15 min, but 50% of the butyl species, Bu_3SnH, was still present after 1 h.

Increasing the flow-rate (100, 150, 200 ml min^{-1}) improved the extraction, but also saturated the hydride trap with water. The use of a water trap filled with Na_2SO_4, or molecular sieves placed between the reaction vessel and the hydride trap, was investigated. Although it was possible to hinder uptake of water (most effectively using 3A molecular sieves at −78 °C), this process also condensed out the higher boiling hydrides (*e.g.*, Bu_3SnH and Ph_2SnH_2). The optimum conditions were established as a 70 ml min^{-1} flow-rate for 1 h without a water trap. For a 10 p.p.m. solution, the transfers of the hydride into the trap were 100, 85, 40 and 15% for Me_3SnH, Et_3SnH, Bu_3SnH and Ph_3SnH, respectively, the remainder being collected by ether extraction. The time required for extraction of the volatile hydrides was reduced for more dilute solutions, *e.g.*, 1 p.p.m. of Et_3SnH was removed 100% in 40 min. Using the helium flow alone we were never able to remove the phenyl compounds or Bu_3SnH completely, in contrast to Hodge *et al.*,[18] who used only a 5-min flow at 70 ml min^{-1} to collect hydrides from ocean samples. Atomic-absorption spectrophotometry was also used to verify that the high-boiling fractions were extracted quantitatively with diethyl ether as described above.

The gas-chromatographic conditions were carefully optimised using the standard solutions to permit the separation given in Tables 1 and 2. We found that the flame-ionisation detector was more sensitive to butyltin hydrides than to phenyl

Table 1. Gas-chromatographic results obtained using syringe injection for R_nSnH_{4-n}. All peaks gave base-line separation

	R_n					
	Et_3	Bu_2	BiP*	Bu_3	Ph_2	Ph_3
Retention time/min	5.4	9.5	15	16	18	31
Relative peak area	8	10	65	20	5	1

* BiP = biphenyl.

Table 2. Gas-chromatographic results obtained using the hydride trap for R_nSnH_{4-n}. All peaks gave base-line separation

	R_n								
	H_2O	Me_2	Me_3	Et_2	Et_3	Bu_2	Bu_3	Ph_2	Ph_3
Retention time/min	4	6	7	9	11	11.5	13	13.5	17

species, and even more sensitive to biphenyl. The detection limit for Bu_2SnH_2 was 2 ng absolute, which, if dissolved in 1 l of water, corresponds to 2×10^{-6} p.p.m. Extraction totally by trap permits complete injection, thus giving a detection limit of 2×10^{-6} p.p.m. Alternatively, ether extraction, using syringe injections of 0.1 µl of a 0.5-ml solution, gives a 5×10^{-3} loss in sensitivity, with a final limit of 1×10^{-2} p.p.m.

The above procedure was extended to include organotin hydroxides, oxides and methoxides. In all instances reduction and extraction were quantitative with detection being the same as observed for the chlorides.

The authors thank Dr. G. Eigendorf for his great assistance in the adaptation of the gas chromatograph to our specific needs.

References

1. Davies, A. G., and Smith, P. J., *in* Wilkinson, G., *Editor*, "Comprehensive Organometallic Chemistry," Volume 2, Pergamon Press, Oxford, 1982.
2. Thapar, I. G., and Mariwala, K. V., *Paintindia Annu.*, 1978, **80**, 85.
3. Loktev, E. A., Gol'dberg, V. M., Kerber, M. L., and Akutin, M. S., *Izv. Vyssh. Uchebn. Zaved., Khim. Khim. Tekhnol.*, 1979, **22**, 723.
4. Meinema, H. A., Burger-Wiersma, T., Versluis-de-Haas, S., and Gevers, E. C., *Environ. Sci. Technol.*, 1978, **12**, 288.
5. Kadeg, R. D., and Christian, G. D., *Anal. Chim. Acta*, 1977, **88**, 117.
6. Everett, G. L., West, T. S., and Williams, R. W., *Anal. Chim. Acta*, 1974, **70**, 291.
7. Braman, R. S., and Tompkins, M. A., *Anal. Chem.*, 1979, **51**, 12.
8. Florence, T. M., and Farrar, Y. J., *J. Electroanal. Chem.*, 1974, **51**, 191.
9. Steinmeyer, R. D., Fentiman, A. F., and Kahler, E. J., *Anal. Chem.*, 1965, **37** 520.
10. Soderquist, C. J., and Crosby, D. G., *Anal. Chem.*, 1978, **50**, 1435.
11. Kuivila, H. G., *Adv. Organomet. Chem.*, 1964, **1**, 47.
12. Van de Kerk, G. J. M., Noltes, J. G., and Luijten, J. G. A., *J. Appl. Chem.*, 1957, **7**, 366.
13. Hayashi, K., Iyoda, J., and Shiihara, I., *J. Organomet. Chem.*, 1967, **10**, 81.
14. Amberger, E., and Kula, M. R., *Chem. Ber.*, 1963, **96**, 2560.
15. Neumann, W. P., and Niermann, H., *Justus Liebigs Ann. Chem.*, 1962, **653**, 164.
16. Tamborski, C., Ford, F., and Soloski, E., *J. Org. Chem.*, 1963, **28**, 237.
17. Birnbaum, E. R., and Javora, P. H., *Inorg. Synth.*, 1970, **12**, 45.
18. Hodge, V. F., Seidel, S. L., and Goldberg, E. D., *Anal. Chem.*, 1979, **51**, 1256.

Paper A4/193
Received June 1st, 1984
Accepted June 28th, 1984

Potentiometric Determination of Milligram Amounts of Organolead in Petroleum*

Sabri M. Farroha, Albertine E. Habboush and Najwa Issaq
Department of Chemistry, College of Science, University of Baghdad, Baghdad, Iraq

For the determination of organolead in petroleum two methods for converting, quantitatively, organolead into lead chloride, and a potentiometric titration method for the measurement of lead chloride, have been developed. The sensitivity, precision and accuracy of the two methods were investigated by analysing a series of standard lead nitrate and synthetic standard solutions. The limits of detection achieved varied from 2.07×10^{-1} to 2.07×10^{-4} g per 100 ml using one method and from 6.22×10^{-1} to 1.66×10^{-4} g per 100 ml using the other method, with an average percentage error of 1–3% and a relative standard deviation that did not exceed ±0.6% for both methods. These two methods were applied successfuly to the determination of lead in petroleum and its fractions before and after treatments.

Keywords: *Organolead determination; potentiometric titration; lead-selective electrode; petroleum analysis*

Several methods have been described for the determination of lead as organolead compounds in gasoline, having the following limits of detection: polarographic, 0.5–6.0 g l^{-1} [1]; atomic absorption, 2.5–25 mg l^{-1} [2]; colorimetric, 2.64–26.4 mg l^{-1} [3]; X-ray spectrophotometric, 0.026–1.32 g l^{-1} [4,5]; and combined gas chromatographic - photometric, 10–1000 p.p.m. of lead.[6] The limit of detection for the technique described in this work is lower than in most of these methods, and the method is simpler and of greater accuracy.

Experimental and Results

Apparatus

The following apparatus was used: a Beckman Model 4500 digital pH meter; an Ingold 157200 lead-selective electrode; a Beckman saturated calomel electrode; a Quickfit reflux set; and a Kjeldhal digestion apparatus.

Reagents

All reagents were obtained from Fluka in the purest available form.

Sodium molybdate dihydrate.
Lead nitrate.
Sodium nitrate.
Methanol.
Lead tetraacetate.
Hydrochloric acid.
Octane.
Benzene.
Sodium hydroxide.
Concentrated nitric acid.
Perchloric acid.
Hydrogen peroxide solution, 30% *V/V*.

Procedures

Determination of lead by potentiometric titration using a lead-selective electrode

The sensitivity, accuracy and precision of the potentiometric determination of lead were determined by titrating 100-ml samples of a standard lead nitrate solution of various concentrations in the range of 10^{-2}–6×10^{-5} M. Each solution was quantitatively transferred into a 250-ml beaker and its pH was adjusted to between 5 and 5.5. The cell was assembled and the solution was titrated potentiometrically against sodium molybdate solution in the range 2.5×10^{-1}–2.0×10^{-4} M using a lead-selective electrode and a double-junction saturated calomel electrode. The results were plotted on Gran's plot paper and the amounts of lead calculated as shown in Table 1.

Table 1. Summary of the results for the potentiometric determination of lead nitrate solutions with sodium molybdate solution as titrant

Theoretical concentration of lead/mmol per 100 ml	Concentration of titrant/M	Lead concentration found/mmol per 100 ml	Absolute error/mmol per 100 ml	Error, %
1.0	2.5×10^{-1}	1.02	$+2.0 \times 10^{-2}$	2.0
1×10^{-1}	2.5×10^{-2}	1.01×10^{-1}	$+1.0 \times 10^{-3}$	1.0
5×10^{-2}	2.5×10^{-2}	4.93×10^{-2}	-7.0×10^{-4}	1.4
4×10^{-3}	2.5×10^{-3}	3.95×10^{-3}	-5.0×10^{-5}	1.3
1×10^{-3}	2.0×10^{-4}	1.02×10^{-3}	$+2.0 \times 10^{-5}$	2.0
6×10^{-4}	2.0×10^{-4}	5.82×10^{-4}	-1.8×10^{-5}	3.0

Preparation and measurement of a synthetic standard solution

Method I. A small amount of lead tetraacetate was weighed accurately and dissolved in about 50 ml of benzene (**Caution**—Benzene is a highly toxic substance and appropriate precautions should be taken) and the solution was quantitatively transferred into a 250-ml long-necked, round-bottomed flask. A 50-ml volume of octane and a 50-ml volume of 35% hydrochloric acid were added to the solution, a double condenser was fitted and the mixture was boiled under reflux for 45 min. The flask was then disconnected and the solution was transferred quantitatively into a separating funnel, the aqueous layer was collected in a beaker and the oily layer was returned to the flask and extracted twice with 10 ml of distilled water. The total extracted solution was boiled to expel the excess of the acid until the volume of the solution was reduced to about 10 ml. This was then cooled and quantitatively transferred into a 100-ml calibrated flask, 40 ml of methanol were added to the solution, the volume was made up to the mark with distilled water and the procedure was continued as before.

The results for seven synthetic standards in which the masses of lead tetraacetate ranged between 4.434×10^{-1} and 4.433×10^{-4} g are listed in Table 2. This method was applied to the determination of lead in petroleum.[7] A 100-ml sample of crude oil, or 100 ml of each of its fractions, was taken and the procedure was followed exactly as before; except for crude

* Presented at SAC 83, the 6th International Conference on Analytical Chemistry, Edinburgh, UK, 17–23 July, 1983.

Table 2. Summary of the results for the determination of lead in synthetic standard samples by method I

Theoretical concentration of lead/ mmol per 100 ml	Concentration of titrant/M	Concentration of lead found/mmol per 100 ml	Standard deviation/ mmol per 100 ml	Relative standard deviation, %	Absolute error/ mmol per 100 ml	Error, %
1.0	2.5×10^{-1}	1.03	5.744×10^{-3}	0.560	$+3.0 \times 10^{-2}$	3.0
		1.03			$+3.0 \times 10^{-2}$	3.0
		1.02			$+2.0 \times 10^{-2}$	2.0
		1.02			$+2.0 \times 10^{-2}$	2.0
5.0×10^{-1}	2.5×10^{-1}	4.93×10^{-1}	2.362×10^{-3}	0.477	-7.0×10^{-3}	1.4
		4.98×10^{-1}			-2.0×10^{-3}	0.4
		4.95×10^{-1}			-5.0×10^{-3}	1.0
		4.93×10^{-1}			-7.0×10^{-3}	1.4
1.0×10^{-1}	2.5×10^{-2}	1.01×10^{-1}	4.966×10^{-4}	0.490	$+1.0 \times 10^{-3}$	1.0
		1.02×10^{-1}			$+2.0 \times 10^{-3}$	2.0
		1.01×10^{-1}			$+1.0 \times 10^{-3}$	1.0
		1.01×10^{-1}			$+1.0 \times 10^{-3}$	1.0
5.0×10^{-2}	2.5×10^{-2}	5.08×10^{-2}	1.153×10^{-4}	0.227	$+8.0 \times 10^{-4}$	1.6
		5.10×10^{-2}			$+1.0 \times 10^{-4}$	2.0
		5.08×10^{-2}			$+8.0 \times 10^{-4}$	1.6
		5.10×10^{-2}			$+1.0 \times 10^{-4}$	2.0
9.12×10^{-3}	2.5×10^{-3}	9.00×10^{-3}	2.061×10^{-5}	0.229	-1.2×10^{-4}	1.3
		9.00×10^{-3}			-1.2×10^{-4}	1.3
		8.98×10^{-3}			-1.4×10^{-4}	1.5
		9.03×10^{-3}			-0.9×10^{-4}	1.0
5.0×10^{-3}	2.6×10^{-3}	5.08×10^{-3}	4.082×10^{-5}	0.804	$+8.0 \times 10^{-5}$	1.6
		5.13×10^{-3}			$+1.3 \times 10^{-4}$	2.6
		5.08×10^{-3}			$+8.0 \times 10^{-5}$	1.6
		5.03×10^{-3}			$+3.0 \times 10^{-5}$	0.5
1.0×10^{-3}	2.0×10^{-4}	9.76×10^{-4}	4.159×10^{-6}	0.427	-2.4×10^{-5}	2.4
		9.70×10^{-4}			-3.0×10^{-5}	3.0
		9.80×10^{-4}			-2.0×10^{-5}	2.0
		9.74×10^{-4}			-2.6×10^{-5}	2.6

Table 3. Summary of the results for the determination of lead in petroleum and its fractions before and after treatment by method I

Fraction	Lead determined directly, % *m/m*	Lead determined by standard additions, % *m/m*	Standard deviation, % *m/m*	Relative standard deviation, %
Light naphtha	Undetectable	2.63×10^{-4}	1.850×10^{-5}	6.62
		2.64×10^{-4}		
		2.97×10^{-4}		
		2.94×10^{-4}		
Heavy naphtha	Undetectable	3.69×10^{-4}	2.166×10^{-5}	6.29
		3.32×10^{-4}		
		3.31×10^{-4}		
Kerosene	Undetectable	2.18×10^{-4}	1.414×10^{-5}	6.20
		2.49×10^{-4}		
		2.23×10^{-4}		
		2.22×10^{-4}		
Gas oil	Undetectable	Undetectable	—	—
Treater outlet	Undetectable	Undetectable	—	—
Reformate	Undetectable	9.22×10^{-4}	2.973×10^{-5}	3.10
		9.75×10^{-4}		
		9.46×10^{-4}		
		9.96×10^{-4}		
Hydrotreater kerosene	Undetectable	3.02×10^{-4}	1.182×10^{-5}	4.15
		2.76×10^{-4}		
		2.80×10^{-4}		
		2.80×10^{-4}		
Premium gasoline without tetraethyllead	Undetectable	4.12×10^{-4}	1.650×10^{-5}	4.15
		4.06×10^{-4}		
		3.76×10^{-4}		
		4.06×10^{-4}		
Super gasoline without tetraethyllead	Undetectable	7.15×10^{-4}	2.031×10^{-5}	2.93
		6.96×10^{-4}		
		6.66×10^{-4}		
		6.97×10^{-4}		
Premium gasoline with tetraethyllead	11.60×10^{-2}	11.67×10^{-2}	3.125×10^{-4}	0.269
	11.62×10^{-2}	11.58×10^{-2}		
	11.64×10^{-2}	11.62×10^{-2}		

Table 3. *Continued*

Fraction	Lead determined directly, % *m/m*	Lead determined by standard additions, % *m/m*	Standard deviation, % *m/m*	Relative standard deviation, % *m/m*
Super gasoline with tetraethyllead	11.64×10^{-2}	11.62×10^{-2}	1.0×10^{-4}	8.60×10^{-2}
	11.62×10^{-2}	11.63×10^{-2}		
	11.62×10^{-2}	11.62×10^{-2}		
Crude oil	2.608×10^{-3}	2.627×10^{-3}	4.681×10^{-5}	1.78
	2.602×10^{-3}	2.593×10^{-3}		
	2.614×10^{-3}	2.720×10^{-3}		

Table 4. Summary of the results for the determination of lead in synthetic standard samples by method II

Theoretical concentration of lead/mmol per 100 ml	Concentration of titrant/M	Concentration of lead found/mmol per 100 ml	Standard deviation/ mmol per 100 ml	Relative standard deviation, %	Absolute error/ mmol per 100 ml	Error, %
3.0	5.0×10^{-1}	3.10	4.966×10^{-3}	0.160	$+1.0 \times 10^{-1}$	3.3
		3.10			$+1.0 \times 10^{-1}$	3.3
		3.10			$+1.0 \times 10^{-1}$	3.3
		3.11			$+1.1 \times 10^{-1}$	3.7
8.0×10^{-1}	2.0×10^{-1}	7.80×10^{-1}	2.580×10^{-3}	0.331	-2.0×10^{-2}	2.5
		7.82×10^{-1}			-1.8×10^{-2}	2.3
		7.78×10^{-1}			-2.2×10^{-2}	2.8
		7.84×10^{-1}			-1.6×10^{-2}	2.0
3.0×10^{-1}	5.0×10^{-2}	3.06×10^{-1}	8.165×10^{-4}	0.266	$+6.0 \times 10^{-3}$	2.0
		3.06×10^{-1}			$+6.0 \times 10^{-3}$	2.0
		3.05×10^{-1}			$+5.0 \times 10^{-3}$	1.7
		3.07×10^{-1}			$+7.0 \times 10^{-3}$	2.3
8.0×10^{-2}	2.0×10^{-2}	8.10×10^{-2}	2.082×10^{-4}	0.257	$+1.0 \times 10^{-3}$	1.3
		8.14×10^{-2}			$+1.4 \times 10^{-3}$	1.8
		8.06×10^{-2}			$+0.6 \times 10^{-3}$	0.8
		8.10×10^{-2}			$+1.0 \times 10^{-3}$	1.3
3.0×10^{-2}	5.0×10^{-2}	2.98×10^{-2}	1.291×10^{-4}	0.434	-2.0×10^{-4}	0.7
		2.96×10^{-2}			-4.0×10^{-4}	1.3
		2.99×10^{-2}			-1.0×10^{-4}	0.3
		2.97×10^{-2}			-3.0×10^{-4}	1.0
7.9×10^{-3}	2.5×10^{-3}	8.00×10^{-3}	2.041×10^{-5}	0.255	$+1.0 \times 10^{-4}$	1.3
		8.02×10^{-3}			$+1.2 \times 10^{-4}$	1.5
		8.00×10^{-3}			$+1.0 \times 10^{-4}$	1.3
		7.98×10^{-3}			$+7.5 \times 10^{-4}$	1.0
3.0×10^{-3}	5.0×10^{-4}	2.95×10^{-3}	8.539×10^{-5}	0.417	-5.0×10^{-5}	1.7
		2.96×10^{-3}			-4.0×10^{-5}	1.3
		2.95×10^{-3}			-5.0×10^{-5}	1.7
		2.94×10^{-3}			-6.0×10^{-5}	2.0
8.0×10^{-4}	2.0×10^{-4}	8.18×10^{-4}	3.416×10^{-6}	0.417	$+1.8 \times 10^{-5}$	2.3
		8.14×10^{-4}			$+1.4 \times 10^{-5}$	1.8
		8.20×10^{-4}			$+2.0 \times 10^{-5}$	2.5
		8.22×10^{-4}			$+2.2 \times 10^{-5}$	2.8

oil it was necessary to add 50 ml of benzene as solvent. The results are shown in Table 3.

Method II. A sample containing a known amount of lead was digested in a micro-Kjeldhal flask with 0.4 ml of 65% nitric acid with the addition of 0.3 ml of 30% hydrogen peroxide and finally 0.4 ml of 70% perchloric acid. the flask was fitted with a double condenser and the mixture was digested under reflux for 45 min. After the mineralisation was complete the digest was allowed to cool, diluted with 10 ml of distilled water and boiled vigorously for 3 min to drive off any oxidising gases present that cause suppression of the electrode response. After cooling, the solution was transferred into a 250-ml beaker and the flask was rinsed with distilled water, 40 ml of methanol were added to the solution and the volume was made up to 100 ml. Further determination of lead in the solution was performed as described under *Method I.*

Eight synthetic standard solutions in which the mass of lead tetraacetate ranged between 3.547×10^{-4} and 1.330 g were prepared and determined by the same procedure. The results are shown in Table 4. This method was also applied to the determination of lead in crude oil and its fractions,[7] where 15 ml of the sample were used and the same procedure was followed. The mixture, after complete mineralisation and driving off the oxidising gases, was quantitatively transferred into a separating funnel, the aqueous layer was separated from the oily layer, 40 ml of methanol were added to the aqueous layer, the volume was made up to 100 ml and the solution was titrated as before. The results are listed in Table 5.

Discussion

The conditions for the quantitative conversion of organic lead compounds into lead chloride were carefully investigated; for method I these were selection of a suitable solvent, amount of acid added, temperature and time required for the reflux and removal of the excess of acid; and for method II proportion of nitric acid, hydrogen peroxide and perchloric acid in the mixture, length of time required for complete mineralisation and removal of the excess of oxidising agent. After optimising each of the conditions in turn, two simple procedures were developed.

The length of time required for the reflux for complete conversion of a given sample of lead tetraacetate containing

Table 5. Summary of the results for the determination of lead in petroleum and its fractions before and after treatment by method II

Fraction	Lead determined directly, % *m/m*	Lead determined by standard additions, % *m/m*	Standard deviation, % *m/m*	Relative standard deviation, %
Light naphtha	Undetectable	2.62×10^{-4}	1.431×10^{-5}	5.12
		2.76×10^{-4}		
		2.86×10^{-4}		
		2.95×10^{-4}		
Heavy naphtha	Undetectable	3.94×10^{-4}	2.311×10^{-5}	5.78
		4.21×10^{-4}		
		4.15×10^{-4}		
		3.70×10^{-4}		
Kerosene	Undetectable	2.06×10^{-4}	1.144×10^{-5}	5.36
		2.25×10^{-4}		
		2.02×10^{-4}		
		2.22×10^{-4}		
Gas oil	Undetectable	Undetectable	—	—
Treater outlet	Undetectable	Undetectable	—	—
Reformate	Undetectable	9.80×10^{-4}	3.919×10^{-5}	3.999
		9.32×10^{-4}		
		10.28×10^{-4}		
		9.80×10^{-4}		
Hydrotreater kerosene	Undetectable	2.52×10^{-4}	1.264×10^{-5}	4.696
		2.82×10^{-4}		
		2.71×10^{-4}		
		2.71×10^{-4}		
Premium gasoline without tetraethyllead	Undetectable	3.45×10^{-4}	1.304×10^{-5}	3.87
		3.37×10^{-4}		
		3.18×10^{-4}		
		3.45×10^{-4}		
Super gasoline without tetraethyllead	Undetectable	7.39×10^{-4}	2.476×10^{-5}	3.48
		6.79×10^{-4}		
		7.13×10^{-4}		
		7.13×10^{-4}		
Premium gasoline with tetraethyllead	11.60×10^{-2}	11.65×10^{-2}	4.283×10^{-4}	0.368
	11.67×10^{-2}	11.69×10^{-2}		
	11.63×10^{-2}	11.59×10^{-2}		
Super gasoline with tetraethyllead	11.60×10^{-2}	11.66×10^{-2}	2.323×10^{-4}	0.200
	11.65×10^{-2}	11.65×10^{-2}		
	11.63×10^{-2}	11.64×10^{-2}		
Crude oil	2.57×10^{-3}	2.52×10^{-3}	3.966×10^{-5}	1.55
	2.55×10^{-3}	2.63×10^{-3}		
	2.56×10^{-3}	2.53×10^{-3}		

1.89×10^{-3} g of lead into lead chloride was 45 min; longer reflux periods (60 and 90 min) for the same sample did not affect the results, but a shorter period (30 min) increased the percentage error from 1.32 to 4.1%.

A number of experiments were performed using 5×10^{-4} M lead nitrate solution and 2.5×10^{-2} M sodium molybdate dihydrate solution as the titrant with different concentrations of methanol (0, 10, 20, 30, 40, 50 and 60%). The errors were found to be 5, 4, 3, 2.5, 1.5, 2.5 and 3%, respectively, and therefore 40% methanol was used throughout this investigation. Further, it was necessary to adjust the pH of the solution to between 5 and 5.5 to ensure the insolubility of the precipitated lead molybdate. Blank experiments were run for methods I and II, and no lead could be detected by either the direct determination or standard additions method.

Sensitivity, Accuracy and Precision of the Potentiometric Measurements

The effect of the concentration of the titrant on the accuracy of the results was considered. The results in Table 1 show that the titration of 10^{-3} M lead nitrate solution with 2×10^{-4} M sodium molybdate dihydrate solution resulted in a 2% error and the titration of a similar sample of lead nitrate solution with a 2.5 $\times 10^{-3}$ M solution of the titrant increased the error to 2.5%. Also, the titration of a 6×10^{-6} M lead nitrate solution with a 2×10^{-4} M solution of the titrant resulted in a 3.0% error, but when a similar lead sample was titrated with a 10^{-4} M solution of titrant the error was increased to 5.0%.

Synthetic Standard

The results in Tables 2 and 4 show that the quantitative conversion of lead tetraacetate into lead chloride was performed successfully and that the amounts of lead recovered were in good agreement with the theoretical values.

Table 2 shows the results of method I, in which the amount of lead used ranged between 2.07×10^{-1} and 2.07×10^{-4} g per 100 ml, the average error ranged between 1.1 and 2.5% and the relative standard deviation did not exceed 0.8%. Table 4 shows the results of method II in which the amount of lead ranged between 6.22×10^{-1} and 1.66×10^{-4} g per 100 ml, the percentage error ranged between 0.8 and 3.4% and the relative standard deviation was not more than 0.42%. These results show that the two methods are similar with respect to sensitivity, accuracy and precision, although method II covers a wider range of concentration.

The results in Tables 3 and 5 show that the two methods were applied successfully to the determination of lead in crude oil and its fractions. The approximate limits of detection achieved directly for the different fractions of petroleum varied

from 2.56×10^{-3} % *m/m* in crude oil to 11.66×10^{-2} % *m/m* in premium and super gasoline with a relative standard deviation not exceeding ±1.8%. These results are in good agreement with the results obtained by the standard additions method (Tables 3 and 5). Further, Tables 3 and 5 show that the standard additions method was necessary to determine lower amounts of lead in petroleum successfully. The lowest amount of lead detected successfully was 2.69×10^{-4} % *m/m* in hydrotreater kerosene with a relative standard deviation not exceeding 4%.

References

1. ASTM Standard, D1269–61 (Reapproved 1968), Part 17, 1973, American Society for Testing and Materials, Philadelphia, PA, 1973, p.448.
2. ASTM Standard, D-3237-79, Part 25, American Society for Testing and Materials, Philadelphia, PA, 1979, p. 112.
3. ASTM Standard, D-3348-79, Part 25, American Society for Testing and Materials, Philadelphia, PA, 1979, p. 253.
4. ASTM Standard, D-3229-73 (Reapproved 1978), Part 25, American Society for Testing and Materials, Philadelphia, PA, 1980, p. 62.
5. "IP Standards for Petroleum and its Products," Part 1, Section 2, Institute of Petroleum, London, 1971, p. 1032.
6. Coker, D. T., *Anal. Chem.*, 1975, **47**, 386.
7. Issaq, N., *MSc Thesis,* University of Baghdad, 1983.

Paper A3/227
Received July 22nd, 1983
Accepted June 6th, 1984

Potentiometric Measurement of the Sodium Content of Sodium Amalgams

Artemio Gellera, Luciano Cavalli and Giancarlo Nucci
Chimica Augusta, Centro Ricerche, Via Reali 4, Paderno D., Milan, Italy

In the electrolysis cells of a chloro-alkali plant it is important to know the sodium concentration in the flowing amalgams in both the inlet and the outlet of the cell. At present the most commonly used technique for analysing these sodium amalgams is still based on an acid - base titration after reaction of a known amount of amalgam with 0.5 N HCl. This technique is both awkward and time consuming to apply accurately to all the electrolysis cells of a plant. Also, it causes serious environmental problems because of the sampling and treatment of amalgams. A few alternative methods have been suggested[1] but they are not in common use. In this paper we describe an electrode developed to measure the sodium concentration of flowing amalgams in an electrolysis cell. The system is already in routine use in some of our plants.

Keywords: *Sodium concentration measurement; potentiometry; sodium amalgams*

Principle of Operation

The sodium electrode, devised in our laboratories, is based on a potentiometric method that provides measurements of the potential of the following cell:

$$Na_o.Hg \mid NaCl\ (1\ M) \mid Ag_o - AgCl$$

the two possible reactions that can occur in each half-cell are as follows.
1st half-cell:

$$Na^+ + e^- \rightleftarrows Na_o.Hg$$

2nd half-cell:

$$AgCl + e^- \rightleftarrows Ag_o + Cl^-$$

The potential of a half-cell as a function of concentration is given by the Nernst equation.
1st half cell:

$$E_1 = E^o_{Na^+ \cdot Na_o.Hg} + 0.059\log[Na^+]$$

2nd half-cell:

$$E_2 = E^o_{Ag_o \cdot AgCl} - 0.059\log[Cl^-]$$

As the circuit is closed, the electrode works as a galvanic cell. The over-all potential, E_{cell}, is positive (the free-energy change is negative) and the spontaneous reactions that take place are the following.

$$(-)\ \text{oxidation: } Na_o \rightarrow Na^+ + e^-\ (E_1)$$

$$(+)\ \text{reduction: } AgCl + e^- \rightarrow Ag^o + Cl^-\ (E_2)$$

$$E_{cell} = E_2 - E_1 + E_L$$

At constant temperature and steady NaCl solution concentration, E_2 (reference potential) and E_L (inter-liquid potential) are constant. Consequently E_{cell} depends on the activity of sodium in the amalgams, namely on its concentration. On the base of laboratory experiments at 75 °C and with NaCl 1 M solutions, the E_{cell} range is approximately 2.0–2.2 V (ref. 2) for sodium concentrations in the amalgam of 0–0.8% *m/m*.

Calibration

Fig. 1 is a schematic diagram of the sodium electrode. The essential parts are an approximately 1 m long plastic tube carrying a porous polymer disc at one end, an approximately 200-ml capacity glass vessel tightly connected to the tube and filled with 1 M NaCl solution, an Ag_o - AgCl reference electrode soaked in the NaCl solution and an isolated wire lead ending with a circular naked Fe wire. The two pin connectors are joined through a millivolt reading device.

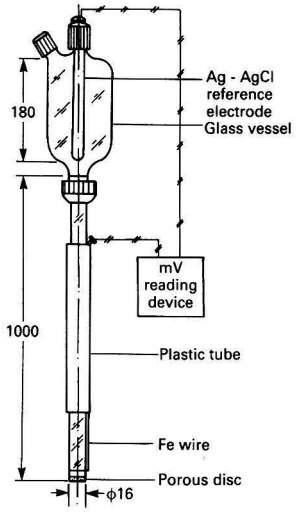

Fig. 1. Schematic diagram of the sodium detector

Table 1. Experimental data for calibration of the sodium electrode. Reference electrode, Ag - AgCl; amalgam temperature, 70 °C

Na concentration, %	Molar fraction of Na ($\times 10^3$)	Potential/mV
0.049	4.26	2060
0.082	7.11	2070
0.105	9.09	2078
0.131	11.32	2085
0.185	15.91	2100
0.228	19.55	2110
0.285	24.33	2120
0.345	29.32	2130
0.420	35.49	2141
0.500	42.0	2150
0.590	49.23	2161
0.635	52.81	2165

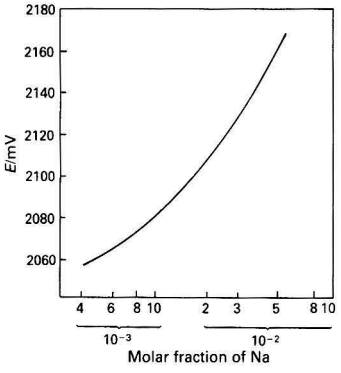

Fig. 2. Calibration graph for sodium amalgams at 70 °C

Using this electrode, a series of amalgams of known sodium concentration were analysed and the results are given in Table 1. Fig. 2 shows the corresponding experimental curve and it can be seen that it does not follow perfect Nernstian behaviour. With the help of a least-squares polynomial regression analysis, a theoretical expression was obtained that fitted well all the experimental points in the approximate sodium concentration range of 0–0.8% *m/m*.

The precision of the method in the above concentration range is about ± 0.005% absolute. The detection limit is about 0.0005% of sodium.

Applications

The millivolt reading detector was conveniently modified to give a battery-charged device, provided with a microprocessor and a small data printer in order to obtain direct sodium concentration readings. This arrangement makes the sodium electrode a useful hand-held device. Using this

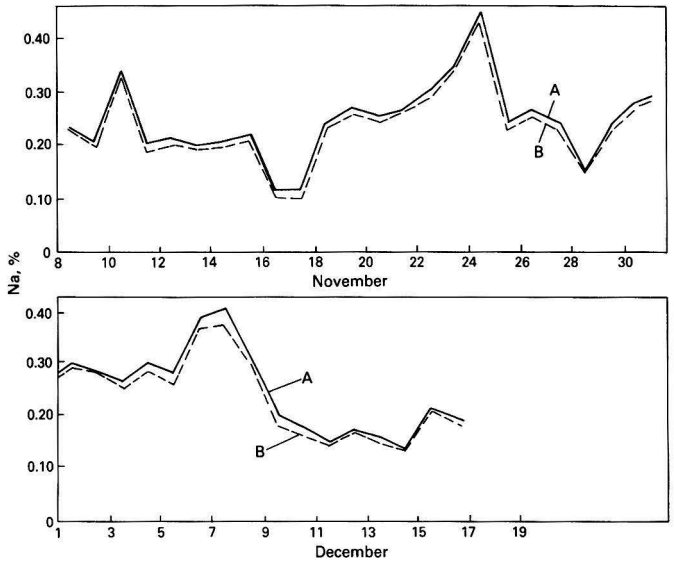

Fig. 3. Results for continuous sodium analysis in one electrolysis cell for about 40 d during November and December. Results obtained (A) electrochemically and (B) by acid - base titration

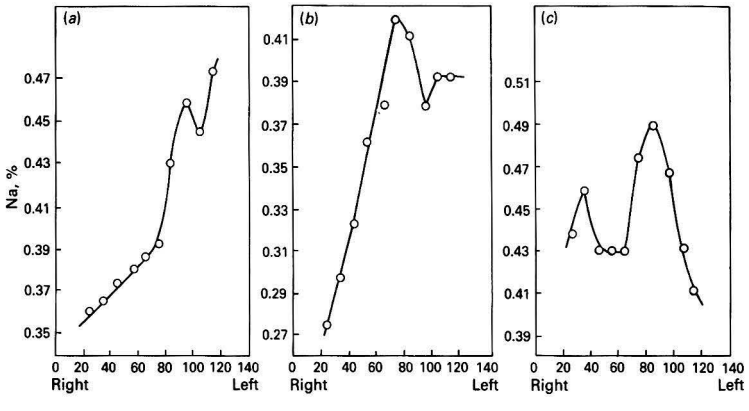

Fig. 4. Sodium concentration patterns of three different electrolysis cells, (*a*), (*b*) and (*c*). The *x* axis is the amalgam front of the cell outlet in cm, right and left referring to the flowing amalgam

electrochemical system we have already carried out extended experiments in the field. Fig. 3 is an example of continuous sodium analysis in one electrolysis cell for *ca.* 40 d. Good agreement between acid - base titration and electrochemical analysis was found. The greatest advantage of the sodium electrode, in addition to routine analysis of amalgams for sodium, is the possibility of performing instant spot checks of the sodium concentration along the front of the amalgams in both the inlet and the outlet of the electrolysis cell. The measurement in the outlet gives a rapid indication of the performance of the electrolysis cell and the measurement in the inlet shows whether the amalgam decomposer is working properly.

These measurements can be performed without mercury sampling, shortening the working time in the cell area. Thirty cells can easily be analysed in 20 min by one operator. A further advantage of the electrochemical system is the possibility of establishing readily whether there are differences in sodium concentration in the front of the amalgams. Fig. 4 shows typical concentration patterns of some cells. These patterns are useful for understanding the working conditions of the cell and make it possible to perform timely cell maintenance.

The sodium electrode as described is a hand-held device, but if properly modified it can also be adapted for continuous process control.

We thank Professor L. Formaro of Milan University for assisting in the work and for fruitful discussion.

References

1. Klotz, H., *Chem.-Ing.-Tech.*, 1980, **52**, 444.
2. Mussini, T., Longhi, P., *Chim. Ind. (Milan)*, 1977, **59**, 163.

Paper A4/2
Received January 4th, 1984
Accepted June 6th, 1984

Automatic Potentiometric Micro-determination of Basic Nitrogen in Organic Compounds

Agostino Pietrogrande, Alfredo Guerrato, Bruno Bortoletti and Gabriella Dalla Fini
Department of Pharmaceutical Sciences, University of Padua, 35131 Padua, Italy

Basic nitrogen is determined at the milligram level by potentiometric titration in a non-aqueous medium. Acetic acid is a suitable solvent for substances with very different structures, except from some amino acids that are soluble in perchloric acid and may therefore be determined by back-titration. The behaviour of some organic nitrogen compounds that do not exhibit a basic character because of a resonance phenomena, contrary to what is expected, is also explained. Titration graphs with sharp inflection points allow exact determinations for all the compounds examined.

Keywords: *Potentiometric micro-determination; basic organic nitrogen*

Among the different determinations in elemental organic analysis, that of basic nitrogen is particularly interesting owing to the frequent presence of amino groups, heterocyclic nitrogen, etc., in organic molecules.

In this work we investigated the limits that characterise the micro-scale determination of organic nitrogen in organic substances with very varied structures by non-aqueous potentiometry. Some studies on the macro-scale have been published.[1–4] Keen and Fritz[5] described micro-determinations, but their investigation was incomplete because of the small number of compounds considered and because it was limited to the primary amino group.

Experimental and Results

The titrations were carried out employing a Metrohm Model 636 Titroprocessor, connected to a Model 635 automatic burette and to an EA 120 combined glass pH electrode. This equipment allows the rapid evaluation of titration curves, which are printed out automatically. By pre-selecting "kinetic T" in the operating programme, it is possible to determine the time range for the delivery of titrating solution. With position 1 of this setting, the 5-s frequency allows one to perform the titration in only a few minutes.

First trials were performed on 5–7 mg of substances with simple aliphatic and aromatic structures, containing a primary amino group, such as D,L-alanine, 4-nitroaniline and aminophenones. The samples were dissolved in acetic acid, the optimum volume of which was found to be 30 ml, and then titrated with 0.01 N perchloric acid. The precise results obtained in acetic acid for the listed compounds (Table 1) allowed us to investigate whether it is possible to generalise the use of this solvent to determine basic nitrogen on other substances with more complex and diverse structures.

In this connection, we thought that the small amounts of the weighed samples would allow the solubilisation of compounds that are poorly soluble in acetic acid. Further, it seemed that under the operating conditions used we could add a few drops of acetic anhydride to the solution being titrated in order to remove any water present, without the risk of adverse effects due to the strong reactivity of this compound (acetylation).

The analytical data obtained in this way met our expectations. The very precise results (average standard deviation 0.07%) are listed in Table 1. The titration volumes are between 1.5 and 4.0 ml of 0.01 N perchloric acid and the potential values are between 300 and 600 mV. Titration curves are shown in Fig. 1(*a*) and (*b*).

Some amino acids, such as L-tyrosine, L-tryptophan and L-glutamic acid, are insoluble in acetic acid, even in amounts smaller than those chosen for other samples. In these instances we followed the procedure of Ciampa *et al.*,[4] in which the substance is dissolved in perchloric acid, the excess of which is back-titrated with sodium acetate. The results are given in Table 2 (average standard deviation 0.11%).

Procedure

Dissolve 5–7 mg of sample in 30 ml of anhydrous acetic acid, stirring electromagnetically. If the substance is a hydro-

Table 1. Determination of basic nitrogen in compounds with different structures

Compound	Basic N calculated, %	Standard deviation, %	Compound	Basic N calculated, %	Standard deviation, %
Allopurinol	10.28	0.10	Levamisole.HCl	5.81	0.08
2-Amino-5-chlorobenzophenone	6.07	0.02	Lorazepam	4.36	0.09
2-Amino-2′,5-dichlorobenzophenone	5.26	0.04	Medazepam	5.17	0.03
2-Amino-5-chloro-2′-fluorobenzophenone	5.61	0.03	Metrodinazole	8.18	0.01
Bromazepam	4.43	0.11	Nitrazepam	4.93	0.06
Chlordiazepoxide base	4.67	0.01	Nitrimidazine	12.38	0.11
Chlordiazepoxide.HCl	4.16	0.06	4-Nitroaniline	10.14	0.04
Clomiphene citrate	2.37	0.04	Oxazepam	4.89	0.08
Clotrimazole	4.06	0.05	Pentazocine base	4.90	0.04
Diazepam	4.92	0.07	Temazepam	4.66	0.05
Dimetridazole	9.92	0.12	Tetramisole.HCl	5.81	0.15
Flunitrazepam	4.47	0.04	Trimetoprim	4.82	0.06
Flurazepam.2HCl	6.08	0.04	3,4,5-Trimethoxyaniline	7.65	0.08
Furaltadone base	4.32	0.06			

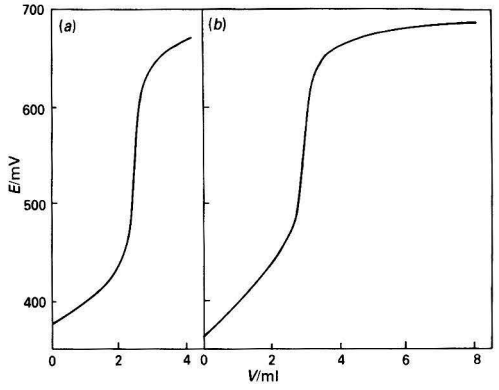

Fig. 1. Titration of micro-amounts of (*a*) diazepam and (*b*) trimetoprim with 0.01 N perchloric acid

Table 2. Determination of basic nitrogen in amino acids

Compound	Basic N calculated, %	Standard deviation, %
D,L-Alanine	15.71	0.12
4-Aminobenzoic acid	10.21	0.07
L-Arginine	16.07	0.12
L-Glutamic acid*	9.52	0.11
L-Histidine	18.05	0.15
L-Leucine	10.67	0.08
D,L-Methionine	9.38	0.12
D,L-Phenylalanine	8.48	0.08
L-Tyrosine*	7.73	0.16
L-Tryptophan*	6.86	0.14

* Insoluble in acetic acid.

chloride, use 25 ml of acetic acid and 5 ml of a 10% solution of mercury(II) acetate in acetic acid.

Dissolve amino acids that are insoluble in acetic acid in an accurately measured volume of 0.01 N perchloric acid (5–6 ml), then dilute the solution to 30 ml with acetic acid.

Before titration, in all instances add three drops of acetic anhydride.

Insert the first "control card" (calculation), giving the mass in milligrams, then the analytical factor, multiplied by the titre. Insert the second "control card" (operation), programmed for "dynamic titration," "kinetic *T*, value 1" (increase in volume every 5 s).

Insert the electrode, taking care that the tip remains a few millimetres above the stirring bar. Start the automatic titration with 0.01 N perchloric acid in anhydrous acetic acid. Stop the titration and stirring after the end-point. The percentages of basic nitrogen are printed with the curves together with volumes (ml) and differences in potential (mV).

Perform the back-titration of perchloric acid that has dissolved the amino acids that are insoluble in acetic acid with 0.01 N sodium acetate solution. Prepare the solution by dissolving the required amount of sodium carbonate in anhydrous acetic acid.

To standardise the perchloric acid solution dissolve 5–7 mg of potassium hydrogen phthalate in 30 ml of anhydrous acetic acid and titrate following the procedure described above.

Discussion

We tested substances with very different structures, but apart from two instances (flurazepam, nitrimidazine) only one of the nitrogen atoms could be titrated in compounds that contained two or more. In order to interpret the limits of this determination we have also tried to explain the interaction between perchloric acid and the nitrogen atoms. As a knowledge of the pK_h values of the different nitrogen atoms does not allow one to establish which nitrogen atom is really involved in the protonation, our explanation is only qualitative.

Titration of the 2-aminobenzophenones is very exact, as shown in Table 1. Benzodiazepines of general formula

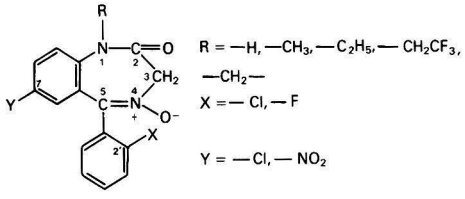

in contrast, cannot be titrated and therefore we can infer that none of the nitrogen atoms is basic enough to undergo the proton attack, with the exception of chlordiazepoxide, which contains two nitrogen atoms that form an amidine system.

Titration curves with sharp and reproducible inflection points can nevertheless be obtained, as shown in Fig. 1, by benzodiazepines of the type

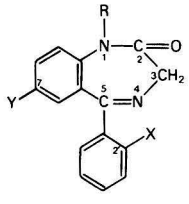

where R, X and Y have the same meaning as above, and with 1,5-benzodiazepines (medazepam). It follows that the nitrogen in position 4 can be protonated, as it provides a pair of unshared electrons, whereas the basicity of that in position 1 appears to be lowered by the inductive and mesomeric effects of the adjacent carbonyl group. Electron-withdrawing effects are also expected to be exerted by the groups in position 7 and by the imine nitrogen in position 4, that is at the end of a mesomeric system of conjugated double bonds; in other words, the nitrogen in position 1 cannot be protonated because of these two factors negatively affecting its electron availability.

In bromazepam the basicity is spread on the two nitrogen atoms in position 4 and in position 2′ of the heterocylic ring; the protonation of one of them will involve the whole mesomeric system. In flurazepam two nitrogen atoms can be protonated: that in position 4 and that in the side-chain.

Some other benzodiazepines contain a hydroxy group in position 3, such as lorazepam, oxazepam and temazepam. Titration of these compounds gives curves with less sharp inflection points than those described above. This result can probably be ascribed to the lower basicity of the nitrogen in position 4, owing to the inductive effect of the oxygen atom in position 3.

The effects discussed above are valid for other compounds with two or more nitrogen atoms such as levamisole, tetramisole, allopurinol, trimetoprim and amino acids. Fig. 1(*b*) shows the curve obtained in the titration of trimetoprim.

In nitroimidazoles, such as dimetridazole, metronidazole and nitrimidazine, the basicity is lowered because of the

presence of the nitro group. In nitrimidazine two nitrogen atoms can be determined: the morpholinic nitrogen and that in the imidazole ring. Among nitrofurans, furaltadone is interesting, as only the morpholine nitrogen is very basic and therefore protonatable. The other nitrogen atoms do not seem to be basic enough to be protonated, as they are bound to strongly electron-withdrawing groups.

Conclusion

Micro-amounts of many organic substances containing basic nitrogen in different forms may be titrated in anhydrous acetic acid with a solution of perchloric acid in acetic acid with very precise results. Under the experimental conditions used we observed the following behaviour: amide nitrogens are not protonated, even if the atom is linked to an alkyl group that increases its basicity; in substituted amidines, only one nitrogen atom is titrated; aromatic imine nitrogens are sufficiently basic to undergo proton attack; nitrogen atoms taking part in an inductive conjugative organic system behave as though only one atom is involved in the titration; and the titration curves of the different substances exhibit inflection points that are sharp enough for the exact percentage of the protonated nitrogen atoms to be calculated.

References

1. Wagner, C. D., Brown, R. H., and Peters, E., *J. Am. Chem. Soc.*, 1947, **69**, 2609.
2. Kleckner, L. J., and Osol, A., *J. Am. Pharm. Assoc., Sci. Ed.*, 1952, **61**, 573.
3. Fritz, J. S., *Anal. Chem.*, 1952, **24**, 672.
4. Ciampa, G., Grieco, C., and Silipo, C., *Farmaco, Ed. Prat.*, 1976, **22**, 70.
5. Keen, R. T., and Fritz, J. S., *Anal. Chem.*, 1952, **24**, 564.

Paper A4/190
Received May 25th, 1984
Accepted July 16th, 1984

Differential-pulse Polarographic Determination of Nitrite

Sadallah T. Sulaiman and Banan A. Akrawi
Department of Chemistry, College of Science, University of Mosul, Mosul, Iraq

A simple, sensitive and rapid method based on the application of the differential - pulse polarography of the diazonium salts of *o*-, *m*- and *p*-aminobenzoic acid for the determination of trace amounts of nitrite is described. The reagents required are readily available and non-toxic. The detection limits using the *o*-, *m*- and *p*-aminobenzoic acids were 0.87×10^{-7}, 1.73×10^{-7} and 4.30×10^{-7} M, respectively, with relative standard deviations of between 9 and 10%.

Keywords: *Differential-pulse polarography; nitrite determination;* o-, m- *and* p-*aminobenzoic acid diazotisation*

The nitrite ion plays an important role as a precursor in the formation of *N*-nitrosamines, many of which have been shown to be potent carcinogens,[1,2] and in view of increasing interest in the quality of various materials and the purity of sewage effluents a sensitive, rapid and accurate procedure for the trace determination of nitrite is desirable.

Several methods have been proposed for the microdetermination of nitrite. Spectrophotometric methods[3,4] have limited sensitivity and most of them depend on unstable colours and are time consuming. The application of polarography to the determination of nitrite has been reported.[5,6] The direct polarographic measurement of nitrous acid has a detection limit of 0.5 p.p.m.[5] The differential-pulse polarographic method for the indirect determination of nitrite reported by Chang *et al.*[6] involves the quantitative reaction of nitrite with diphenylamine to yield diphenylnitrosamine (DPN). Although this method is sensitive (the detection limit is 4.6 p.p.b.), DPN is toxic and may be carcinogenic.

We propose here a simple, sensitive and rapid method based on the application of the differential-pulse polarography of the diazonium salts of *o*-, *m*- and *p*-aminobenzoic acid for the trace determination of the nitrite ion.

Experimental

Apparatus

Differential-pulse polarograms were determined using a Metrohm Polarecord E506 in conjunction with an E505 polarography stand equipped with a mechanical drop timer.

A three-electrode system was used, the working electrode being a dropping-mercury electrode (DME), the reference electrode Ag - AgCl, KCl with a ceramic liquid junction and the counter electrode a platinum wire. Except when stated otherwise, a 2-s drop time and a pulse magnitude of 100 mV were used throughout and the scan rate was 5 mV s^{-1}. All polarographic measurements were carried out at room temperature (25 °C). The solution was de-aerated by passing through it a slow stream of helium for 15 min. All pH measurements were made by using a Sargent Welch Model NX pH meter.

Reagents

Unless stated otherwise, all reagents were of anlaytical-reagent grade and triply distilled, de-ionised water was used.

Nitrite solutions. Dilute solutions of nitrite were prepared from a 2.17×10^{-3} M (100 μg ml^{-1}) stock solution of $NaNO_2$ by appropriate quantitative dilution or by direct pipetting into samples.

Aminobenzoic acid solutions. Standard solutions (10^{-2} M) of *o*-, *m*- and *p*-aminobenzoic acid were prepared in 1 N HCl.

Buffer solutions. The modified universal series of Britton - Robinson buffers were used as supporting electrolytes and prepared as described by Britton.[7]

Procedure

A differential-pulse polarogram was run on a de-aerated solution (25 ml) containing an excess (2.0 ml) of a 10^{-2} M solution of either *o*-, *m*- or *p*-aminobenzoic acid, Britton - Robinson buffer (5 ml for *o*- and 2.5 ml for *m*- and *p*-aminobenzoic acid) and 1 N HCl (2.5 ml for *m*- and *p*-aminobenzoic acid). The pH of this solution was measured and found to be about 1.4, and the background current was recorded. To this solution was added a certain amount of sodium nitrite, the polarogram was recorded again and the

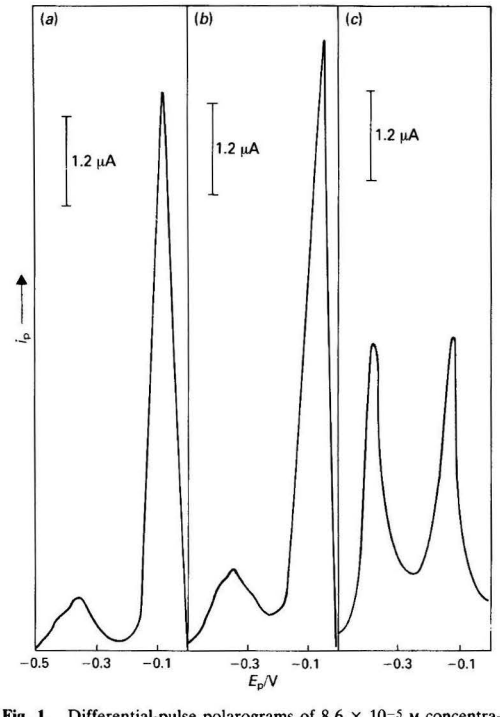

Fig. 1. Differential-pulse polarograms of 8.6×10^{-5} M concentrations of (*a*) DMABA, (*b*) DPABA and (*c*) DOABA in Britton - Robinson buffer at pH 1.4

Table 1. Effect of pH on differential-pulse peaks and peak currents of DOABA, DPABA and DMABA

	DOABA				DPABA				DMABA			
pH	E_{p1}/ V	I_{p1}/ 10^{-2} μA	E_{p2}/ V	I_{p2}/ 10^{-2} μA	E_{p1}/ V	I_{p1}/ 10^{-2} μA	E_{p2}/ V	I_{p2}/ 10^{-2} μA	E_{p1}/ V	I_{p1}/ 10^{-2} μA	E_{p2}/ V	I_{p2}/ 10^{-2} μA
1.4	0.13	53.0	0.37	46.0	0.07	99.60	0.36	12.3	0.07	100.8	0.36	11.4
1.7	0.10	51.1	0.38	47.2	0.06	97.80	0.36	12.3	0.06	99.0	0.36	10.8
2.1	0.06	89.0	0.42	54.6	0.03	144	0.36	10.0	0.03	114.0	0.36	9.6
3.3	0.06	86.3	0.46	15.5	0.10	130	0.38	6.1	0.05	27.6	0.34	3.6
4.1	0.03	38.2	0.42	V. small	—	—	—	—	—	—	0.34	2.1

Table 2. Effect of time on differential-pulse peaks and peak currents of DOABA, DPABA and DMABA

	DOABA				DPABA				DMABA			
Time/h	E_{p1}/ V	I_{p1}/ 10^{-2} μA	E_{p2}/ V	I_{p2}/ 10^{-2} μA	E_{p1}/ V	I_{p1}/ 10^{-2} μA	E_{p2}/ V	I_{p2}/ 10^{-2} μA	E_{p1}/ V	I_{p1}/ 10^{-2} μA	E_{p2}/ V	I_{p2}/ 10^{-2} μA
0.33	0.05	112.0	0.39	41.4	0.06	106.2	0.36	10.2	0.07	100.8	0.36	11.4
0.50	0.05	108.0	0.39	40.0	0.06	105.0	0.36	10.2	0.07	103.8	0.35	11.4
0.67	0.06	107.3	0.39	40.0	0.06	105.0	0.36	10.2	0.07	104.6	0.35	11.5
0.83	0.06	105.3	0.39	39.0	0.06	105.0	0.36	10.2	0.07	105.3	0.35	11.7
1.30	0.06	105.4	0.39	39.0	0.07	104.4	0.36	10.2	0.07	106.8	0.35	12.0
2.42	0.06	105.4	0.39	39.0	0.07	106.2	0.36	10.2	0.07	110.4	0.35	12.0
3.42	0.06	105.4	0.39	39.0	0.07	106.2	0.36	10.2	0.07	110.4	0.35	12.0
Overnight	0.08	66.2	0.34	23.1	0.09	63.0	0.32	6.6	0.10	61.8	0.31	7.8

Table 3. Determination of nitrite in solutions of known concentration; I_p(corr.) = I_p (sample) − I_p (blank)

	DCABA		DMABA:	DPABA:
Nitrite concentration/ 10^{-6} M	I_{p1}(corr.)/ 10^{-2} μA	I_{p2}(corr.)/ 10^{-2} μA	I_{p1}(corr.)/ 10^{-2} μA	I_{p1}(corr.)/ 10^{-2} μA
0.087	—		—	0.15
0.174	0.54		—	0.30
0.260	0.75		—	0.48
0.434	1.41		1.05	0.80
0.868	2.73		1.10	1.58
1.736	4.78		1.20	2.68
2.604	6.30		2.23	3.62
4.340	10.07		4.33	5.78
8.680	13.56		9.81	13.53
17.360	17.80		26.73	29.24
26.040	21.30		43.87	47.77
43.400	27.42	30.91	78.95	83.18
86.800	46.54	84.87	122.43	120.65

background current was subtracted from the current observed after addition of the sample, to give the value for the corrected current. Nitrite ion was then determined by the method of standard additions.

Results and Discussion

Typical differential-pulse polarograms for diazotised *o*-, *m*- and *p*-aminobenzoic acid are shown in Fig. 1. Diazotised *o*-aminobenzoic acid (DOABA) yielded two well defined reduction peaks of almost equal height. On the other hand, diazotised *m*- (DMABA) and *p*-aminobenzoic acid (DPABA) showed one well defined major peak and a small, poorly defined peak.

Both the peak potential (E_p) and the peak current (I_p) for the three diazotised products varied with pH (Table 1). Although at pH 2–2.1 a maximum peak current was obtained for all three compounds, the peak current was very sensitive and a small change in pH caused a large change in I_p. The optimum pH range was chosen as 1.4–1.7 because firstly, the peak currents were stable in this pH range, secondly, it was easy to prepare solutions in this pH range by the addition of HCl to Britton - Robinson solutions and finally, the diazotised products were found to be very stable in this pH range (see below).

Stability of Diazonium Salts

The differential-pulse polarograms of DOABA, DPABA and DMABA were recorded at different times (Table 2). It can be seen that the diazotised products were stable for more than 3 h in a solution containing a mixture of Britton - Robinson buffer and HCl as a supporting electrolyte (pH = 1.4).

Effect of Concentration

The differential-pulse polarograms were recorded separately at different concentrations of DOABA, DPABA and DMABA. The results obtained indicated that at low concentrations of the diazotised product (less than 1.2 p.p.m. with respect to nitrite), the peak current of the first peak only was proportional to the concentration and very good calibration graphs were obtained. On the other hand, at higher concentrations (above 2 p.p.m.), the second peak of DOABA was also proportional to concentration.

Interferences

The following ions were found not to interfere even if present at a concentration 50 times greater than that of the nitrite ion: Na^+, K^+, Co^{2+}, Ni^{2+}, NH_4^+, F^-, Cl^-, NO_3^-, $C_2O_4^{2-}$, PO_4^{3-}, BO_3^{3-} and CH_3COO^-. Cu^{2+}, Hg^{2+}, $S_2O_3^{2-}$ and all other ions that could reduce at the same peak potential as the diazotised amine did, however, interfere.

Trace Determination of Nitrite

The optimum conditions for the determination of nitrite in aqueous solution from the diazotisation of *o*-, *m*- and *p*-aminobenzoic acid were found to be pH 1.4 (with a mixture of Britton - Robinson buffer and HCl as the supporting electrolyte), pulse amplitude 100 mV and drop time 2 s. For the pulse amplitude and drop time, a series of experiments were performed using pulse amplitudes of 100, 80, 60, 40 and 20 mV and drop times of 0.6, 1.0, 1.4 and 2.0 s and the

maximum response for the diffusion current was obtained at a pulse amplitude of 100 mV and a drop time of 2 s.

The working ranges for nitrite determination were found to be 4 p.p.b.–2 p.p.m. (8.68×10^{-8}–4.34×10^{-5} M) from diazotisation of PABA, 8 p.p.b.–4 p.p.m. (1.74×10^{-7}–8.68×10^{-5} M) from diazotisation of OABA (using two calibration graphs) and 20 p.p.b.–4 p.p.m. (4.34×10^{-7}–8.68×10^{-5} M) from diazotisation of MABA. Some typical results for simple aqueous solutions are given in Table 3. This table shows the results of the application of the differential-pulse method to a series of known nitrite solutions, prepared by adding an appropriate aliquot of nitrite stock solution to 25 ml of reagent solution containing 10^{-2} M of either PABA, OABA or MABA and buffer solution at pH 1.4. The data appear to be good and peak currents are linearly related to concentration. The detection limits were 0.87×10^{-7}, 1.73×10^{-7} and 4.30×10^{-7} M, respectively, with relative standard deviations ranging between 9 and 10%, which is reasonable for such low concentrations.

Conclusion

From the results in Table 3, it seems clear that the diazotisation of *o*-, *m*- and *p*-aminobenzoic acid provides the basis for a sensitive and rapid analytical method for the determination of nitrite ion using differential-pulse polarography. The analysis time is short and the reagents required are readily available and non-toxic. The best results were obtained using the diazotisation of *p*-aminobenzoic acid.

References

1. Wolff, I. A., and Wasserman, A. E., *Science*, 1972, **177**, 15.
2. Choi, K. K., and Fung, K. W., *Analyst*, 1980, **105**, 241.
3. Szekely, E., *Talanta*, 1968, **15**, 795.
4. Flamerz, S., and Bashir, W. A., *Analyst*, 1981, **106**, 243.
5. "Application Brief N-1," Princeton Applied Research, Princeton, NJ, 1974.
6. Chang, S., Kozeniauskas, R., and Harrington, G. W., *Anal. Chem.*, 1977, **49**, 2272.
7. Britton, H. T. S., "Hydrogen Ions," Second Edition, Volume 1, Chapman and Hall, London, 1952, p. 362.

Paper A4/59
Received February 7th, 1984
Accepted May 24th, 1984

Characterisation and Application of an Oxygen Membrane Polarographic Detector in a Flow System for Studying Oxygen-evolving Reactions

Andrew Mills and Carl Lawrence
Department of Chemistry, University College of Swansea, Singleton Park, Swansea SA2 8PP, UK

A study has been made on the characteristics of an oxygen membrane polarographic detector (O_2-MPD) in a flow system, *i.e.*, a system in which an inert gas, such as N_2, is used to sweep out the O_2 from a reaction vessel to the detector. Over a wide range of carrier gas flow-rates (10–215 cm^3 min^{-1}) the response of the detector appeared to be fast enough ($t_{95\%}$ <1 min), accurate enough (±5%) and sensitive enough (P_{O_2} < 100 p.p.m.) toward injections of O_2 into the reaction vessel for the present applications. However, claims have been made for response times of less than 1 s and accuracies of ±0.01% for the metallised-membrane electrode, which, unlike the Clark electrode, was designed specifically for use in the gas phase. The detector response was also found to be proportional, over at least three orders of magnitude, to the volume of O_2 injected. A brief study of two well documented O_2-evolving systems (one chemical and one photochemical) yielded results that were in good agreement with those reported in the literature. The difficulties that arise when the oxygen is dissolved in a liquid, and the need for time for it to be transferred from solution to the gas phase, were examined and discussed.

Keywords: *Oxygen determination; flow system; membrane electrode; polarographic detector*

In recent years there has been a great deal of interest in aqueous photochemical and chemical systems capable of evolving O_2, particularly if the O_2 originates from water as it is this step that has proved difficult to achieve in the numerous attempts to photodissociate water into H_2O and O_2.[1] In much of this work gas chromatography has been used for the analysis of the head space above the aqueous O_2-evolving system of interest,[1,2] however, this technique is expensive and often not of a sufficient sensitivity (usually <1 μl).[2] In addition, the total amount of O_2 produced can prove difficult to determine, as this requires a knowledge of the amount of O_2 dissolved in the solution [and in order to determine this quantity either additional chromatography[3] or use of an oxygen-membrane polarographic detector (O_2-MPD)[4] would be necessary]. In order to overcome such problems and to obtain a continuous record of the total amount of O_2 produced many workers have turned to using an inert gas such as N_2 to flush continuously the O_2 from the solution to the detector. Obviously such "flow" systems are ideal for studying photochemical or chemical systems in which the O_2 generated can act as a quencher and/or undergo additional reactions.

The detector used with a flow system must be: (*a*) very sensitive, (*b*) fast in responding to rapid changes in O_2 concentration and (*c*) selective toward O_2. One type of detector often used is a zirconium oxide sensor,[5] however, it requires an operating temperature of 600–800 °C, and therefore care must be taken to remove possible interfering substances.[6] For example, oxidisable species such as NO, CO and H_2 can react with any O_2 present and so lead to lower O_2 readings than expected.[6] In contrast, a species such as RuO_4 or OsO_4 that decomposes at high temperatures to release O_2 could lead to O_2 readings that were higher than expected. Indeed, this latter effect may be responsible for the conflicting reports made by Grätzel and co-workers of a 100% yield of O_2 from a Ce^{4+} - $RuO_2.xH_2O$ system as measured with a ZrO_2-type sensor in a flow system,[7] compared with their more recent report[8] of only a 73% O_2 yield with, this time, a liquid N_2 cold trap incorporated into the detection system to remove any interfering substances. The discrepancy between these two O_2 yields may be due to RuO_4, which we have shown recently[1] to be produced by oxidation of $RuO_2.xH_2O$ by Ce^{4+}.

Another type of O_2 detector often employed in a flow system is the micro-fuel cell.[6,9] This detector is very sensitive (1 p.p.m.–100%), selective and stable; however, in most of the forms commercially available the gas stream has a long path to traverse over the electrode and a large rate of oxygen consumption per unit area; and as a result the carrier gas containing the O_2 must flow over the detector at a minimum rate (*e.g.*, for a Teledyne fuel cell $f_{min.} > ca.$ 100 cm^3 min^{-1}) in order to prevent a substantial depletion layer forming on the surface of the exposed membrane, which in turn would lead to low O_2 readings.

In general, in their commercial forms, both the ceramic oxide sensor and the micro-fuel cell are expensive (*i.e.*, more than £2000). In contrast the O_2-MPD is a relatively cheap device (*e.g.*, less than £500 from Rank Bros., Cambridge) as well as being sensitive (10 p.p.m.–100%), selective, stable and insensitive to carrier gas flow-rate (as the depletion of the oxygen in the carrier gas flow is kept to a negligible level by the low permeability of the non-porous membrane and the short path of the flow over the relatively small electrode). Calzaferri and Sulzberger[10] have briefly described a flow system with an O_2-MPD that they used to study an O_2-evolving photochemical system. In this paper we investigate further characteristics and limitations of an O_2-MPD in such a flow system, before going on to use it to study two, well documented, O_2-evolving systems, one chemical, one photochemical.

Experimental

Apparatus

Flow system

The main components of the flow system used are shown in Fig. 1. A fine control of the N_2 flow-rate was achieved using an Edwards needle valve (Model LB1B) attached at the cylinder head. Flow-rates were measured with a calibrated flow meter (Glass Precision Engineering Ltd. Model RS1/C) incorporated in the line (see Fig. 1). The N_2 carrier gas flowed from the cylinder into the reaction vessel (a 125 cm^3 Pyrex Drechsel bottle, modified to receive a rubber septum) and then on to the O_2-MPD where any O_2 present could then be detected. Note that because the O_2-MPD measures partial pressure care has to be taken to keep the pressure of gas reaching the detector stable.

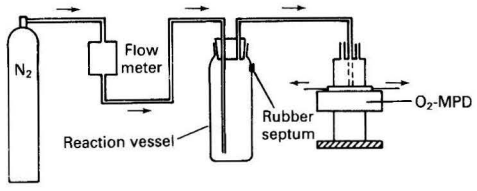

Fig. 1. Schematic diagram of the flow system. The arrows indicate the direction of carrier gas flow

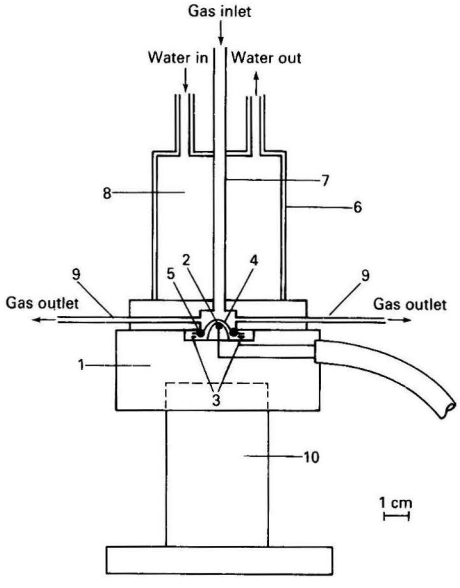

Fig. 2. Sectioned side view of the O_2-MPD used in the flow system. 1, Plastic base; 2, platinum disc working electrode (diameter 2 mm); 3, silver - silver chloride ring counter reference electrode; 4, PTFE membrane (12.5 μm); 5, silicone rubber O-ring; 6, plastic cell top; 7, stainless-steel tubing (~2 mm i.d.); 8, thermostated water jacket; 9, stainless-steel vents (~1 mm i.d.); and 10, Perspex stand

Oxygen membrane polarographic detector

The O_2-MPD (Fig. 2) consisted of a plastic base (1) (purchased from Rank Bros., Cambridge) containing both the Pt working electrode (2) and the Ag - AgCl counter electrode (3). Over these a PTFE membrane (4) (12.5 μm thick) was situated clamped firmly into position by the silicone rubber O-ring (5). This O-ring was held in position by the homemade cell top (6), which, in turn, was clamped to the base (1) by two spring-loaded clips (not shown on this diagram). The homemade Perspex cell top (6) consisted of a length of stainless-steel tubing (7) (2.0 mm i.d.), part of which was surrounded by a thermostated water jacket (8); this maintained the detector at a constant temperature (usually 25 ± 0.5 °C). The carrier gas from the reaction vessel flowed down the tubing (7) to the sensing electrode (2), and then vented to the atmosphere via two steel tubes (9) (1 mm i.d.) placed diametrically opposite each other. The O_2-MPD was usually placed on a plastic stand (10). A description of the principles of operation, electrochemical characteristics and the setting-up procedure for the O_2-MPD can be found elsewhere.[4] The constant polarising voltage of −0.7 V *versus* the Ag - AgCl counter reference electrode (3) applied at the Pt working electrode (2), and necessary for the operation of the O_2-MPD, was provided by a Metrohm potentiostat (Model E611). In this device the current produced by the O_2-MPD is converted into a voltage by means of an operational amplifier. The output of the O_2-MPD, in the form of a voltage, was recorded on a Servogor 210 *x/t* chart recorder. The O_2-MPD described here is now available from Rank Bros., Cambridge.

Reagents

All reagents used were of analytical-reagent grade and obtained from BDH Chemicals Ltd. The Ce^{4+} solutions employed were made up from ammonium cerium(IV) nitrate using 1 M H_2SO_4 as the solvent. Working solutions of H_2O_2 were prepared by dilution of a 20-volume standard solution with water.

Procedure Notes

The concentrations of all H_2O_2 solutions used were determined by titration with an appropriate standard Ce^{4+} solution, using ferroin as an indicator.[11] All irradiations were performed using the full output of a 250-W Xe arc lamp (Applied Photophysics Ltd.). In this latter work a quartz, thermostatically controlled (25 ± 0.5 °C) reaction vessel, similar in design to the cell top of an H_2-MPD described in a previous paper[12] (total volume *ca.* 38 cm^3), was used in the flow system in place of the Pyrex Dreschel bottle. Areas under the $i_d(t)$ *versus* time profiles obtained from the O_2-MPD were measured by a cut-and-weigh technique.

Results and Discussion

Characteristics of an O_2-MPD in a Flow System

On switching on the O_2-MPD in the flow system, a steady-state, diffusion-controlled current (i_d) is achieved (usually after 1–2 min) which is related to the partial pressure of oxygen (P_{O_2}) in the gas phase above the detector by equation (1):

$$i_d = \frac{nAFP_m}{b} P_{O_2} \quad \ldots \quad \ldots \quad \ldots \quad (1)$$

where n = number of electrons transferred in the electrochemical reaction; F = Faraday's constant (9.65 × 10^4 C mol^{-1}); P_m = permeability coefficient of the membrane (mol cm^{-1} s^{-1}); b = membrane thickness (cm); and A = working electrode surface area (cm^2).

As the N_2 carrier gas sweeps any O_2 in the reaction vessel to the O_2-MPD, the value of P_{O_2} measured at any time should be related directly to the amount of O_2 present in the reaction vessel. In addition, a sudden (or step-wise) change in this amount of O_2 should lead to a step-wise change in P_{O_2}, and then, with an ideal O_2-MPD, to a step-wise change in i_d. However, this was not found to be the case in practice, as the O_2-MPD required a minimum time to respond (t_r)[13] represented by equation (2):

$$t_r \sim b^2/D_m \quad \ldots \quad \ldots \quad \ldots \quad \ldots \quad (2)$$

where D_m = the diffusion coefficient of O_2 in the membrane. This is due to the relatively slow step, in the over-all process, of mass transport by diffusion through the membrane.[13] Under the typical conditions employed in this work (*i.e.*, $b \sim$ 12.5 μm; $D_m \sim 10^{-11}$ m^2 s^{-1}), equation (2) predicts the time taken for a 100%, full-scale response (*i.e.*, t_r) to be *ca.* 16 s. In practice, however, we found a 90% response in *ca.* 18 s and a 99% response in 50–60 s. Similar results have been observed by other workers,[13,14] and indicate that in the type of O_2-MPD used mass transfer resistance is not due solely to diffusion through the membrane. Possible causes for this type of

sluggish behaviour in O_2-MPDs (which include membrane tautness, electrode age, the electrolyte layer and lateral diffusion) have been discussed elsewhere.[14] It is worth mentioning that many of these problems are removed with metallised-membrane electrodes.[15,16]

As the O_2-MPD has a limited response time, it follows that it will not be able to detect accurately very rapid changes in P_{O_2}. One possible approach to investigate just how this limits the use of an O_2-MPD, for making accurate quantitative O_2 measurements in a flow system, would be to expose the O_2-MPD to a range of O_2 levels that varied with time in a manner which could be both predicted and controlled; the expected and observed response of the detector could then be compared. In fact we can readily achieve this using the flow system (see Fig. 1), because if V_i cm^3 of O_2 is injected into the reaction vessel, through which the N_2 carrier gas is flowing (at a rate of f cm^3 min^{-1}), then the rate of decrease in O_2 partial pressure in the reaction vessel (P_{O_2}) at any time (t) after injection will be given by equation (3):

$$-\frac{d(P_{O_2})}{dt} = \frac{fP_{O_2}}{V_0} \quad \ldots \quad (3)$$

where V_0 = volume of the gas phase in the reaction vessel (cm^3). (This equation assumes perfect mixing of the injected and carrier gas in the reaction vessel.)

Equation (3) indicates that the initial partial pressure of O_2 produced in the reaction vessel following injection will decay in an exponential manner, and at a rate that is dependent upon f and V_0, both of which are controllable quantities. It follows from equations (1) and (3), that with such a system the response of an "ideal" O_2-MPD (*i.e.*, one in which t_r = O) placed directly after the reaction vessel would be given by equation (4):

$$i_d(t) = \frac{V_i}{V_0} i_{O_2} . \exp(-ft/V_0) \quad \ldots \quad (4)$$

where $i_d(t)$ = diffusion-controlled current at time (t) after injection; and i_{O_2} = diffusion-controlled current when O_2, instead of N_2, is flowed through the system.

From equation (4), it follows that the diffusion-controlled current (or peak current) observed immediately (t = 0) after injection (i_d^0), would be given by equation (5):

$$i_d^0 = \frac{V_i}{V_0} i_{O_2} \quad \ldots \quad (5)$$

If, as is often the case, the O_2-MPD is placed at a distance from the reaction vessel (see Fig. 1), a delay time (t_d) is observed between injection (or O_2 production) at the reaction vessel and the subsequent detector response. This delay time can be estimated by equation (6):

$$t_d = V'/f \quad \ldots \quad (6)$$

where V' = volume of N_2 gas in the line between the reaction vessel and the O_2-MPD.

Using the equations developed by Heineken[17] for the response of an O_2-MPD to an exponential change in P_{O_2} it can be shown that the "ideal" behaviour for an O_2-MPD described by equation (5) would only be possible if equation (7) was valid.

$$\frac{V_0}{f} \gg \frac{b^2}{D_m} \quad \ldots \quad (7)$$

In most of our experiments dealing with the response of the O_2-MPD, V_0 = 156 cm^3, and it follows from equation (7) that if the O_2-MPD is to respond as described by equation (4), then f must be $\ll$ 600 cm^3 min^{-1}. A typical output from the O_2-MPD for an injection of 1 cm^3 of air (f = 215 cm^3 min^{-1}) is shown in Fig. 3 and compares favourably with the set of points calculated using equation (4), and plotted on the same figure. At high flow-rates (*i.e.*, f > 220 cm^3 min^{-1}) the observed O_2-MPD response begins to differ significantly from that predicted by equation (4) (due to the long response time of the detector) and as a result all subsequent work was carried out using flow-rates of less than 220 cm^3 min^{-1}.

Over the flow-rate range (10–215 cm^3 min^{-1}) the O_2-MPD was found to respond to a large variety of injections of O_2 (V_i = 0.02–30 cm^3), as described by equation (5). For example the peak current (i_d^0) was found to be: (*a*) proportional to V_i over at least three orders of magnitude (up to five has been achieved both in this and other[10] laboratories); and (*b*) independent of flow-rate. In addition, for each flow-rate used, a 1-cm^3 injection of air gave a peak profile, which when plotted as ln [$i_d(t)$] *versus* t produced a straight line over at least 2.5 half-lives, t being measured from the peak maximum. This is in agreement with equation (4) and, as expected from (4) the subsequent plot of the gradients (m = f/V_0) against their respective values for f gave an average value for V_0 of 145 ± 5 cm^3 (calculated by the method of least squares, see Fig. 4) which compared favourably with the measured value of 156

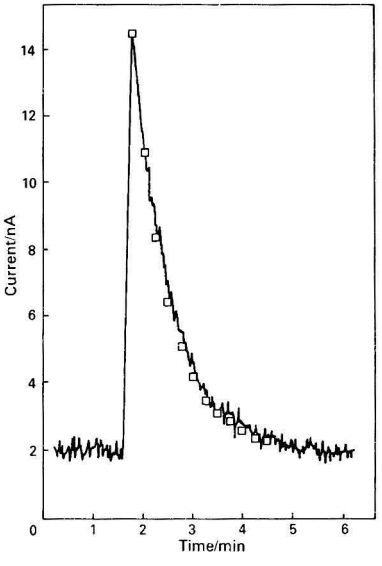

Fig. 3. Typical output from the O_2-MPD for an injection of 1 cm^3 of air, into the reaction vessel of the flow system (f = 215 cm^3 min^{-1}). □, Points calculated using equation (4). The time origin is arbitrary

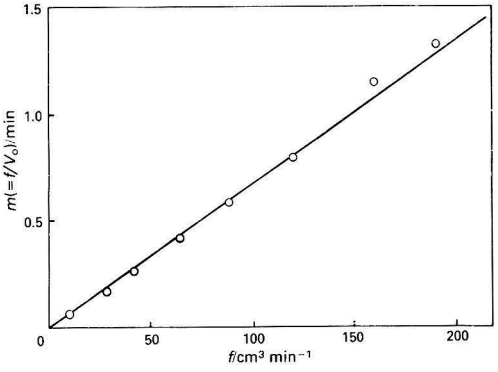

Fig. 4. Graph of m(= f/V_0) *versus* f. (Least-squares analysis give V_0 = 145 ± 5 cm^3)

cm^3. Incomplete mixing of the injected sample with the N_2 in the reaction vessel may be responsible for the difference between these two values for V_0. A variation in V_0 was achieved by filling the reaction vessel with different volumes of water (V_w = 0–120 cm^3); V_0 was then calculated using expression (8):

$$V_0 = 156 - V_w \quad .. \quad .. \quad .. \quad (8)$$

As predicted by equation (5) the peak current (i_d^0) was found to be inversely proportional to the gas-phase volume in the reaction vessel (V_0).

The integral of equation (4) from $t = 0$ to ∞ provides us with an equation for the area under a peak (A_p), *i.e.*, equation (9):

$$A_p = \frac{V_i \cdot i_{O_2}}{f} \quad .. \quad .. \quad .. \quad .. \quad (9)$$

In agreement with this equation we were able to show that the peak area (A_p) was: (*a*) proportional to V_i (V_i = 0.02–30 cm^3 of O_2) over at least three orders of magnitude; (*b*) inversely proportional to the flow-rate; and (*c*) independent of V_0.

From the work described here we can say that when used in a flow system with $10 < f < 200$ cm^3 min^{-1}, the O_2-MPD used behaved as a sensitive and accurate device for the measurement of P_{O_2} in the reaction vessel. Thus if any O_2-evolving system is placed in the reaction vessel of the flow system, it should be possible to use the O_2-MPD to measure both the amount and rate of O_2 production, and to study the parameters that affect them. In order to demonstrate this possible application, two well documented, O_2-evolving systems were chosen for study: one chemical and one photochemical, and in this work an N_2 flow-rate of 180 cm^3 min^{-1} was always employed, in order to minimise the time taken to flush out the O_2 from the reaction vessel.

Oxygen Evolution from a Chemical System

The chemical system chosen was based on the spontaneous reaction[11,18] given in equation (10):

$$2Ce^{4+} + H_2O_2 \rightarrow 2Ce^{3+} + O_2 + 2H^+ \quad .. \quad (10)$$
$$G = -147 \text{ kJ mol}^{-1} \text{ of } O_2$$

Because in our experiments reaction (10) can be considered to occur almost instantaneously (*i.e.*, <10 s), we could have expected the $i_d(t)$ *versus* t profile, produced on addition of an H_2O_2 solution (2 cm^3, at 5×10^{-2} M) to 80 cm^3 of a Ce^{4+} solution (1.35×10^{-2} M) contained in the reaction vessel, to be similar in shape to that shown in Fig. 3, with a half-life ($t_{\frac{1}{2}}$) given by equation (11).

$$t_{\frac{1}{2}} = \frac{V_0 . \ln 2}{f} \quad .. \quad .. \quad .. \quad .. \quad (11)$$

In fact what is observed (see Fig. 5) is a peak with a much longer exponential decay than predicted by equation (4), with $t_{\frac{1}{2}}$ *ca.* 90 s rather than *ca.* 18 s, as calculated using equations (8) and (11). This was found to be so for all injections of H_2O_2 and can be explained in terms of the mass-transfer resistance of O_2 when going from the liquid phase (where it is produced) to the gas phase (in which it is subsequently detected). This effect has been well studied by workers measuring the aeration capacity of bioreactors and waste water treatment units.[19] An often quoted measure of this transfer resistance is the oxygen mass-transfer coefficient (*i.e.*, $k_La = \ln 2/t_{\frac{1}{2}}$), and the value calculated using the data in Fig. 5 ($k_La = 0.0077$ s^{-1}) compares favourably with those reported in the literature[20] (*i.e.*, k_La *ca.* 0.0080 s^{-1}) for solutions where the gas bubbles and the liquid phase were well mixed. This mixing can be improved further if the solution is stirred, and this in turn leads to an increase in k_La (typically k_La increased from 0.0077 to 0.0116 s^{-1}).

Obviously, in a flow system, the resistance to mass transfer

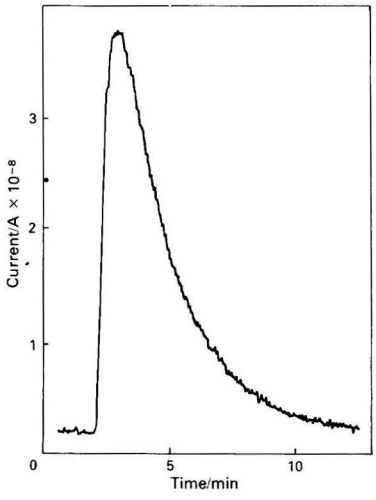

Fig. 5. Typical output from the O_2-MPD resulting from the addition of 2 cm^3 of a H_2O_2 solution (5×10^{-2} M) to 80 cm^3 of a Ce^{4+} solution (1.35×10^{-2} M) contained in the reaction vessel. The time origin is arbitrary

(for both stirred and unstirred solutions) would always make it difficult to follow rapid changes in the O_2 evolved from a solution irrespective of the detector employed. As a consequence, this would seriously limit the use of any flow system for measurement of O_2 evolution rates. However, it should not hinder measurement of the total amount of O_2 evolved from any system as, when using a O_2-MPD in conjunction with a flow system, equation (9) relates the area under a peak to the number of moles of O_2 present (N), *i.e.*, equation (9) can be rewritten as equation (12):

$$A_p = NK \quad .. \quad .. \quad .. \quad .. \quad (12)$$

where K is a constant.

With the studies involving O_2-evolving systems, the value of K was determined beforehand by injecting known volumes of gaseous O_2 saturated with water into the reaction vessel containing the solution under study. These volumes could then be related to the number of moles of O_2 present (N) via the gas equation. The plot of peak area (A_p) *versus* N always yielded a straight line from which K could be calculated (±5%) using equation (12).

When studying reaction (10) it was found that, on injection of a small volume (1–5 cm^3) of a variety of H_2O_2 solutions of different strengths to a Ce^{4+} solution (usually 90 cm^3 and 2.4×10^{-2} M), O_2 was evolved and could be subsequently detected at the O_2-MPD (Fig. 5 shows a typical output from the detector). The number of moles of O_2 generated could then be calculated, via equation (12), from the peak area. It was found that over a wide range of H_2O_2 additions (1.7×10^{-4}–1.6×10^{-6} moles), the number of moles of H_2O_2 injected always equalled (±5%) the number of moles of O_2 evolved. These results are in good agreement with those reported by other workers[18] and are as expected from the stoicheiometry of reaction (10). It should be pointed out that, with a liquid in the reaction vessel, the partial pressure of oxygen will be diluted by some constant but small amount (estimated at *ca.* 3%) owing to the vapour pressure of the liquid; however, this did not prove a problem in our measurements.

O_2 Evolution from a Photochemical System

The photochemical system chosen involved the UV photolysis of hydrogen peroxide,[20] equation (13):

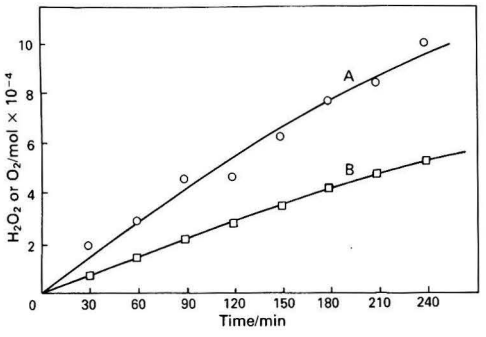

Fig. 6. A, Number of moles of H_2O_2 decomposed, and B the corresponding number of moles of O_2 evolved after irradiation for t min. The curve drawn through the circles was the best fit by eye

$$2H_2O_2 \xrightarrow{\text{UV light}} 2H_2O + O_2 \quad .. \quad .. \quad (13)$$

and as UV light was required to drive this reaction, the Pyrex Dreschel bottle usually used in the flow system (see Fig. 1) was replaced with a quartz, thermostatically controlled (at 25 °C) reaction vessel (total volume 38 cm^3). On irradiation of 25 ml of an H_2O_2 solution (0.099 M) placed in the quartz reaction vessel, O_2 was produced and the H_2O_2 concentration was found to decay concomitantly. The concentration of the H_2O_2 solution was monitored at 30-min intervals before and during irradiation by removing 0.5-ml samples and titrating them with a standard Ce^{4+} solution.[11] This work allowed us to calculate the number of moles of H_2O_2 decomposed during the irradiation ($N_{H_2O_2}$), and to compare this with the corresponding number of moles of O_2 produced (N_{O_2}), as measured by the O_2-MPD in the flow system. The results are shown in Fig. 6, and indicate that the number of moles of O_2 evolved were always about half that of H_2O_2 decomposed. In fact a plot of N_{O_2} *versus* $N_{H_2O_2}$ yielded a straight line, with a correlation coefficient of 0.9984, a gradient of 0.55 ± 0.03 and an intercept of $(-1.4 \pm 2.2) \times 10^{-5}$ mol, as calculated by the method of least squares, and this is in reasonable agreement with the values of 0.5 and 0, respectively, as predicted from the stoicheiometry of reaction (13).[21] Problems associated with the accurate syringing-up and titration of small volumes of H_2O_2 were found to be responsible for the scatter in the $N_{H_2O_2}$ *versus* t data (see Fig. 6).

We thank the S.E.R.C. for financial support of this work.

References

1. Mills, A., *J. Chem. Soc., Dalton Trans.*, 1982, 1213, and references cited therein.
2. Lehn, J. M., Sauvage, J. P., and Ziessel, R., *Nouv. J. Chim.*, 1980, **4**, 355.
3. Valenty, S. J., *Anal. Chem.*, 1978, **50**, 669.
4. Mills, A., *in* Harriman, A., and West, M., *Editors*, "Photogeneration of Hydrogen," Academic Press, New York, 1982, p. 1.
5. Kalyanaswndaram, K., Micic, O., Pramauro, E., and Grätzel, M., *Helv. Chim. Acta*, 1979, **62**, 2434.
6. Bobeck, R. F., *Chem. Eng.*, 1980, 113.
7. Kiwi, J., and Grätzel, M., *Chimia*, 1979, **33**, 289.
8. Kiwi, J., Grätzel, M., and Blondeel, G., *J. Chem. Soc., Dalton Trans.*, 1983, 2215.
9. Duonghong, D., Borgarello, E., and Grätzel, M., *J. Am. Chem. Soc.*, 1981, **103**, 4685.
10. Calzaferri, G., and Sulzberger, B., *J. Photochem.*, 1982, **19**, 321.
11. Vogel, A. I., "Textbook of Quantitative Inorganic Analysis," Fourth Edition, Longman, London, 1978, p. 369.
12. Mills, A., Harriman, A., and Porter, G., *Anal. Chem.*, 1981, **53**, 1254.
13. Hale, J. M., and Hitchman, M. L., *J. Electroanal. Chem.*, 1980, **107**, 281.
14. Benedeck, A. A., and Heideger, W. J., *Water Res.*, 1970, **4**, 627.
15. Bergman, I., and Windle, D. A., *Ann. Occup. Hyg.*, 1972, **15**, 329.
16. McCallum, C., and Pletcher, D., *Electrochim. Acta*, 1975, **20**, 811.
17. Heineken, F. G., *Biotechnol. Bioeng.*, 1971, **13**, 599.
18. Baer, S., and Stein, G., *J. Chem. Soc.*, 1953, 3176.
19. Lee, Y. H., and Tsao, G. T., *Adv. Biochem. Eng.*, 1979, **13**, 35.
20. Linek, V., *Biotechnol, Bioeng.*, 1972, **14**, 285.
21. Volman, D. H., and Chen, J. C., *J. Phys. Chem.*, 1959, **81**, 4141.

Paper A4/137
Received April 4th, 1984
Accepted July 12th, 1984

Improved pH Cells for Over-all Temperature Compensation in the Measurement of the pH of Boiler Feedwater

Kenneth Torrance
Central Electricity Generating Board, Central Electricity Research Laboratories, Kelvin Avenue, Leatherhead, Surrey KT22 7SE, UK

The pH of boiler feedwater is raised by the addition of ammonia to a level at which corrosion of the boiler is limited and consequently the measurement of pH is of primary operational interest. It is considered necessary to refer this measurement to a standard temperature of 25 °C because under conditions of varying sample temperatures, some pH meters will record changes in pH that are solely due to the effects of temperature on the chemical equilibrium of the ammonia-dosed water. At present, readings at a reference temperature can be made by controlling the sample temperature or by inclusion of additional compensation circuits in the pH meter. An attractive alternative to either of these methods is the use of self-temperature-compensating electrodes whose physico-chemical properties compensate for the temperature-induced changes in the pH of the sample.

When the experimental glass and reference electrodes were tested in simulated ammonia-dosed boiler feedwater over the temperature range 15–35 °C the temperature compensation gave an accuracy of *ca.* ±0.05 pH about the value predicted at 25 °C. Use of these electrodes gives an improvement over those previously reported, in that glass electrodes are more stable and their thermal capacities match more closely those of the reference electrodes.

Keywords: *pH measurement; boiler feedwater; temperature compensation*

The Central Electricity Generating Board (CEGB) specification for the measurement of the pH of ammonia-dosed boiler feedwater requires that the pH is referred to a standard temperature of 25 °C. This has been considered necessary because under conditions of varying sample temperatures the measurement of pH by instruments that display the correct pH at the temperature of the sample will actually record changes in pH that are solely due to the effects of temperature on the chemical equilibrium of the sample. These effects can be considerable because the temperature coefficient of feedwater is of the order of −0.033 pH °C^{-1} and without additional information, plant operators can be in doubt as to whether a difference in pH arises from a change in the ammonia content of the feedwater or simply a change in sample temperature. In a previous paper,[1] pH cells having over-all temperature compensation were described in which the intention was to display the pH at 25 °C for samples with temperatures in the range 15–35 °C. Using experimental glass electrodes and silver - silver chloride or calomel reference electrodes the temperature-induced variations in pH were of the order of ±0.05 pH over the previously stated temperature range. While the principle of self-temperature-compensating electrodes was clearly and successfully demonstrated, the electrodes used were not entirely suitable for all types of flow cells mainly owing to the large difference in the thermal capacities of the glass and reference electrodes. An additional disadvantage was that the temerature dependence of the cells did not behave as predicted theoretically. In practice, this meant that the ideal composition of the electrolyte in the reference electrode was found empirically.

In the work reported here a combination of glass and reference electrodes was produced that was both self-temperature-compensating and behaved in a way that could be predicted from existing theories of the glass electrode. This is particularly important if any extension of the principle of self-temperature-compensation is to be applied to other electrode systems.

Theory and Electrode Design

The temperature dependence of the e.m.f. of a pH cell, E_{cell}, can be written in terms of the potential of the internal reference electrode, $E_{int.}$, which is inside the glass electrode, and the pH of the solution in which it is immersed, $pH_{int.}$, together with the pH of the external solution, $pH_{ext.}$, and the potential of the reference electrode, $E_{ref.}$ If no consideration is given to the temperature coefficient of the form

$$\frac{dE_{cell}}{dT} = \frac{dE_{int.}}{dT} + \frac{k dpH_{int.}}{dT} + pH_{int.}\frac{dk}{dT} - \frac{k dpH_{ext.}}{dT} - pH_{ext.}\frac{dk}{dT} - \frac{dE_{ref.}}{dT} \quad \ldots \quad (1)$$

where k is the Nernst coefficient, equal to $2.303RT/F$. In a previous paper,[1] the cell coefficient dE_{cell}/dT, obtained with the internal and external reference electrodes containing 3 mol l^{-1} potassium chloride solution, was 0.5–0.6 mV °C^{-1}. A coefficient this large was not predicted from equation (1). It was concluded that this equation possibly oversimplified the temperature dependence of the glass electrode, especially when the internal solution contained a high concentration of alkali metal ions. The electrodes described in this paper contained a much more dilute (0.1 mol l^{-1}) potassium chloride solution and, as this concentration of electrolyte is comparable to that found in most conventional glass electrodes, a better agreement with the theoretical behaviour [as described in equation (1)] was expected.

In an ideal temperature-compensating electrode system, changes in the cell e.m.f. are due only to changes in the concentration of the species being determined; all thermally induced changes in the potential of one electrode should be cancelled by simultaneously occurring changes in the potential of the other. This null requirement in temperature dependence means that the thermal capacity of both electrodes should be equal and the chemistry, position and geometry of the internal reference electrodes should be the same.

Most forms of glass pH electrodes have an internal silver - silver chloride reference electrode and its associated electrolyte, contained entirely within the glass sensing bulb and the glass stem connected to the bulb contains no solution. In contrast, the external reference electrode is usually entirely filled with solution and has the reference element (*e.g.*, silver - silver chloride) in the upper half of the glass stem. Under the circumstances it was simplest to re-design a glass pH electrode

such that the stem was entirely filled with the internal reference electrolyte and the reference electrode was relocated near the top of the glass stem. The internal electrolyte solutions that were used in the glass electrodes were 0.1 mol l^{-1} potassium chloride solution, adjusted to about pH 9 by an appropriate base. Solutions of this type, when used in a reference electrode with an open reservoir, would absorb carbon dioxide unless sealed from the atmosphere. Consequently, it was decided to seal the reference element and its basic electrolyte into a separate compartment and use an additional junction from this to a salt bridge solution. The final arrangement for both the glass and reference electrodes is shown in Fig. 1. With this arrangement it was intended that the bottom 20–30 mm of the electrodes were equally immersed in the sample solution and as such the electrodes were suitable for use in a Model 7680 pH system EIL flow cell (Kent Industrial Measurements, EIL Analytical Instruments), which is a type currently used widely by the CEGB for boiler feedwater pH analysis.

Experimental

Apparatus for the Measurement of Temperature Dependence of pH Cells

Full details of the apparatus used for the determination of pH in simulated ammonia-dosed boiler feedwater have been previously described.[1] Briefly, it consisted of a stream of de-ionised water to which ammonia had been added by means of a diffusion membrane. Under conditions of constant temperature, flow-rate of de-ionised water and addition of ammonia, the pH of the resulting stream can be calculated from an accurate measurement of the electrical conductivity. The temperature of such a stream was controlled at 15, 20, 25, 30 and 35 °C by passing it through a stainless-steel heat-exchanger coil immersed in a temperature-controlled water-bath. Following temperature equilibration, the stream passed through a conductivity cell and then through a glass flow cell (Fig. 1) containing the pH and reference electrodes. The e.m.f.s were measured by a Model 10 Corning digital pH meter or a Keithley differential electrometer; the changes in e.m.f. were recorded on a Servoscribe potentiometer recorder. Measurements of conductivity were made using a Model B642 Wayne Kerr autobalance bridge.

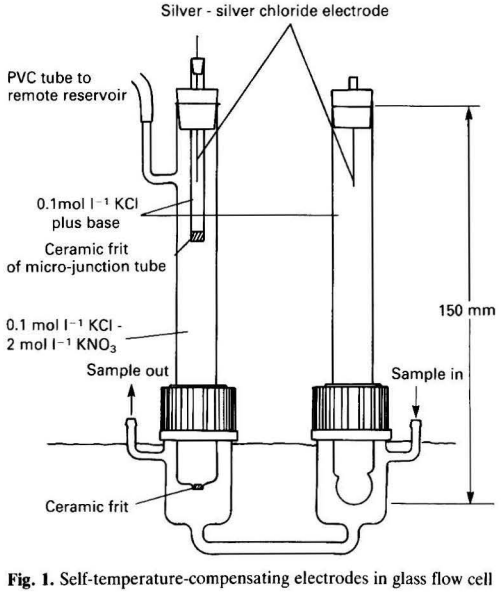

Fig. 1. Self-temperature-compensating electrodes in glass flow cell

Electrolyte Solutions for the Glass and Reference Electrodes

The electrolyte solutions consisted of 0.1 mol l^{-1} potassium chloride containing either ammonia or Tris [tris(hydroxymethyl)aminomethane] adjusted to a pH comparable to that of ammonia-dosed boiler feedwater (pH ≈ 9–9.2). The choice of Tris for this purpose has been discussed previously.[1] Solutions were prepared containing both 10^{-2} and 10^{-3} mol l^{-1} of Tris, the pH being adjusted to the required range with nitric acid.

Assembly of the Glass Electrodes

Unfilled glass electrodes, which had the same sensing-bulb glass as that used in the EIL wide-range pH electrodes, were obtained with dilute hydrochloric acid to remove any excess of alkali, then washed with de-ionised water. The electrodes were filled with the appropriate electrolyte solution for about 24 h then emptied and re-filled with a fresh portion of the same solution. The top of each electrode was sealed by means of a silicone-rubber bung through which passed the chloridised silver wire internal reference electrode. No attempt was made to fit an electrostatic screen (normal in most production pH electrodes) to these experimental electrodes and consequently they were prone to electrical interference. A coaxial socket was soldered to the external portion of the silver wire for connection to the measuring circuit.

The over-all length of these electrodes was 150 mm and the stem diameter was 12 mm.

Assembly of Reference Electrodes

The external dimensions of the reference electrodes were the same as those of the glass electrodes, the silver - silver chloride wire electrode was mounted in a small silicone-rubber bung and this was sealed into a remote microjunction tube filled with the same solution as used in the corresponding glass electrode (0.1 mol l^{-1} potassium chloride with added base). This microjunction tube was then sealed into the main body of the reference electrode through a second silicone-rubber bung. The salt bridge solution filling the main body of the electrode contained the same concentration of potassium chloride (0.1 mol l^{-1}) as the microjunction tube and, in addition, potassium nitrate (2 mol l^{-1}). By substantially increasing the conductivity over that of 0.1 mol l^{-1} potassium chloride alone, the potassium nitrate improved the performance of the ceramic-frit junction in contact with the external solution. A side-arm on the barrel of the reference electrode (see Fig. 1) was connected, via a length of PVC tubing, to an external reservoir containing the salt bridge solution. An approximately 500-mm head of electrolyte was used.

Flow Cells

A glass flow cell was constructed from two 50-mm lengths of 22-mm external diameter Quickfit and Quartz screw joints, such that the lower half of the cell could be immersed in a temperature-controlled water-bath (Fig. 1). The electrodes were held in place by plastic screw caps that had silicone-rubber sealing washers cut to provide a tight fit around the stem of the electrodes. In all the experiments the reference electrode was placed downstream of the glass electrode.

A limited number of experiments were carried out using the metal flow cell used in the EIL pH system for low-conductivity water (EIL Model 7680 pH system). This cell was not suitable for partial immersion in a water-bath and, therefore, was not ideally suited for use with the apparatus designed to produce ammonia solutions of known conductivity and temperature.

Results

Response of Cell to Changes in Air Temperature

It is essential for compensation that any changes in potential of the silver - silver chloride reference electrode brought about by changes in temperature are cancelled by equal changes in the potential of the internal silver - silver chloride electrode of the glass electrode. With the silver - silver chloride electrodes at the top of the glass stems, changes in air temperature could change the cell e.m.f. even though the bottoms of the electrodes were in solutions of constant temperature and pH. The extent of any such effect was measured as follows.

The electrodes were immersed to a depth of about 25 mm in a buffer solution whose temperature was controlled at 25 °C. The air temperature was varied by flowing a stream of warm air across the electrode stems. A change in air temperature from 21 to 27 °C produced a decrease in cell e.m.f. of 0.5 mV and a change from 21 to 38 °C produced a decrease of 0.9 mV. The electrode design was considered to be adequately robust as the larger of these two changes is only equivalent to *ca.* 0.015 pH unit.

pH Electrodes Using Ammonia as the Added Base

Electrodes were prepared using an electrolyte solution of 0.1 mol l^{-1} potassium chloride whose pH was adjusted to 9.3 by the addition of ammonia. The potential of the glass electrode *versus* a saturated calomel electrode was measured in 0.01 mol l^{-1} disodium tetraborate(III) buffer solution within 1 d of its assembly and remeasured at intervals over a period of 10 d. The direction of change of e.m.f. (becoming more negative with time) suggested that the pH of the internal filling solution had decreased and when this was measured, by inserting a microcombination pH electrode in the internal solution, it was found to be pH 7. This loss of basicity was possibly due to the loss of ammonia by volatilisation and the use of ammonia as a filling solution was discontinued.

Previous work had shown that Tris could be used in the internal electrolyte solution to provide a base solution with properties analogous to those of dilute ammonia solution, but with the added advantage of lower volatility. The results obtained with this compound are described below.

pH Electrodes Using Tris as the Added Base

Electrodes were prepared using a filling solution containing 0.1 mol l^{-1} potassium chloride and either 10^{-3} or 10^{-2} mol l^{-1} Tris. The pH values of these solutions were adjusted to 9.2–9.3. The slope factors, $k = 2.303RT/F$, of electrodes were determined by measuring the e.m.f.s in NBS standard disodium tetraborate(III) and phosphate (1 + 1) buffer solutions. At 25 °C the value of k was always greater than 99% of its theoretical value.

A simple test for the compensation characteristics of an electrode pair was to measure the changes in e.m.f. in a standard 0.01 mol l^{-1} disodium tetraborate(III) buffer solution over the temperature range 20–30 °C. This test was carried out in a temperature-controlled beaker and the results were obtained quickly, relative to the tests using the ammonia diffusion apparatus.

Ideally, from equation (1), the cell coefficient, dE_{cell}/dT, measured in disodium tetraborate(III) buffer solution should be

$$\frac{dE_{cell}}{dT} = \frac{k\,dpH}{dT}(\text{ammonia solution}) - \frac{k\,dpH}{dT}[\text{disodium tetraborate(III) solution}]$$

as the electrodes are intended to compensate for dilute ammonia solution but are actually responding to the temperature-induced changes in the disodium tetraborate(III) buffer solution. In this example, the theoretical cell coefficient was calculated to be about −0.13 mV °C^{-1}. The experimentally obtained values when the electrodes were filled with either 10^{-3} or 10^{-2} mol l^{-1} Tris were in the range −0.11 to −0.12 mV °C^{-1}.

The temperature-compensation characteristics of the glass and reference electrode pair containing 10^{-2} mol l^{-1} Tris and 0.1 mol l^{-1} potassium chloride solutions were measured in a flowing stream of simulated ammonia-dosed feedwater using the glass cell shown in Fig. 1. The results obtained over the temperature range 15–35 °C for a series of solutions having values of pH at 25 °C of 8.8, 9.0, 9.1 and 9.3 are shown in Table 1.

From these results it can be seen that the compensation characteristics predicted by the temperature response in disodium tetraborate(III) buffer solution were verified in simulated feedwater solutions.

The suitability of the electrodes for use in an EIL stainless-steel industrial flow cell (as fitted in the EIL Model 7680 pH system) was investigated using the simulated feedwater. In this instance the flow cell was not immersed in the water-bath and the temperature of the solution in the cell was, in part, dependent on the room temperature (25 ± 0.3 °C). A sample flow-rate of 50 ml min^{-1} was maintained and the temperature inside the cell measured by a platinum resistance

Table 1. Temperature dependence of electrodes containing 0.01 mol l^{-1} Tris in simulated ammonia-dosed feedwaters

pH at 25 °C	Temperature/°C	pH calculated from conductivity*	E.m.f./mV	pH from e.m.f.†
8.87	20	9.04	13.8	8.90
	25	8.87	15.1	8.87
	30	8.82	16.9	8.84
	35	8.52	18.9	8.81
9.01	15	9.35	9.8	9.05
	20	9.18	10.9	9.03
	25	9.01	11.9	9.01
	30	8.86	12.4	9.00
	35	8.70	12.9	9.02
9.09	15	9.43	0.3	9.13
	20	9.26	1.6	9.11
	25	9.09	2.7	9.09
	30	8.93	3.5	9.08
	35	8.78	4.7	9.06
9.33	20	9.49	−13.7	9.35
	25	9.33	−12.6	9.33
	30	9.17	−11.2	9.30
	35	9.02	−10.1	9.28

* Conductivity measured in μS cm^{-1}.

† Values of pH at each temperature have been normalised with respect to the conductivity value at 25 °C.

Table 2. Temperature dependence of electrodes containing 10^{-2} mol l^{-1} Tris using an EIL stainless-steel flow cell with simulated ammonia-dosed feedwater at pH 9.12 and 25 °C

Temperature/°C	pH calculated from conductivity*	E.m.f./mV	pH from e.m.f.
16.0	9.51	−19.5	9.23
20.6	9.35	−18.0	9.20
25.6	9.18	−16.5	9.18
30.1	9.04	−14.0	9.14
34.7	8.91	−11.5	9.09

* Conductivity measured in μS cm^{-1}.

† Values of pH at each temperture have been normalised with respect to the value at 25.6 °C.

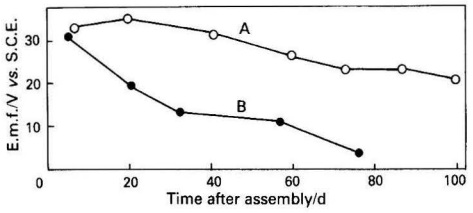

Fig. 2. Stability of experimental glass electrode containing Tris. A, 0.1 mol l^{-1} KCl containing 10^{-2} mol l^{-1} Tris (pH 9.23); and B, 0.1 mol l^{-1} KCl containing 10^{-3} mol l^{-1} Tris (pH 9.22)

thermometer. In order to avoid any spurious e.m.f. measurements caused by earth loops through the metal flow cell, the cell potential was measured by a Keithley differential amplifier. The results for a solution of pH 9.2 at 25 °C are shown in Table 2.

Stability of the Glass Electrodes Containing Tris

The stability of two glass electrodes containing 10^{-3} and 10^{-2} mol l^{-1} Tris in 0.1 mol l^{-1} potassium chloride were measured in standard buffer solution *versus* a saturated calomel electrode over a period of about 3 months. The variations in e.m.f. over this period in disodium tetraborate(III) buffer are shown in Fig. 2. It can be seen that the e.m.f.s of both the electrodes decreased with time and the rate of change was greater in the electrode containing the lower concentration of Tris. The over-all change for this was of the order of −35 mV while the electrode containing 10^{-2} mol l^{-1} of Tris changed by about −12 mV during the same period.

Discussion

The results obtained using the electrodes containing 10^{-2} mol l^{-1} Tris at temperatures between 15 and 35 °C (Table 1) were accurate to within 0.05 pH of the value at 25 °C. In every instance there was a trend in compensation that arose from the small but positive value of the cell temperature value of the cell temperature coefficient ($dE_{cell}/dT \approx 0.1$–0.3 mV °C^{-1}). However, the magnitude of this error was not too great and an average value of ±0.05 pH would be considered acceptable for most feedwater applications.

The results obtained in the EIL stainless-steel flow cell had the same trend as those described above, though in this instance the error was about ±0.09 pH. Part of this error was thought to arise from the imprecision in the calculation of pH from the theoretical conductivity - temperature relationship as the temperature of the solution in the cell could not be accurately controlled.

Unlike the previously reported work on self-temperature-compensation systems[1] where the glass electrodes contained 3 mol l^{-1} potassium chloride plus added base, the behaviour of these electrodes followed that predicted by equation (1). Even the small cell temperature coefficient obtained can be explained on the basis of this equation. If one assumes that the only two terms of this equation that do not cancel are $k\mathrm{dpH_{int.}}/dT$ and $k\mathrm{dpH_{ext.}}/dT$ (because the internal solution is Tris and the external solution is dilute ammonia), then the cell coefficient should be,

$$\frac{dE_{cell}}{dT} = k\left(\frac{\mathrm{dpH_{Tris}}}{dT} - \frac{\mathrm{dpH_{ammonia}}}{dT}\right)$$

Using a value of $\mathrm{dpH_{ammonia}}/dT = -0.033$ (ref. 2) and $\mathrm{dpH_{Tris}}/dT = -0.28$ (ref. 3) a cell coefficient of about 0.3 mV °C^{-1} was calculated.

The stability of the Tris-filled glass electrodes was also much greater than that previously reported. This could be due to the much larger volume of liquid present in the electrodes reported here (16 ml compared with <1 ml) providing a larger buffer capacity for any change in pH due to impurities on the glass surfaces. The changes in e.m.f. that were observed over about 3 months were only equivalent to a decrease of 0.15 pH for the electrode containing 10^{-2} mol l^{-1} Tris and 0.5 pH for the electrode containing 10^{-3} mol l^{-1} Tris. Losses as small as this would not affect their compensation characteristics but in order to avoid frequent standardisation the more stable system (*i.e.*, 10^{-2} mol l^{-1} Tris) is preferred. The experiments in dilute ammonia solution, at any one pH value, described in this paper were carried out over time periods (approximately 6 h) that are short relative to the time between standardisation of electrodes in an industrial monitor. Extended performance tests would be necessary before these experimental systems could be considered for plant applications.

The cooperation of Mr. A. E. Bottom of Kent Industrial Measurements is acknowledged, particularly for the loan of flow cells and the gift of glass electrode bodies. This work was carried out at the Central Electricity Research Laboratories of the Central Electricity Generating Board, Technology Planning and Research Division and is published by permission of the Central Electricity Generating Board.

References

1. Midgley, D., and Torrance, K., *Analyst*, 1982, **107**, 1297.
2. Torrance, K., Note RD/L/N 103/78, Central Electricity Research Laboratories, Leatherhead, 1978.
3. Bates, R. G., "Determination of pH," Wiley, London, 1973, p. 458.

Paper A4/200
Received June 12th, 1984
Accepted July 6th, 1984

Determination of Vanadium by Means of Its Catalytic Effect on the Potassium Bromate Oxidation of Pyrogallol Red

A. Sevillano-Cabeza, J. Medina-Escriche and F. Bosch-Reig
Department of Analytical Chemistry, Faculty of Chemical Sciences, Valencia University, Burjasot (Valencia), Spain

The method is based on the oxidation of Pyrogallol Red (PGR) by potassium bromate. Vanadium is determined by means of its catalytic effect on this oxidation, under the following conditions: pH 4, ionic strength 0.1 M, temperature 25 °C and at a wavelength of 490 nm. The decrease in absorbance of PGR (6×10^{-5} M) in the presence of $KBrO_3$ (4.4×10^{-3} M), at a fixed time, is proportional to the concentration of vanadium(V) over the range 0–50.94 p.p.b. The limit of detection of vanadium is found to be 0.61 p.p.b. The precision and accuracy of the method, using a fixed time of 5 min, is described. The selectivity of the method with respect to the possible interference of 23 species is also described. Starting from the oxidation of PGR (6×10^{-5} M), at pH 4, and by means of the V(V) - $KBrO_3$ - PGR and V(V) - PGR systems it is possible to carry out the determination of vanadium(V) between 0.61 p.p.b. and 1.83 p.p.m., measuring the absorbance values at times of 5 and 10 min, with and without $KBrO_3$.

Keywords: *Vanadium determination; catalytic oxidation; Pyrogallol Red; potassium bromate; kinetic - spectrophotometric method*

In the literature, there are few references to the oxidation of Pyrogallol Red (PGR) and its applications, by means of kinetic studies, to the determination of different species. The determination of trace amounts of lead[1,2] and iodide,[3] by means of their catalytic effect on the oxidation of PGR by persulphate and hydrogen peroxide, respectively, has been described. Previous work by us described the kinetic - spectrophotometric determination of vanadium(V) based on the oxidation of PGR.[4] We have studied the oxidation of the reagent by Mn(VII),[5] and by Cr(VI) and Ce(IV) (unpublished data), and were able to carry out determinations of them. It is known that many redox systems are catalysed by metal ions; of these systems it is found that some oxidations by bromate are catalysed by vanadium.[6] Costache and Sasu[7] determined vanadium in the range 0.61–6.16 p.p.b., starting from the reaction between Pyrogallol Bromide Red and potassium bromate. Based on these facts it is thought that is possible to determine vanadium by means of the catalytic effect on the oxidation of PGR by $KBrO_3$.

Experimental

Reagents

All reagents used were of analytical-reagent grade unless otherwise specified.

Vanadium(V) stock solution, 10^{-2} M. Dissolve 1.232 g of sodium vanadate ($NaVO_3$, E. Merck) in distilled water (by warming) and then dilute to 1 l. The solution was standardised with iron(II) ethylenediammonium sulphate (general-purpose reagent grade) titrimetric standard. The 10^{-6} and 10^{-5} M working solutions were prepared by the appropriate dilution of the stock solution.

Potassium bromate solution, 1.1×10^{-1} M. Dissolve 9.232 g of $KBrO_3$ (E. Merck) in distilled water and then dilute to 500 ml.

Buffer solution, 2.2 M acetic acid - 0.5 M sodium acetate, pH 4.

Pyrogallol Red solution, 8×10^{-4} M. Dissolve 0.080 g of PGR (E. Merck) in 250 ml of methanol. This solution is stable for at least 1 month.

Apparatus

All the spectrophotometric measurements were made on a Pye Unicam SP 8–100 spectrophotometer using 1-cm cells. A Crison-501 pH meter, equipped with a Metrohm EA-121 Ag - AgCl electrode system, was used for measuring the pH of the solutions. The pH should be measured to an accuracy of ±0.01 pH unit. A Frigedor Selecta-398 refrigerator unit for use in a water-bath and a Thermotronic Selecta-389 immersion thermostat capable of maintaining the temperatures within 0.05 °C, were also used.

Results and Discussion

Influence of Potassium Bromate Concentration on the Oxidation Rate of PGR and the Vanadium(V) - PGR System

Solutions of PGR, in the presence of $KBrO_3$ (*ca.* 10^{-3} M), which were unable to oxidise the reagent, underwent a rapid decomposition (Fig. 1) when vanadium(V), at the parts per billion level, was added. Similar spectra were obtained to the ones observed for the vanadium(V) - PGR system,[4] which required longer times and higher vanadium concentrations. On the basis of this, it was thought that vanadium acts as a catalyst in the V(V) - $KBrO_3$ - PGR system.

Initially, the influence of the potassium bromate concentration on solutions of PGR, 6×10^{-5} M at a pH of 4 [the optimum working pH for the V(V) - PGR system][4] with or without 2.04, 4.07 or 50.94 p.p.b. of vanadium(V), was studied for 15 min, in order to determine the maximum concentration of bromate allowed before the reagent is oxidised.

For this purpose, the following tests were carried out. Into a series of 25-ml calibrated flasks, 5 ml of 2.2 M acetic acid - 0.5 M sodium acetate buffer solution were added. Volumes of vanadium(V) solution, 10^{-6} or 10^{-5} M, were then added to obtain a final concentration of 2.04, 4.07 or 50.94 p.p.b. of vanadium(V). Increasing volumes of 1.1×10^{-1} M $KBrO_3$ solution were then added and the solution was diluted to *ca.* 20 ml with distilled water. This solution was shaken gently whilst 2 ml of 8×10^{-4} M PGR were added. The stopwatch was turned on when the last drop had been added and the solution was diluted to the mark with distilled water. The absorbance was measured at 490 nm at a temperature of 25 °C against water as a reagent blank and at a fixed time.

The results show that in the absence of vanadium(V) and $KBrO_3$ (0–30.8×10^{-3} M), the oxidation of PGR, for a time between 1.5 and 5 min, did not proceed. In the concentration range 0–8.8×10^{-3} M of $KBrO_3$ the absorbance values remain unchanged over the 15-min period studied, whereas there is a linear correlation between the absorbance *versus* time between 5 and 15 min for $KBrO_3$ in the range 13.2×10^{-3}–30.8×10^{-3} M. There is also a linear correlation between the oxidation rate of PGR *versus* the concentration of $KBrO_3$ over the range 8.8×10^{-3}–30.8×10^{-3} M (Fig. 2).

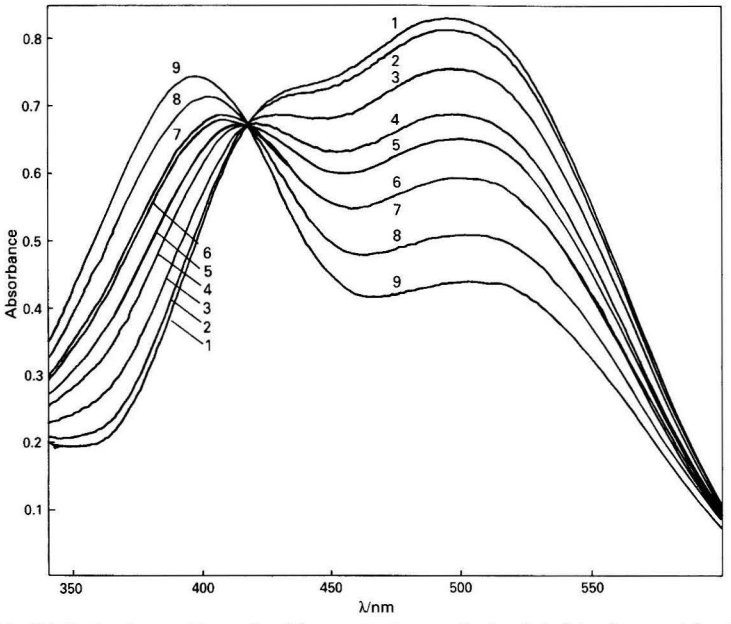

Fig. 1. Variation of PGR - $KBrO_3$ absorbance with vanadium(V) concentration, at a fixed period of time between 1.5 and 3.5 min. [V(V)]: 1, 0.00; 2, 2.04; 3, 8.15; 4, 14.26; 5, 20.38; 6, 26.49; 7, 30.56; 8, 40.75; and 9, 50.94 p.p.b. Conditions as follows: 6.4×10^{-5} M PGR; 4.4×10^{-3} M $KBrO_3$; pH, 4.0; I, 0.1 M; and temperature, 25 °C

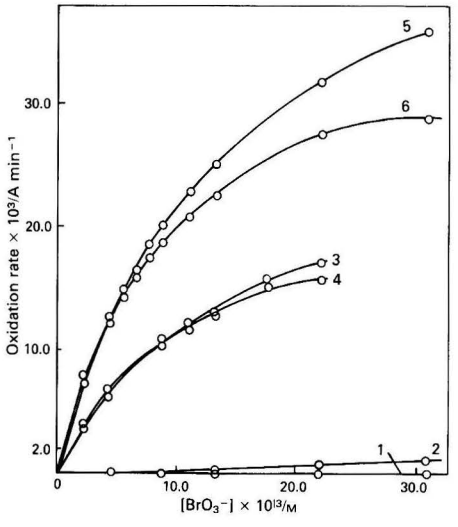

Fig. 2. Influence of potassium bromate concentration on the oxidation rate (absorbance units per minute) of PGR with and without vanadium(V). [V] (p.p.b.) and time (min), respectively: 1, 0.00 and 1.5–5.0; 2, 0.00 and 5.0–15.0; 3, 2.04 and 1.5–5.0; 4, 2.04 and 1.5–15.0; 5, 4.07 and 1.5–5.0; and 6, 4.07 and 1.5–15.0. Conditions as follows: 6.4×10^{-5} M PGR; pH, 4.0; I, 0.1 M; and temperature, 25 °C

In the presence of 2.04 and 4.07 p.p.b. of vanadium(V) there is a linear correlation between the absorbance *versus* time, both between 1.5 and 5 min and between 5 and 15 min. There is also a linear correlation between the oxidation rate of PGR *versus* the $KBrO_3$ concentration in the range 2.2×10^{-3}–8.8×10^{-3} M.

From these results, 4.4×10^{-3} and 8.8×10^{-3} M of $KBrO_3$ were the chosen concentrations because they fall within the linear range.

Calibration Graphs

In order to obtain the linear range of the V(V) - $KBrO_3$ - PGR system as a function of the vanadium(V) concentration (c_V), two series of tests, with $KBrO_3$ concentrations of 8.8×10^{-3} and 4.4×10^{-3} M, following the procedure and the order of addition of reagents given above, were carried out.

The plot of absorbance *versus* time is linear for each concentration of vanadium(V) (c_V) used. The slope of the straight line obtained for each c_V is the oxidation rate of PGR. Therefore the oxidation rate of the reagent is a linear function of c_V. This linearity was obtained under the following conditions: (*i*) with a $KBrO_3$ concentration of 8.8×10^{-3} M and vanadium(V) concentrations of 0.41–14.26 p.p.b. ($y = 1.04 \times 10^{-3} + 4.24 \times 10^{-3} c_V$, $r = 0.998$) and 14.26–22.41 p.p.b. ($y = 20.05 \times 10^{-3} + 2.76 \times 10^{-3} c_V$, $r = 0.998$); and (*ii*) with a $KBrO_3$ concentration of 4.4×10^{-3} M and vanadium concentrations of 0.61–22.41 p.p.b. ($y = 0.47 \times 10^{-3} + 2.83 \times 10^{-3} c_V$, $r = 0.998$) and 26.49–50.94 p.p.b. ($y = 35.89 \times 10^{-3} + 1.24 \times 10^{-3} c_V$, $r = 0.998$); 50.94 p.p.b. of V(V) is the theoretical limit of detection ($K = 2$; K is a numerical factor chosen according to the confidence level desired) and the experimental limit for the V(V) - PGR system, in the absence of $KBrO_3$.[4]

However, for calibration graphs of absorbance *versus* c_V (Table 1), at times of 5 and 10 min, higher slopes and correlation coefficients were obtained than for calibration graphs of v (oxidation rate of PGR) *versus* c_V. The results show that using a $KBrO_3$ concentration of 8.8×10^{-3} M and with c_V in the range 0.41–14.26 p.p.b., the correlation coefficient at a fixed time of 5 min is better than for 10 min, but the sensitivity or slope of the calibration graph is lower. The intercept of the straight line obtained using a fixed time of 5 min agrees with the absorbance results of the PGR - $KBrO_3$ system in the absence of vanadium(V). However, for 10 min there is no such agreement. Therefore, 5 min was chosen as the most suitable measuring time. For this time, when comparing the calibration graphs using a $KBrO_3$ concentration of 4.4×10^{-3} M with the one obtained using 8.8×10^{-3} M, an increase of the linear range and a decrease in sensitivity

Table 1. Calibration graphs for absorbance *versus* c_V. Conditions: PGR 6.5 × 10^{-5} and 6.4 × 10^{-5} M for $KBrO_3$ 8.8 × 10^{-3} and 4.4 × 10^{-3} M, respectively; pH 4.0; *I*, 0.1 M; λ, 490 nm; and temperature, 25 °C

	8.8 × 10^{-3} M $KBrO_3$			4.4 × 10^{-3} M $KBrO_3$		
Time/min	c_V, p.p.b.	Calibration graph	*r*	c_V, p.p.b.	Calibration graph	*r*
5	0–14.26	$y = 0.836–0.0230c_V$	−0.9995	0–26.49	$y = 0.829–0.0142c_V$	−0.9996
	14.26–26.49	$y = 0.761–0.0174c_V$	−0.9990	26.49–50.94	$y = 0.713–0.0094c_V$	−0.9998
10	0–14.26	$y = 0.821–0.0383c_V$	−0.9966			

were obtained and the correlation coefficients were practically equal. The decrease in the slopes of the calibration graphs in the range 14.26–26.49 and 26.49–50.94 p.p.b. of vanadium(V) using $KBrO_3$ concentrations of 8.8 × 10^{-3} and 4.4 × 10^{-3} M, respectively, were attributed to a possible change in the mechanism of the oxidation process, which was observed by changes in the colour of the solutions. In the first linear plot (*A versus* c_V or *v versus* c_V) the PGR predominates over its oxidised form giving a reddish coloured solution; for the second linear plot the colour is orange, owing to the existence of the two species, and finally the colour is yellow in the presence of larger concentrations of vanadium(V), owing to the predominance of the oxidised form of the reagent.

The theoretical limits of detection (c_L)[8] for numerical factors $K = 2$ and $K = 3$ (confidence level) are shown in Table 2. The absorbance values at 490 nm for the PGR - $KBrO_3$ system (8.8 × 10^{-3} and 4.4 × 10^{-3} M $KBrO_3$) agree with the absorbance of PGR, and the standard deviation of the blank (s_{bl}) is then obtained for 11 independent solutions of 6 × 10^{-5} M PGR, s_{bl} = 4.08 × 10^{-3} absorbance units. The experimental limit of detection is 0.41 or 0.61 p.p.b. of vanadium(V) in the presence of 8.8 × 10^{-3} or 4.4 × 10^{-3} M $KBrO_3$, respectively.

Precision and Accuracy

A study of the precision was performed with five independent solutions of various concentrations of vanadium(V) and a fixed concentration of $KBrO_3$ and PGR. The vanadium concentration was calculated by substituting the absorbance values, at a fixed time of 5 min, into the corresponding equation of the calibration graph. The results are shown in Tables 3 and 4, the relative standard deviations (s_r) being in the range 5–0.4% for c_V from 0.41 to 50.94 p.p.b.

A study of the accuracy[9–12] was performed for 0.41–10.19 p.p.b. of vanadium with 8.8 × 10^{-3} M $KBrO_3$ and for 2.04–20.38 and 26.49–50.94 p.p.b. with 4.4 × 10^{-3} M $KBrO_3$ and 6 × 10^{-5} M PGR. The homogeneity of the variances of the analysed samples was confirmed by application of Bartlett's test. The linear regression of the values obtained for each analysis of each sample and the corresponding real values were obtained. The statistical *t*-test was applied to the study of the slope and the intercept of the straight line was obtained. From this study we can affirm that the method proposed does not present a constant-type error (a slope equal to unity) and it does not need a blank correction (an intercept equal to zero).

Optimum Working Conditions

From the results obtained, a $KBrO_3$ concentration of 4.4 × 10^{-3} M was chosen, as there is a linear correlation between absorbance (measured at λ 490 nm) *versus* c_V over the range 0.61–26.49 p.p.b. and in the range 26.49–50.94 p.p.b. of vanadium. The latter (50.94 p.p.b.) agrees with the theoretical limit of detection ($K = 2$) and the experimental one in the absence of $KBrO_3$ at the same initial concentration of PGR (6 × 10^{-5} M)[4] and this allows the determination of vanadium between 0.61 p.p.b. and 1.83 p.p.m. by combination of the V(V) - $KBrO_3$ - PGR and V(V) - PGR[4] systems, by measuring the absorbance values at fixed times of 5 and 10 min, respectively, under the following conditions: pH 4, ionic strength 0.1 M, temperature 25 °C and wavelength of 490 nm.

Table 2. Limit of detection. Conditions: 6 × 10^{-5} M PGR; pH, 4.0; temperature, 25 °C; time, 5 min; and λ, 490 nm

	8.8 × 10^{-3} M $KBrO_3$, 0–14.26 p.p.b. V(V)	4.4 × 10^{-3} M $KBrO_3$, 0–26.49 p.p.b. V(V)
Slope of calibration graph	0.0230	0.0142
Limit of detection . .	0.35 ($K = 2$) 0.53 ($K = 3$)	0.57 ($K = 2$) 0.86 ($K = 3$)

Table 3. Precision data for the method. Equation of calibration graph: $y = 0.831–0.0259\ c_V$ ($r = -0.9998$). Pairs of values of absorbance/c_V: 0.828/0.00; 0.820/0.41; 0.807/1.02; 0.725/4.07; 0.566/10.19. Conditions: 6.4 × 10^{-5} M PGR; 8.8 × 10^{-3} M $KBrO_3$; pH, 4.0; *I*, 0.1 M; λ, 490 nm; temperature, 25 °C; and time, 5 min. Results are in p.p.b.

True concentration of V(V)	Mean concentration of V(V) found	Standard deviation
0.41	0.40	0.02
1.02	0.99	0.04
4.07	4.10	0.03
10.19	10.20	0.03

Table 4. Precision data for the method. Equation of calibration graph: $y = 0.827–0.0167c_V$ ($r = -0.9998$). Pairs of values absorbance/c_V 0.828/0.00; 0.793/2.04; 0.690/8.15; 0.584/14.26; 0.489/20.38. Equation of calibration graph: $y = 0.628–0.0083c_V$ ($r = -0.99999$). Pairs of values of absorbance/c_V: 0.409/26.49; 0.376/30.56; 0.291/40.75; 0.207/50.94). Conditions: 6.4 × 10^{-5} M PGR; 4.4 × 10^{-3} M $KBrO_3$; pH 4.0; *I*, 0.1 M; λ, 490 nm; temperature, 25 °C; and time, 5 min. Results are in p.p.b.

True concentration of V(V)	Mean concentration of V(V) found	Standard deviation
2.04	2.04	0.07
8.15	8.12	0.07
14.26	14.49	0.06
20.38	20.31	0.05
26.49	26.4	0.2
40.75	40.5	0.2
50.94	51.0	0.2

Influence of Temperature

A study of the influence of temperature on the oxidation of PGR in the presence of 4.4 × 10^{-3} M $KBrO_3$ with different concentrations of vanadium(V) (in the ranges 0.61–26.49 and 26.49–50.94 p.p.b.) at pH 4 was performed at 15, 20, 25, 30, 35 and 40 °C. The rate constant (*k*) and the order of reaction (*n*) with respect to vanadium(V) were calculated by the differential method and determining the initial rate of reaction (v_0) (Table 5). The reaction is first order in the range 0.61–26.49 p.p.b. of vanadium(V) but the order of reaction decreases for the 26.49–50.94 p.p.b. range. This decrease was attributed to a possible change in the mechanism of the oxidation process.

In order to calculate the activation energy (*E*) and the frequency factor (*A*), the Arrhenius equation was applied in the range 0.61–50.94 p.p.b. of V(V); the plot ln *k versus* $1/T$ is a straight line; $\ln k = 11.30 - 6347.38 \times 1/T$, with a correlation coefficient, $r = -0.99$ when E = 12.61 Kcal mol^{-1} and A = 80738.14 s^{-1}.

Table 5. Dependence of rate constant (k) and reaction order (n) on temperature. Conditions: 6.6×10^{5} M PGR; 4.4×10^{-3} M $KBrO_3$; pH, 4.0; I, 0.1 M; and λ, 490 nm

	0.61–26.49 p.p.b. V(V)		26.49–50.94 p.p.b. V(V)		0.61–50.94 p.p.b. V(V)	
T/K	$k \times 10^{-3}/s^{-1}$	n	$k \times 10^{-3}/s^{-1}$	n	$k \times 10^{-3}/s^{-1}$	n
288	1.28	1.16	3.03	0.88	1.46	1.09
293	1.53	1.17	4.91	0.79	1.67	1.10
298	2.83	1.08	10.25	0.62	2.57	1.02
303	3.50	1.01	15.46	0.54	3.83	0.94
308	5.54	0.90	23.48	0.44	6.01	0.83
313	6.67	0.87	36.39	0.33	7.35	0.79

Table 6. Interfering species. Conditions: 6.3×10^{-5} M PGR; 4.4×10^{-3} M $KBrO_3$; 10.00 p.p.b. V(V); pH 4.0; λ, 490 nm; temperature, 25 °C; and time, 5 min. Maximum tolerance ± 2% of the original absorbance (0.662)

Species	Concentration, p.p.m.	Ratio of [V(V)] to species	Absorbance (490 nm)
Ti(IV) ($TiOSO_4$)	0.02	1:2	0.675
Sn(IV) ($SnCl_4$)	0.05	1:5	0.676
Mo(VI) [$(NH_4)_6Mo_7O_{24}.4H_2O$]	0.05	1:5	0.673
Mn(VII)($KMnO_4$)	0.05	1:5	0.649
Ce(IV) [$Ce(NH_4)_2(NO_3)_6$]	0.06	1:6	0.648
Cr(VI) ($K_2Cr_2O_7$)	0.07	1:7	0.648
Cr(III) [$Cr(NO_3)_3.9H_2O$]	0.1	1:10	0.667
W(VI) ($Na_2WO_4.2H_2O$)	0.1	1:10	0.672
Al(III) [$Al(NO_3)_3.9H_2O$]	0.3	1:30	0.675
Sb(V) ($SbCl_5$)	0.5	1:50	0.660
Fe(III)[$Fe(NO_3)_3.9H_2O$]	0.6	1:60	0.675
Zr(IV) ($ZrOCl_2.8H_2O$)	1	1:100	0.676
Nb(V) (Nb_2O_5)	2	1:200	0.647
Cu(II) [$Cu(NO_3)_2.5H_2O$]	4	1:400	0.649
$C_6H_5O_7^{3-}$ ($Na_3C_6H_5O_7.2H_2O$)	10	1:1000	0.674
F^- (NaF)	50	1:5000	0.674
Ni(II)[$Ni(NO_3)_2.6H_2O$]	50	1:5000	0.650
Co(II)[$Co(NO_3)_2.6H_2O$]	70	1:7000	0.651
Pb(II) [$Pb(NO_3)_2$]	75	1:7500	0.650
B($Na_2B_4O_7.10H_2O$)	80	1:8000	0.675
P(Na_2HPO_4)	100	$1:10^4$	0.674
As(V)($Na_2HAsO_4.7H_2O$)	7000	$1:7 \times 10^5$	0.676
Mn(II) ($MnSO_4.H_2O$)	10000	$1:10^6$	0.654

Table 7. Interfering species. Conditions: 6.3×10^{-5} M PGR; 4.4×10^{-3} M $KBrO_3$; 30.00 p.p.b. V(V); pH, 4.0; λ, 490 nm; temperature, 25 °C; and time, 5 min. Maximum tolerance ±2% of the original absorbance (0.423)

Species	Concentration, p.p.m.	Ratio of [V(V)] to species	Absorbance (490 nm)
Sn(IV) ($SnCl_4$)	10^{-3}	1:0.03	0.433
Ti(IV) ($TiOSO_4$)	0.01	1:0.3	0.431
Al(III) [$Al(NO_3)_3.9H_2O$]	0.04	1:1.3	0.433
Mo(VI) [$(NH_4)_6Mo_7O_{24}.4H_2O$]	0.05	1:1.7	0.433
Mn(VII) ($KMnO_4$)	0.05	1:1.7	0.415
W(VI) ($Na_2WO_4.2H_2O$)	0.05	1:1.7	0.431
Ce(IV) [$Ce(NH_4)_2(NO_3)_6$]	0.06	1:2.0	0.416
Cr(VI) ($K_2Cr_2O_7$)	0.07	1:2.3	0.414
Sb(V) ($SbCl_5$)	0.08	1:2.7	0.421
Cr(III) [$Cr(NO_3)_3.9H_2O$]	0.2	1:6.7	0.424
Fe(III) [$Fe(NO_3)_3.9H_2O$]	0.3	1:10	0.430
Zr(IV) ($ZrOCl_2.8H_2O$)	0.5	1:16.7	0.430
Nb(V) (Nb_2O_5)	1	1:33.3	0.413
$C_6H_5O_7^{3-}$ ($Na_3C_6H_5O_7.2H_2O$)	3	1:100	0.432
Cu(II) [$Cu(NO_3)_2.5H_2O$]	15	1:500	0.414
F^-(NaF)	20	1:667	0.432
B($Na_2B_4O_7.10H_2O$)	40	1:1333	0.432
Ni(II) [$Ni(NO_3)_2.6H_2O$]	50	1:1667	0.414
Co(II) [$Co(NO_3)_2.6H_2O$]	70	1:2333	0.415
Pb(II) [$Pb(NO_3)_2$]	75	1:2500	0.414
P(Na_2HPO_4)	100	1:3333	0.431
As(V) ($Na_2HAsO_4.7H_2O$)	1500	$1:5 \times 10^4$	0.431
Mn(II) ($MnSO_4.H_2O$)	10000	$1:3 \times 10^5$	0.430

From this study we can conclude that at the temperature studied, the Arrhenius equation was followed.

Interferences

The influence of 23 different species on the oxidation of 6×10^{-5} M PGR in the presence of 4.4×10^{-3} M $KBrO_3$ at two different concentrations of V(V) (10.00 and 30.00 p.p.b.) were studied. These c_V values were chosen from the two straight line graphs of absorbance *versus* c_V obtained for the V(V) - $KBrO_3$ - PGR system. The results are shown in Tables 6 and 7.

From this study we can conclude that for concentrations greater than those given in Tables 6 and 7 the species Ti, Sn, Mo, Mn(VIII), Ce, Cr, W, Al, Sb, Fe, Zr and Nb cause a strong interference; the species Cu, cit^{3-} and F^- cause less interference and finally Ni, Co, B, Pb, P, As and Mn(II) do not interfere. If these interferences are compared with those for the V(V) - PGR system,[4] it can be seen that V(V) - $KBrO_3$ - PGR is generally more selective because the V(V) to species ratios are less.

Recommended Procedure

Samples containing between 0.015 and 1.273 μg of vanadium(V) were placed in 25-ml calibrated flasks, 5 ml of 2.2 M acetic acid - 0.5 M sodium acetate buffer solution and 1 ml of 1.1×10^{-1} M $KBrO_3$ were added and the contents diluted to 20 ml with distilled water. This solution was shaken gently while 2 ml of 8×10^{-4} M PGR were added. The stopwatch was turned on when the last drop had fallen and the solution was diluted to the mark with distilled water. The absorbance was measured at 490 nm and at a temperature of 25 °C against water as a reference blank, at a time of 5 min. The corresponding vanadium concentration was calculated from the corresponding equation of the calibration graph.

References

1. Jasinskiene, E., and Kalesnikaite, S., *Liet. TSR Aukst. Mokyklu Mosklo Darb., Chem. Chem. Technol.*, 1969, **11**, 51; *Zh. Anal. Khim.*, 1970, **25**, 87.
2. Anderson, R. G., and Brown, B. C., *Talanta*, 1981, **28**, 368.
3. Jasinskiene, E., and Umbraziunaite, O., *Zh. Anal. Khim.*, 1973, **28**, 2025; *Chem. Abstr.*, 1974, **80**, 66402r.
4. Medina Escriche, J., Sevillano Cabeza A., de la Guardia Cirugeda, M., and Bosch Reig, F., *Analyst*, 1983, **108**, 1402.
5. Sevillano-Cabeza, A., Medina-Escriche, J., de la Guardia-Cirugeda, M., *Analyst*, 1984, **109**, 1303.
6. Yatsimirskii, K. B., "Kinetic Methods of Analysis," Pergamon Press, Oxford, 1966.
7. Costache, D., and Sasu, S., *Rev. Roum. Chim.*, 1973, **18**, 913.
8. IUPAC, "Compendium of Analytical Nomenclature," Pergamon Press, Oxford, 1978.
9. Mandel, J., and Linnig, F. J., *Anal. Chem.*, 1957, **29**, 743.
10. Commissariat à l'Energie Atomique, "Statistique Appliquée l'Explotation de Mesures," Masson, Paris, 1978.
11. de la Guardia, M., Salvador, A., and Berenguer, V., *An. Quim.*, 1981, **77**, 129.
12. de la Guardia, M., Salvador, A., and Berenguer, V., paper presented at "5° Encontro Anual da Sociedade Portuguesa de Química," 1982.

Paper A4/187
Received May 23rd, 1984
Accepted July 16th, 1984

Spectrophotometric Determination of Hafnium as a Mixed-ligand Complex With *N*-*p*-Tolyl-*p*-methoxybenzohydroxamic Acid and Xylenol Orange

Y. K. Agrawal and U. Dayal
Analytical Laboratory, Pharmacy Department, Faculty of Technology and Engineering, M.S. University of Baroda, Kalabhavan, Baroda-390001, India

A selective and sensitive method for the extraction and spectrophotometric determination of hafnium in microgram amounts based on the formation of the hafnium - *N*-*p*-tolyl-*p*-methoxybenzohydroxamic acid - xylenol orange ternary complex is described. Hafnium is extracted from hydrochloric and perchloric acids with *N*-*p*-tolyl-*p*-methoxybenzohydroxamic acid into chloroform. Xylenol orange solution is subsquently added to the organic phase and the absorbance is measured at 540 nm. The molar absorptivities of the hafnium complexes are 8.40×10^4 and 6.97×10^4 l mol^{-1} cm^{-1}, respectively. Various parameters for optimum extraction and colour development are described.

Keywords: *Hafnium determination; spectrophotometry; mixed-ligand chelates;* N-p-*tolyl*-p-*methoxybenzohydroxamic acid; xylenol orange*

Few methods have been reported for the determination of trace amounts of hafnium. Previously, 1-(2-pyridylazo)-2-naphthol,[1] Formazan II,[2] Arsenazo III,[3,4] 2,6,7-trihydroxy-3-isoxanthane,[5] 3,4-dihydroxyazobenzene,[6] 3-hydroxychromone,[7] antipyrene and pyrocatechol sulphanphthalein[8,9] have been used as spectrophotometric reagents for its determination.

Hydroxamic acids having the bidentate group CONOH are excellent complexing agents for various metal ions,[10-12] and although the complexing properties of hafnium with *N*-phenylbenzo-, *N*-phenyl-*o*,*m*,*p*-trifluoromethylbenzo- and *N*-phenyl-*N*-3-trifluoromethyl-5-nitrobenzohydroxamic acids have been reported,[13-20] they have not been utilised in a spectrophotometric method for its quantitative determination. *N*-*p*-Tolyl-*p*-methoxybenzohydroxamic acid (*N*-*p*-T-*p*-MBHA) has been found to be a sensitive reagent for vanadium.[21] In this work *N*-*p*-T-*p*-MBHA was used for the extraction and spectrophotometric determination of hafnium.

The possibility of using dye molecules to act as secondary ligands, with the aim of producing analytically useful colour reactions, was also studied and the results showed that xylenol orange is able to act as a secondary ligand in the spectrophotometric determination of hafnium.

Experimental

Reagents and Chemicals

All chemicals were of AnalaR or general-reagent grades obtained from BDH Chemicals and E. Merck, respectively, unless specified otherwise.

N-p-*T*-p-*MBHA*. Synthesised from *p*-methoxybenzoyl chloride and *p*-tolylhydroxylamine as described previously.[22] The purity of the reagent was checked by its melting-point and IR and UV spectra. A 0.1% *m*/*V* solution of the reagent was prepared in chloroform and used for most of the extraction work.

Hafnium solution. A stock solution of hafnium was prepared by heating 0.0125 g of hafnium dioxide in a platinum dish (150-ml capacity) with 50 ml of water and 1 ml of 40% hydrofluoric acid. The contents were evaporated to dryness, the residue was moistened with sulphuric acid and evaporation was continued until dense white fumes appeared. The residue was dissolved in 250 ml of 0.2 M perchloric acid and its final concentration (2.3×10^{-4} M) was determined spectrophotometrically.[19]

Xylenol orange solution, 0.1%. Prepared in absolute ethanol.

Apparatus

The absorption measurements were carried out on a Hitachi recording double-beam spectrophotometer.

Extraction Procedure

Transfer an aliquot of hafnium solution (2.3×10^{-5} M) into a 60-ml separating funnel and add 1 ml of 5.0 M HCl and water so as to give a final volume of 10 ml. Add 5.0 ml of reagent solution in chloroform, shake vigorously for 2 min, allow the layers to separate completely and transfer the organic layer into a 10-ml calibrated flask after drying over anhydrous sodium sulphate. Repeat the extraction with an additional 2.0 ml of reagent solution and combine with the previous extract. Add 1 ml of xylenol orange solution (0.1% *m*/*V* in absolute ethanol) and dilute to volume with chloroform. Measure the absorbance at 530 nm against a blank prepared similarly.

Results and Discussion

Absorption Spectra

The colourless complex of hafnium - *N*-*p*-T-*p*-MBHA showed maximum absorbance at 330 nm in chloroform, the reagent at 287 nm (in chloroform) and the ternary complex of hafnium - *N*-*p*-T-*p*-MBHA - xylenol orange at 540 nm.

Effect of Acidity

The maximum colour intensity was obtained in 0.5 M HCl. Lower and higher acidities gave incomplete extraction (Table 1).

Table 1. Effect of the concentration of HCl on the extraction of the Hf - *N*-*p*-T-*p*-MBHA complex. Hafnium = 0.41 p.p.m.; solvent = chloroform; and $\lambda_{max.}$ = 330 nm

HCl concentration/ M	Extraction, %	Molar absorptivity/ l mol^{-1} cm^{-1}
0.2	82.9	7.01×10^4
0.3	87.8	7.40×10^4
0.4	95.1	8.01×10^4
0.5	100.0	8.42×10^4
0.6	97.6	8.10×10^4
0.7	85.3	7.14×10^4
0.8	80.5	6.75×10^4
0.9	69.5	6.00×10^4
1.0	62.2	5.36×10^4

Effect of Chromogenic Indicators

The chromogenic indicators Arsenazo II, Alizarin Red S and xylenol orange were chosen for the mixed-complex study. Arsenazo III only formed a complex after heating, Alizarin Red S had a very poor sensitivity and so xylenol orange, found to be the most sensitive, was considered the most suitable.

Effect of Xylenol Orange Concentration

A 1.0-ml volume of a 0.1% *m/V* solution of xylenol orange in absolute ethanol was sufficient for maximum colour development of the Hf - *N*-*p*-T-*p*-MBHA - xylenol orange complex. Further addition of xylenol orange increased the absorbance of the blank (Table 2).

Time for Colour Development

The maximum colour intensity was developed in 2 min after the addition of xylenol orange solution and it remained constant for at least 30 min (Table 3). There was no significant change in the colour intensity after 1 h.

Effect of Reagent Concentration

The extraction of hafnium was studied with varying concentrations of the reagent under the optimum conditions. The results showed that a single extraction with 5.0 ml of 0.1% reagent solution was sufficient for quantitative extraction of hafnium. Lower concentrations gave incomplete extraction. A slight excess of the reagent could be used without any difficulty.

Validity of Beer's Law

Beer's law was obeyed over the range 0.08–2.05 p.p.m. as a binary Hf - *N*-*p*-T-*p*-MBHA complex and 0.16–2.87 p.p.m. as a ternary Hf - *N*-*p*-T-*p*-MBHA - xylenol orange complex. The molar absorptivities were 8.40×10^4 and 6.97×10^4 l mol^{-1} cm^{-1}, respectively.

Effect of Diverse Ions

The effects of various ions on the determination of Hf were studied using the recommended procedure. A 1.02-μg mass of hafnium was successfully determined in the presence of 25 μg of the following ions: Zn(II), Co(II), Cu(II), Ni(II), Cd(II), Hg(II), Sn(II), Mn(II), Fe(II), Fe(III),W(VI) and Cr(VI). However, it was found that Nb(V) (>1.5 mg), Mo(VI) (>2.0 mg) and Ti(IV) and V(V) interfered in the determination of hafnium. The interference of Nb(V), Mo(V) and Ti(IV) was removed by masking with tartrate and oxalate and V(V) was reduced with iron(II) sulphate. Hafnium could also be determined in the presence of Zr(IV) by masking zirconium with H_2O_2 (10 ml, 1%) in the presence of sulphate ions (10 ml, 2%). The results are given in Table 4.

Composition of the Complexes

The composition of the hafnium mixed-ligand complex was studied by the slope ratio method,[21] *i.e.*, by plotting the logarithm of the distribution of metal [log$D_{(M)}$] *versus* the logarithm of the ligand concentration (log[ligand]). The extraction was carried out by taking a fixed amount of hafnium in the presence of (*a*) a constant amount of xylenol orange and varying the concentration of *N*-*p*-T-*p*-MBHA and (*b*) a constant amount of *N*-*p*-T-*p*-MBHA and varying the concentration of xylenol orange. In both instances the plot of log $D_{(M)}$ and $-$log[ligand] gave a straight line of slope 2, which indicated that the compositions of the complexes are (*a*) hafnium to *N*-*p*-T-*p*-MBHA = 1:2 and (*b*) hafnium to *N*-*p*-T-*p*-MBHA to xylenol orange = 1:2:1. The possible reaction mechanisms are as follows:

$$Hf(SO_4)_2 + 2HA \rightleftharpoons [Hf(A)_2SO_4]^{2-} + 2H^+$$

where HA = *N*-*p*-T-*p*-MBHA and

$$[Hf(A)_2SO_4]^{2-} + Ox_2 \rightleftharpoons [Hf(A)_2(Ox_2)] + 2H^+ + SO_4^{2-}$$

where Ox_2 = xylenol orange.

Hafnium was determined in standard samples and the results are given in Table 5.

Table 2. Effect of xylenol orange on the extraction of Hf - *N*-*p*-T-*p*-MBHA complex. Hafnium = 0.41 μg; solvent = chloroform; $\lambda_{max.}$ = 540 nm; and xylenol orange = 0.1% *m/V* solution in absolute ethanol

Volume of xylenol orange solution/ml	Extraction, %	Molar absorptivity/ l mol^{-1} cm^{-1}
0.10	46	3.27×10^4
0.20	73	5.09×10^4
0.40	82	5.79×10^4
0.60	90	6.31×10^4
0.80	98	6.84×10^4
1.00	100	6.97×10^4
1.20	98	6.84×10^4
1.40	94	6.66×10^4
1.60	92	6.49×10^4
1.80	89	6.31×10^4
2.00	81	5.66×10^4

Table 3. Effect of time on the colour development of Hf - *N*-*p*-T-*p*-MBHA - xylenol orange complex. Hafnium = 0.41 μg; solvent = chloroform; $\lambda_{max.}$ = 530 nm; and xylenol orange = 1 ml of 0.1% *m/V* solution in absolute ethanol

Time/ min	Extraction, %	Molar absorptivity/ l mol^{-1} cm^{-1}
1.0	95.6	6.62×10^4
2.0	100.0	6.97×10^4
5.0	100.0	6.97×10^4
7.0	100.0	6.97×10^4
10.0	100.0	6.97×10^4
30.0	100.0	6.97×10^4

Table 4. Determination of hafnium in the presence of zirconium. Solvent = chloroform; $\lambda_{max.}$ = 540 nm; and xylenol orange = 0.1% *m/V* solution in absolute ethanol

Hafnium taken/ μg	Zirconium added/ mg	Hafnium found/ μg	Relative error, %
1.50	1.0	1.49	−0.66
	5.0	1.50	0.00
	10.0	1.51	+0.66
2.00	20.0	2.00	0.00
	30.0	2.01	+0.50
4.00	20.0	4.01	+0.25
	30.0	3.98	−0.50
	40.0	3.99	−0.25

Table 5. Determination of hafnium in standard samples [Geological (USGS) and IAEA Soil-5 samples]

Sample	Hf in standard, %	Hf found, %	Relative error, %
BCR-I	4.70	4.70	0.21
W-I	2.65	2.66	0.38
AGV-I (74/19)	5.07	5.10	0.60
GSP-I (17/22)	15.50	15.49	0.07
Soil-5	6.00	6.02	0.33

References

1. Subrahmanyam, B., and Eshwar, M. C., *Microchim. Acta*, 1976, **2**, 585.
2. Mandzhgaladze, O. V., *Zh. Anal. Khim.*, 1976, **31**, 1567.
3. Boganova, A. N., and Nomodruk, A. A., *Zavod. Lab.*, 1978, **44**, 15.
4. Akimov, V. K., and Gvelesiani, L. T., *Zavod. Lab.*, 1981, **47**, 4.
5. Holler, P., and Vrbsky, J., *Anal. Chem.*, 1977, **55**, 289.
6. Vilkova, O. M., and Ivanov, V. M., *Zh. Anal. Khim.*, 1979, **34**, 720.
7. Ito, T., and Murata, A., *Anal. Chim. Acta*, 1981, **125**, 155.
8. Young, I. D., and White, J. C., *Talanta*, 1958, **1**, 263.
9. Wood, D. F., and Gaus, J. T., *Analyst*, 1965, **90**, 125.
10. Agrawal, Y. K., *Rev. Anal. Chem.*, 1980, **5**, 3.
11. Agrawal, Y. K., *Russ. Chem. Rev.*, 1979, **48**, 1773.
12. Agrawal, Y. K., and Patel, S. A., *Rev. Anal. Chem.*, 1980, **4**, 237.
13. Fouche, K. F., Le Roux, H. J., and Phillips, F., *J. Inorg. Nucl. Chem.*, 1970, **32**, 1949.
14. Fouche, K. F., *Talanta*, 1968, **15**, 1295.
15. Hala, J., *J. Less-Common Met.*, 1972, **26**, 117.
16. Hala, J., and Sotularova, L., *J. Inorg. Nucl. Chem.*, 1969, **31**, 2247.
17. Hala, J., *J. Inorg. Nucl. Chem. Lett.*, 1968, **4**, 67.
18. Hala, J., *J. Inorg. Nucl. Chem.*, 1967, **29**, 187; 1967, **29**, 1977.
19. Le Roux, H. J., and Fouche, K. F., *J. Inorg. Nucl. Chem.*, 1970, **32**, 3059.
20. Busev, A. I., Tiptsova, V. G., and Ivanov, V. M., "Analytical Chemistry of Rare Elements," MIR, Moscow, 1981, p. 165.
21. Tandon, U., and Tandon, S. G., *J. Indian Chem. Soc.*, 1969, **46**, 983.
22. Agrawal, Y. K., *J. Chem. Eng. Data*, 1977, **70**, 22.

Paper A4/147
Received April 11th, 1984
Accepted July 6th, 1984

Spectrophotometric Determination of Histamine in Mast Cells, Muscle and Urine by Solvent Extraction With Copper(II) and Tetrabromophenolphthalein Ethyl Ester

Tadao Sakai and Noriko Ohno
Department of Chemistry, Gifu College of Dentistry, 1851-1, Hozumi, Hozumi-cho, Gifu 501-02, Japan
and Masaya Tanaka and Toyohiko Okada
Faculty of Engineering, Tottori University, Koyama Minami, Tottori 680, Japan

A simple and sensitive method for the determination of histamine in mast cells, rat muscle and urine using solvent extraction and spectrophotometry is described. The method is based on the formation of a Cu(II) - histamine chelate cation, followed by extraction of the ion associate with tetrabromophenolphthalein ethyl ester into 1,2-dichloroethane and measurement of the absorbance of the complex to determine histamine. Low levels (0.2 μg ml^{-1}) of histamine in rat mast cells, rat muscle and urine can be directly determined without purification from other derivatives and biogenic amines. A linear calibration graph is obtained in the concentration range 1×10^{-6}–5×10^{-6} M (0.2–1 μg ml^{-1}) of histamine in aqueous solution. The molar absorptivity is 3.4×10^4 l mol^{-1} cm^{-1} at 515 nm. The precision of the method is ±2.5%.

Keywords: *Histamine assay; extraction - spectrophotometry; rat mast cells, rat muscle and urine; histamine - Cu(II) - TBPE complex*

It is well known that histamine (HA) is produced from decarboxylation of histidine and is stored in mast cells. The amount of histamine in tissues varies when the tissues are affected by inflammation due to allergy. Its activity is significant because it has an important physiological effect in the central nervous system. For example, when tissues are inflamed when drugs are being administered, the histamine content of the mast cells and muscle decreases temporarily. Therefore, its measurement in mast cells, tissues, body fluids, brain or urine is of importance in clinical chemistry.

Numerous investigations have been reported on the determination of histamine by means of fluorimetry after column chromatography,[1,2] high-performance liquid chromatography[3] and radioisotope techniques using [^{14}C]histamine.[4,5] Although these procedures are very sensitive, they are time consuming and complicated, as pre-treatment and/or purification of the biological samples is essential. For example, the bioassay procedures suffer from problems of instability of the products, inconsistency under incubation conditions and reproducibility. The fluorimetric procedure, which is dependent on the fluorescence of an HA - *o*-phthalaldehyde (OPT) complex, requires a preliminary and time-consuming purification of the tissues before assaying.[6] Tsuruta *et al.*[3] obtained good results by HPLC separation followed by fluorescence detection. However, the pH of the phosphate solution in the mobile phase affects the capacity factor of the OPT derivatives because the optimum pH range is very narrow. For all these methods, the precision is poor, generally in the range 7–15%.

There is a need to develop simple, fast and accurate procedures for the determination of histamine in biological samples. This paper describes a simple, rapid, selective and accurate spectrophotometric method without the need for the separation and purification of histamine from other amines and histamine derivatives, for the assay of HA in rat mast cells, rat muscle and urine. The method is based on the formation of a chelate between Cu(II) and HA, and the formation of an ion associate with tetrabromophenolphthalein ethyl ester (TBPE) in 1,2-dichloroethane. Its extractability is selective. Metallic ions such as cobalt, nickel and lead do not interfere at levels up to a 1.5-fold molar ratio to Cu(II). Catecholamines such as noradrenaline and dopamine also do not interfere at levels up to a 5-fold concentration compared with HA. However, spermidine interferes in the determination of HA and, if the sample contains spermidine, it is necessary to separate it using column chromatography prior to the determination.

Experimental

Reagents

Reagent solutions were prepared from analytical-reagent grade chemicals and were dissolved in distilled water.

Histamine standard solution. A stock solution of 1×10^{-2} M histamine was prepared by dissolving 1.8407 g of its dihydrochloride in distilled water and diluting to 1 l.

Copper (II) solution, 5×10^{-3} M. Prepared from copper(II) chloride.

TBPE solution, 4×10^{-3} M. Prepared by dissolving 0.2800 g of TBPE, potassium salt (Tokyo Kasei Kogyo) in 100 ml of ethanol.

Buffer solution. A borate phosphate buffer solution (pH 9.5) was prepared by mixing equal volumes of 0.3 M potassium dihydrogen orthophosphate solution and 0.1 M sodium tetraborate solution and adjusting the pH with 1 N sodium hydroxide solution or 1 N sulphuric acid.

Apparatus

A Hitachi Model 100–50 spectrophotometer was used for the measurement of absorbance. pH measurements were carried out with a Toa Model HM-5B pH meter and an Iwaki Model KM shaker was used for extraction. Centrifugation was carried out with a Hitachi Model 05P-21 centrifuge.

Recommended Procedure

Mix 3 ml of sample solution containing about 5 μg ml^{-1} of HA, 1 ml of 5×10^{-3} M Cu(II) chloride solution, 15 ml of buffer solution (pH 9.5) and allow the mixture to stand for 5 min. Add 2 ml of 4×10^{-3} M TBPE and dilute to 50 ml with distilled water. Transfer the aqueous solution into a 100-ml separating funnel and shake for 10 min with 10 ml of 1,2-dichloroethane until a red colour is completely developed. After centrifuging for 10 min, the organic layer is separated and its absorbance is measured at 515 nm using a reagent blank as a reference.

Results and Discussion

Absorption Spectra

It is well known that histamine forms complexes with transition metal ions such as copper, zinc, cobalt, nickel and iron. Of these elements, it was found that the complex with copper(II) was the most stable.[7] The absorption spectra of the Cu(II) - HA - TBPE ion associate and the reagent blank in the range 470–630 nm are shown in Fig. 1. The cationic complex reacts with monoprotic acid dyes such as picric acid (PCA),[8] 2,6-dichlorophenolindophenol (DCIP),[9] resazurine and tetrabromophenolphthalein ethyl ester (TBPE)[10] to form simple, coloured ion associates in the organic phase.

Of these dyes, TBPE, being hydrophobic, shows the highest sensitivity, best extractability and largest molar absorptivity.

The reaction mechanism for the formation of the Cu(II) - HA complex and the TBPE ion associate is shown in Scheme 1. The complexing ratios of both Cu(II) to HA and HA to TBPE were examined by the continuous variations method.

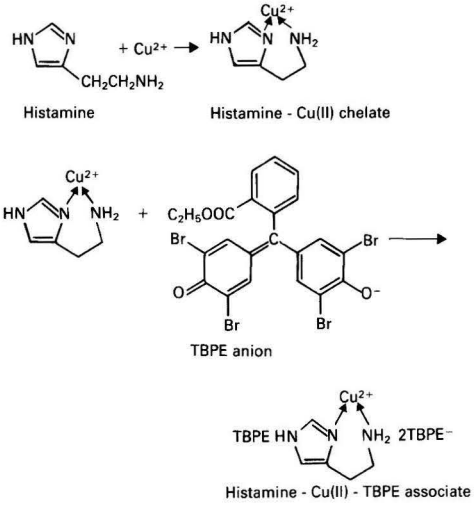

Scheme 1

The molar ratio of Cu(II) to HA was found to be 1 : 1 and that of HA to TBPE was 1 : 3. Consequently, the results obtained suggest that the empirical formula of the extracted species is HA - Cu(II)·$(TBPE)_3$. The complex between Cu(II) - HA and the TBPE anion has a $\lambda_{max.}$ at 515 nm (Fig. 1). As can be seen, as the absorbance of the TBPE molecule at 410 nm is very high, it is necessary to measure the absorption of the Cu(II) - HA - TBPE complex at 515 nm using a reagent blank as a reference. Of the solvents investigated, 1,2-dichloroethane was the best.

Effect of pH on Extraction

The effect of pH on the absorbance of the ion associate was investigated in the pH range 4–11, as shown in Fig. 2. The largest and most constant absorbance was observed over the pH range 9.3–9.7. A lower pH may result in poor formation of Cu(II) - HA and a higher pH causes instability of TBPE, so subsequent extractions were carried out at pH 9.5.

Effect of Copper(II), TBPE and Buffer Concentrations

Various amounts of Cu(II) were added to the aqueous solution of histamine and measurements were carried out as recommended. The results are illustrated in Fig. 3. Maximum absorbance was observed at Cu(II) concentrations above 3×10^{-6} M, which shows a 1 : 1 molar ratio in the chelate formed with histamine. To prevent precipitation of copper(II) hydroxide, 1 ml of 5×10^{-3} M solution was used, *i.e.*, a 30-fold molar excess over histamine. Volumes of 2 ml of various concentrations of TBPE ($0.5–2 \times 10^{-4}$ M) were used to study the effect of TBPE concentration. Constant absorbance was observed at concentrations above 1.6×10^{-4} M and a sufficient amount of TBPE was needed for quantitative extraction of the

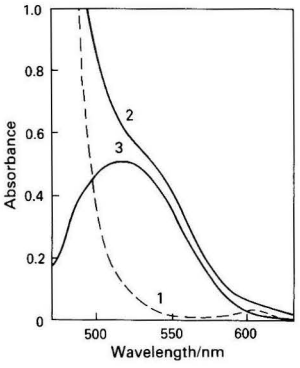

Fig. 1. Absorption spectra. 1 = Reagent blank (reference, water); 2 = 3×10^{-6} M histamine (reference, water); and 3 = 3×10^{-6} M histamine (reference, reagent blank). Copper(II) chloride concentration, 1×10^{-4} M; TBPE concentration, 1.6×10^{-4} M; pH, 9.5; solvent, 1,2-dichloroethane

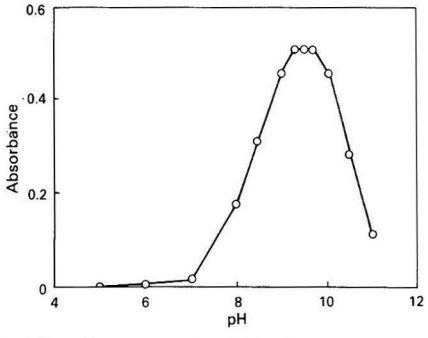

Fig. 2. Effect of pH on extraction of histamine associate. Histamine concentration, 3×10^{-6} M; copper(II) chloride concentration, 1×10^{-4} M; TBPE concentration, 1.6×10^{-4} M; reference, reagent blank

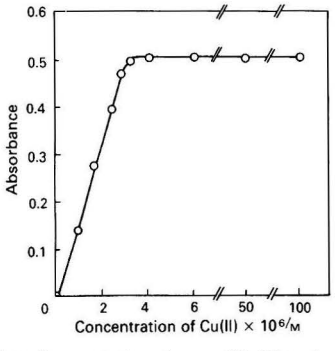

Fig. 3. Effect of concentration of copper(II). Histamine concentration, 3×10^{-6} M; TBPE concentration, 1.6×10^{-4} M; pH, 9.5; reference, reagent blank

Table 1. Effect of various substances on the determination of histamine

Substance	Molar ratio [Ion] to [HA]	Molar ratio [Ion] to [Cu(II)]	Recovery of histamine, %
Sodium chloride	1000	30	101.9
	500	15	99.0
Potassium chloride	1000	30	102.9
	500	15	100.2
Sodium nitrate	100	3	101.0
Sodium carbonate	100	3	102.0
	50	1.5	99.8
Calcium chloride	50	1.5	97.8
	10	0.3	98.9
Magnesium chloride	50	1.5	96.1
	10	0.3	98.6
Cobalt chloride	100	3	96.4
	50	1.5	97.8
	10	0.3	100.5
Lead chloride	50	1.5	101.4
Nickel sulphate	50	1.5	96.7
	10	0.3	98.4
Zinc acetate	10	0.3	98.1
	5	0.15	99.8
Iron(III) nitrate	50	1.5	96.0
	5	0.15	99.8
Ammonium chloride	10	0.3	102.7
	5	0.15	99.6
Potassium iodide	50	1.5	102.3
	5	0.15	100.9
Histidine	20	0.6	94.7
	10	0.3	100.5
Acetylcholine	50	1.5	95.5
	20	0.6	99.3
Serotonine	20	0.6	97.9
	10	0.3	100.3
Imidazole-4-acetic acid	20	0.6	97.6
	10	0.3	99.5
Adrenaline	1	0.03	99.1
Noradrenaline	5	0.15	95.5
	2	0.06	97.4
Levodopa	5	0.15	96.4
	2	0.06	99.6
Dopamine	2	0.06	97.6
	1	0.03	100.4
Spermidine	0.1	0.003	110.0

hydrophilic Cu(II) - HA cation. In this procedure, 2 ml of 4×10^{-3} M TBPE solution were used, corresponding to about a 50-fold excess over histamine.

Various amounts of buffer solution were used in the investigation to establish its effect on absorbance. There was almost no influence on the absorbance up to 15 ml, but an amount of less than 8 ml resulted in unsatisfactory separation of the organic phase during extraction.

Effect of Shaking Time

Shaking for 30 s was sufficient for extraction, but prolonged shaking is apt to lead to emulsion formation. Therefore, shaking for 10 min was applied in the procedure. The stability of the colour of the extract in 1,2-dichloroethane was excellent for more than 1 h. Also, a single extraction resulted in 96.3% colour development.

Interferences from Diverse Substances

To a solution containing 3×10^{-6} M histamine and 1×10^{-4} M Cu(II), various amounts of foreign compounds were added and their interferences were examined. The results are summarised in Table 1. Common inorganic salts did not interfere and several metallic ions, such as calcium, magnesium, cobalt, nickel, lead and iron(III), had no significant effect at a 50-fold molar excess over histamine (1.5-fold excess over Cu). On the other hand, histidine, serotonine and acetylcholine, which give strong interferences in the usual fluorimetric determination using *o*-phthalaldehyde, did not interfere in the present method even when present in a 20-fold molar excess.

Catecholamines such as adrenaline, noradrenaline, dopamine and levodopa, which coexist with histamine in biological materials, did not interfere at 1–5-fold molar ratios in excess of HA.

Medina and Shore[11] modified the Kremzner and Pfeiffer procedure to separate spermidine from histamine by the use of a phosphorylated cellulose column and obtained good results.

Table 2. Recovery of added histamine in urine by the present method. Samples I and II were prepared by dissolving 0.25 ml of 1×10^{-2} M standard histamine solution in 10 and 25 ml, respectively, of human urine

Sample taken/ml	Recovery, % Sample I	Recovery, % Sample II
0.4	98.2	—
0.6	97.2	—
0.8	96.1	—
1.0	91.4	89.8
1.2	89.7	—
1.5	—	87.0

Table 3. Determination of histamine in rat mast cells and muscle

Sample	Sample No.	Mast cells/ml	Histamine concentration/pg per cell: This method*	Histamine concentration/pg per cell: OPT method†
Mast cells	1	7.2×10^5	53.4 ± 1.9	—
	2	5.6×10^5	50.8 ± 3.1	40.6
			Amount of histamine/μg	
		Muscle mass/g	This method*	OPT method†
Muscle	1	1.19	26.1	23.7
	2	0.74	36.8	40.4
	3	0.74	39.4	37.8

* Mean values of three determinations.
† The OPT method is based on the fluorescence of the histamine - *o*-phthalaldehyde complex.

However, the histamine concentration in the midbrain and other organs such as the liver, kidney and cerebral cortex is very low[12] compared with that of spermidine. Accordingly, it is difficult to determine small concentrations of histamine in the midbrain and other tissues directly. However, microgram amounts of histamine in mast cells, muscle and urine can be selectively determined by the present method without any purification.

Calibration Graph and Precision

The calibration graph was plotted with a histamine standard solution under the optimum conditions. It showed good linearity over the range 1×10^{-6}–5×10^{-6} M (*ca.* 0.2–1.0 μg ml^{-1}). The molar absorptivity was 3.4×10^4 l mol^{-1} cm^{-1}. The range of linearity of the method is about ten times better than that found using atomic-absorption spectrophotometry.[7]

Recovery of Added Histamine from Urine

Portions of 0.25 ml of 1×10^{-2} M histamine solution were added to 25 and 10 ml of human urine and 0.4–1.5-ml aliquots were used for the determination. The results are shown in Table 2. The recovery of histamine decreased with increasing volume of urine, independent of its absolute amount. When 1 ml of urine was used in the analysis, more than 90% of the histamine was recovered.

Determination of Histamine in Rat Mast Cells and Muscle

The mast cells were prepared according to the method proposed by Sullivan *et al.*[13] as follows. A rat (about 150 g) was anaesthetised with diethyl ether, exsanguinated by decapitation and the thoracic and abdominal cavities were opened. Mast cells were harvested and processed in a medium containing 150 mM NaCl, 3.7 mM KCl, 3.0 mM Na_2HPO_4, 3.5 mM KH_2PO_4, 0.9 mM $CaCl_2$, 5.6 mM glucose and heparin, 10 units ml^{-1}, pH 6.80. This medium does not include bovine serum albumin and gelatine in Sullivan's medium because of some interferences on the ion associates with TBPE. Mast cells in the media are heated in boiling water for 30 min and histamine is eluted from the cells.

The muscle (1 g) obtained from the rat legs is homogenised[14] in 9 ml of 0.4 N $HClO_4$ and centrifuged (3000 rev min^{-1} for 15 min, 4 °C). A 4-ml aliquot of the supernatant fluid, 10 ml of butan-1-ol, 0.5 ml of 5 N NaOH and 1.5 g of NaCl are added and the mixture is shaken for 10 min and centrifuged for 10 min at room temperature. A 15-ml volume of heptane and 5 ml of 0.1 N H_2SO_4 are added to 9 ml of the butan-1-ol phase. Histamine in the aqueous phase is measured after shaking for 10 min and centrifuging as follows: a 3-ml volume of the sample solution is pipetted into a separating funnel, 1 ml of 5×10^{-3} M Cu(II) solution and 15 ml of buffer solution (pH 9.5) are added, the volume is made up to 25 ml with distilled water and the mixture is shaken for 10 min with 1,2-dichloroethane to remove the interfering polyamines. A 5-ml volume of buffer solution and 2 ml of 4×10^{-3} M TBPE solution are added to the residual aqueous solution after discarding the organic phase, followed by shaking with 10 ml of 1,2-dichloroethane. The absorbance of the ion associates in the organic phase is measured according to the Recommended Procedure.

The results are shown in Table 3. The concentrations of histamine determined by this method are higher than those given by the OPT method.[6] However, the present method is simple, selective and rapid for the determination of histamine in biological samples as elaborate sample treatment procedures are not required.

We express our gratitude to Dr. Y. Azuma, Gifu College of Dentistry, for technical assistance.

References

1. Seki, T., and Wada, H., *J. Chromatogr.*, 1974, **102**, 251.
2. Yamatodani, A., and Wada, H., *Bunseki*, 1978, 842.
3. Tsuruta, Y., Kohashi, K., and Ohkura, Y., *J. Chromatogr.*, 1981, **224**, 105.
4. Kobayashi, Y., and Mandsley, D. V., *Anal. Biochem.*, 1972, **46**, 85.
5. Beaven, M. A., Jacobsen, S., and Horakavo, Z., *Clin. Chim. Acta*, 1972, **37**, 91.
6. Michaelson, I. A., and Coffman, P. Z., *Anal. Biochem.*, 1969, **27**, 257.
7. Sakai, T., Ohno, N., Wakisaka, T., and Kidani, Y., *Bull. Chem. Soc. Jpn.*, 1982, **55**, 3464.
8. Takagi, M., Nakamura, H., Sanui, Y., and Ueno, K., *Anal. Chim. Acta*, 1981, **126**, 185.
9. Sakai, T., Hara, I., and Tsubouchi, M., *Chem. Pharm. Bull.*, 1977, **25**, 2451.
10. Sakai, T., *Analyst*, 1982, **107**, 640.
11. Medina, M., and Shore, P. A., *Biochem. Pharmacol.*, 1966, **15**, 1627.
12. Michaelson, I. A., and Coffman, P. Z., *Biochem. Pharmacol.*, 1967, **16**, 1636.
13. Sullivan, T. J., Parker, K. L., Stenson, W., and Parker, C. W., *J. Immunol.*, 1975, **114**, 1473.
14. Shore, P. A., Burkhalter, A., and Cohn, V. H., *J. Pharmacol. Exp. Ther.*, 1959, **127**, 182.

Paper A4/48
Received January 31st, 1984
Accepted July 17th, 1984

Spectrophotometric Determination of Silver in Lead and Lead Concentrates With Thiocyanate and Rhodamine B

Ignacio López García, Manuel Hernández Córdoba and Concepción Sánchez-Pedreño*
Department of Analytical Chemistry, Faculty of Sciences, University of Murcia, Murcia, Spain

The formation of a violet coloration when Rhodamine B is treated with silver in the presence of a large excess of thiocyanate is used for the spectrophotometric determination of silver. The colour is stabilised by adding poly(vinyl alcohol). At 600 nm the calibration graph is linear in the range 5–30 μg of silver per 25 ml of final solution with a relative standard deviation of 0.8% for 0.6 μg ml^{-1} of silver. The molar absorptivity is 3.3×10^4 l mol^{-1} cm^{-1}. The sensitivity can be enhanced by recording the second-derivative spectrum and a sensitivity of 0.06 μg ml^{-1} of silver can be achieved. The selectivity can be improved using the separation of silver with lead chloride as a collector. The method is applied to the determination of silver in metallic lead and lead concentrates.

Keywords: *Silver determination; Rhodamine B; spectrophotometry; ion association; lead and lead concentrates analysis*

In recent years, several spectrophotometric methods for the determination of silver based on the formation of ion-association compounds have been described.[1–8] Usually, the spectral characteristics of an ion associate are very similar to those of its component ions and, as a consequence, a separation step, such as a solvent extraction, is needed. However, in some instances significant colour changes do occur on ion-pair formation. From an examination of the literature, it is apparent that some dyes show a change in their absorption spectrum on formation of ion pairs with metallic complexes.[9–12] If this occurs, the need for a solvent extraction process can be avoided and the spectrophotometric method can be carried out with minimum manipulation. Therefore, we have examined the reaction of several basic dyes with silver in the presence of large amounts of chloride, bromide, iodide or thiocyanate with the aim of developing a rapid method for the spectrophotometric determination of silver without extraction. Preliminary results showed that Rhodamine B and thiocyanate offered the best possibilities.

In this work, the formation of an ion-association compound between Rhodamine B and silver in an excess of thiocyanate was studied, the conditions for the spectrophotometric determination of silver were established and the method was applied to the determination of this element in metallic lead and lead concentrates.

Experimental

Apparatus

A Pye-Unicam SP8-200 spectrophotometer with 10-mm glass cells was used for recording spectra and absorbance measurements. Derivative spectra were obtained with a Perkin-Elmer 550 SE spectrophotometer.

Reagents

All inorganic chemicals used were of analytical-reagent grade and were used without further purification. Doubly distilled water was used exclusively.

Rhodamine B solution, 4×10^{-3} M. Prepared from the commercial product (Merck) by dissolving 0.9580 g in water and diluting to 500 ml.

Thiocyanate solution, 0.4 M. Prepared by dissolving ammonium thiocyanate (19.4 g) in distilled water to give 500 ml of solution.

Standard silver solution, 0.01 M. Prepared by drying silver nitrate at 105 °C to constant mass. The dried compound (0.8493 g) was dissolved in distilled water to give 500 ml of solution. Working solutions (5×10^{-5} M) were prepared every day.

Poly(vinyl alcohol) (PVA) solution. Prepared by dissolving 2 g of commercially available PVA (Merck) in 200 ml of hot water and used after filtering through filter-paper.

Preparation of Reagent Solution

The reagent solution was prepared by mixing 200 ml of 4×10^{-3} M Rhodamine B solution, 200 ml of 1% *m/V* PVA solution and 13 ml of concentrated sulphuric acid (97%). About 60 min after mixing, the solution is ready to use.

General Procedure

Transfer up to 20 ml of the sample solution containing not more than 30 μg of silver into a 25-ml calibrated flask and dilute to 20 ml with water. Add 1 ml of 0.4 M thiocyanate solution, 1 ml of 4.5 N sulphuric acid and 2 ml of reagent solution. After 10 min, measure the absorbance at 600 nm against a reagent blank. Beer's law is obeyed over the concentration range 5–30 μg of silver per 25 ml of solution. When the silver content of the final solution is too low (less than 5 μg of silver), record the second derivative spectrum from 700 to 550 nm against a reagent blank using the response time No. 6 (10 s) and a scan speed of 120 nm min^{-1}. Measure the second-derivative value (the vertical distance from a peak to a trough or that from the base line to a trough of the peak) so that the calibration graph is useful between 1.5 and 10 μg of silver per 25 ml of solution.

Procedure for the Determination of Silver in Lead Concentrates

Decompose a 0.2-g sample with 5 ml of nitric acid and cool. Add 5 ml of perchloric acid, evaporate to white fumes, cool and add 20 ml of 0.2 M lead nitrate solution. Warm, then precipitate lead and silver by the dropwise addition of 3 ml of 1 M sodium chloride solution. Cool, and filter through a sintered-glass crucible (porosity 4), washing well with water. Dissolve the precipitate in 50 ml of 2 M ammonia solution plus 3 ml of 25% citric acid solution and dilute to 100 ml. Take a suitable aliquot, neutralise with sulphuric acid to the colour change of phenolphthalein and determine silver by the general procedure using citrate in the calibration graph.

*To whom correspondence should be addressed.

Procedure for the Determination of Silver in Lead

Dissolve a 1-g sample in dilute nitric acid (1 + 3) and evaporate nearly to dryness. Add 20 ml of water and 4 ml of 2 M potassium sulphate solution, warm and filter through a sintered-glass crucible (porosity 4). Dilute to 50 ml, take an aliquot of up to 20 ml and determine silver by the general procedure.

When the level of silver in lead is less than 100 μg g^{-1} or there are serious interferents, take a 1-g sample and use the procedure described above for the determination of silver in lead concentrates, employing lead chloride as a collector.

Results and Discussion

The reaction between silver(I) in the presence of a large excess of thiocyanate and a large number of basic dyes (crystal violet, methyl violet, Rhodamine B, 6G and S, malachite green, Victoria blue, Hoffman's violet, methyl green, brilliant green and fuchsin) was examined for shift in the spectral characteristics of the dye. With malachite green, methyl green, brilliant green and Rhodamines, a noticeable spectral shift was observed, but with Rhodamine B the reaction proceeded inmediately and the coloration was the best of all the dyes examined. However, the violet ternary complex that resulted on the addition of the dye to the aqueous solution of silver containing thiocyanate was unstable and gradual precipitation on standing was observed. Stabilisation was achieved by the addition of the protective colloid PVA, which successfully retarded precipitation of the complex even on leaving to stand overnight.

Fig. 1 shows the absorption spectra of Rhodamine B with different amounts of silver in the presence of an excess of thiocyanate solution in a 0.27 N sulphuric acid medium. It is evident that the interaction between the silver thiocyanate complex and Rhodamine B proceeded with a considerable bathochromic shift and that the complex showed maximum absorption at 600 nm, as against that of the reagent at 556 nm. All absorbance measurements were carried out at 600 nm.

Effect of Acidity

The acidity of the solution affected the development of the colour. The effect of the sulphuric acid concentration was examined by varying the content of acid in the final solution and the results are shown in Fig. 2. Maximum and constant absorbances at 600 nm were obtained over the range 0.09–0.5 N in sulphuric acid. All subsequent investigations were carried out in 0.27 N suphuric acid medium. Experimentally, it was found that better reproducibility and faster development of the colour were achieved when the dye solution was previously acidified. Taking all these results into account, the optimum acidity in 25 ml of the final solution was supplied using 2 ml of reagent solution prepared as described under Experimental and 1 ml of 4.5 N sulphuric acid.

Effect of the Amount of Thiocyanate and Rhodamine B and Stoicheiometry of the Complex

Fig. 3 shows the effect of thiocyanate on the colour when using 19.6 μg of silver in 25 ml of final solution. A 0.016 M thiocyanate concentration was chosen, providing a low reagent blank.

Several series of experiments were carried out to investigate the influence of the Rhodamine B concentration on the development of the colour at 600 nm. As can be seen in Fig. 4, a 1.6×10^{-4} M Rhodamine B concentration is adequate to ensure the highest, constant absorbance value.

In order to elucidate the stoicheiometry of the ternary complex, the reaction was investigated by the method of continuous variations. The results showed that a species with a Rhodamine B to silver molar ratio of 1:1 is formed.

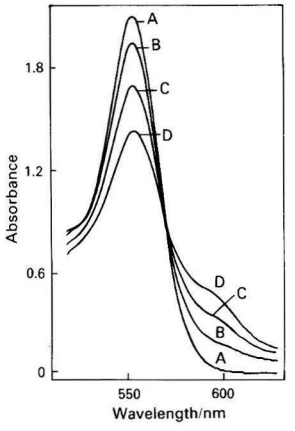

Fig. 1. Absorption spectra of the silver - thiocyanate - Rhodamine B complex. Total volume, 25 ml; 1-cm cells. A, 1.6×10^{-4} M Rhodamine B; 0.016 M thiocyanate; 0.27 N sulphuric acid; 0.04% *m/V* PVA. B, C and D, as in A with the addition of 5, 15 and 25 μg of silver, respectively

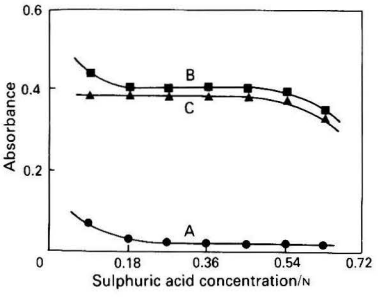

Fig. 2. Effect of sulphuric acid concentration on absorbance at 600 nm. A, Reagent blank; reference water. B and C, with 19.6 μg of silver and with water and reagent blank, respectively, as reference

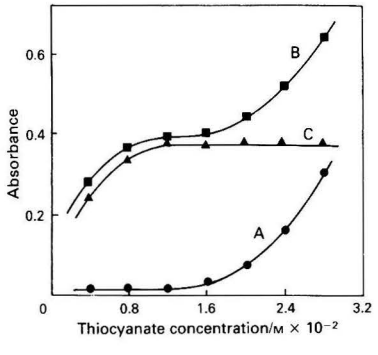

Fig. 3. Effect of thiocyanate concentration on absorbance at 600 nm. A, Reagent blank; reference water. B and C, with 19.6 μg of silver and with water and reagent blank, respectively, as reference

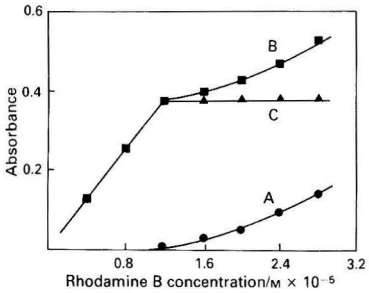

Fig. 4. Effect of Rhodamine B concentration on absorbance at 600 nm. A, Reagent blank; reference water. B and C, with 19.6 μg of silver and with water and reagent blank, respectively, as reference

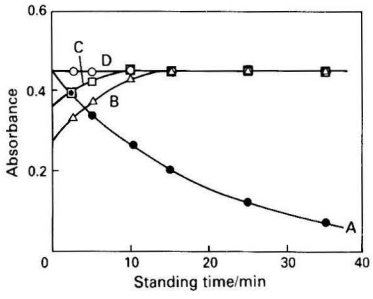

Fig. 5. Effects of poly(vinyl alcohol) and standing time on absorbance at 600 nm. Rhodamine B, 1.6×10^{-4} M; sulphuric acid, 0.27 N; silver, 25 μg. A, Without PVA; B, C and D, PVA added before, with and after the acidified dye, respectively

Consequently, it was concluded that the ternary complex has the composition $[R^+ Ag(SCN)_2^-]$, where R^+ represents the Rhodamine B cation.

Effect of Poly(vinyl Alcohol)

PVA plays an important role and the order of its additon affected the development of the colour. Without PVA the colour faded gradually, whereas on addition of PVA before addition of the dye, the colour was developed gradually. When the PVA was added after the dye, the reproducibility of the absorbance at 600 nm was unsatisfactory. The best results were obtained when the PVA was added together with the acidified dye solution as is recommended in the procedure. When the temperature was higher than 25 °C a noticeable decrease in the absorbance value at 600 nm was observed. All the measurements were carried out at room temperature (18–20 °C) and the results are shown in Fig. 5.

Calibration Graph, Reproducibility and Stability

Under the described conditions, Beer's law is obeyed over the range 5–30 μg of silver in a final volume of 25 ml. The molar absorptivity is 3.3×10^4 l mol^{-1} cm^{-1} with a Sandell's sensitivity of 3.2×10^{-3} μg cm^{-2}. The precision of the method was evaluated for ten measurements of 0.6 μg ml^{-1} of silver and the results are shown in Table 1. The sensitivity of the method can be enhanced by plotting the second-derivative value of coloured solutions *versus* the silver concentration, which gives calibration graphs that are linear in the range 60–400 μg l^{-1} of silver when either the peak to trough values or the base line to trough values are plotted.

Effect of Diverse Ions

An aliquot of solution containing various amounts of foreign ions and 10 μg of silver was treated exactly as described in the recommended procedure. The results are given in Table 2. The limiting value of the concentration of foreign ion was taken as that value which caused an error of not more than ±3% in the absorbance value. An enhancement in the selectivity can be achieved by using lead chloride as a collector for silver chloride. In order to verify that this collection procedure is effective for the complete recovery of silver, several experiments were carried out. Table 3 shows the results of these recovery tests at different levels of silver, using the procedure described under Experimental. As can be seen in Table 3, the recovery for silver is excellent and the collection with lead chloride avoids the interference of foreign ions adequately. Thus, gold, iron, palladium, mercury, molybdenum and tungsten, even in a 100:1 molar ratio (maximum molar ratio tested), do not interfere.

Determination of Silver in Metallic Lead and Lead Concentrates

The method has been applied satisfactorily to the determination of silver in lead and lead concentrates. The results, shown in Table 4, are compared with those obtained by atomic-absorption spectrophotometry. Good agreement is shown between the two methods.

Table 1. Results showing the precision of the method for measurements taken after different times of reagent preparation

		Time			
Sample	Parameter	1 h	4 h	8 h	1 d
Reagent blank	$\bar{x}$*	0.028	0.029	0.030	0.030
	S.d.	0.0016	0.0010	0.0010	0.0020
	R.s.d., %	5.6	3.4	3.3	6.6
Silver (15 μg)	$\bar{x}$†	0.325	0.325	0.324	0.320
	S.d.	0.0025	0.0023	0.0020	0.0020
	R.s.d., %	0.8	0.7	0.6	0.6

* Average absorbance of reagent blank for ten experiments; reference, water.

† Average absorbance of silver for ten experiments; reference, water.

Table 2. Effect of diverse ions on the determination of silver. Silver taken, 10 μg

Ion added	Molar ratio, [ion added]:[Ag(I)]
Nitrate, fluoride, EDTA, Co(II), Ni(II), Al(III), acetate, citrate, tartrate	>10000*
Cd(II), Cr(III), phosphate, Fe(III)†	1000
V(V)	500
Perchlorate, Bi(III)	200
Mo(VI), Zn(II), Cu(II), Ga(III), In(III), Cr(VI)	25
W(VI), Fe(III)	5
Hg(II), Au(III), Pd(II)	<1

* Maximum molar ratio tested.

† Limiting ratio tolerated in the presence of fluoride.

Table 3. Recovery of silver by collection with lead chloride

Lead added/ g l^{-1}*	Silver content of sample/ mg l^{-1}	Silver recovered, %†
10.0	100.0	99.8
10.0	10.0	100.5
10.0	1.0	99.2
10.0	0.1	100.3

* Added as lead nitrate.

† Average of five determinations.

Table 4. Determination of silver in lead and lead concentrates

Sample	Silver found/ mg g^{-1}	
	Proposed method*	AAS
Lead 1	5.2	5.2
Lead 2	3.3	3.3
Lead 3	2.7	2.6
Lead 4	1.2	1.2
Lead 5	0.74	0.75
Lead 6	0.01†	0.01
Lead concentrate 1	1.5†	1.5
Lead concentrate 2	1.0†	1.0
Lead concentrate 3	0.92†	0.91
Lead concentrate 4	0.89†	0.88
Lead concentrate 5	0.86†	0.86
Lead concentrate 6	0.63†	0.63

* Average of five determinations.
† Using collection with lead chloride.

The authors thank to the Sociedad Minero-Metalúrgica Peñarroya-España for the kind gift of the metallic lead and lead concentrate samples.

References

1. Koh, T. and Katoh, M., *Anal. Chim. Acta*, 1979, **109**, 107.
2. Markham, J. J., *Anal. Chem.*, 1967, **39**, 241.
3. Mehra, M. C., and Bourque, C., *Analusis*, 1975, **3**, 299.
4. Busev, A. I., and Sheztidesyatnaya, N. L., *Zh. Anal. Khim.*, 1974, **29**, 1138.
5. Bochkareva, I. A., and Blyum, I. A., *Zh. Anal. Khim.*, 1975, **30**, 874.
6. Likussar, W., and Raber, H., *Anal. Chim. Acta*, 1970, **50**, 173.
7. Sheztidesyatnaya, N. L., Kotelyanskaya, L. I., and Chuchulina, I. A., *Zh. Anal. Khim.*, 1975, **30**, 1303.
8. Sánchez-Pedreño, C., Hernández Córdoba, M., and López García, I., *An. Quim.*, 1982, **78**, 252.
9. Ramakrishna, T. V., Aravamudan, G., and Vijayakumar, M., *Anal. Chim. Acta*, 1976, **84**, 369.
10. Prasada Rao, T., and Ramakrishna, T. V., *Analyst*, 1982, **107**, 704.
11. Dagnall, R. M., and West, T. S., *Talanta*, 1961, **8**, 711.
12. Dagnall, R. M., and West, T. S., *Talanta*, 1964, **11**, 1533.

Paper A4/139
Received April 6th, 1984
Accepted June 22nd, 1984

Spectrophotometric Determination of Trace Amounts of Mercury With Phenanthroline and Eosin

Jayateerth R. Mudakavi
Department of Chemical Engineering, Indian Institute of Science, Bangalore-560012, India

A sensitive method has been developed for the determination of mercury (0.2–1.2 p.p.m.) using phenanthroline and eosin in an aqueous medium. The reaction occurs at pH 4.5. Various metal ion interferences have been evaluated.

Keywords: *Mercury(II) determination; spectrophotometry; phenanthroline; eosin*

Owing to the toxicity of mercury in the environment, the determination of trace amounts of mercury has attracted great attention.[1,2] The conventional technique of dithizone extraction is not always favoured because the procedure is cumbersome, sensitive to light and is subject to interferences from other metal ions.[3] Analytical methods based on ternary complex formation seem to offer superior sensitivity and selectivity. A number of ternary systems[4–7] have been proposed for the determination of mercury, among which the tetrabromomercurate(II) - methylene blue system is the most sensitive. However, most of the ternary systems involve an additional extraction step. Colour development and measurement in aqueous solution itself would alleviate this difficulty, leading to a rapid, more accurate and precise analytical method.

A survey of the various ternary systems proposed for mercury revealed that anionic mercury complexes are coupled with cationic dyes to form the ternary complex. On the other hand, the reaction of mercury with neutral ligands and anionic dyes can be utilised to form ternary complexes.

A detailed examination of the reaction of mercury with phenanthroline-type compounds and anionic dyes showed that the colour reaction of mercury, phenanthroline and eosin could be used to advantage with an aqueous finish. This paper describes studies conducted on this system.

Experimental

Apparatus

A Shimadzu Graphicord UV-240 spectrophotometer with 10-mm matched quartz cells and a Toshniwal pH meter with a combined glass electrode was used.

Reagents

All reagents were of analytical-reagent grade unless stated otherwise.

Mercury(II) solution, 1 mg ml^{-1}. Dissolve 0.3385 g of mercury(II) chloride in water and dilute to 250 ml. Dilute an appropriate volume of this solution to provide a 10 p.p.m. solution of mercury(II).

Phenanthroline solution, 0.05%. Dissolve 0.05 g of 1,10-phenanthroline monohydrate in 100 ml of water. Store in an amber-coloured bottle.

Acetate buffer, pH 4.5. Mix 124 ml of 1 N acetic acid with 50 ml of 1 N sodium hydroxide solution and dilute to 500 ml with distilled water. Adjust the final pH of the solution to 4.50.

Eosin solution, 0.05%. Dissolve 0.125 g of eosin (C.I. 45380) in water and dilute to 250 ml.

EDTA solution, 0.05 M. Dissolve 1.8615 g of EDTA in 100 ml of distilled water.

Gelatine solution, 0.05%. Dissolve 0.025 g of gelatine in 50 ml of hot water. Prepare fresh daily.

Procedure

To a series of solutions containing 5–30 μg of mercury(II) add 1.0 ml of 0.05 M EDTA solution, 5 ml of pH 4.5 buffer, 2 ml of 0.05% 1,10-phenanthroline solution and 1 ml of 0.05% gelatine solution. Mix the contents well and add 5 ml of 0.05% eosin solution. Again mix the solutions and dilute to 25 ml. Measure the absorbance of the samples in 10-mm cells at 552 nm against a reagent blank. Prepare a calibration graph for 5–30 μg of mercury.

Develop the colour similarly for the unknown and determine its concentration by refering to the calibration graph.

Results and Discussion

Preliminary studies of the reaction of mercury, 1,10-phenanthroline and eosin indicated that the reaction proceeded immediately after mixing the reagents. However, owing to the colloidal nature of the products, precipitation from both the sample and the reagent blank occurred on standing. Addition of poly(vinyl alcohol) or sodium carboxymethylcellulose stabilised the colour system, but under these conditions the absorbance decreased slowly over a period of time. Gelatine, on the other hand, solubilised the precipitate and allowed the absorbance to remain constant for more than 6 h. To avoid the precipitation, therefore, gelatine was added before the addition of eosin.

Fig. 1 shows the absorption spectra of varying concentrations of the mercury - 1,10-phenanthroline - eosin complex at pH 4.5. The interaction between mercury and the reagents proceeds with a bathochromic shift. The complex showed an absorption maximum at 550 nm and the maximum absorbance difference between the complex and the reagent was at 552 nm.

Effect of Experimental Variables

The optimum pH for the reaction was examined over the pH range 1.0–8.0. To a series of solutions containing 25 μg of mercury(II) solution in 25-ml beakers, 1 ml of 0.05 M EDTA solution, 2 ml of 0.05% 1,10-phenanthroline solution, 1 ml of 0.05% gelatine solution and 5 ml of 0.05% eosin solution were added and the pH was adjusted to cover the range 1.0–8.0 using dilute hydrochloric acid or sodium hydroxide solution and a pH meter. The absorbances of these solutions, diluted to 25 ml, were measured against blanks at 552 nm. Fig. 2 shows that maximum complex formation occurs over the pH range 4.3–4.7 As the absorbance of the reagent blank also varies with pH (Fig. 3), it is necessary that the pH of the sample and reference should be very close. A pH of 4.50 was maintained in all subsequent investigations, by using an acetate buffer of 0.1 M concentration. As the reaction was unaffected in the presence of EDTA, it was decided to add 1.0 ml of 0.05 M EDTA solution to all samples to suppress the interferences of any other foreign metal ions.

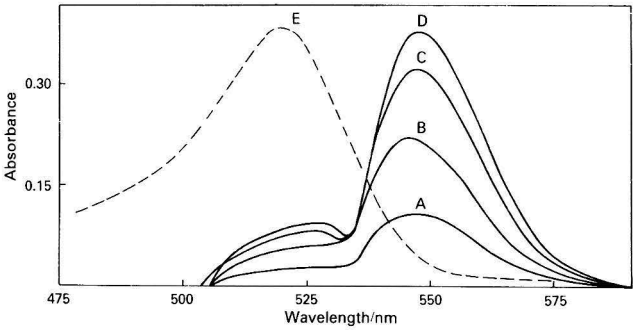

Fig. 1. Absorption spectra of Hg(II) complexes for varying concentrations of Hg(II). A: Hg(II), 5 μg; EDTA solution, 1 ml; 1,10-phenanthroline solution, 2 ml; gelatine solution, 1 ml; buffer solution, 5 ml; and eosin solution, 5 ml in 25 ml; 10-mm cells. B–D, as A but with 15, 20 and 25 μg of Hg(II), respectively

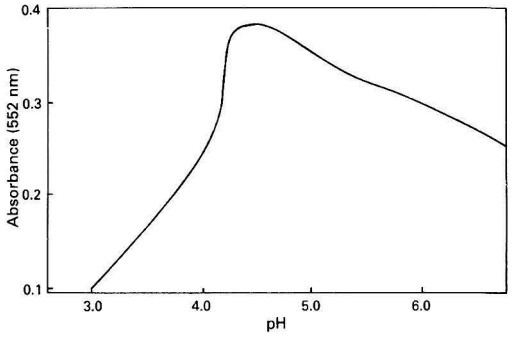

Fig. 2. Effect of pH on absorbance. Conditions: Hg(II), 25 μg; EDTA solution, 2 ml; 1,10-phenanthroline solution, 1 ml; gelatine solution, 1 ml; buffer solution, 5 ml; and eosin solution, 5 ml in 25 ml; 10-mm cells

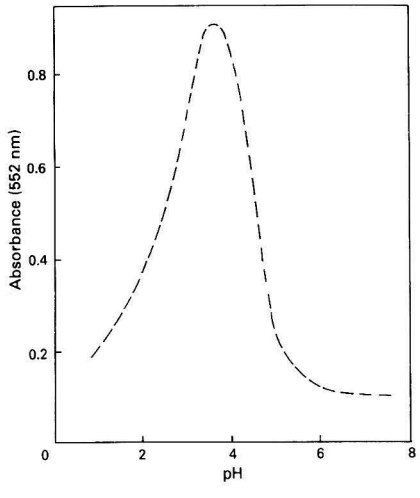

Fig. 3. Variation of absorbance of reagent blank with pH. Conditions as in Fig. 2, except no Hg(II) and using 5-mm cells

The influence of 1,10-phenanthroline was investigated next. To a series of solutions containing 25 μg of mercury(II), 5 ml of pH 4.5 acetate buffer, 1 ml of 0.05 M EDTA solution and varying volumes of 0.05% 1,10-phenanthroline solution were added. Colour development was completed by adding 1 ml of 0.05% gelatine solution and 5 ml of 0.05% eosin solution and diluting to 25 ml. When the volume of 1,10-phenanthroline solution added was 2 ml or greater, the absorbance attained a constant maximum value. However, at volumes greater than 2 ml, a tendency for precipitation to occur was shown by the blank. A volume of 2 ml was therefore considered to be optimal and was maintained in subsequent investigations.

To determine the effect of eosin, a similar experiment was carried out by varying the dye concentration. The absorbance of the complex reached a maximum at 3.5 ml of 0.05% eosin solution and remained constant when larger volumes were used. A volume of 5 ml of the dye was added in all further experiments.

The order of addition was not critical except that when the gelatine was added after the reagents the reproducibility became poor. Therefore, in subsequent work the gelatine was added before introducing the dye solution.

Beer's Law and Precision

Beer's law was obeyed over the range 5–30 μg of mercury in a final volume of 25 ml. Under the conditions described the molar absorptivity was 8.0×10^4 l mol^{-1} cm^{-1} for mercury. The Sandell sensitivity corresponding to 0.001 absorbance was 6 ng cm^{-2}. The relative standard deviation for ten determinations of 25 μg of mercury was 0.053%.

Nature of the Complex

Phenanthroline coordinates readily with mercury(II) to form mono, bis and tris complexes. Bisphenanthroline - mercury(II) complexes of the type HgX_2B_2 precipitate on mixing ethanolic solutions of phenanthroline and mercury(II) halide.[8] A trisphenanthroline - mercury(II) complex has been isolated as the perchlorate salt from aqueous solution.[9] Under the experimental conditions, as an excess of 1,10-phenanthroline is present only bis and tris complexes are expected to be predominant. Further, addition of perchlorate salt did not precipitate the complex but an ethanolic solution of 1,10-phenanthroline did precipitate the mercury, indicating that the experimental conditions are favourable for the formation of the bis complex,[10] *viz.*, $HgCl_2(o\text{-phen})_2$, $\log \beta_2 = 19.65$.

The ratio of eosin to mercury was determined to be 1 : 1 by the molar ratio and Job's continuous variations methods.

Hence the complex appears to have empirical composition $[Hg(o\text{-phen})_2]R$, where R represents a divalent eosin anion. This stoicheiometry was further confirmed by employing Adron's[11] modified procedure, with which he showed that for any two reacting species A and B forming a coloured product A_1B_1 the plot of 1/absorbance *versus* 1/reagent concentration would be a straight line, provided that reagent concentration is high. In the present work the graph of 1/absorbance *versus* 1/[eosin] was linear and the apparent formation constant of the complex was calculated to be 4.7×10^3, which shows that the complex is weak and that a large excess of reagent is necessary for the reaction to go to completion.

Interference of Foreign Ions

The interference of various ions in the determination of 25 μg of mercury was determined by carrying out the reaction according to the recommended procedure in the presence of 1.0 mg of the desired metal ion. The results are summarised in Table 1.

Among the anions, thiocyanate and cyanide interfered seriously. The interference of Al(III), Ti(IV), Mn(II) and V(V) was overcome by the addition of 1 ml of 0.1 M sodium fluoride solution. The interference due to Bi(III), Cr(VI) and Mo(VI) could be removed with 1 ml of 0.1 M citric acid. Tungsten(VI) did not affect the determination of mercury when tartaric acid was present. Up to 100 μg of Cu(II) and Co(II) could be extracted by solvent extraction with 8-hydroxyquinoline in chloroform. The tolerance limits for other ions were Zn 20, Ni 45 and Pb 4 p.p.m.

Table 1. Results of interference studies

Interferent	Interference
Li(I), Ca(II), Sr(II), Ba(II), Mg(II), Be(II), U(VI), Cr(III), Fe(III), Tl(III), La(III), Ce(IV), Zr(IV), Pt(IV), Pd(II), Se(IV), Te(IV), As(V), sulphate, sulphite, borate, fluoride, oxalate, citrate, tartrate, nitrate, chloride, bromide	No interference
Cyanide, thiocyanate, iodide, Mo(VI), Tl(I), Bi(III)	Interfere by decreasing the absorbance
Mn(II), Al(III), Cr(VI), Pb(II), Zn(II), Th(IV), Sb(V), Co(II), Ni(II), Cu(II), V(V), W(VI), Ti(IV)	Interfere by increasing the absorbance

Application of the Method

The validity of the method was checked by analysing a factory effluent containing mercury and synthetic sea-water samples by the standard additions technique. The results shown in Table 2 are in good agreement with the expected values.

Conclusions

The proposed method is simple, sensitive and rapid. It is less laborious and less sensitive to light than the dithizone method. The few interferences encountered can be eliminated by simple masking and extraction techniques.

References

1. Ure, A. M., *Anal. Chim. Acta*, 1975, **76**, 1.
2. Chilov, S., *Talanta*, 1975, **22**, 206.
3. Sandell, E. B., "Colorimetric Methods of Analysis," Interscience, 1959, p. 445.
4. Lebedeva, S. P. A., *Arm. Khim. Zh.*, 1975, **25**, 303.
5. Tanaka, T., *Chem. Pharm. Bull.*, 1978, **26**, 3139.
6. Shestidesyatnya, N. L., Voronich, O. G., and Motyl, V. A., *Zh. Anal. Chim.*, 1977, **32**, 260.
7. Kovalenko, A. A., Uvaroa, K. A., Usatenko, Yu. I., and Zubtsova, T. I., *Zh. Anal. Khim.*, 1977, **32**, 270.
8. Sutton, G. J., *Aust. J. Chem.*, 1952, **12**, 637.
9. Schilt, A. A., and Taylor, R. C., *J. Inorg. Nucl. Chem.*, 1958, **9**, 211.
10. Anderegg, G., *Helv. Chim. Acta*, 1963, **46**, 2397.
11. Adron, M., *J. Chem. Soc.*, 1957, 1811.

Paper A3/184
Received June 23rd, 1983
Accepted July 6th, 1984

Table 2. Determination of mercury in a factory effluent and in synthetic sea water

Effluent			Synthetic sea water		
Added/μg	Found/μg	Recovery, %	Added/μg	Found/μg	Recovery, %
0	7.5	—	0	0	—
5	12.0	96	10	9.4	94
10	16.5	95	15	14.5	97
15	23.0	102	30	29.2	97

Extraction - Fluorimetric Determination of Mercury With 2-Phenylbenzo[8,9]quinolizino[4,5,6,7-*fed*]phenanthridinylium Perchlorate

Tomás Pérez-Ruiz, Joaquín A. Ortuño and Concepción Sánchez-Pedreño*
Department of Analytical Chemistry, Faculty of Sciences, University of Murcia, Murcia, Spain

The characteristics of 2-phenylbenzo[8,9]quinolizino[4,5,6,7-*fed*]phenanthridinylium perchlorate (PQPP) as a reagent for the formation of ion-association complexes with metal - bromide anions and its application to the fluorimetric determination of mercury are described. This reagent forms a 1 : 1 complex with $HgBr_3^-$ that is slightly soluble in water and can be extracted with butyl acetate. The influence of the acidity, bromide ion concentration and foreign ions were investigated. Mercury can be determined in the range 1.5–15 ng ml^{-1}. The stoicheiometry and apparent stability constant of the complex were determined. The method is applicable to the determination of mercury in sphalerites and organomercurials in cleaning solutions for contact lenses.

Keywords: *2-Phenylbenzo[8,9]quinolizino[4,5,6,7-fed]phenanthridinylium perchlorate; spectrofluorimetry; mercury determination; organomercurials determination; sphalerite*

The determination of small amounts of mercury, present in both organic and inorganic combinations, is of interest in contamination analysis and geochemical prospecting. Many methods have been developed for the determination of mercury,[1–5] but there is still a need for more simple, sensitive and selective methods that will allow samples to be analysed without removing interferences.

A recent fluorimetric reagent, 2-phenylbenzo[8,9]-quinolizino[4,5,6,7-*fed*]phenanthridinylium perchlorate (PQPP) forms ion-association complexes with a small number of metal - halogen ions. These complexes may be used for the fluorimetric determination of the metal after extraction with the appropriate solvents. The formation and extraction of metal - chloride complexes and its application to the fluorimetric determination of gold(III) and thallium(III) have been reported.[6,7]

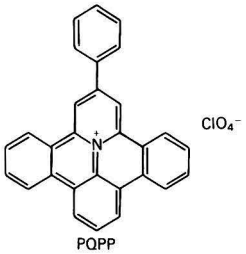

PQPP

This paper discusses the formation and extraction of metal - bromide complexes with PQPP and a selective fluorimetric method for the determination of trace amounts of mercury is proposed. This method is more sensitive than other fluorimetric,[5] spectrophotometric[5] and conventional atomic-absorption[1] methods for the determination of mercury.

Experimental

Apparatus

Fluorescence spectra and quantitative spectrofluorimetric measurements were obtained with a Perkin-Elmer Model 3000 spectrofluorimeter, equipped with a quantum counter. Excitation spectra were corrected, but emission spectra were not. A Perkin-Elmer Model 240B elemental analyser, a Perkin-Elmer 177 grating infrared spectrophotometer, a Hewlett-Packard 5980A mass spectrometer and a Varian FT-80 nuclear magnetic resonance spectrometer were used for identification of PQPP.

Reagents

All inorganic chemicals used were of analytical-reagent grade. Acetophenone, benzaldehyde (Aldrich) and butyl acetate (Merck) were used as received. Doubly distilled water was used exclusively.

2-Phenylbenzo[8,9]*quinolizino*[4,5,6,7-fed]*phenanthridinylium perchlorate*. This was synthesised from 1,2,4,6-tetraphenylpyridinium perchlorate (TPPP) by dissolution in methanol and irradiation with a UV lamp, as described previously.[6]

2-Phenylbenzo[8,9]*quinolizino*[4,5,6,7-fed]*phenanthridinylium perchlorate solution*, 5×10^{-5} M. Prepared by dissolving 0.012 g of the reagent in 500 ml of ethanol. The solution is stable for several weeks.

Mercury(II) standard solution, 0.01 M. Prepared by dissolving mercury(II) nitrate in 0.1 M nitric acid and standardised by titration with EDTA.[8] Working standards were prepared from this solution as required.

Procedure for Determination of Mercury(II)

To a volume of sample solution in a separating funnel containing up to 750 ng of mercury(II) add 1 ml of 10 N sulphuric acid, 1 ml of 0.4 M sodium bromide solution and 3 ml of 5×10^{-5} M PQPP solution. Dilute to 50 ml with doubly distilled water and extract the mixture with 5 ml of butyl acetate. Shake the funnel vigorously for 2 min, allow the phases to separate for 10 min, then transfer the organic layer into a centrifuge tube and centrifuge it to give a water-free organic layer. Activate at 300 nm and read the fluorescence of the complex at 460 nm. Under the recommended conditions, the calibration graph is linear over the range 64–640 ng of mercury per 5 ml of butyl acetate.

* To whom correspondence should be addressed.

Table 1. Extraction efficiencies of metal - bromide complexes with PQPP in butyl acetate. Conditions: sodium bromide concentration, 0.008 M; sulphuric acid concentration, 0.2 N; PQPP concentration, 3×10^{-6} M; ratio of aqueous phase to butyl acetate, 10 + 1 (*V/V*)

Metal ion	Extraction, %	Metal ion	Extraction, %
Au(III)	100	Bi(III)	0.4
Tl(III)	100	Pb(II)	0.08
Hg(II)	85.5	Cu(II)	0.007
Ag(I)	14.0	Cd(II)	0.003
In(III)	1.3	Fe(III)	0.001

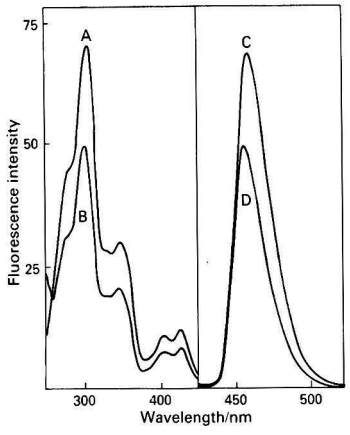

Fig. 1. Excitation (A and B) and emission (C and D) spectra of A and C, mercury complex ($PQP^+ HgBr_3^-$) in butyl acetate, and B and D, reagent in ethanol

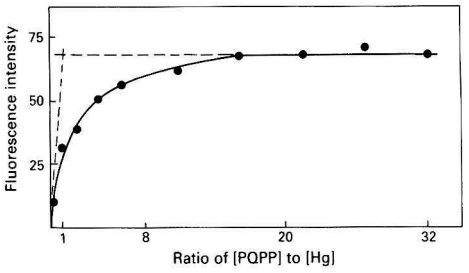

Fig. 2. Stoicheiometry of mercury - PQPP complex determined by the molar ratio method. Mercury(II) concentration, 7.13×10^{-8} M

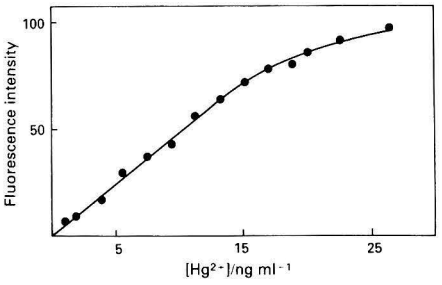

Fig. 3. Calibration graph for mercury

Results and Discussion

Preliminary Studies

PQPP reacts with some metal ions in an acidic medium containing an excess of bromide ion to form ion-association complexes that can be extracted into butyl acetate. The extraction efficiencies of these complexes under the selected conditions are shown in Table 1. Gold(III), mercury(II) and thallium(III) have high extraction efficiencies whereas other metal ions are only slightly extracted.

The extraction efficiencies of the corresponding metal - chloride complexes with PQPP are also high for gold(III) and thallium(III) and low for mercury.[6,7] Therefore, the study of the bromide - mercury(II) system seems to be interesting for the determination of mercury whereas there is no advantage with respect to sensitivity with the use of bromide - thallium(III) and gold(III) complexes over chloride - metal complexes for the determination of these two ions.

Fluorescence Spectra

The excitation and emission spectra of the reagent (in ethanol) and $PQP^+ HgBr_3^-$ (in butyl acetate) are shown in Fig. 1. The excitation spectra have maxima at 300, 346 and 428 nm and the emission spectra have maxima at 460 nm.

Effect of Acidity

The effect of acidity on the formation of the $PQP^+ HgBr_3^-$ complex and its extraction into butyl acetate was studied using fixed concentrations of mercury(II) (12 ng ml^{-1}), sodium bromide (0.008 M) and PQPP (3×10^{-6} M) and varying the sulphuric acid concentration from 0.001 to 2 N. The maximum fluorescence intensity was obtained with a 0.2 N sulphuric acid concentration.

Effect of Bromide Ion Concentration

The influence of the bromide ion concentration was studied using 12 ng ml^{-1} of mercury(II) solution in 0.2 N sulphuric acid and sodium bromide solutions ranging from 0.001 to 0.015 M. Increasing the bromide ion concentration in this range caused an increase in fluorescence intensity with a maximum at 0.008 M, the intensities decreasing again at higher bromide concentrations.

Composition of the Complex

To establish the composition of the complex, the continuous variation[9,10] and molar ratio[11] methods were applied. The molar ratio of mercury to PQPP was found to be 1 : 1 by these two methods. Fig. 2 shows that a molar ratio of [PQPP] to [Hg(II)] of higher than 16 is necessary for the complete formation and extraction of the complex. The apparent stability constant of the complex was calculated from the results of the molar ratio and continuous variation methods by the procedures of Momoki *et al.*[12] and Likussar and Boltz[13] and an average value of log $K = 7.9 \pm 0.1$ at 20 °C was obtained.

Extraction Efficiency and Stability

The selected ratio of aqueous phase to butyl acetate was 10 + 1 (*V/V*) and the extraction efficiency was 85.5%.

The fluorescence intensities of the complex extracted into butyl acetate remained constant for 24 h.

Table 2. Interference of other ions in the determination of mercury. Concentration of mercury(II), 15 ng ml^{-1}

Ion added	Molar ratio, [ion added]/[Hg(II)]	Ion added	Molar ratio, [ion added]/[Hg(II)]
Bi(III)	10	Pt(IV)	1
Cd(II)	1000	Ag(I)	0.2
Cr(III)	10^4	Tl(III)	0.02
Cu(II)	500	Zn(II)	10^5*
Au(III)	0.02	Chloride	10^5
In(III)	2	Nitrate	1000
Fe(III)	5000	Perchlorate	100
Pb(II)	50	Sulphate	10^6*
Mn(II)	50		

* Maximum molar ratio tested.

Table 3. Determination of mercury and organomercurials in sphalerite and cleaning solutions for contact lenses

Sample	Content	Found, %
Sphalerite	0.064% of mercury*	0.067
Cleaning solutions for contact lenses:		
1	0.004% of sodium ethylmercurithiosalicylate† (thiomersal)	0.0045
2	0.0033% of phenylmercury nitrate†	0.0031

* Value obtained by atomic-absorption spectrometry.
† Certified by Laboratory Pharmaceuticals.

Effect of Shaking Time

The extraction of the complex into butyl acetate was rapid and no change was observed when the shaking time was varied from 1 to 4 min.

Calibration Graphs, Sensitivity and Precision

The slope of the calibration graphs increases with increase in mercury concentration and, under the recommended conditions, the calibration graph was linear over the concentration range 1.5–15 ng ml^{-1} (Fig. 3).

The standard deviations for 15 and 8 ng ml^{-1} of mercury(II) (ten determinations each) were 0.65 and 0.51 ng ml^{-1}, respectively, and the relative errors were 3.1 and 4.5%, respectively.

Effect of Other Ions

In the determination of 15 ng ml^{-1} of mercury(II), extraneous ions can be tolerated at the levels given in Table 2. The limiting value of the concentration for each ion was taken as that value which caused an error of not more than 4% in the fluorescence intensity. Cations were added as chlorides, nitrates or sulphates, and anions in the form of sodium or potassium salts.

Positive interferences are attributed to the fact that the elements concerned also form ion-pair compounds with the reagent in sodium bromide media and so are slightly extracted into the organic solvent. Thallium, gold and silver cause the largest interferences.

Applications

The method has been applied satisfactorily to the determination of mercury in different materials that contain trace amounts of mercury present in organic or inorganic combinations.

Determination of Mercury in Sphalerites

A suitable amount (0.1 g) of sample was dissolved in aqua regia, then sulphuric acid was added and the solution was boiled until white fumes were evolved. After transferring the solution into a 200-ml calibrated flask and diluting to volume with doubly distilled water, a suitable volume (2 ml) of solution was treated following the recommended procedure. The results are given in Table 3.

Determination of Organomercurials in Cleaning Solutions for Contact Lenses

A suitable volume (1 ml) of sample was taken in a 200-ml calibrated flask, 20 ml of 10 N sulphuric acid were added and the solution was diluted to volume with doubly distilled water. Bromine vapour was added, the mixture was allowed to stand for 2 min then an air current was passed through the solution for 5 min to remove the bromine. A suitable volume (5 ml) of solution was treated following the recommended procedure. The results are given in Table 3.

Conclusions

PQPP was found to be satisfactory for the fluorimetric determination of mercury by the formation of an ion-association complex that is extracted into butyl acetate. This method could be particularly useful in routine analytical work for the determination of mercury without a prior separation procedure.

References

1. Chilov, S., *Talanta*, 1975, **22**, 205.
2. Mercury Analysis Working Party of BITC, *Anal. Chim. Acta*, 1974, **72**, 37; 1976, **84**, 231.
3. Analytical Methods Committee, *Analyst*, 1965, **90**, 515.
4. López-Rivadulla, M., and Fernández, E., *Quim. Anal.*, 1976, **30**, 251.
5. Snell, F. D., "Photometric and Fluorimetric Methods of Analysis, Part 1," Wiley, New York, 1978, p. 101.
6. Pérez-Ruiz, T., Sánchez-Pedreño, C., Ortuño, J. A., and Molina-Buendía, P., *Analyst*, 1983, **108**, 733.
7. Pérez-Ruiz, T., Ortuño, J. A., and Molina, P., *Microchem. J.*, in the press.
8. Přibil, R., Körös, E., and Barcza, L., *Acta Pharm. Hung.*, 1957, **27**, 145.
9. Job, P., *Justus Liebigs Ann. Chem.*, 1928, **9**, 113.
10. Irving, H., and Pierce, T. B., *J. Chem. Soc.*, 1959, 2565.
11. Yoe, J. H., and Jones, A. L., *Ind. Eng. Chem., Anal. Ed.*, 1944, **16**, 111.
12. Momoki, K., Sekino, J., Sato, H., and Yamaguchi, N., *Anal. Chem.*, 1969, **41**, 1286.
13. Likussar, W., and Boltz, D. F., *Anal. Chem.*, 1971, **43**, 1265.

Paper A4/164
Received April 25th, 1984
Accepted June 5th, 1984

Fluorimetric Determination of Aluminium With Morin After Extraction With Isobutyl Methyl Ketone

Part I. Fluorescence of the Aluminium - Morin Complex in an Isobutyl Methyl Ketone - Ethanol - Water System

F. Hernandez Hernandez and J. Medina Escriche
Analytical Chemistry, University College of Castellón, University of Valencia, Castellón de la Plana, Spain

A method for the fluorimetric determination of aluminium with morin (3,5,7,2',4'-pentahydroxyflavone) in an isobutyl methyl ketone (IBMK) - ethanol - water system is proposed, with a 3- to 4-fold increase in sensitivity over the conventional method. The optimum conditions were found to be as follows: 40% of IBMK, 20% of an aqueous solution containing the aluminium and HCl - KCl to adjust the pH and 40% of methanol - ethanol - water (86 + 9 + 5) solution, which is necessary for the dispersion of the IBMK in water, and in which the reagent, morin, is dissolved. The optimum pH is 3.7–3.8 (HCl - KCl buffer) and the fluorescence is measured after 1 h at 495 nm, with excitation at 418 nm, at 25 °C.

Using a morin concentration of 0.005%, the calibration graph is linear for concentrations up to 40 p.p.b., and the limit of detection of the method is 0.2 p.p.b. A study of 17 interfering ions showed that the most important interferences are due to Be^{2+}, Zn^{2+}, Pb^{2+}, Fe^{3+}, Cu^{2+} and F^-, and in most instances it was found that the tolerance limits are higher than with the conventional method for the determination of aluminium with morin.

Keywords: *Aluminium determination; fluorescence analysis; aluminium - morin complex; isobutyl methyl ketone - ethanol - water*

Various methods for the fluorimetric or spectrophotometric determination of metals using the extraction of metal complexes with morin in different organic solvents have been proposed. Ga, Mo, V and Fe have been determined in this way after extraction of their complexes in chloroform, isobutyl methyl ketone (IBMK), pentanol or isoamyl alcohol.[1–4] IBMK has been widely used for the extraction of aluminium, usually as a complex with quinolin-8-ol, especially in water analysis.[5,6]

This paper reports part of a complete study that includes the fluorimetric determination of Al with morin after extraction in IBMK, and subsequent dispersion of IBMK in ethanol - water, using as calibration standards determination in IBMK - ethanol - water without extraction. In this paper the fluorescence of the Al - morin complex in the presence of 40% IBMK, which is dispersed in water using 40% of ethanol - methanol - water (86 + 9 + 5) solution, is reported. Also, the fact that ethanol - methanol enhances the quantum yield of the fluorescent reaction of aluminium with morin[7] meant that a method for the fluorimetric determination of aluminium in an IBMK - ethanol - water system could be developed with a 3- to 4-fold increase in sensitivity compared with the conventional method proposed by Will.[8]

Morin was chosen because it is a reagent widely used in the fluorimetric determination of aluminium, and because comparative studies have shown that morin is the most sensitive reagent.[9–11]

Experimental

Apparatus

Fluorescence intensity (I_F) measurements were made on a Perkin-Elmer Model 3000 spectrofluorimeter with a Termotronic S-389 thermostat, which measures temperature to ±0.5 °C.

pH was measured using a Crison Model Digilab 517 pH meter (pH ± 0.001).

Reagents

Analytical-reagent grade chemicals (Merck) were used, and the water used to prepare solutions was distilled and deionised.

A stock solution of Al was prepared by dissolving 0.1758 g of $AlK(SO_4)_2.12H_2O$ in water, adding 1 ml of H_2SO_4 (1 : 1) and diluting to 1 l.

Morin solution was prepared by dissolving 0.0125 g of the reagent in 100 ml of ethanol containing 9% of methanol and 5% of water.

General Procedure

A 20-ml volume of IBMK and 20 ml of the morin solution were placed in a 50-ml beaker and an aliquot of the aluminium solution was added. The pH was adjusted to different values using HCl and NaOH solutions and various buffers. The mixture was then diluted to 50 ml with water. The I_F was measured at various temperatures at a wavelength of 495 nm, with excitation at 418 nm, and the stability of the system over a period of time was studied.

Results and Discussion

Firstly, the solubility of IBMK in the ethanol - water medium was studied, using proportions of IBMK between 5 and 40%. The concentration of ethanol that was necessary to disperse the IBMK varied in each instance, from 25 to 40%, and below this level the two phases appeared separately. The necessary volume of ethanol was introduced with the morin solution.

Fig. 1 shows the excitation and emission spectra of the Al - morin complex (I) and Al - morin in the presence of IBMK

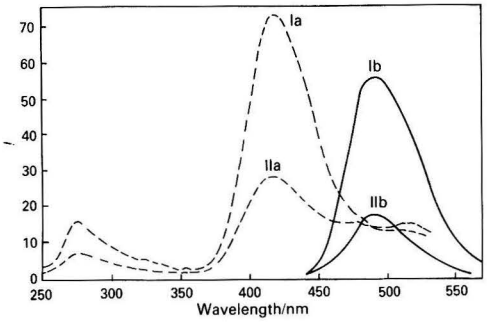

Fig. 1. (a) Excitation and (b) emission spectra of I, aluminium - morin/IBMK - ethanol - water and II, aluminium - morin. Conditions: aluminium, 5 p.p.b.; morin, 0.005%; IBMK, 40%

(II). It can be seen that the presence of IBMK - ethanol does not cause any shift in the wavelengths, although a clear hyperchromic effect does take place as the I_F of the Al - morin complex is 3–4 times greater in the presence of IBMK - ethanol. In both instances the maximum fluorescence is obtained at 495 nm with excitation at 418 nm.

Effect of pH

The effect of pH was studied over a range from 1 to 10, adjusted by means of HCl and NaOH solutions. Fig. 2 shows the relation between I_F and pH for different measurement times; the graph shows that the maximum fluorescence intensity is obtained at a pH between 2 and 3 in all instances. However, for pH values below 3.5 it was found that the I_F of the complex was very unstable and decreased considerably with time. Fig. 3 shows the variation of fluorescence with time at different pH values; it is concluded that the fluorescence hardly varies after 1 h at pH $\geqslant$3.5. Although the maximum fluorescence was obtained at pH 2–3, the instability of the system was the reason why higher pH levels were tested in order to find the optimum range, even though there was some sacrifice of sensitivity.

After pH levels near to 3.5 had been chosen, HCl - KCl was utilised to adjust the pH in the range between 2.90 and 4.10 in order to determine the optimum pH of the system. Fig. 4 shows the fluorescence of the Al - morin complex in IBMK - ethanol - water at different pH values adjusted with HCl - KCl, and also the variation of fluorescence with time; pH values below 3.5 could not be used because it would be necessary to place severe restrictions on the measurement time. pH 3.7–3.8 was chosen because here the system is stable with time and rigorous control of pH is not required. Variations between 3.55 and 3.95 can be tolerated if the measurements are made after 1 h, with very little variation in fluorescence. The blanks (morin - IBMK - ethanol - water), however, are stable at all of the pH values tested.

Effect of Temperature

The effect of temperature on the I_F of the Al - morin complex in the presence of IBMK was studied. No great differences in fluorescence were observed with temperature variations between 15 and 40 °C, unlike the Al - morin complex in the absence of IBMK, which is very sensitive to variations in temperature.[12] Fig. 5 shows the variation of I_F with temperature for a fixed measurement period of 1 h.

However, it should be pointed out that the behaviour of the fluorescence system is not identical at the various temperatures studied. At temperatures below 25 °C the fluorescence decreases gradually with time, whereas at higher temperatures a slight increase in I_F is observed. At 25 °C there is first a slight decrease in I_F, but this becomes completely stable 1 h after the addition of the reagents. A temperature of 25 °C, with a measuring time of 1 h, was therefore chosen for subsequent experiments, owing to the greater stability of the system under these conditions (Fig. 6).

Recommended Procedure

After optimising the above experimental parameters the following procedure can be recommended. Place 20 ml of IBMK and 20 ml of 0.0125% morin solution in a 50-ml beaker and add an aliquot of aluminium solution, with a final content between 0.01 and 2 μg. Adjust the pH to 3.7–3.8 with HCl - KCl and dilute the mixture to 50 ml with water. After 1 h measure the I_F at 25 °C, with emission at 495 nm and excitation at 418 nm.

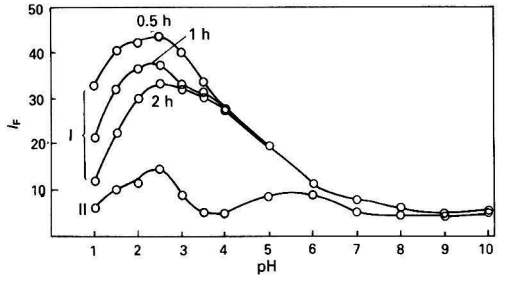

Fig. 2. Effect of pH on the aluminium - morin/IBMK - ethanol - water system. I, Aluminium (5 p.p.b.) - morin/IBMK - ethanol - water; II, morin - IBMK - ethanol - water

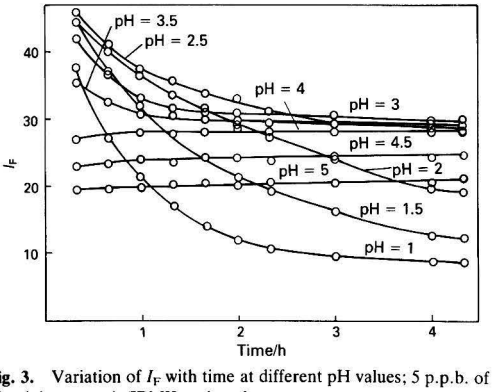

Fig. 3. Variation of I_F with time at different pH values; 5 p.p.b. of aluminium - morin/IBMK - ethanol - water

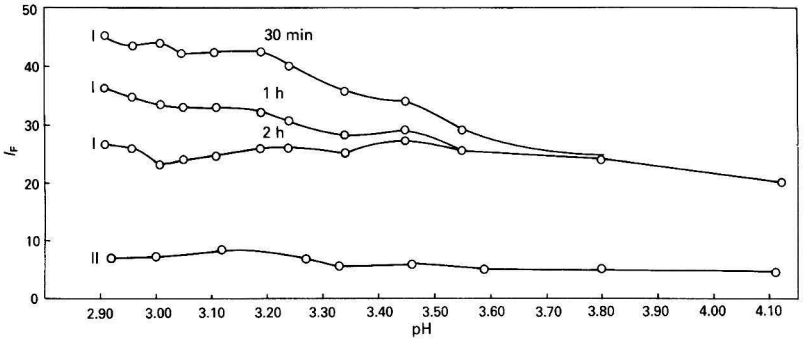

Fig. 4. Variation of I_F with pH at different times. I, Aluminium (5 p.p.b.) - morin/IBMK - ethanol - water; II, morin/IBMK - ethanol - water

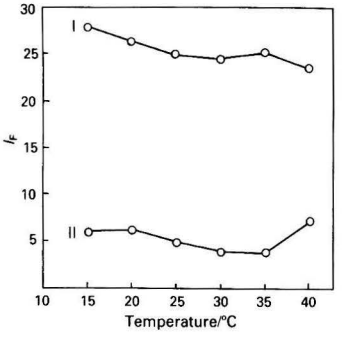

Fig. 5. Effect of temperature. I, Aluminium (2 p.p.b.) - morin/IBMK - ethanol - water; II, morin/IBMK - ethanol - water

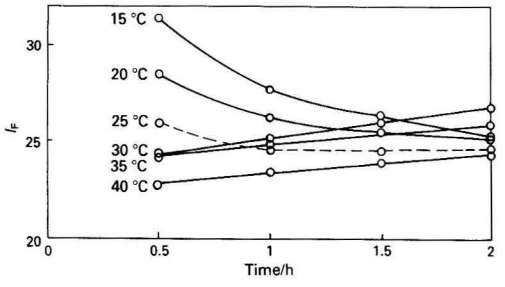

Fig. 6. Variation of I_F with time at different temperatures; 2 p.p.b. of aluminium - morin/IBMK - ethanol - water

Analytical Characteristics

Range of applicability

The linearity range of the method was studied by constructing various calibration graphs. Good correlation coefficients were obtained with a linear fluorescence response at aluminium levels up to 40 p.p.b.

Precision

The standard deviation, s, for the analysis of 12 replicates of a solution containing 2 p.p.b. of Al was equivalent to 0.1 p.p.b. (relative standard deviation $s_r = 5\%$). When the content was increased to 30 p.p.b., s_r was 1%.

Detection limit

The detection limit, defined as the minimum concentration of the analyte that can be detected and differentiated from the blank,[13] is given by the equation $C_L = Ks_{bl}/S$, where K is a numerical factor chosen according to the confidence level desired, s_{bl} is the standard deviation of the blank measurements and S is the sensitivity of the calibration graph. A value of 3 for K is recommended, and in a practical sense the $3s_{bl}$ value usually corresponds to a confidence level of about 90%. The detection limit was 0.2 p.p.b., considerably lower than those reported for the Al - morin system (5 and 1 p.p.b.),[10,14] and identical with that for the Al - morin complex sensitised by the addition of non-ionic surfactants.[15]

Interferences

Interferences were studied using a solution with an Al content of 2 p.p.b. (Table 1). The tolerance in the I_F measurements was taken to be the same as the relative standard deviation of the method, *i.e.*, an interference is tolerated if its effect on the fluorescence signal is less than the relative standard deviation. The tolerances for various ions found in the Al - morin system[8] were compared with those obtained with the present Al - morin/IBMK - ethanol - water system. Interferences common to both methods were observed with fluorides, copper and iron. The IBMK - ethanol system, in addition to stabilising the complex, also eliminated interferences from Cr^{3+}, Mg^{2+} and NH_4^+, and greatly increased the tolerance for PO_4^{3-}, in the same way as with the Al - morin system sensitised by the addition of surfactants.[15]

However, there was a considerable increase in the I_F produced by the presence of Zn^{2+} and Pb^{2+} ions. Will[8] did not mention these as interferences.

The effect of the six ions that produced the greatest interference (F^-, Be^{2+}, Cu^{2+}, Fe^{3+}, Pb^{2+}, Zn^{2+}) was studied, increasing the Al concentration to 20 p.p.b. It was discovered that F^-, Cu^{2+} and Fe^{3+}, which have a "quenching" effect on the I_F, maintained their tolerance levels, whereas Zn^{2+}, Pb^{2+} and Be^{2+}, which interfere by increasing the I_F of the system, gave considerably lower interferences, particularly Pb^{2+}, for which the tolerance increased from 80 to 1000 p.p.b.

Table 1. Tolerances to diverse ions

Ion	Limiting concentration, p.p.b. Al - morin	Al - morin/IBMK - ethanol - water
CH_3COO^-	—	>10000
F^-	5	25 (15†)
NO_3^-	—	>10000
PO_4^{3-}	3	800
SO_4^{2-}	>1000	>1000
SiO_3^{2-}	>1000	>5000
Be^{2+}	—	4 (20†)
Ba^{2+}	—	5000
Ca^{2+}	>1000	>5000
Co^{2+}	>1000	>1000
Cr^{3+}	30	>10000
Cu^{2+}	20	50 (70†)
Fe^{3+}	100	70 (60†)
Mg^{2+}	200	>10000
NH_4^+	500	>5000
Ni^{2+}	>1000	>5000
Pb^{2+}	1000	80 (1000†)
Zn^{2+}	>1000	70 (100†)

* Data published by Will[8] for the Al - morin system (2 p.p.b. Al).
† Al, 20 p.p.b.

Conclusion

The proposed method for the fluorimetric determination of aluminium with morin in an IBMK - ethanol - water system allows aqueous standards to be introduced and improves the stability, sensitivity, selectivity and range of applicability compared with the conventional method.

In Part II, the optimum conditions for the extraction of the Al - morin complex in IBMK will be reported; the organic extract is dispersed in water with the help of ethanol - methanol and the I_F measurements are made under the conditions outlined here.

The authors express their thanks to Dr. M. de la Guardia Cirugeda for professional assistance.

References

1. Bradacs, L. K., Feigl, F., and Hecht, F., *Mikrochim. Acta*, 1954, 269.
2. Murata, A., and Yamamuchi, F., *Rep. Fac. Eng. Shiz. Univ. (Jpn.)*, 1958, **9**, 97.

3. Kohara, H., Ishibashi, N., Hamamira, Y., and Ueno, K., *Bunseki Kagaku*, 1966, **15**, 938.
4. Kohara, H., Ueno, K., and Ishibashi, N., *Bunseki Kagaku*, 1966, **15**, 1252.
5. Pinta, M., "Spectrometrie d'Absorption Atomique, Tome II, Application a l'Analyse Chimique," Masson, Paris, 1980.
6. American Public Health Association, American Water Works Association and Water Pollution Control Federation, "Standard Methods for the Examination of Water and Wastewater," Fifteenth Edition, American Public Health Association, Washington, DC, 1981.
7. Babko, A. K., Volkova, A. I., and Get'man, T. E., *Zh. Anal. Khim.*, 1968, **23**, 39.
8. Will, F., *Anal. Chem.*, 1961, **33**, 1360.
9. Paul, A. D., and Gibson, J. A., Jr., *J. Chem. Educ.*, 1962, **39**, 398.
10. Golovina, A. P., Alimarin, I. P., Kuznetsov, D. I., and Filyugina, A. D., *Zh. Anal. Khim.*, 1966, **21**, 163.
11. Babko, A. P., Volkova, A. I., and Get'man, T. E., *J. Anal. Chem. USSR, Engl. Transl.*, 1967, **22**, 842.
12. White, C. E., Mcfarlane, H. C. E., Fogt, J., and Fuchs, R., *Anal. Chem.*, 1967, **39**, 367.
13. IUPAC, "Compendium of Analytical Nomenclature," Pergamon Press, Oxford, 1978.
14. Katyal, M., and Prakash, S., *Talanta*, 1977, **24**, 367.
15. Medina Escriche, J., De la Guardia Cirugeda, M., and Hernandez Hernandez, F., *Analyst*, 1983, **108**, 1386.

Paper A4/126
Received March 27th, 1984
Accepted July 27th, 1984

Determination of Arsenic, Antimony, Bismuth, Cadmium, Copper, Lead, Molybdenum, Silver and Zinc in Geological Materials by Atomic-absorption Spectrometry

John G. Viets, Richard M. O'Leary and J. Robert Clark
US Geological Survey, Box 25046, Denver Federal Center, MS 955, Denver, CO 80225, USA

Arsenic, antimony, bismuth, cadmium, copper, lead, molybdenum, silver and zinc are very useful elements in geochemical exploration. In the proposed method, geological samples are fused with potassium pyrosulphate and the fusate is dissolved in a solution of hydrochloric acid, ascorbic acid and potassium iodide. When this solution is shaken with a 10% *V/V* Aliquat 336 - isobutyl methyl ketone organic phase, the nine elements of interest are selectively partitioned in the organic phase. All nine elements can then be determined in the organic phase using flame atomic-absorption spectrometry. The method is rapid and allows the determination of Ag and Cd at levels down to 0.1 p.p.m., Cu, Mo, and Zn down to 0.5 p.p.m., Pb, Bi and Sb down to 1 p.p.m. and As down to 5 p.p.m. in geological materials.

Keywords: *Atomic-absorption spectrometry; trace metal determination; geological materials; organic separation*

Geochemical exploration for mineral deposits is based on the systematic measurement of elements or groups of elements associated with mineral deposits in rocks, soils, sediments, water and vegetation. Anomalously high concentrations of these elements due to their dispersion by physical and chemical means often delineate target areas worthy of further exploration. As an example, stream sediments may be enriched in base metals many kilometres below their mineralised source in a stream drainage.

As stated by Levinson,[1] to be useful in geochemical exploration analytical methods must be sufficiently accurate and precise for the particular project, be sensitive to detect background levels, and be rapid and inexpensive. For exploration purposes, analytical precision is generally more important than accuracy. Reproducibility is important because the explorationist is primarily concerned with differences in the concentration of an element above the normal background for a particular rock type within the area of study. A reasonable accuracy is, of course, necessary. Although expensive and time-consuming total digestions of silicate constituents of rock, soil or sediment samples will increase the accuracy, the added time and expense are not generally warranted, because most elements derived from a mineralised source are not in the silicate portion of a sample.

Other desirable attributes of an analytical method are multi-element determinations from a single digestion, sensitivity for elements indicative of a variety of mineral deposit types and interference-free determinations for a wide variety of sample matrices. For large regional exploration programmes these attributes are particularly attractive as a given region may have potential for a variety of metal deposit types and include many diverse rock types.

Recently, the USGS has developed a flame atomic-absorption method, which has all of the above desirable features, for the determination of Ag, As, Bi, Cd, Cu, Mo, Pb, Sb and Zn. Over the past 2 years this method has been used for the determination of these metals in thousands of samples collected for mineral resource assessment programmes. Previously, four separate analytical methods were required to determine these nine elements. With the proposed method they may now all be determined using a single digestion and extraction procedure. An experienced analyst can determine all nine elements in as many as 50 samples per day, thus saving considerable time and expense.

The proposed method is similar to a method described by Viets,[2] but is much more useful because As, Sb and Mo can also be determined. As and Sb are extremely useful in the search for disseminated epithermal Au deposits and Au - Ag vein deposits. Instead of a hydrochloric acid - potassium chlorate digestion, a potassium pyrosulphate fusion is used, which adequately digests non-silicate-bound metals, yet does not result in the loss of As and Sb as in the previous method. Interferences due to major elements in the digestion solution are eliminated by extracting the metals of interest from an aqueous phase containing hydrochloric acid, potassium iodide and ascorbic acid into a 10% *V/V* solution of tricaprylylmethylammonium chloride (Aliquat 336) in isobutyl methyl ketone (IBMK). Au and Te, which were extracted using the hydrochloric acid - potassium chlorate digestion, are not quantitatively digested using the potassium pyrosulphate fusion.

During development of the method, experimental extraction curves were prepared to determine the efficiency of extraction of the nine metals into the organic phase as a function of acid concentration. Once the optimum range of acidity had been determined, five replicate analyses of each of six international geochemical reference standards were performed. Values for the nine elements were found generally to show good agreement with published values for the reference samples.

Experimental

Reagents and Apparatus

All chemicals were of analytical-reagent grade. The aqueous reagent solutions were prepared using distilled, de-ionised water. Aliquat 336 was obtained from General Mills Chemical Division, Minneapolis, MN, USA.*

Individual 1000 μg ml^{-1} standards of Ag, As, Bi, Cd, Cu, Mo, Pb, Sb and Zn were prepared in 10 M hydrochloric acid using Specpure metals or metal oxides obtained from Johnson Matthey Chemicals. Standards prepared in other acids, particularly nitric acid, must not be used, as nitrate ions will deactivate the exchange sites on Aliquat 336.

All atomic-absorption measurements were made with a Perkin-Elmer 603 atomic-absorption spectrometer equipped with background correction. As, Bi and Sb were determined using electrodeless discharge lamps and with deuterium arc background correction. Electrodeless discharge lamps were used to determine As, Bi and Sb. All other elements were determined using conventional hollow-cathode lamps. A

* Any use of trade names is for descriptive purposes only and does not imply endorsement by the USGS.

single-slot, 10-cm burner was used with an air - acetylene flame for all elements except Mo, which was determined using a 5-cm dinitrogen oxide burner with dinitrogen oxide - acetylene flame. The operating parameters used were those recommended by the instrument manufacturer, and the burner position, flame conditions and aspiration rates were optimised for maximum absorbance and linear response while aspirating known organic standards.

Procedure

Weigh 0.50 g of powdered sample into a 150 × 16 mm disposable Pyrex test-tube. Add two 1-g scoops of potassium pyrosulphate and mix thoroughly. Fuse the sample over a hot gas burner for 2 min. The flame should be hot but below the temperature that melts or deforms the Pyrex test-tube. After fusing, manipulate the tube to coat the tube walls while the melt is solidifying. Avoid any large accumulation of melt in the bottom of the tube. After the tubes have cooled to room temperature, add 6 ml of 6.0 M hydrochloric acid and place in a boiling water-bath. Mix the contents of the tubes periodically with a vortex mixer until the melt has disintegrated; disintegration usually occurs within 30 min. Allow the samples to cool, add 4 ml of an aqueous solution containing 30% *m/V* ascorbic acid and 15% *m/V* potassium iodide, completely mix on a vortex mixer and allow to stand for 20 min. Accurately add 8.0 ml of a 10% *V/V* Aliquat 336 in IBMK to each tube, cap with silicone-rubber stoppers and shake for 5 min. Centrifuge the samples to separate the organic phase and determine the metal content of the organic phase by atomic-absorption spectrometry.

Samples containing significant amounts of organic matter may bubble excessively during fusion. If the samples are roasted in a muffle furnace for 8 h at 250 °C prior to adding potassium pyrosulphate, bubbling will be reduced. Care should be taken not to exceed 275 °C while roasting because loss of As may occur. No loss of the nine elements was observed for the six geochemical reference samples after roasting at 250 °C for 8 h.

Standard Preparation

Combined acid standards

From the individual 1000 μg ml^{-1} standards, prepare 100 ml of three combined standards in 10 M hydrochloric acid containing the amounts of metal listed in Table 1.

Organic standards

One set of standards should be prepared for approximately every 20 samples. Add 0.50-ml aliquots of combined standard 1, 2 and 3 to each of three 150 × 16-mm test-tubes. Add 5.0 ml of 6.0 M HCl, 0.5 ml of distilled water, 4 ml of 30% *m/V* ascorbic acid - 15% *m/V* potassium iodide reagent and two 1-g scoops of potassium pyrosulphate and mix thoroughly. To each standard add 8.0 ml of 10% *V/V* Aliquat 336 - IBMK solution, cap and shake for 5 min. With each set of standards a reagent blank should be prepared as above except that 6 ml of 6.0 M HCl should be used.

A working blank of 300 ml of 10% *V/V* Aliquat 336 - IBMK solution shaken over 100 ml of 4 M HCl may be used between samples and for burner warm-up. The reagent blank should be used for instrument calibration because it will compensate for any reagent contaminants. Organic standards and unknown organic solutions should be used within 2 d of preparation.

Table 1. Concentrations of each element in 10 M HCl combined standards

Element	Concentration/μg ml^{-1} Standard 1	Standard 2	Standard 3
Ag	2.00	5.00	10.0
As	50.0	100.0	200.0
Bi	20.0	50.0	100.0
Cd	2.00	5.0	10.0
Cu	20.0	50.0	100.0
Mo	20.0	50.0	100.0
Pb	20.0	50.0	100.0
Sb	20.0	50.0	100.0
Zn	50.0	100.0	200.0

Results and Discussion

The method proposed in this paper is similar to a method previously described by Viets.[2] The latter method, however, had the disadvantage that Sb and As, which are extractable into the organic phase and are important "pathfinder" elements in geochemical exploration, were partially lost as volatile chlorides during the sample digestion. The extraction of Mo was not investigated by Viets, but was found to be efficiently extracted in this study.

Investigations were begun to find an alternative sample digestion procedure that would not volatilise As and Sb, yet was rapid and compatible with the organic separation chemistry for the metals determined with the original method. A variety of mineral acid and fusion digestions were tested on six geochemical reference samples, described by Allcott and Lakin,[3] to determine the efficiency of the digestion for the desired elements and their extraction into the organic phase. Except for the digestion, the reagent concentrations and proportion were the same as those used in the original method.

A fusion of 0.50 g of sample with 2 g of potassium pyrosulphate was found to yield values for Ag, Bi, Cd, Cu, Zn, Sb, As and Mo that were in good agreement with published values. Only Pb had values significantly lower than those reported in the literature. Pursuing the potassium pyrosulphate fusion further, the amount of ascorbic acid and potassium iodide used in the original method was reduced by 25% to eliminate the precipitate that was observed at the higher reagent concentration. When the nine elements of interest were again determined in the reference samples using the modified fusion procedure, all nine elements generally showed good agreement with reported values. Lead was apparently lost in the precipitate when using the more concentrated reagents.

As in the development of the original method, extraction curves were prepared to determine the optimum hydrochloric acid concentration for the extraction of the nine elements of interest into the Aliquat 336 - IBMK organic phase.

The nine elements were extracted by shaking the organic phase for 5 min with 10 ml of aqueous phases of varying acid concentrations containing 2 g of dissolved - fused potassium pyrosulphate, 1.2 g of ascorbic acid and 0.6 g of potassium iodide.

Table 2. Description of six geochemical reference samples

Sample	Description
GXR-1	Jasperoid
GXR-2	Soil
GXR-3	Fe, Mn, W-rich hot-spring deposit
GXR-4	Porphyry copper mill heads
GXR-5	B-horizon soil
GXR-6	B-horizon soil

Table 3. Comparison of values obtained with the proposed method with other published values*

Arsenic, p.p.m.

Sample	A	RSD, %	B	C	D	E
GXR-1	410	6.0	460 ± 30	349	332	436
GXR-2	19	11.8	31 ± 5	16.25	18.2	23.3
GXR-3	4420	6.5	4000 ± 450	—	4564	3980
GXR-4	78	7.3	98 ± 10	—	89	103
GXR-5	12	22.8	12 ± 3	—	9.8	11.8
GXR-6	256	10.6	340 ± 30	304	329	297

Lead, p.p.m.

Sample	A	RSD, %	B	F	G	J
GXR-1	768	1.7	670 ± 20	692	712	825
GXR-2	664	1.7	615 ± 15	651	722	725
GXR-3	16.8	12.2	15 ± 2	—	13	20
GXR-4	47.6	5.3	—	41	46.2	54
GXR-5	16.2	13.4	22 ± 2	15	16.2	16
GXR-6	97	2.8	110 ± 10	96	84.2	100

Silver, p.p.m.

	A	RSD, %	F	G
GXR-1	30.8	2.7	32.6	32.6
GXR-2	17.2	4.9	17.7	17.4
GXR-3	0.11	20.3	—	0.06
GXR-4	3.34	4.0	3.8	3.64
GXR-5	0.73	6.1	0.77	0.82
GXR-6	0.31	7.2	0.35	0.29

Molybdenum, p.p.m.

	A	RSD, %	B	K
GXR-1	19.4	4.6	20 ± 5	20.1
GXR-2	1.2	22.8	1.5 ± 0.5	1.3
GXR-3	7.8	10.7	L(6)	6.77
GXR-4	320	2.2	310 ± 25	340
GXR-5	30.8	3.6	30 ± 4	32.3
GXR-6	2.3	11.9	1.7 ± 0.4	2.27

Bismuth, p.p.m.

	A	RSD, %	H	G
GXR-1	1720	2.6	1700	1725
GXR-2	L(2)	—	0.360	0.4
GXR-3	L(2)	—	—	L(0.2)
GXR-4	19	5.3	22	21.2
GXR-5	L(2)	—	0.349	0.4
GXR-6	L(2)	—	0.212	0.2

Antimony, p.p.m.

	A	RSD, %	B	C	L
GXR-1	102	5.6	124 ± 6	115	97.6
GXR-2	39.8	3.7	48 ± 5	41.04	43.6
GXR-3	32	6.6	40 ± 3	—	21.9
GXR-4	2.8	15.9	4.4 ± 0.8	—	5.1
GXR-5	1.2	37.2	2 ± 1	—	1.6
GXR-6	2.6	21.1	3.8 ± 0.7	3.92	2.8

Cadmium, p.p.m.

	A	RSD, %	F	G
GXR-1	2.82	5.3	4.0	3.0
GXR-2	3.88	2.8	4.7	3.94
GXR-3	0.38	7.2	—	0.39
GXR-4	0.32	8.6	0.5	0.34
GXR-5	0.12	22.8	0.22	0.14
GXR-6	0.11	20.3	0.18	0.11

Zinc, p.p.m.

	A	RSD, %	B	G	F	I
GXR-1	798	1.4	740 ± 110	640	670	675
GXR-2	510	2.0	500 ± 60	428	425	470
GXR-3	204	2.7	220 ± 70	124	—	204
GXR-4	68	4.0	64 ± 10	59	63	76
GXR-5	47	5.8	50 ± 5	41	37	51
GXR-6	122	6.9	120 ± 20	78	104	100

Copper, p.p.m.

	A	RSD, %	B	F	G	I
GXR-1	1298	1.1	1300 ± 100	999	1080	1129
GXR-2	76	5.5	L(100)	71	69	63.4
GXR-3	13.4	17.2	L(100)	—	10.8	14.2
GXR-4	6660	2.0	6500 ± 200	6487	6840	6780
GXR-5	358	2.3	360 ± 20	323	350	308
GXR-6	74	5.7	105 ± 12	54	55	63.9

* RSD = relative standard deviation; L( ) = less than bracketed value; — = not determined; A, mean of 5 replicates, proposed method; B, recommended values and ranges by various methods[4]; C, aqua regia digestion, hydride generation, atomic-absorption determination[5]; D, mean of 5 replicates, perchloric - nitric acid digestion, hydride generation into silver nitrate solution, graphite furnace atomic-absorption determination[6]; E, perchloric - nitric - hydrofluoric acid digestion, hydride generation into hydrogen flame, atomic-absorption determination[7]; F, mean of 5 replicates, potassium chlorate - hydrochloric acid digestion, Aliquat 336 - IBMK separation, inductively coupled plasma spectrometry determination[8]; G, same as F with atomic-absorption determination[2]; H, mean of 2 replicates by electrothermal atomic absorption[9]; I, mean of 5 replicates, nitric - hydrofluoric acid digestion, organic separation, atomic-absorption determination[10]; J, mean of 5 replicates, hydrofluoric - hydrochloric acid, hydrogen peroxide digestion, organic separation, atomic-absorption determination[11]; K, mean of 5 replicates, hydrofluoric - nitric perchloric acid digestion, dithiol separation, spectrometric determination[12]; L, mean of 5 replicates, ammonium iodide fusion, organic separation, atomic-absorption determination.[13]

Figs. 1 and 2 show the percentages of the nine elements extracted into the organic phase as a function of hydrochloric acid concentration of the aqueous phase. Between acid concentrations of 2.8 and 3.8 M, 95% or more of all nine elements were partitioned into the Aliquat 336 - IBMK phase. Mo limits the lower acid concentration and Zn limits the upper end of the optimum extraction range.

Based on the extraction curves, the proposed fusion method was further modified by changing the hydrochloric acid concentration of the aqueous phase to 3.6 M, which is near the upper limit for optimum extraction. An acid concentration near the upper limit was chosen because both As and Mo show a rapid decrease in extractability close to the lower limit. Also, a more acidic aqueous phase would adequately maintain the acidity within the optimum range when analysing limestone or dolomite samples that could potentially lower the acidity of the aqueous phase.

To test the accuracy and precision of the new method, the nine elements were determined in five replicates of the six geochemical reference samples described in Table 2.

Table 3 gives the mean values obtained with the proposed method, other published values and the relative standard

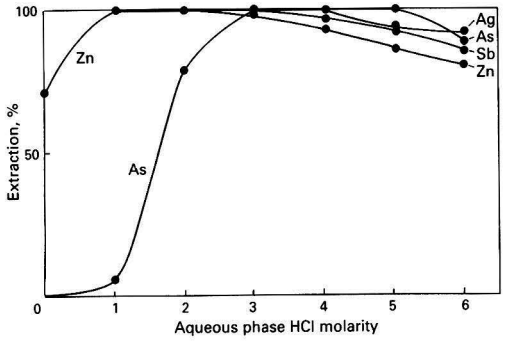

Fig. 1. Extraction of Ag, As, Sb and Zn into the organic phase

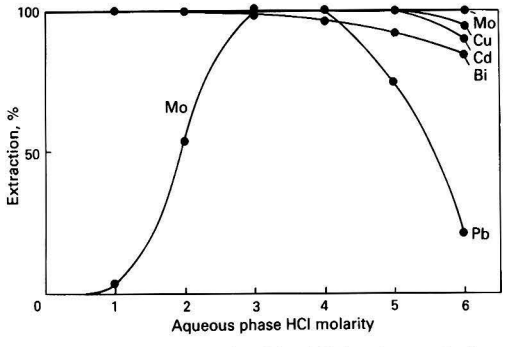

Fig. 2. Extraction of Mo, Cd, Cu, Bi and Pb into the organic phase

deviation for the five replicates of the GXR series. In general, the values obtained by the proposed method are in good agreement with other published values. The As and Sb values were lower than the neutron activation values,[13] but were in general agreement with other literature values. As would be expected, the precision declines as the detection limit for an element is approached. The worst precision observed was for Sb in GSR-5 with a relative standard deviation of 37.2%. Practical limits of determination for the nine elements based on the authors' experience with routine samples are As 5, Ag 0.1, Bi 1, Cd 0.1, Cu 0.5, Pb 1, Mo 0.5, Sb 1, and Zn 0.5 p.p.m., although lower limits are often attainable.

In terms of accuracy, most values agree well with published values, although there are several exceptions. The As values for sample GXR-6 are lower than published values and we can offer no explanation. Values for the other eight elements agree well with published values. As, Ag, Bi and Sb in GXR-4 are lower than published values by varying amounts. The remaining values for sample GXR-4 show good agreement, however, suggesting that in this high-sulphide sample As, Ag, Bi and Sb may be present in a separate mineral phase not completely attacked by the pyrosulphate fusion. Although these few values are lower than published values, their precision is adequate for geochemical exploration purposes.

References

1. Levinson, A. A., "Introduction to Exploration Geochemistry," Applied Publishing, Calgary, 1974, p. 241.
2. Viets, J. G., *Anal. Chem.*, 1978, **50**, 1097.
3. Allcott, G. H., and Lakin, H. W., "Geochemical Exploration 1974," Elsevier, Amsterdam, 1975, p. 659.
4. Gladney, E. S., Perrin, D. R., Owens, J. W., and Knab, D., *Anal. Chem.*, 1979, **51**, 1557.
5. Aslin, G. E. M., *J. Geochem. Explor.*, 1976, **6**, 321.
6. Sanzolone, R. F., Chao, T. T., and Welsch, E. P., *Anal. Chim. Acta*, 1979, **108**, 357.
7. Terashima, S., *Anal. Chim. Acta*, 1976, **86**, 43.
8. Motooka, J. M., Mosier, E. L., Sutley, S. J., and Viets, J. G., *Appl. Spectrosc.*, 1979, **33**, 356.
9. Ficklin, W. H., and Ward, F. N., *J. Res., U. S. Geol. Surv.*, 1976, **4**, 217.
10. Sanzolone, R. F., Chao, T. T., and Crenshaw, G. L., *Anal. Chim. Acta*, 1979, **105**, 247.
11. Sanzolone, R. F., and Chao, T. T., *Anal. Chim. Acta*, 1976, **86**, 163.
12. Terashima, S., *Geostand. Newsl.*, 1980, **4**, 9.
13. Welsch, E. P., and Chao, T. T., *Anal. Chim. Acta*, 1975, **76**, 65.

Paper A4/184
Received May 17th, 1984
Accepted July 26th, 1984

Studies of Nickel Absorption in Rats Using Inductively Coupled Plasma Atomic-emission Spectrometry and Liquid Scintillation Counting

Paul B. Hayman, David M. L. Goodgame and Richard D. Snook*
Department of Chemistry, Imperial College of Science and Technology, London SW7 2AY, UK

A comparison of the absorption by rats of orally dosed soluble $^{63}NiCl_2$ and insoluble Raney nickel in polyethylene glycol 200 is reported. ^{63}Ni in whole blood was determined by liquid scintillation counting. The analytical technique used for the determination of Ni derived from the absorption of Raney Ni was inductively coupled plasma atomic-emission spectrometry to avoid the use of radiolabelled Raney Ni.

Keywords: *Nickel absorption; rats; inductively coupled plasma atomic-emission spectrometry; liquid scintillation counting*

Nickel has recently been recognised as an essential element in nutrition, normal individuals having typical blood plasma concentrations of 2.6 ± 0.8 μg l^{-1},[1] with the nickel being bound to the serum proteins. Excess levels are encountered after myocardial infarction and deficiencies commonly occur in cases of liver cirrhosis and chronic uraemia.

However, it is now clear that human exposure to nickel in excess of the body's requirements can lead to serious health problems. Nickel in some form(s) can lead to cancer of the lung and nasal cavity and haemorrhage of the bronchials. Nickel solutions used in electroplating cause dermatitis, and may aggravate eczema. There is also evidence for the toxicity of nickel when present at high levels in foodstuffs, although the contamination of food by nickel leached from cooking vessels is not thought to be serious. Tobacco smoke also contains nickel.

A particular problem in the past has been the accurate determination of nickel levels in blood, especially as the absorption of the element in the digestive tract is poor. It is possible to follow blood nickel levels after dosing with a radiolabel, but this is not feasible in occupational exposure. Neutron-activation analysis, although offering the required sensitivity, is not generally available for routine use. Other methods include electrothermal atomic-absorption spectrophotometry; while this method is relatively free from interferences, it lacks sensitivity for untreated blood and entails relatively time-consuming sample preparation with its attendant risks of contamination during sample handling. Typically the blood requires acid digestion, followed by chelation and pre-concentration by solvent extraction before analysis.[2]

Several workers[3–5] have demonstrated the sensitivity of inductively coupled plasma atomic-emission spectrometry (ICP-AES) for the detection of nickel in blood, with its associated reduction in the absolute detection limit and in the volume of sample required.

The report by Christensen and Lagesson[6] of a blood nickel concentration profile after dosing a soluble form of nickel to human subjects showed a peak blood concentration of nickel 150 min after dosing. In this study we dosed rats orally with soluble and insoluble forms of nickel and determined the blood nickel levels at selected time periods, after dosing, either by IPC-AES or liquid scintillation counting (LSC), in order to investigate the absorption of these forms of nickel from the intestines of rats.

* To whom correspondence should be addressed.

Experimental

Apparatus

The ICP-AES instrumentation has been fully described elsewhere[7] and consists of a high-frequency generator operating at 27.12 MHz with a continuously variable power output of 0–2.5 kW (IPC Model 120.27). The output of the generator is fed to a 1.5-turn load coil via an impedence-matching network and coupled to the plasma, which is sustained in a concentric demountable silica torch. The spectrometer employed was a 1-m Hilger Monospek 1000 (grating, 1200 lines mm^{-1}; blaze, 300 nm; reciprocal linear dispersion, 8 A mm) equipped with an EMI 6256B photomultiplier tube. Signal registration was achieved using a fast-response chart recorder (Servoscribe 541.20).

Sample introduction was effected using a nebuliser (Meinhard Model T-230-A3) for line selection and a programmable graphite rod vaporisation device[7] for the direct introduction of blood serum samples.

LSC was performed using a Packard Tri-Carb 460CD scintillation spectrometer.

Reagents

$^{63}NiCl_2$ (specific activity 1 mCi cm^{-3}) was obtained from Amersham International and $NiCl_2.6H_2O$ (Gold Label grade) from Aldrich Chemicals. Raney nickel of particle size 4–6 μm was obtained from Goodfellow Metals and polyethylene glycol 200 from BDH Chemicals. The nickel standards for calibration of the ICP-AES method were prepared by serial dilution of a 1000 mg dm^{-3} solution of Ni in 0.1 M $HClO_4$ (BDH Chemicals) with distilled, de-ionised water.

The nickel stock solutions for LSC were prepared from $^{63}NiCl_2$ and $NiCl_2.6H_2O$ to yield a solution concentration of 0.1 g dm^{-3} (10 mCi dm^{-3}) of Ni.

Procedures

All glass and polypropylene vessels used for sampling, storage and manipulation of the blood and serum samples were previously cleaned in 1 + 1 nitric acid and rinsed with distilled de-ionised water.

Six male Alderley Park Wistar derived (AP) rats (mass range 180–200 g) were dosed orally with 0.5 cm^3 of a suspension of the Raney nickel in PEG 200 (10 mg cm^{-3}) for the ICP-AES determinations. For the LSC determination five AP rats were dosed orally with 1.0 cm^3 of a solution of $^{63}NiCl_2$ in water (0.1 g cm^{-3} of Ni; 20 μCi cm^{-3}).

Table 1. Plasma and vaporiser operating conditions

Plasma			
Viewing height			35 mm above load coil
Forward power			1000 W
Ar coolant flow-rate			16 l min^{-1}
Ar (carrier gas) injector flow-rate			0.8 l min^{-1}
Vaporiser			
		Temperature/°C	Time/s
Evaporation	First	100	30
	Second	140	30
Ashing	First	1100	80
	Second	1100	10
Vaporisation		2700	4

Samples of rat blood (0.5 cm^3) were taken from the tail vein (discarding the first two drops) at the intervals reported under Results and Discussion. For the ICP-AES determinations the samples were allowed to clot for 40 min, centrifuged and the serum fractions stored in polypropylene vials at −80 °C for subsequent analysis.

The procedure for analysis of the serum samples was to pipette 10 µl of a 0.4% solution of Triton X-100 on to the graphite rod followed by 10 µl of blood serum. This mixture was then desolvated, ashed and vaporised into the plasma under the conditions described in Table 1. The resulting emission from the plasma was observed at the 352.5-nm nickel line. A blank was determined to account for nickel in the Triton X-100 solutions and results were subsequently corrected for this level. A control serum sample was prepared to ascertain the background level of nickel in a rat dosed only with PEG 200. The blood was taken from an anaesthetised rat by cardiac puncture.

For LSC determinations the blood sample was stored in lithium heparin-lined tubes to prevent clotting. Duplicate 0.15-cm^3 aliquots of the blood were digested with 1.5 cm^3 of Soluene 350 - isopropanol (1 + 1) in a glass vial for 20 min. These solutions were bleached with 0.5 cm^3 of 33% hydrogen peroxide for 10 min and then heated at 40 °C for 20 min and allowed to cool. To each vial 15 cm^3 of a standard liquid scintillation cocktail (Instagel, Packard Instruments) were added. The vials were placed in the dark for 3 h to allow chemiluminescence processes to decay and then assayed by LSC. Counts were automatically corrected for background scintillation and counting efficiencies were determined using external standard quench correction curve data with ^{226}Ra as the gamma source. The corrected disintegration per minute (d.p.m.) values were automatically derived from the appropriate quench curve data stored in the instrument computer. Samples were counted either for 10 min or to a statistical precision of 1.0% relative standard deviation (r.s.d.).

Results and Discussion

The absorption of two forms of nickel by rats was studied: soluble nickel-63 chloride and a suspension of insoluble Raney nickel in PEG 200. The amounts of the soluble nickel-63 in rat blood were conveniently monitored by LSC. In this determination the background level of natural nickel in the rats was discriminated as no nickel-63 was expected to be present. Soluble nickel was expected to be absorbed in greater amounts than the insoluble form, and consequently we chose a slightly more sensitive technique for the determination of nickel in the blood of rats given Raney nickel. Thus inductively coupled plasma atomic-emission spectrometry was employed to give a detection limit of 10 ng cm^{-3} and a linear range with respect to concentration at levels up to 1 mg cm^{-3}. An advantage of employing ICP-AES is that the radiolabelled form of Raney nickel is not required for detection.

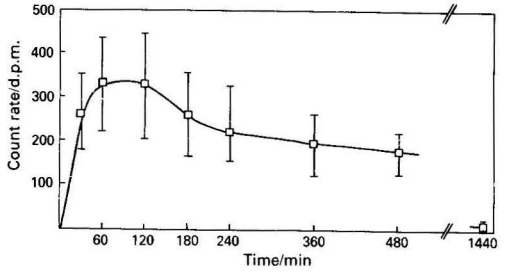

Fig. 1. Concentration of ^{63}Ni in rat blood determined by liquid scintillation counting *versus* time

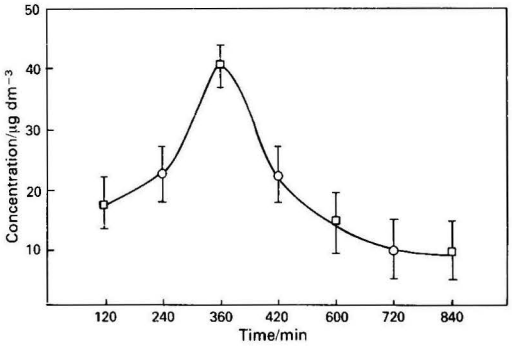

Fig. 2. Concentration of Ni, derived from Raney nickel, in rat blood determined by ICP-AES *versus* time. □, Group 1 rats; and ○, group 2 rats

Fig. 1 shows the average temporal distribution of nickel in the blood of the five AP rats dosed with $^{63}NiCl_2$. The bar limits represent the standard deviation of the ^{63}Ni levels in the five rats for each particular sample collection time.

The highest ^{63}Ni level was found between 60 and 120 min after dosing. The average maximum concentration of radioactivity found was at 90 min and corresponds to a concentration of 10.5 mg l^{-1} (10.5 p.p.m.).

Fig. 2 shows the average Ni levels in the serum of rats at particular time periods after dosing with Raney nickel in PEG 200. Six male rats were dosed for this experiment and divided into two groups of three, from which blood was sampled at alternate time intervals. The peak level of nickel was observed between 4 and 8 h after dosing and corresponds to 41 µg l^{-1}. To assess the validity of the procedure with two different sets of rats the experiment was repeated and the results were found to be reproducible, *i.e.*, the peak nickel serum concentration was within the same experimental error (41 ± 8 µg l^{-1}) with the peak concentration occurring at 6 h. No nickel was detected in the blood serum of the control rat.

From these figures we can compare the time at which the maximum concentration of nickel occurs in the rats' blood. The soluble nickel is absorbed more rapidly than the insoluble Raney nickel and the concentration of nickel in blood derived from the soluble nickel is higher, as would be expected considering the higher dose concentration and solubility.

The important comparison, however, is between the times at which the peak concentration of nickel in rat blood occurs, which has important implications when assaying blood nickel concentrations in humans exposed to insoluble forms of nickel. It is essential that the time of maximum nickel concentration in the blood is ascertained, so that during routine monitoring blood is sampled at the appropriate time.

Conclusions

The peak nickel concentration in rat blood occurs *ca.* 6 h after dosing with Raney nickel in PEG 200 compared with 1.5 h for soluble $^{63}NiCl_2$ in water. This implies that the Raney nickel is slowly solubilised in the digestive tract of the rat.

The ICP-AES determination of nickel in blood serum has advantages over LSC as radioactive ^{63}Ni is not required and it employs only microlitre volumes of sample. The technique of ICP-AES with graphite rod vaporisation for sample introduction also offers the clinical analyst a rapid and sensitive technique for this type of determination. As the sample can be determined directly by vaporisation from the graphite rod into the ICP, the opportunity for contamination of the sample is minimised.

We acknowledge the support of the SERC CASE Studentship to P.B.H. and the Laboratory of the Government Chemist for support to R.D.S.

References

1. McNeeley, M. D., Sunderman, F. W., Jr., Nechay, M. W., and Levine, H., *Clin. Chem.*, 1971, **17**, 1123
2. Belling, G. B., and Jonwa, G. B., *Anal. Chim. Acta*, 1975, **80**, 179.
3. Larson, G. F., Fassel, V. A., Scott, R. M., and Knisely, R. N., *Anal. Chem.*, 1975, **47**, 238.
4. Boumans, P. W. J. M., and de Boer, F. J., *Spectrochim. Acta, Part B*, 1976, **31**, 355.
5. Camara Rica, C., Kirkbright, G. F., and Snook, R. D., *At. Spectrosc.*, 1981, **2**, 172.
6. Christensen, O. B., and Lagesson, V., *Ann. Clin. Lab. Sci.*, 1981, **11**, 119.
7. Long, S. E., and Snook, R. D., *At. Spectrosc.*, 1982, **3**, 171.

Paper A4/192
Received May 31st, 1984
Accepted June 21st, 1984

Electrochemical Pre-concentration Technique for Use With Inductively Coupled Plasma Atomic-emission Spectroscopy

Part II*

David A. Ogaram and Richard D. Snook†
Trace Analysis Laboratory, Department of Chemistry, Imperial College, London SW7 2AY, UK

Two new electrochemical cells are described for the pre-concentration of trace elements from flowing solutions. The cells operate under controlled hydrodynamic conditions and are therefore suitable for in-line use with the nebuliser sample introduction system of the inductively coupled plasma. Their performances as pre-concentration cells are compared with the wall-jet cell described in Part I.

Keywords: *Electrochemical pre-concentration; inductively coupled plasma atomic-emission spectroscopy; trace metals; controlled hydrodynamics*

In Part I[1] we described an electrochemical cell that could be used for the pre-concentration of trace elements prior to their determination using inductively coupled plasma atomic-emission spectroscopy (ICP-AES). The cell described was of the wall-jet type and operated under controlled hydrodynamic conditions at a volume flow-rate of 3 cm^3 min^{-1}, which was compatible with the nebuliser of the ICP. Although effective pre-concentration could be achieved after 10 min by reduction of the trace metal of interest at the glassy carbon electrode and subsequent rapid stripping of the analyte back into solution, the cell was not designed primarily for this role. Consequently, the plating efficiency, which determines the amount of analyte stripped from solution, was typical for this type of cell (*ca.* 8%). The cell volume into which the plated analyte was stripped was also larger than necessary (710 μl), which resulted in a lower than optimum concentration for injection into the nebuliser of the ICP.

The new cells have been designed and evaluated with the intention of improving the over-all pre-concentration factor obtainable by electrochemical means. The first cell is called the concentric slot electrode and has been designed to minimise the cell volume to the volume of the diffusion layer into which the analyte is stripped and where the resulting concentration is high. The second cell employs a reticulated vitreous carbon[2] flow-through electrode (RVCE), which combines the advantages of a large electroactive surface area, flow-through capabilities and a small cell volume. The RVCE has an open pore structure, similar to a frit, and can therefore be considered as an assembly of minute cell volumes into which plated analyte is stripped.

Both cells have been used in this study as electrochemical pre-concentration cells by operating them in the anodic-stripping voltammetric mode. Each cell, however, can be used as an electrochemical detector in its own right.

Experimental

Instrumentation

The ICP spectrometer employed was described in Part I[1] and the compromise operating conditions of the instrument described there were also employed in this study. The potentiostat used in Part I was of simple construction but this has now been superseded by the use of a PAR 174 scanning potentiostat (Princeton Applied Research, Princeton, NJ, USA) for control of the electrochemical cells.

The concentric slot electrode consists of a central probe that has incorporated an annulus of platinum of diameter 5 mm and length 2 mm. Solution entering the cell flows over this electrode. Downsteam of the platinum electrode the probe is tapered smoothly into a rounded point, as shown in Fig. 1. The concentric slot around the electrode is formed by a cup that surrounds the tapered region of the probe. When fixed in the operating position the distance between the inner surface of

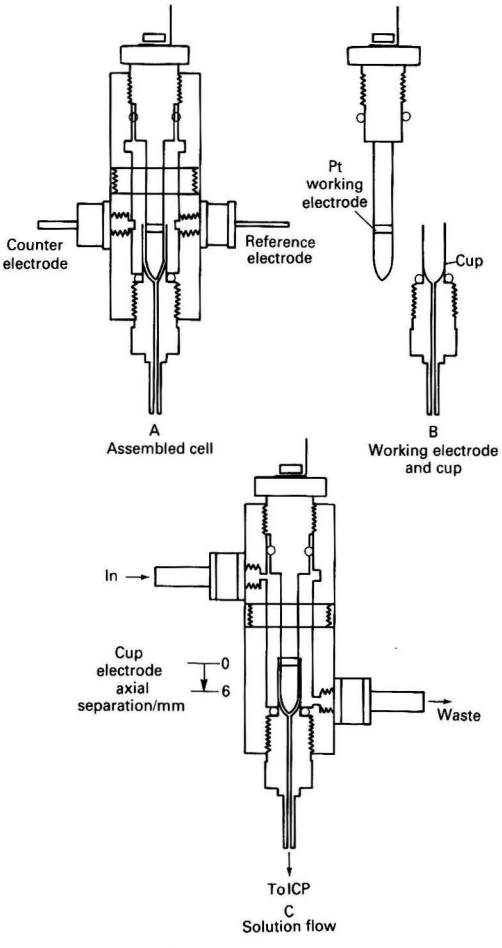

Fig. 1. The concentric slot electrode

* For Part I of this series, see reference 1, p. 1601.
† To whom correspondence should be addressed.

the cup and the probe is 0.15 ± 0.05 mm, which provides a small volume (30 µl) into which plated analyte is stripped, thus resulting in a higher concentration than was obtainable for the same amount of stripped analyte using the wall-jet cell. The counter and reference electrodes are positioned radially opposite the working electrode.

The RVCE (Fig. 2) is contained in a flow-through cell through which the electrolyte solution is pumped. The RVC is 3 mm thick and has perforations through it approximately 50 µm in diameter. The holes through the frit follow tortuous routes to the obverse surface and thus we have available a large electroactive surface area in comparison with the glassy carbon electrode described in Part I and the concentric slot electrode described above. The RVC flow-through cell has a volume behind the electrode of 200 µl into which plated analyte is stripped.

For both cells we employed a Pt counter electrode and an Ag - AgCl (1 M KCl) reference electrode. Solutions were pumped through the cells and hence to the nebuliser with a peristaltic pump (Technicon AutoAnalyzer). The cells were interfaced directly to the nebuliser during the analysis cycle to allow the ICP to be used for other purposes during the plating stage of the pre-concentration.

The most successful of the two cells for pre-concentration purposes was the RVC flow-though cell and consequently most attention is directed towards its characterisation in the remainder of this paper.

Reagents

Throughout this work reagents of the highest purity available were prepared in doubly distilled, de-ionised water. Copper was removed from blanks and reagent solutions using an Amberlite IRC 718 ion-exchange column of bed dimensions 20 × 2 cm diameter. The base electrolyte was 0.1 M KCl solution and solutions were deoxygenated prior to use by passing argon through them for 20 min.

Results and Discussion

The most important factor when considering continuous on-line pre-concentration is the maintenance of controlled hydrodynamics so that we can predict the efficiency of the cell with respect to the volume flow-rate of solution through it and the concentration range for which it is being employed. Ideally, the efficiency of the cells should remain constant with respect to these parameters. For the wall-jet cell we showed that the flow-rate dependence remained constant between flow-rates of 0.5 and 10.0 $cm^3\ min^{-1}$ and for a concentration range of two orders of magnitude.

The diffusion current and hence mass plated at the working electrode of the wall-jet cell was shown to be proportional to the volume flow-rate, *i.e.*, $i_d \propto V^{3/4}$.

Concentric Slot Electrode

The performance of the concentric slot electrode as a pre-concentration cell was optimised with respect to the cup-electrode separation. When the cup is screwed away from the electrode the effective volume into which the analyte is stripped is increased, and we would expect the final concentration of stripped analyte to change. The possibility that the hydrodynamic conditions may change was also investigated, as it is the change in volume flow-rate dependence of the limiting current and stripping current that reflects a change in hydrodynamic conditions.

To assess the flow-rate dependence of this cell we used a purely electrochemical procedure in which the diffusion current of the hexacyanoferrate(III) reduction is monitored for different cup-electrode separations and flow-rates.

$$Fe(CN_6)^{3-} + e \rightleftharpoons Fe(CN_6)^{4-}$$

Thus, $K_3Fe(CN)_6$ (4×10^{-4} M) in KCl (0.5 M) was buffered to pH 6.9 and the potential of the working electrode was scanned from +0.6 to −0.6 V and the limiting current measured for different cup-electrode separations and, independently, at the different cup-electrode separations, for different volume flow-rates.

The cup-electrode separation was found not to be critical and large diffusion currents could be obtained at separations between 0 mm, when the probe is located in the cup, to 5 mm out of the cup. The volume flow-rate dependence of the limiting current was determined at the different cup-electrode separations. The results of this experiment are shown in Fig. 3, in which the limiting current is plotted against the volume flow-rate of solution through the concentric cup cell. The graphs are linear (correlation coefficient 0.99) between flow-rates of 1.0 and 10 $cm^3\ min^{-1}$ and all have a gradient of 0.33, which, according to our conditions for hydrodynamic flow described in Part I, shows that the limiting current i_l is proportional to $V^{0.33}$, where V is the volume flow-rate. This is the flow-rate dependence that we would expect for an open-tubular electrode as reported by Blaedel and Klatt.[3]

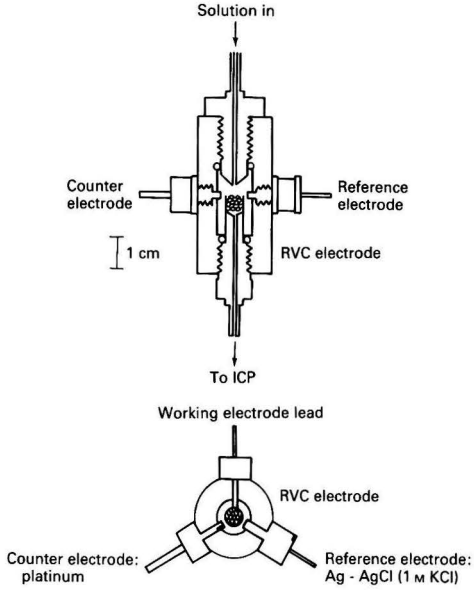

Fig. 2. Demountable reticulated vitreous carbon flow-through cell

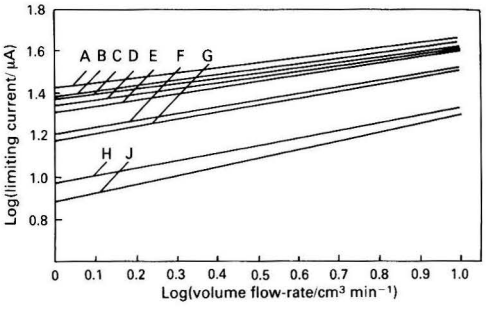

Fig. 3. Dependence of limiting current on solution volume flow-rate for $Fe(CN)_6^{3-}$ (0.5 mM) in KCl (0.1 M) at different electrode cup separations: A, 0; B, 0.5; C, 0.25; D, 0.75; E, 1.0; F, 1.25; G, 1.5; H, 2.0; and J, 2.5 mm

The volume flow-rate dependence of the limiting current is not surprising as the platinum electrode is an annulus, as is an open tube, and differs only in that its outer surface, rather than its inner surface, is the electroactive area. For completeness we also assessed the volume flow-rate dependence of i_l using the plateable species Cd^{2+} (30 μg cm^{-3}) in 0.1 M KCl and a plating potential of −0.95 V. The same result was obtained, *i.e.*, $i_l(Cd^{2+}) \propto V^{0.33}$, over the range of flow-rates from 1.0 to 10 cm^3 min^{-1}.

Having established that the concentric cup electrode does indeed operate under controlled hydrodynamic conditions, we assessed its use as a pre-concentration cell with the ICP. Cadmium was used as the diagnostic species for this experiment. The best emission line for cadmium was found to be the Cd I 228.8 nm line at the compromise ICP-AES operating conditions described previously.[1] The optimum pH was found to be pH 9.0.

Typical ICP signals obtained by scanning across the Cd I 228.8 nm line whilst nebulising a solution containing 2 μg cm^{-3} of Cd were compared with signals observed at the cadmium I 228.8 nm line when a discrete amount of cadmium was injected into the plasma from the concentric slot electrode after pre-concentration for 10 min and subsequent stripping at a potential scan rate of 500 mV s^{-1}. In the latter instance the peak width at half-height is 5.3 s, whereas the time taken to strip the cadmium from the annular platinum electrode is less than 1 s when measured electrochemically. This apparent peak broadening is caused by the dilution of the cadmium into the cup volume and further by dilution of the analyte into the gas stream in the spray chamber of the nebuliser system. Nevertheless, an improvement in detection power, determined by peak-height measurement, is obtainable. The magnitude of this improvement is small, improving our detection limit by a factor of 3 from 0.09 to 0.03 μg ml^{-1}. This is comparable to the improvement obtained with the wall-jet cell described in Part I, which is not surprising as the areas of the electrodes are similar (0.39 and 0.32 cm^2, respectively) and their efficiencies with respect to plating, which we measured as described in Part I, are the same (8%). Also, the diffusion coefficients for the depolarisers (Cd^{2+} and Cu^{2+}) are similar (0.72×10^5 and 0.78×10^5 cm^2 s^{-1}, respectively). One might expect that the concentric slot electrode would be superior for pre-concentration, however, as the volume into which the analyte is stripped is smaller (200 μl compared with 710 μl in the wall-jet cell) by a factor of 3.5. On closer inspection, however, we see that the sensitivity of the concentric slot electrode towards plating at a fixed rate is determined by the power of the volume flow-rate term and, with the concentric slot electrode, this power is 0.33 compared with 0.75 in the wall-jet cell. Hence we can now conclude there should be no serious quantitative difference in the over-all pre-concentration efficiency between two cells, which is in fact what we observe.

Reticulated Vitreous Carbon Electrode

The RVCE (Fig. 2) has a large electroactive surface area owing to the porous nature of the material. The RVC has a pore size that varies between 20 and 100 μm and a void volume of 97%. Because of the open nature of the RVC there is no resistance to flowing solutions and the material can be successfully used as a flow-through electrode. Hence in these experiments we pumped solutions through the RVCE and employed anodic-stripping voltammetry for pre-concentration of trace elements. The cell employs a platinum counter electrode and an Ag - AgCl reference electrode positioned radially to the RVC working electrode. Control of the cell was achieved using the PAR 174 potentiostat.

The volume flow-rate dependence of the limiting current, i_l, for this cell was determined using hexacyanoferrate(III) reduction described previously. The double logarithmic plot of i_l *vs.* volume flow-rate is shown in Fig. 4. From this graph we can conclude that the volume flow-rate dependence is $i_l \propto V^{0.35}$ for solution volume flow-rates between 1.0 and 10 cm^3 min^{-1}.

The same volume flow-rate dependence of i_l was determined using Cu as the platable species by measuring the limiting current for the reaction:

$$Cu^{2+} + 2e \rightleftharpoons Cu^0$$

The volume flow-rate dependence of i_l was found to be the same as that determined using the hexacyanoferrate(III) reduction. The volume flow-rate has been shown by Blaedel and Wang[4] to be dependent on the thickness of the RVC in the direction of solution flow and increases in value as the thickness increases. It is important, therefore, to determine the volume flow-rate dependence for each new electrode installed in the cell. In practice this is not a disadvantage as the lifetime of the electrode materials is a few months in this application.

The useful potential range of the RVCE in aqueous solution was determined at different pH values. The potential range is limited by two processes: in the cathodic direction by the reduction of H^+:

$$2H^+ + 2e \rightarrow H_2\uparrow \quad (1)$$

and in the anodic direction by the oxidation of water:

$$2H_2O \rightarrow 4H^+ + 4e + O_2(g) \quad (2)$$

The potential range therefore changes with change in pH. The pH values used in this experiment were between 1 and 13 and the reagents used to obtain these pH values are shown in Table 1.

For this experiment the solution volume flow-rate was set at 3.4 cm min^{-1} and a potential scan rate of 5 mV s^{-1} was applied to the working electrode between +1.2 and −1.2 V. From the resulting current - potential graphs the potentials at which reactions (1) and (2) occured were determined to be the potential at which a current of 1 μA was exceeded. Fig. 5 shows a graph of potential *vs.* pH of solution and reveals that the RVCE has a wide potential range (up to 2 V) except when strongly acidic solutions are used, which adversely affect cathodic reactions.

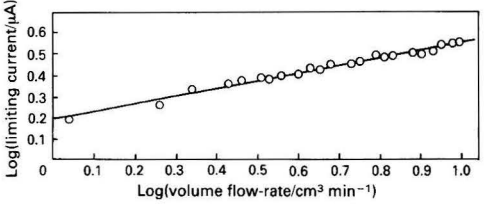

Fig. 4. Dependence of limiting current on solution volume flow-rate for the reticulated vitreous carbon electrode. $Fe(CN)_6^{3-}$ concentration, 0.4 mM; pH, 6.9. Gradient = 0.35

Table 1. Buffer solutions used to assess the working potential range of the RVCE. Final volume, 100 cm^3

pH	Reagent solution
1	67 cm^3 HCl (0.2 M) + 25 cm^3 KCl (0.2 M)
2	6.5 cm^3 HCl (0.2 M) + 25 cm^3 KCl (0.2 M)
4	100 cm^3 KCl (0.1 M) - $C_6H_4(COOH)_2$ (0.25 M) buffer
6.86	100 cm^3 KCl (0.1 M) - Na_2HPO_4(0.025 M + NaH_2PO_4(0.025 M)
9	100 cm^3 KCl (0.1 M) - $Na_2B_4O_7$(0.01 M) buffer
12	26.9 cm^3 NaOH (0.1 M) + 50.0 cm^3 Na_2HPO_4 (0.05 M)
13	66 cm^3 NaOH (0.2 M) + 25 cm^3 KCl (0.2 M)

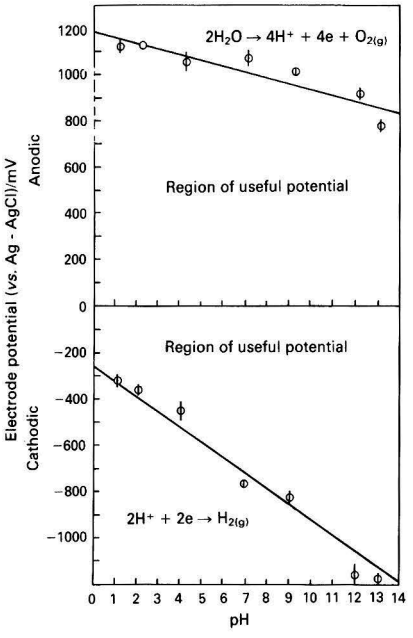

Fig. 5. Useful pH range for the reticulated vitreous carbon electrode

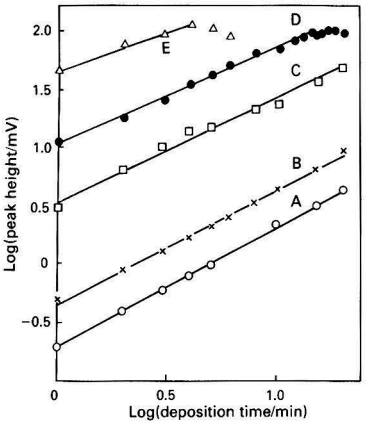

Fig. 6. Stripping peak height *versus* deposition time. Cu^{2+} concentration: A, 0.05; B, 0.1; C, 0.5; D, 1.0; and E, 5.0 μg cm^{-3}

To assess the analytical utility of the RVCE flow-through cell as a device for trace element pre-concentration with the ICP we again chose copper as the trace element of interest to enable us to compare efficiencies directly with those obtained with the glassy carbon electrode used with the wall-jet cell described in Part I. Using a solution containing 0.1 μg dm^{-3} of Cu^{2+} in 0.1 M KCl we optimised the plating and stripping efficiency with respect to pH using the pH reagents shown in Table 1. The ICP was used in these studies to measure the amount of analyte stripped from the RVCE, which is directly

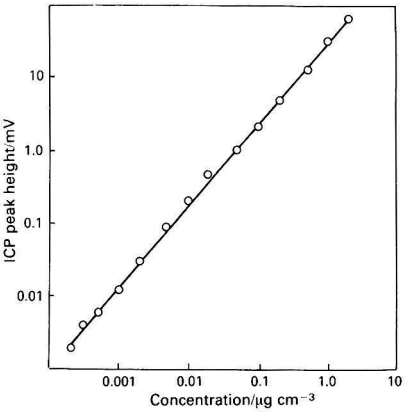

Fig. 7. Linear range with respect to concentration for copper. pH, 3.5; 324.7 nm

Table 2. Electrochemical conditions for the pH optimisation for Cu^{2+} using the RVCE

Deposition time	5 min
Deposition potential	−400 mV
Anodic potential scan rate	200 mV s^{-1}
Solution volume flow-rate	3.4 cm^3 min^{-1}

proportional to the stripping current. The ICP operating conditions were the same as those given in Part I (forward power, 1.0 kW; injector gas flow-rate, 0.8 l min^{-1}; coolant gas flow-rate, 13 l min^{-1}) and the electrochemical conditions are given in Table 2.

The optimum pH range for this particular element was found to be 3.0–3.5 and therefore solutions of this pH were used for the remainder of the experiments.

The dependence of the peak height observed with the ICP on the deposition time was also investigated for different concentrations of copper. The deposition time was varied between 1 and 20 min and, after deposition, the copper was stripped from the electrode under the conditions shown in Table 2 and pumped to the ICP for quantification. The double logarithmic plots of ICP emission intensity recorded at the Cu I 324.7 nm line *vs.* deposition time are shown in Fig. 6. It is apparent that the relationship is linear over a wide range of concentrations and deposition times. Curvature is noticed, however, after long deposition times for solutions containing 1.0 and 5.0 μg ml^{-1} of Cu^{2+}. The onset of curvature occurs at the same mass deposition on the electrode (calculated from the deposition time where onset occurs and the concentration) and is thought to be due to the current demand for the potentiostat exceeding its maximum during the stripping cycle.

The plating efficiency of the cell has been determined by the method described in Part I and was found to be 35% (*ca.* 8% wall jet). Using this value, we can calculate that the maximum amount of Cu that can be reduced and subsequently stripped from the electrode using the PAR 174 is 19 μg, which is large considering the application of this technique to trace element analysis.

The actual linear range of the technique with respect to concentration was determined at the optimum pH and for deposition time of 5 min. The results of this experiment are shown in Fig. 7, which indicates that the signal intensity and hence amount of copper plated and subsequently stripped from the electrode is linear with respect to concentration over

four orders of magnitude, and therefore matches well with the excellent dynamic concentration range of the ICP. Using Milli-Q Water (resistance 18 MΩ) we established a detection limit of 100 pg ml^{-1} for Cu^{2+} compared with 20 ng ml^{-1} using the ICP alone. We also established that the reproducibility is good, with a relative standard deviation of 1.7% obtained by 10 replicate determinations of 0.1 μg ml^{-1} of copper after a plating time of 5 min and a day-to-day relative standard deviation of 5.7%.

The lifetime of the RVCE is good under the conditions described, and we have been using one electrode for 8 months without serious degradation of its performance. Blaedel and Wang[5] reported that background currents become significant after 10–20 d of operations of this type of electrode, and we have confirmed this observation. However, the rise in the background and consequent decrease in the signal to background ratio observed in electrochemical measurements do not affect the ICP measurement of the copper concentration and apparently do no affect the performance of the cell with respect to quantitative plating and stripping, which are prerequisites for effective pre-concentration procedures.

Conclusions

Of the two cells investigated, the most efficient as a pre-concentration cell is that which employs RVC as the working electrode. The plating efficiency of this cell is 35% compared with 8% obtainable with the platinum concentric slot electrode and the glassy carbon wall-jet cell, described in Part I. All of the cells described operated under controlled hydrodynamics and therefore the volume flow-rate dependence of their limiting currents does not change and hence their efficiency does not change with volume flow-rate, which is an important consideration if one considers the range of nebuliser operation solution flow-rates for which this technique might be applied. The electrodes made of carbon show a superior dynamic range with respect to concentration and are therefore more suited to use with the ICP. There is a slight advantage in using the solid electrodes (Pt and glassy carbon) as these can be periodically cleaned by mechanical means to remove reduced impurities from the surface. For most applications, however, this advantage is outweighed by the superior pre-concentration efficiency of the RVCE and the wider linear range with respect to concentration.

Owing to the simplicity and absence of chemical manipulation in this form of electrochemical pre-concentration, we believe that this technique could be applied to the analysis of real samples, especially for the determination of trace metals in seawater where the dissolved sodium chloride is a natural base electrolyte. Experiments are currently under way to assess this application in our laboratory.

We thank the Uganda Government for the support of D.A.O. and the Laboratory of the Government Chemist for the support of this work and R.D.S. We also acknowledge helpful discussions with Dr. Jaim Lichtig, University of São Paulo, Brazil, visiting on study leave, and S. E. Long, Georgia Institute of Technology, USA.

References

1. Long, S. E., and Snook, R. D., *Analyst*, 1983, **108**, 1331.
2. Wang, J., *Electrochim. Acta*, 1981, **26**, 1721.
3. Blaedel, W. J., and Klatt, L. N., *Anal. Chem.*, 1966, **38**, 879.
4. Blaedel, W. J., and Wang, J., *Anal. Chem.*, 1979, **51**, 799.
5. Blaedel, W. J., and Wang, J., *Anal. Chem.*, 1979, **51**, 1724.

Paper A4/223
Received July 4th, 1984
Accepted July 19th, 1984

Selection of the Receiver Electrolyte for the Donnan Dialysis Enrichment of Cations

James A. Cox, Thomas Gray, Kyung S. Yoon, Yeon-Taik Kim and Zbigniew Twardowski
Department of Chemistry and Biochemistry, Southern Illinois University, Carbondale, IL 62901, USA

The Donnan dialysis of cations is typically performed with a sulphonated ion-exchange membrane. Factors that govern the selection of the receiver electrolyte when such membranes are used are described. In terms of providing high enrichment factors that are similar for a variety of cations and constituting a medium that is compatible with various quantification methods, a mixture containing 0.2 M $MgSO_4$ and 0.5 mM $Al_2(SO_4)_3$ at pH 1 is the recommended electrolyte. For use with cadmium and copper ion-selective electrodes, the pH is adjusted to 3.5–4 after the dialysis. For quantification with a lead ion-selective electrode, the receiver consists of the nitrate salts of Mg(II) and Al(III).

Keywords: *Donnan dialysis; pre-concentration; atomic-absorption spectrometry; ion-selective electrodes; copper, lead, cadmium and zinc*

The procedure of a Donnan dialysis experiment is to pre-concentrate ions from an aqueous sample across an ion-exchange membrane into a concentrated electrolyte (receiver solution). Depending on the charge sign of the fixed ionic sites on the membrane, either anions or cations can be pre-concentrated. Although Donnan dialysis can be used to enrich selectively a given ionic species from a set of ions of the same charge sign,[1] more typically the objective is to pre-concentrate either the entire set, or a significant subset, of analytes by approximately the same factor. Concomitantly, the experiment is designed to obtain high enrichment factors without the need to employ long dialysis times. The receiver volume and composition must be compatible with the attendant analytical procedure. Finally, the enrichment factor for a given ion should not be significantly affected by the composition of the sample.

Donnan dialysis has characteristics that make it a potentially important separation technique in analytical chemistry. In contrast with solvent extraction, the Donnan dialysis receiver is an aqueous electrolyte that is ideally suited to polarographic and ion-selective electrode potentiometric quantification; it is also compatible with flame spectrometric techniques. The linear range is greater than that observed with solvent extraction and the precision is higher than obtained by other ion-exchange methods such as column chromatography and batch separations.[2] The rate of Donnan dialysis is independent of the sample matrix over a wide range of conditions,[3] so enrichments can be performed from many kinds of sample without a preliminary chemical step. The last point is especially important in the design of remote monitors.

In an earlier report[4] we established that a 0.2 M $MgSO_4$ - 0.5 mM $Al_2(SO_4)_3$ mixture is a suitable receiver for the Donnan dialysis of divalent cations. The applicability of that receiver electrolyte to the Donnan dialysis of Cu(II), Cd(II), Pb(II) and Zn(II) from several types of aqueous samples was demonstrated.[3] The efficacy of the Mg - Al mixture was suggested to be related to the fact that the Mg(II) and Al(III) affinities for the sulphonate sites on the membrane were higher than those of the analyte ions.[5,6] Therefore, the analyte ions were displaced into the neutral channels of the membrane that connect the pools (inverse micelles) that contain the fixed ionic sites at high concentration. It was noted[6] that an ideal cation-exchange membrane for Donnan dialysis would have continuous polyelectrolyte networks rather than the inverse micelle structure; the receiver electrolyte selection would then be trivial, as ion transport through the membrane would proceed by site-to-site diffusion. Such a membrane was devised for anions but not for cations.[6]

Recently, the use of a receiver electrolyte that contains 0.9 M $MgCl_2$, 0.016 M $AlCl_3$, 0.9 M HCl, 1.7 M NaCl and 0.02 M 2-mercaptoethanol was reported for the pre-concentration of Pb(II) by Donnan dialysis.[7] Enrichment factors of 100 were obtained in 17 min, and with quantification by flame atomic-absorption spectrometry the enrichment factor was independent of sample concentration over four orders of magnitude.

This paper reports a comparison of these and other receiver systems. In addition, a suitable receiver for use with potentiometric ion-selective electrodes is described.

Experimental

The Donnan dialysis experiments with the objective of achieving high enrichment factors were performed with a previously characterised blender cell.[8] The sample (1000 ml) was placed in a polystyrene copolymer container of an Osterizer 848–34 blender, and the receiver solution was contained within a coil of Nafion 811 cation-exchange tubing. The length of the tubing (about 10 m) was adjusted to contain 5.0 ml of the receiver solution. The experiments were initiated by immersing the coil, which was held on a Plexiglas frame, in the sample and turning on the blender at its slowest speed. After 15 min, the dialysate was pumped into a 10-ml beaker, transferred into a 10-ml calibrated flask and diluted to volume with distilled water.

Before each experiment, the cation-exchange tubing was conditioned by pumping a solution with a concentration five times greater than that of the receiver through the coil at 3 ml min^{-1} for 5 min. A 5-min water-rinse followed. The final step of the conditioning was likewise to pump a solution of the same composition and concentration as the receiver through the coil. With the receiver solution described by Bruce *et al.*,[7] the conditioning solution was identical to the receiver. With the NaCl - EDTA receiver, only the NaCl was more concentrated in the conditioning solution.

Certain diagnostic experiments were performed in a Donnan dialysis cell that was constructed from a glass cylinder. A sheet of P-1010 (RAI Research Corp., Hauppauge, NY, USA) or Nafion 125 (DuPont Polymer Products, Wilmington, DE, USA) cation-exchange membrane was used to close one end (4 cm^2). The membrane was held by PTFE tape and an O-ring. The dialysis cell contained 5 ml of receiver solution and was placed in 100 ml of sample (magnetically stirred) to initiate the experiment. The dialysis times were 30 min. The membranes were soaked in receiver electrolyte for 15 min as a conditioning step. The quantification was carried out by pulse polarography (PAR Model 174), flame atomic-absorption

spectrometry (Varian 475) or by ion-selective electrode potentiometry (Orion Model 701A). The electrodes for the latter were cadmium (Orion 94–48), lead (Orion 94–82) and copper (Orion 94–29).

All chemicals used were of analytical-reagent grade. The Mg - Al receiver electrolytes were purified by electrolysing a 1 M Mg(II) - 0.025 M Al(III) mixture at a mercury pool at −1.3 V *vs.* S.C.E. for 1 week. The HCl used in the receiver electrolytes was purified by distillation. Only the constant-boiling, middle third of the distillate was retained. The house-distilled water was purified by passing it through Cole-Parmer Research, Universal and Adsorber cartridges.

The data are reported in terms of the enrichment factor, *EF*. Unless otherwise stated, *EF* is the ratio of analyte concentration in the receiver electrolyte, after dialysis and dilution, to the initial concentration of the analyte in the sample.

Results and Discussion

Preliminary experiments verified our earlier suggestion[4] that a 0.2 M $MgSO_4$ - 0.5 mM $Al_2(SO_4)_3$ mixture, which has a pH of about 4, is a useful receiver for the Donnan dialysis of divalent cations. For example, with the blender cell the enrichment factors for 1.0×10^{-6} M Pb(II), Cd(II), Cu(II) and Zn(II) alone (and in a mixture of nitrate salts of the four cations) were 21 (22), 27 (27), 27 (28) and 29 (32), respectively. The relative standard deviation of replicate experiments (10 trials) was 8%. The enrichment factor for each analyte was independent of concentration from 1×10^{-5} to 1×10^{-7} M. Except for Pb(II), which forms a precipitate with sulphate, the range also extended to higher concentrations. Except for Cu(II), which is an impurity in the blender system, the range was extended down to 5×10^{-9} M.

The utility of the receiver is related to the affinities of Mg(II) and Al(III) for the sulphonate sites on the membrane. Other cations, such as Ag(I) and Tl(I), that interact strongly with sulphonate[9] are useful components of a receiver electrolyte. The enrichment factors for 5.0×10^{-6} M Cu(II) into a cylindrical cell containing 0.2 M $NaClO_4$; 0.2 M $MgSO_4$; 0.2 M $MgSO_4$ - 0.5 mM $Al_2(SO_4)_3$; 0.2 M $MgSO_4$ - 5 mM $TlNO_3$; or 0.2 M $NaClO_4$ - 5 mM $AgNO_3$ are 5.2, 7.0, 8.1, 9.0 and 7.7, respectively. Because of the higher cost and toxicity of Ag(I) and Tl(I) salts, Al(III) is preferred as a receiver electrolyte component.

The Mg(II) – Al(III) mixture alone is not a suitable receiver for the Donnan dialysis of monovalent ions. The problem is exemplified by the following data. With a cylindrical cell, the enrichment factor for Na(I) into a 0.2 M $MgSO_4$ - 0.5 mM $Al_2(SO_4)_3$ mixture is 2.0, or less than half of the values for divalent metals. Adding either proton or lithium ion to the receiver increases the value to the range for divalent metals. The results are shown in Table 1. The enrichment factors are listed for only one concentration, but they are constant within experimental error over at least the range 1×10^{-4} to 1×10^{-7} M. The need to include a monovalent receiver cation for the Donnan dialysis of Na(I) is probably related to maintaining local charge balance at points within the membrane.

A test of the 0.2 M Mg(II) - 0.5 mM Al(III) receiver a pH 1 in the blender cell demonstrated that not only does it yield similar enrichment factors for monovalent and divalent cations, but also that the enrichment factors for the latter are about a factor of two higher than the above-reported values with Mg(II) - Al(III) at pH 4. With a mixture containing 1.0×10^{-8} M Pb(II), Cd(II), Zn(II) and Na(I), the enrichment factors were 48, 51, 49 and 46, respectively.

Bruce *et al.*[7] reported that 0.9 M $MgCl_2$ - 0.16 M $AlCl_3$ - 0.9 M HCl - 1.7 M NaCl - 0.02 M 2-mercaptoethanol was an optimised mixture for a receiver electrolyte for the Donnan dialysis of Pb(II). The results in Table 2 support their conclusion and also demonstrate the utility of that receiver for other cations. It is noteworthy that the enrichment factors were higher than were obtained with the 0.2 M Mg(II) - 0.5 mM Al(III) receiver at pH 1. Further, except for Zn(II), the values do not change significantly when mixed samples are used.

A comparison of the enrichment factors in Table 2 with the values reported with the Mg(II) - Al(III) receivers is misleading. With the former, the 5-ml receiver is diluted to 9.5 ml by osmosis during the 15-min dialysis. With the latter, the dilution is only from 5.0 ml to 5.3 ml. Hence, if quantifications were performed on the undiluted dialysate, the latter receiver would yield the higher enrichment factors. In addition, because of the high concentrations of solutes, the Table 2 receiver tends to clog atomic-absorption burners. The relatively complex matrix may also be poorly suited for use with other analytical methods.

In the above examples, receiver cations with high affinities towards sulphonate were used to displace analytes from the sulphonate sites. The possible exception is the use of 2-mercaptoethanol in the experiments summarised in Table 2; it has an uncertain role in acidic solution. An alternative approach is to use a chelating agent at a pH at which reactions with the analytes can be anticipated. The chelation will minimise hold-up on the fixed exchange sites on the membrane. Based on this model, mixtures of NaCl and EDTA at pH 8.5 were used as receiver electrolytes.

Table 3 lists the enrichment factors for Cu, Cd, Pb and Zn, alone and from the four-component mixture. The enrichment factors are higher than the values observed with the other receiver electrolytes; however, they varied with the composition of the sample. In fact, with the four-component mixture they approached the limit of 100 for the experimental design (1000-ml sample, 10-ml diluted receiver volume).

In an attempt to devise a procedure whereby the EDTA-containing receiver would provide high and constant enrichment factors, the effect of dialysis time on the preconcentration was examined. At 1, 5, 10 and 15 min, the enrichment factors with a 1.0×10^{-6} M Cd(II) sample were 11, 40, 54 and 77, respectively. Subsequent studies were therefore performed with 5-min dialyses, at which the approach to Donnan equilibrium was avoided.

Even with 5-min dialyses, the EDTA-containing receiver did not provide analytically useful pre-concentrations. The enrichment factor depended on the Cd(II) concentration. With 5.0×10^{-7}, 1.0×10^{-6} and 1.5×10^{-6} M Cd(II), the enrichment factors were 30, 40 and 54, respectively. Moreover, a repeat of the Table 3 experiments, but with 5-min dialyses, resulted in an increase in the enrichment factor from 40 to 49 when the four-component mixture, rather than Cd(II) alone, was the sample. Changing the receiver component concentrations, using $Na_2MgEDTA$ and adding an excess of a divalent metal to the sample all failed to alleviate these problems.

Because it provided the most rapid Donnan dialyses of the systems that were investigated, the EDTA-containing receiver may find application in studies where removal of metals from aqueous samples is the objective. In addition, the data obtained demonstrate that semi-quantitative results can be attained with the system.

If ion-selective electrode potentiometry is to be used for quantification, the choice of the receiver electrolyte is restricted. It cannot contain complexing agents as the response is related to the free ion activity. The Mg(II) - Al(III) solutions are candidates for Donnan dialysis receivers that are compatible with ion-selective electrodes. Table 4 summarises the results of plots of electrode potential (mV) *versus* the common logarithm of the concentration of metals in 0.2 M $MgSO_4$ - 0.5 mM $Al_2(SO_4)_3$ at various pHs. In the recommended ionic strength adjustment buffer, 0.1 M $NaNO_3$, the electrodes gave the theoretical slope of 29 mV.

In the pH 4 solution, the Cd(II) ion-selective electrode responded as well as in the recommended ionic strength adjustment buffer. The Cu(II) electrode gave a lower slope

Table 1. Donnan dialysis enrichment factors into a 0.2 M Mg(II) - 0.5 mM Al(III) receiver at pH 1. Cylindrical cell with 4 cm^2 P-1010 membrane; all metals 5×10^{-6} M chloride salts except that $Pb(NO_3)_2$ was used. *EF* = the ratio of the concentration of the analyte in the diluted receiver after dialysis to the initial concentration in the sample

	EF			
Sample	Na	Cu	Ni	Pb
Na	5.2			
Cu		4.6		
Na - Cu	5.3	4.6		
Ni			5.1	
Ni - Na - Cu	5.4	4.7	5.2	
Pb				5.6
Pb - Na - Cu - Ni	5.5	4.7	5.0	5.6

Table 2. Donnan dialysis enrichment factors into an acidified mixture of Mg(II), Al(III), Na(I) and 2-mercaptoethanol. Blender cell with the receiver: 0.9 M $MgCl_2$ - 0.16 M $AlCl_3$ - 0.9 M HCl - 1.7 M NaCl - 0.02 M 2-mercaptoethanol

Sample	*EF*
1.0×10^{-6} M Pb(II)	57
1.0×10^{-6} M Cu(II)	60
1.0×10^{-6} M Cd(II)	66
1.0×10^{-6} M Zn(II)	61
Mixture containing:	
1.0×10^{-6} M Pb(II)	60
1.0×10^{-6} M Cu(II)	62
1.0×10^{-6} M Cd(II)	68
1.0×10^{-6} M Zn(II)	69

Table 3. Donnan dialysis enrichment factors into a 0.2 M $NaNO_3$ - 0.02 M EDTA receiver at pH 8.5. The blender cell was used with 15-min dialyses

	EF	
Analyte	Single-component sample	Four-component mixture
1.0×10^{-6} M Cu(II)	75	87
1.0×10^{-6} M Pb(II)	82	86
1.0×10^{-6} M Cd(II)	77	97
1.0×10^{-6} M Zn(II)	87	97

Table 4. Ion-selective electrode responses in $MgSO_4$ - $Al_2(SO_4)_3$ solutions

Analyte	Solution* pH	*S*†/mV	Range‡/mol l^{-1}
Cd(II)	1	16	10^{-3}–10^{-5}
	2	28	10^{-2}–10^{-6}
	4	29	10^{-2}–10^{-6}
Cu(II)	1	16	10^{-3}–3×10^{-5}
	2	21	10^{-3}–3×10^{-5}
	4	24	10^{-3}–1×10^{-5}
Pb(II)	1	5	10^{-3}–10^{-4}
	2	15	10^{-3}–10^{-4}
	4	22	10^{-3}–10^{-4}

* 0.2 M $MgSO_4$ - 0.5 mM $Al_2(SO_4)_3$ adjusted to the tabulated pH with H_2SO_4.

† Slope of *E* (mV) *vs.* log c_m at 22 °C.

‡ Concentration range for which the graph is linear.

than observed in the recommended medium; in addition, the detection limit was poorer by an order of magnitude. The Pb(II) electrode did not yield useful quantitative data in the Table 4 experiments. Because the failure of the Pb(II) ion-selective electrode is undoubtedly related to sulphate, the experiments in Table 4 were repeated using 0.2 M $Mg(NO_3)_2$ - 1.0 mM $Al(NO_3)_3$ solutions at pH 4. The slopes for the Cd(II), Cu(II) and Pb(II) ion-selective electrodes were 27, 27 and 28 mV, respectively. The ranges over which straight-line calibration graphs were obtained were 10^{-3}–10^{-6} M Cd(II), 10^{-3}–10^{-6} M Cu(II) and 10^{-2}–5×10^{-5} M Pb(II).

The results of the above experiments suggest that the cadmium ion-selective electrode can be used in either 0.2 M $MgSO_4$ - 0.5 mM $Al_2(SO_4)_3$ or 0.2 M $Mg(NO_3)_2$ - 1.0 mM $Al(NO_3)_3$ at pH 4. By combining a 15-min Donnan dialysis in the blender cell with ion-selective electrode quantification, cadmium concentrations at the 10^{-8} M level can be determined. The copper electrode response does not match the theoretical slope in either the nitrate or sulphate forms of the Mg(II) - Al(III) electrolyte, and the lower limit of the working range is about an order of magnitude less than expected. Nevertheless, with the nitrate salts the combination of Donnan dialysis and ion-selective electrode potentiometry can be used down to the 10^{-8} M level. Likewise, the lead electrode can be used to quantify samples down to the 5×10^{-7} M level with the $Mg(NO_3)_2$ - $Al(NO_3)_3$ receiver.

Generally, sulphate is preferred over nitrate as the anion in the receiver for Donnan dialysis because it Donnan-penetrates the cation-exchange membrane to a lesser extent. The enrichment factors are therefore higher.[6] In either instance, the dialyses should be performed at pH 1; adjustment to pH 4 should be performed prior to ion-selective electrode quantification.

With flame atomic-absorption spectrometry or pulse polarography as the quantification technique, the 0.2 M $MgSO_4$ - 0.5 mM $Al_2(SO_4)_3$ receiver at pH 1 is recommended because the enrichment factors are high and similar for a variety of cations and the experimental procedure is simple. If the burner can tolerate high concentrations of solutes and meticulous rinsing between trials is performed, the mixture described in Table 2 is superior for atomic absorption.

Although the research described in this paper was funded in part by the US Environmental Protection Agency under assistance agreement number CR-809397 to Southern Illinois University, it has not been subjected to the Agency's required peer and administrative review and therefore does not necessarily reflect the view of the Agency and no official endorsement should be inferred.

References

1. Cox, J. A., Olbrych, E., and Brajter, K., *Anal. Chem.*, 1981, **53**, 1308.
2. DiNunzio, J. E., *PhD Dissertation*, Southern Illinois University, Carbondale, IL, 1978.
3. Cox, J. A., and Twardowski, Z., *Anal. Chim. Acta*, 1980, **119**, 39.
4. Cox, J. A., and DiNunzio, J. E., *Anal. Chem.*, 1977, **49**, 1272.
5. Cox, J. A., and Twardowski, Z., *Anal. Lett.*, 1980, **13**, 1283.
6. Cox, J. A., and Gajek, R., Litwinski, G. R., Carnahan, J. W., and Trochimczuk, W., *Anal. Chem.*, 1982, **54**, 1153.
7. Bruce, M. L., Carnahan, J. W., and Caruso, J. A., Pittsburgh Conference on Analytical Chemistry and Applied Spectroscopy, Atlantic City, NJ, March, 1983, Abstr. No. 268.
8. Cox, J. A., and Litwinski, G. R., *Anal. Chem.*, 1983, **54**, 1640.
9. Rieman, W., and Walton, H. F., "Ion Exchange in Analytical Chemistry," Pergamon Press, New York, 1970, Chapter 3.

Paper A4/219
Received July 3rd, 1984
Accepted August 1st, 1984

An Examination of Instrumental Systems for Reducing the Cycle Time in Atomic-absorption Spectroscopy With Electrothermal Atomisation

M. Hossein Bahreyni-Toosi, John B. Dawson,* Duncan J. Ellis and Roger J. Duffield
Department of Medical Physics, The General Infirmary, Leeds LS1 3EX, UK

The sensitivity, detection limit, reproducibility, matrix effects and cycle time of five atomic-absorption systems with electrothermal atomisation were determined to assess their suitability for the determination of copper and zinc in plasma protein fractions separated by ion-exchange column chromatography. The systems were: a Massmann furnace with a graphite or metal tube, a mini-Massmann atomiser with graphite tubes or cups, a Massmann furnace with an interchangeable graphite cup insert and a Massmann tube furnace coupled to a mini-Massmann graphite cup atomiser. It was found that the Massmann furnace was analytically the most sensitive system, but it was also the slowest. The coupled furnaces suffered the least interference and the fastest system was the Massmann tube with interchangeable sample cup insert. Although all systems had adequate sensitivity it was concluded that none was sufficiently simple and rapid to meet the needs of the proposed analysis.

Keywords: *Electrothermal atomisation; atomic-absorption spectroscopy; copper determination; zinc determination*

In a previous paper[1] we reported a study of instrumental techniques used to increase the sensitivity of flame atomic absorption with a view to developing a rapid and sensitive procedure for the determination of zinc and copper in blood plasma separated by ion-exchange column chromatography.[2] We concluded that no flame-based method could fully meet our requirements and therefore undertook a study of furnace atomising systems. The outstanding advantage of atomic-absorption spectroscopy with electrothermal atomisation (ETA-AAS) for our purpose was its great sensitivity[3]; its major disadvantages were interferences and a long cycle time. By use of the L'vov platform,[4] or one of its variants, *e.g.*, the graphite probe[5] or inner miniature cup,[6] in combination with matrix modification, background correction and integrated absorbance measurement, interference problems can be largely overcome. However, the cycle time for these procedures is of the order of 2 min.

The time-consuming stages in ETA-AAS are drying and pyrolysis of the sample and the cooling of the furnace before the next sample may be injected. While it was considered that changes in furnace design and operating procedures could lead to some reduction in cycle time, it seemed unlikely that a major improvement could be achieved. It was therefore decided to investigate the feasibility of instrumental systems in which the sample was prepared for atomisation remote from the optical axis of the instrument and was then brought into the absorbance path only for the brief period required for atomisation. Two approaches are possible, one in which several atomising chambers are moved sequentially into the optical path, the other a single atomising chamber fixed on the optical axis into which a support carrying a pre-processed sample is inserted. In the former approach, while the sample is being dispensed into the first chamber, the second chamber is drying its sample, another sample is being ashed in the third chamber while atomisation is taking place in the fourth chamber (positioned in the optical path of the spectrophotometer) and, at the same time, the fifth furnace is cooling in preparation for sample injection. In the latter approach samples in small cups are dried and pyrolysed batchwise and introduced sequentially into the furnace tube for atomisation. Pilot studies of both approaches were carried out and provided information on the technical feasibility of the instrumental configuration being examined. The systems examined include micro-furnaces, metal atomisers, a tube furnace with sample cup and a coupled furnace system in which one furnace atomises the sample into the furnace in which the AAS measurements are made. The performance of these systems with respect to accuracy, precision, speed, ease of operation and reliability was examined in relation to the determination of copper and zinc in 0.1 M HNO_3 and in the ion-exchange eluting buffer. The purpose of this paper is to record our experiences of the advantages and limitations of the alternative approaches that we examined and relate these to the general development of atomic-absorption spectroscopy with electrothermal atomisation.

* To whom correspondence should be addressed.

Experimental

Apparatus

A laboratory-assembled optical system (Fig. 1) was used for all atomic-absorption measurements with the several furnace systems. The design of each furnace and the results obtained will be presented later in the paper.

The sources of resonance radiation were hollow-cathode lamps (Cathodeon Ltd.) operated in the pulse mode (400 Hz, 300 μs, 30 mA) with background correction provided by a deuterium lamp (Cathodeon Ltd. Type C71-2V-HDl). The radiation from the D_2 lamp was modulated at 400 Hz by a rotating chopper disc, which also generated trigger pulses for the hollow-cathode lamp power supply.

The aperture of the prism monochromator was *f* 10 and its wavelength range was 200–600 nm; the reciprocal dispersion was 2 nm mm^{-1} at 213.9 nm (zinc) and 10 nm mm^{-1} at 324.8 (copper). The wavelength dependence of the focal length of the light-collecting lens was accommodated by adjusting the position of the lens to give the maximum output from the photomultiplier (Hamamatsu, R456) for each of the elements determined. The atomic-absorption signal was extracted by a lock-in amplifier (Brookdeal 401A) as the difference between signals generated by the hollow-cathode and deuterium lamps. The reference signal for the lock-in amplifier was taken from the hollow-cathode lamp power supply. This method of signal processing is suitable for the measurement of small absorbances. It is simple and sensitive and gives total correction for furnace emission and first-order correction for background absorption. The output of the amplifier was

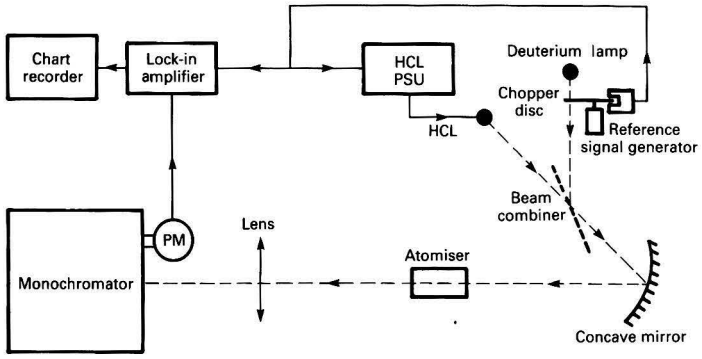

Fig. 1. Schematic diagram of atomic-absorption apparatus. HCL, Hollow cathode lamp; PM, photomultiplier; and PSU, power supply unit

displayed on a potentiometric chart recorder (Smiths Industry, Servoscribe 1S). The response time of the system was *ca.* 0.3 s, hence when atomisation was rapid the trace obtained did not accurately represent the true atomic-absorption signal.

Two atomiser systems were required. One was a Massmann-type furnace with graphite or metal tubes, (effective length, 28 mm; i.d., 5 mm) and the other used either a miniature graphite tube (length, 12.5 mm; i.d., 3.5 mm) or a "cup" (height 3 or 6 mm; i.d., 3.5 mm), supported by graphite rods and similar in design to the CRA 90 (Varian Techtron). Both systems were constructed "in-house" with special attention being given to efficient water cooling and gas shielding of the furnaces.

Two laboratory-made atomiser power supply units were required. One was of the full wave rectified, programmable voltage ramp type incorporating four stages with a maximum output of 300 A at 12 V; this unit was used to drive the Massmann-type furnace systems. The other unit, used to drive rod and cup atomisers, was triac controlled and provided adjustable increases of output current in four stages of 30, 60, 30 and 6 s. All furnace tubes and cups were manufactured "in-house" from Ringsdorf Spectrograde graphite. A flow meter (G. A. Platon Ltd., Gapmeter, 0–2 l of air) was used to monitor the shield gas supply to the furnace system. Furnace temperatures were measured by an optical pyrometer (Cambridge Industrial Instruments Type 13422) and by a calibrated photodiode (R. S. Components Ltd. Type RS308–067).

Reagents

AnalaR or Aristar grade materials were used to minimise trace element contamination. Commercial standard solutions for atomic-absorption spectroscopy (BDH Chemicals Ltd.), were diluted to give working solutions for copper and zinc in two matrices: 0.1 M nitric acid (pure solution) and 0.05 M tris(hydroxymethyl)methylamine - hydrochloric acid, 0.2 M sodium chloride, pH 7.4 (tris buffer solution).

Oxygen-free nitrogen (BOC Ltd.) was used as the furnace shield gas unless stated otherwise. The alternative gases were argon (BOC Ltd., welding grade) and an argon - methane (90 + 10%) mixture (BOC Ltd., Special Gases) which was used when pyrolytic coating of graphite furnaces or support electrodes were required.

Results and Discussion

Preliminary Experiments

The performance of the basic furnace systems, the Massmann tube and mini-Massmann tube and cup, operated in conventional mode, *i.e., in situ* drying and pyrolysis of the sample, was first examined in order to provide a base line against which modifications to the systems could be measured.

The ends of the Massmann tube furnace were closed by quartz windows and an internal gas flow was provided to prevent deposition of debris from the sample on the windows. The performance of the furnace is summarised in Table 1 and is comparable with that reported by Gardiner *et al.*[3] for a commercial system. The sensitivity and detection limits were more than adequate to measure copper and zinc in fractionated blood plasma but in this instance the reproducibility was barely satisfactory, matrix effects were substantial and the cycle time unacceptably long. The lack of reproducibility and interference effects may arise from non-optimised operating conditions, incomplete ashing of organic material in the inert atmosphere of the furnace and from trapped salt vapour. The efficient cooling systems achieved a cooling time of 15–30 s but led to condensation and subsequent re-vaporisation of sample material during the atomisation stage. This effect was later overcome by the removal of the quartz windows. The lifetime of the furnace was rather short (*ca.* 100 firings) but was at least doubled if the tube was pyrolytically coated. The coating was produced by heating a new furnace to *ca.* 2500 K for 5 s in an argon - methane atmosphere and repeating the cycle three times. The performance of the furnace was maintained by repeating the coating procedure after every 50 firings.

When the mini-Massmann tube and cup furnaces were constructed, particular care was required to ensure that the ends of the support electrodes were machined to a radius equal to that of the tube or cup. Uneven heating of the furnace tube resulted when its length was greater than 15 mm and also when the supporting electrodes aged. When using the cup system, the optical axis passed either just over the lip of the cup (internal depth, 2.5 mm) or through an aperture 1 mm above the bottom of the cup (internal depth, 4.0 mm). The mini-Massmann tube system tended to generate double atomic-absorption peaks, particularly as the furnace aged. With a cup system the second peak was insignificant but as the cup aged it again increased in magnitude. The cause of the double peaks was not investigated.

The experimental results for the mini-Massmann tube and cup systems are summarised in Table 2. The data for the cup system relates to the configuration in which the optical axis passes through an aperture close to the base of the cup as this was the most sensitive system. The mini-Massmann tube furnace achieves lower concentration sensitivity and detection limits (p.p.b.) for copper than does the cup but in absolute terms (pg) owing to its lower sample volume, the cup is the more sensitive. For zinc, a more volatile metal, the cup is more sensitive in both concentration and absolute terms. The suppressant effect of the matrix and the reproducibility of measurements are similar for both tube and cup though the cycle time for the latter is slightly shorter. The lifetime of the

Table 1. Performance of a Massmann-type furnace in the determination of copper and zinc

Element and atomisation temperature	Detection limit		Sensitivity (0.0044 absorbance unit)		C.V.*, %	Sample volume/ µl	Cycle time/ s	Effect of matrix B, %
	ng ml^{-1}	pg	ng ml^{-1}	pg				
Copper (2910 K): A†	0.26	7.8	1.04	31	4.0	30	130	−35
B†	0.38	11.5	1.6	48	6.0			
Zinc (2240 K): A†	4.6×10^{-3}	0.092	7.5×10^{-3}	0.15	4.6	20	120	−76
B†	2.0×10^{-2}	0.40	3.1×10^{-2}	0.62	7.2			

* C.V., coefficient of variation.
† Matrix: A, 0.1 M nitric acid; and B, Tris - HCl buffer, 0.2 M NaCl solution.

Table 2. Mini-Massmann tube (1) and cup (2) furnace performance in the determination of copper and zinc

Furnace	Element and atomisation temperature	Detection limit		Sensitivity (0.0044 absorbance unit)		C.V.*, %	Sample volume/ µl	Cycle time/ s	Effect of matrix B, %
		ng ml^{-1}	pg	ng ml^{-1}	pg				
1	Copper (2870 K): A†	3.0	60	10	200	4.9	20	110	−38
	B†	4.9	98	16	320	5.3			
1	Zinc (2170 K): A†	0.22	2.2	0.4	4.0	6.1	10	100	−68
	B†	0.65	6.5	1.23	12.3	7.2			
2	Copper (2900 K): A†	4.2	21	18	92	4.3	5	80	−34
	B†	6.6	33	28	140	5.2			
2	Zinc (2150 K): A†	0.16	0.8	0.2	1.0	6.0	5	80	−58
	B†	0.40	0.2	0.48	2.4	6.3			

* C.V., coefficient of variation.
† Matrix A, 0.1 M nitric acid; and B, Tris - HCl buffer, 0.2 M NaCl solution.

tubes and cups was 70–100 firings. The sensitivity of both systems is adequate for the determination of copper and zinc in blood plasma fractions but the reproducibility and matrix effects would require improvement; the cycle time is unacceptably long.

In all systems, the sensitivity and reproducibility of measurements using pure solutions were better than those for the buffer solution. The suppressant effect of the matrix was similar for all systems and was greatest for zinc. Some of this effect may be attributable to limitations of the background correction electronic system. The conventional Massmann furnace gave the greatest sensitivity and, analytically, is the preferred system but was the slowest of those examined.

From the studies using the mini-Massmann tube, graphite cups and the Massmann furnace tube two conclusions were drawn. First, by virtue of their sensitivity, electrothermal atomisers were the preferred means for the determination of Cu and Zn in separated plasma fractions; second, the design and construction of a rotating multi-furnace system as considered at the beginning of the paper using any of the present furnaces was not as feasible as it had been originally thought. The problems lay in finding ways for the accurate alignment of the atomisers in the optical path and of providing the required shield gas, cooling water and electrical connections for the system. Also a multiplicity of power supplies would be required to provide power for drying, ashing and atomisation of each furnace independently but simultaneously such that the time interval and temperature of each furnace could be programmed. Owing to these problems, although the possibility of developing such a system was not completely ruled out, it was decided that a technique in which a single atomic-absorption furnace remained fixed on the optical axis and the sample delivered to it by a variety of auxiliary devices should be examined.

Cup-in-tube Atomiser

The L'vov platform[4] and its variations have been shown to give sensitive analysis with the minimum of interference. When the platform or miniature cup is used *in situ* for drying and pyrolysis of the sample prior to atomisation the cycle time is long. It is therefore attractive to examine the feasibility of increasing the sample throughput by drying and pyrolysing the samples in batches external to the furnace and to use the furnace for atomisation only. Preliminary treatment of the sample external to the furnace is used in the graphite probe system,[5] but as samples are treated singly there is no improvement in sample throughput. The design of most platforms is such that insertion into the furnace is not a simple, rapid operation. We therefore developed a modified sample container whereby samples could be changed rapidly.

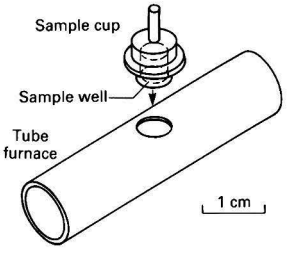

Fig. 2. Cup-in-tube atomiser

The final design of the sample container (cup) and its position relative to the main Massmann furnace is shown in Fig. 2. In order that the sample cup heats rapidly it was made as small and as light as possible (170 mg) compatible with ease of handling and adequate sample volume. The effects of contamination that could arise from handling the cup were minimised by ensuring that no handled surface came into contact with the furnace. The cups were handled by the "tail" using cleaned stainless-steel tweezers. To accommodate the cups, it was necessary to modify the furnace tube design by increasing the diameter of the tube to 10 mm and that of the sample injection port to 6 mm. The cup was a light "press fit" into the injection port to ensure reproducible heating.

Table 3. Performance of the cup-in-tube furnace system in the determination of zinc. Processing temperatures: dry, 20–30 s at 365 K; ash, 30–40 s at 720 K; atomise, 8 s at 2200 K. Average time per sample (batch of 40 samples): 50 s

Matrix*	Detection limit ng ml^{-1}	Detection limit pg	Sensitivity (0.0044 absorbance unit) ng ml^{-1}	Sensitivity (0.0044 absorbance unit) pg	C.V.†, %	Sample volume/ µl	Effect of matrix B, %
A	0.035	0.35	0.07	0.7	5.0	10	−46
B	0.066	0.66	0.13	1.3	6.3	10	

* Matrix: A, 0.1 M nitric acid; and B, Tris - HCl buffer, 0.2 M NaCl solution.
† C.V., coefficient of variation.

Sample volumes of up to 20 µl could be accommodated by the cups. Care was necessary when dispensing samples to avoid trapping bubbles of air in the cup. To prepare samples for analysis, a batch of sample-containing cups is placed on a stainless-steel drying - ashing plate with 60 cup holes and heated by an electric hot-plate from above during the drying stages (20–30 s) and from below during the ashing stage (30–40 s). The cups are transferred, in turn, to the furnace which is then heated as rapidly as possible to a temperature sufficient to atomise the sample from the cup into the furnace (*ca.* 8 s). The furnace is then allowed to cool (25 s) before the next cup is inserted. A batch of 40 samples can be analysed in under 35 min.

Results obtained with the cup-in-tube system for the determination of zinc are presented in Table 3. Compared with previous results obtained by atomisation from the tube wall (Table 1) there is a four- to eight-fold loss of sensitivity when measuring pure solutions but only a two- to three-fold loss when analysing buffer solution. The matrix effect and cycle time per sample are also reduced. As all measurements are based on absorbance peak height the slower evolution of the atom vapour from the cup and the increased volume of the furnace tube may contribute to the large loss of sensitivity, peak-area measurement would perhaps reduce this effect.

The performance of the system for the determination of copper, cadmium and lead was also examined. The results for cadmium and lead were satisfactory and gave sensitivities of 0.3 and 12.5 pg, respectively. For copper, however, the technique was not successful owing to the inadequate heating of the cup via the furnace wall.

It was concluded that the cup-in-tube system is satisfactory for the determination of volatile elements. It is relatively rapid and suffers from less interference than the tube alone. For less volatile elements the heating of the sample cup is inadequate and some system of applying additional heat to the sample cup is necessary.

Coupled Furnace Atomiser

In the original design of the L'vov furnace[7] for atomic absorption the sample was atomised from an arc-heated electrode into an electrically heated graphite tube furnace. This system though very sensitive was cumbersome and not very precise and has not found popular use. A more recent system described by Frech and Jonsson,[8] combines an electrically heated graphite cup atomiser with a tube furnace. The former is fastened tightly into an aperture on the lower side of the latter and sample injection is via a sampling port in the upper surface of the furnace tube. The sample is dried by heating the tube to *ca.* 850 K and the cup to 370 K for 20–40 s. The tube is then heated to a pre-selected temperature dependant upon the element to be determined. When this temperature is reached the cup is heated as rapidly as possible to the same temperature. The results obtained with the system showed a small loss of sensitivity (*ca.* 30%) compared with an equivalent commercial system but comparable reproducibility. Using peak-area measurements in the determination of lead in a variety of matrices no differences between pure water and salt solutions were found. Identical analytical conditions can be used for many elements that could facilitate multi-element analysis. By separating the atomisation chamber from the absorption chamber fundamental reactions in each chamber can be studied independently. As our interest in a two-chamber system is directed at increasing the sample throughput, it is unlikely that the system of Frech and Jonsson, which uses *in situ* sample preparation, would achieve that goal. However, we have developed a similar system in which the graphite cup atomiser is mounted on a movable arm. This atomiser is removed from the tube furnace when changing the sample-containing cup. The samples are prepared external to the atomiser in a manner similar to the previously described cup-in-tube system.

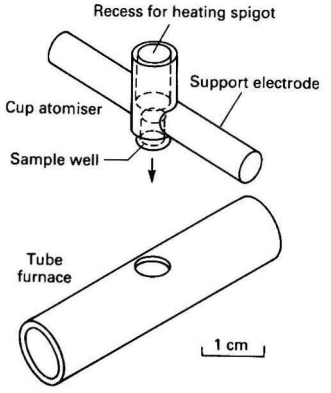

Fig. 3. Coupled-furnace atomisation system

The coupled-furnace system is shown schematically in Fig. 3. It is based on a combination of the furnace previously used in the cup-in-tube system and the cup atomiser used in the preliminary experiments. The auxiliary furnace was attached to an arm that, when rotated, brought the sample cup into an aperture in the main furnace tube. Accurate positioning of the cup with respect to the furnace aperture was critical if reliable results were to be obtained. This was achieved by locating a conical tipped screw attached to a plate beside the main furnace into a V-shaped groove on the furnace mount. The purpose of the recess in the base of the cup is to reduce the thermal mass of the cup and to provide efficient thermal connection between the cup and the hot-plate when drying and pyrolysing the sample.

Preliminary trials of the system indicated that the protrusion of the cup into the furnace tube had a major effect on the atomic-absorption sensitivity, the latter being doubled as the lip of the cup moved from the tube wall to a protrusion of 2.5 mm. A greater protrusion led to a significant obstruction of the optical beam and less reproducible results. For subsequent studies a protrusion of 2.0 mm was used.

Table 4. Performance of the coupled-furnace system in the determination of copper and zinc. Processing temperatures: dry, 30–40 s at 350–380 K; pyrolyse, 30–40 s at 725 K (zinc) or 930 K (copper); atomise, 5–6 s at 2230 K (zinc) or 2900 K (copper). Average time per sample (batch of 40 samples): 60 s

Element	Detection limit		Sensitivity (0.0044 absorbance unit)		C.V.*, %	Sample volume/ µl	Effect of matrix B, %
	ng ml^{-1}	pg	ng ml^{-1}	pg			
Copper: A†	0.41	8.2	1.5	30	4.8	20	−30
B†	0.7	14	2.15	43	6.3		
Zinc: A†	0.01	0.1	0.013	0.13	5.6	10	−38
B†	0.016	0.16	0.021	0.21	7.5		

* C.V., coefficient of variation.
† Matrix: A, 0.1 M nitric acid; and B, Tris - HCl buffer, 0.2 M NaCl solution.

Samples were prepared batchwise for analysis using the hot-plate system described earlier. The holes in the sample-holding plate were replaced by pins to hold the sample cups for this work. To position a cup accurately between the atomiser support electrodes, a spacer block was placed on the shield gas baffle below the electrode. The cup was placed on the block between the spring-loaded electrodes, which when released, held the cup tightly in the correct position. The tube furnace power supply was switched on 2–4 s before the cup atomiser was rotated to it. As soon as the latter was in position its power supply was switched on for 5–6 s. The tube furnace supply was switched off 2–5 s after that of the cup atomiser. The flow of shielding gas (nitrogen) was 2 l min^{-1}. The internal gas flow of the tube furnace was 200 ml min^{-1} rising to 750 ml min^{-1} for the period (2–5 s) between the switch-off of the two furnaces to remove the atom vapour from the system.

The results obtained with the coupled-furnace system are presented in Table 4. The general performance of this system was promising in that it was capable of determining copper, its sensitivity was only slightly worse than that for "off the wall" atomisation for a Massmann furnace, interference effects were acceptable and the average cycle time per sample for a batch of 40 samples was 60 s.

The suitability of the coupled-furnace system for the rapid determination of copper and zinc in plasma protein fractions was, however, limited by several factors. The alignment of the cup in its supporting electrodes was a time-consuming step (20–30 s) and thus slowed up the operation. Further, it was suspected that the method of cup handling led to random contamination by zinc. With copper, there was a problem of carryover from one sample to the next as a result of condensation of sample vapour on the wall of the tube furnace. This difficulty was partly overcome by drilling a hole in the wall of the tube furnace directly opposite the sampling port so that vapour could escape before condensing on the walls of the tube. In practice, however, this latter tube was found to be too fragile to be used routinely.

Metal Atomisers

In the early stages of development of the coupled-furnace system consideration was given to replacing the graphite tube atomiser with one made of metal. The object of the change was to achieve a stronger tube that could withstand the stresses created by cutting a large sampling aperture and extra gas escape hole through the tube wall.

Metal atomisers in the form of either filaments or tubes have been used in atomic-absorption analysis for over a decade and have been reported to give greater sensitivity with fewer interferences than graphite.[9–12] The metals used included tantalum, molybdenum and tungsten. In our study we examined the suitability of tantalum, tungsten and two alloys, nimonic and stainless steel. Use of the latter was considered feasible in that as atomisation was from the graphite cup, the furnace temperature need not exceed *ca.* 1800 K. All tubes were fabricated from sheet metal with the exception of the stainless-steel tubes. The sampling port was drilled in the flat sheet before forming the tube. The tubes were operated in an argon atmosphere to avoid the formation of nitrides.

The alloys were found to be unsatisfactory as tube furnace materials because although the metal withstood the operating temperature of the furnace when heated alone, when the sample cup was inserted into the tube and heated, the edges of the sampling hole melted.

The fabrication of the tungsten tube was difficult and required heating with an argon arc during the bending process. The final product was brittle and had a short working life. Of five tubes constructed, the highest number of firings achieved with any one tube was about 50. Tantalum tubes were easier to fabricate and, given adequate gas shielding, lifetimes in excess of 300 firings could be achieved. However, it was found that if the tubes were heated to temperatures in excess of 2800 K for cleaning purposes, a copper signal was generated that was subsequently identified as an impurity in the tantalum metal.

The most important characteristics of a material to be used for the fabrication of furnace tubes and cups are: high melting-point, very low level of impurities, chemical inertness, high strength, machinable, low thermal expansion and maintenance of a stable shape. Our experiences with metal atomisers showed that they do not meet these criteria as well as graphite. We concluded that carbon in one or other of its forms is the most suitable material for furnace construction at the present time.

Conclusions

In the course of attempting to develop a sensitive and rapid method for the determination of copper and zinc in plasma protein fractions we have investigated several atomic-absorption systems with electrothermal atomisation based on the Massmann furnace and on the mini-Massmann tube and cup atomisers. Of all the systems examined the Massmann furnace was the most sensitive while the coupled-furnace system suffered the least interference.

Using the cup-in-tube technique, satisfactory results were obtained for zinc and other volatile elements but owing to insufficient heating of the sample cup it was not successful for the determination of copper. Matrix interferences were reduced when samples were ashed externally in air followed by atomisation into a pre-heated absorption tube. This is consistent with the observations of many workers using the L'vov platform and graphite probe *e.g.*, Slavin *et al.*[13] This approach led to the development of the coupled-furnace system. The sensitivities and detection limits obtained from the coupled-furnace system were similar to those of the conventional Massmann systems. The precision of all systems was comparable and ranged from 4.0 to 5.6% for measurements of pure solutions to 5.3 to 7.5% for buffer solutions.

The analysis time per sample was greatest for the Massmann furnace (130 s) and shortest for the cup-in-tube system (50 s). As the range of elements to which the latter system can be applied is limited, the fastest usable system is the coupled furnace. In its present form, this system is mechanically elaborate and requires skilled manual handling of the sample cups. In our opinion, it is unlikely that significant improvements can be made with respect to these limitations to this or any other similar system and therefore increased sample throughput in atomic absorption with electrothermal atomisation is more likely to be achieved by refinement of existing systems. Following this approach, the cycle time of a conventional Massmann system has been reduced to approximately 1 min by omitting the pyrolysis step[14] and, using a specially developed segmented graphite rod atomiser in which the sample solution is atomised directly without prior drying and pyrolysis, we achieved an analysis time as short as 30 s,[15] which is adequate for the determination of copper and zinc in plasma protein fractions.

References

1. Bahreyni-Toosi, M. H., Dawson, J. B., and Duffield, R. J., *Analyst*, 1984, **109**, 943.
2. Dawson, J. B., Bahreyni-Toosi, M. H., Ellis, D. J., and Hodgkinson, A., *Analyst*, 1981, **106**, 153.
3. Gardiner, P. E., Ottaway, J. M., Fell, G. S., and Burns, R. R., *Anal. Chim. Acta*, 1981, **124**, 281.
4. L'vov, B. V., *Spectrochim. Acta, Part B*, 1978, **33**, 153.
5. Littlejohn, D., Marshall, J., Carroll, J., Cormack, W., and Ottaway, J. M., *Analyst*, 1983, **108**, 893.
6. Atsuya, I., and Itoh, K., *Spectrochim. Acta, Part B*, 1983, **38**, 1259.
7. L'vov, B. V., *Spectrochim. Acta*, 1961, **17**, 761.
8. Frech, W., and Jonsson, S., *Spectrochim. Acta, Part B*, 1982, **37**, 1021.
9. Cantle, J. E., and West, T. S., *Talanta*, 1973, **20**, 459.
10. McIntyre, N. S., Cook, M. G., and Boase, D. G., *Anal. Chem.*, 1974, **46**, 1983.
11. Sychra, V., Kolihova, D., Vyskocilova, O., Hlavac, R., and Puschel, P., *Anal. Chim. Acta*, 1979, **105**, 263.
12. Ohta, K., and Suzuki, M., *Talanta*, 1979, **26**, 207.
13. Slavin, W., Carnrick, G. R., Manning, D. C., and Pruszkowska, E., *At. Spectrosc.*, 1983, **4**, 69.
14. Halls, D. J., *Analyst*, 1984, **109**, 1081.
15. Bahreyni-Toosi, M. H., and Dawson, J. B., *Analyst*, 1983, **108**, 225.

Paper A4/169
Received May 2nd, 1984
Accepted July 11th, 1984

SHORT PAPERS

Investigations on the Determination of Aluminium in Aluminium Alkoxides and Carboxylates Using Direct Carbon-furnace Atomisation

Duncan Thorburn Burns, Darioush Dadgar, Michael Harriott, Kevin McBride and W. James Swindall
Department of Pure and Applied Chemistry, The Queen's University of Belfast, Belfast BT9 5AG, UK

Keywords: *Aluminium determination; aluminium alkoxide; aluminium carboxylate; carbon-tube atomisation; atomic-absorption spectrophotometry*

Aluminium alkyls, alkoxides and carboxylates, important as organic intermediates,[1,2] are normally analysed following hydrolysis[3] titrimetrically using EDTA or one of its analogues or spectrophotometrically with, for example, 8-hydroxyquinoline,[4] depending on the amount of material available. Although many aluminium alkoxides and carboxylates are of sufficient stability and of low enough vapour pressure to suggest that direct carbon-tube atomisation atomic-absorption spectrophotometry, as for other organometallic compounds,[5] might be feasible, no prior study of this topic has been reported.

Determination of inorganic aluminium by carbon-tube atomisation is well established, although some doubt remains as to the atomisation mechanism. Aggett and Sprott[6] showed that whilst atomisation by reduction of Al_2O_3 by carbon was thermodynamically feasible at 1550 °C, carbon did not act as a reducing agent as there was no significant difference in atomisation behaviour between tantalum and carbon. The vapour in equilibrium Al_2O_3 (solid - liquid) is known to be a complex mixture of atomic and molecular species: Al, AlO, Al_2O, Al_2O_2, O_2 and O have been reported.[7,8] Sturgeon *et al.*[9] agreed that carbon was not involved and suggested that the aluminium atoms were produced by dissociation of Al_2O_3 in a two-stage process; however, Persson and co-workers[10,11] considered this an oversimplification and that the role of other compounds must be considered. Later Sturgeon and Chakrabarti[12] noted that no single mechanism could account for the observed E_a and, on the basis of the change of sensitivity with sheathing gas, considered that AlCN was a possible precursor in the formation of aluminium atoms. The atomisation signal for aluminium depends on the nature of the graphite surface, with normal graphite a single peak was reported whilst with pyrolytically coated graphite two peaks were observed. However, in the presence of a hydrogen diffusion flame only a single peak occurred.[12]

Frech and Cedergren[13,14] have shown that hydrogen evolution by reaction of adsorbed water with carbon was much larger from a normal graphite tube than that from a pyrolytically coated tube. Hence, the change in atomisation characteristics of aluminium in pyrolytically coated graphite may be related to its inability to produce hydrogen,[12] although the exact role of the hydrogen in producing compounds of differing volatility was not discussed. Maruta *et al.*[15] also observed double peaks for aluminium and utilised a hydrogen diffusion flame around the graphite tube to overcome the interference of matrix iron.

In this work sharp, single, aluminium peaks were observed using pyrolytically coated tubes whilst broader peaks with a shoulder were obtained with normal graphite tubes. This is the reverse of the behaviour described by Sturgeon and Chakrabarti.[12] We think that because the atomisation takes place during a very fast temperature ramp, the system is probably under kinetic as opposed to thermodynamic control. Thus it is difficult to predict the exact role, if any, of hydrogen in the atomisation process. Because there was no major change in sensitivity in the presence of hydrogen it is unlikely that hydrogen acts as a reducing agent. The double peaks or the shoulder on the broader peak are unlikely to be due to differences in the free energies of α- and γ-alumina *per se* as the atomisation temperature is above the melting point of Al_2O_3. The peak broadening in this study may be due to penetration of the sample into the more porous untreated graphite.

Experimental

Apparatus

The data were obtained by using a Perkin-Elmer 4000 double-beam atomic-absorption spectrophotometer fitted with a deuterium lamp background correction facility and a Perkin-Elmer HGA 76 graphite furnace; a PRS-10 printer sequencer was used to record peak heights. Sample solutions were introduced into the graphite furnace using an Eppendorf microlitre pipette. The graphite tubes were coated pyrolytically using methane - argon (1 + 9 *V/V*) at a flow-rate of 0.5 l min^{-1} for 10 min at an ashing temperature of 2100 °C.[16] Tantalum carbide-coated tubes were prepared according to the procedure of Hocquellet and Labeyrie.[17] Both types of coated tube were stable for 60 firings and then discarded.

Final Procedure

Atomise 10-μl aliquots (using the HGA 76 graphite furnace) in a pyrolytically coated graphite tube under the conditions given in Table 1. Determine the aluminium from a calibration graph constructed from 10-μl aliquots of standard solutions containing 0–2 p.p.m. of aluminium. The stock standard solution (1000 p.p.m. of Al) is prepared from aluminium ammonium sulphate; dilute standard solutions are prepared just prior to use. Sample and standard results must be corrected against the appropriate solvent blank (see Table 2).

Table 1. Atomisation conditions. Peak height absorbances are measured at 309.0 nm with slit width 0.7 nm, and in the peak-height mode; t = 5 s

	Dry	Ash	Atomise
Temperature/°C ..	100	1400	2650
Time/s	20	30	10
Gas mode	Flow	Flow	Stop

Table 2. Analysis of organoaluminium compounds

Ref. No.	Compound*	Solvent	Calculated Al, %	Estimated Al (mean of 4 results), %			
				Gravimetric	Carbon	Ta_2O_5-coated	Pyrolytically coated
1	$(CH_3COO)_4OAl_2.3H_2O$	H_2O	14.98	15.2	21.3	25.1	15.1
2	$Al_2(SO_4)_3(NH_4)_2SO_4.24H_2O$	H_2O	5.95	5.7	5.1	6.6	5.8
3	$Al(C_{18}H_{35}O_2)_3$	Acetylacetone	3.07	3.0	3.1	4.2	3.1
4	$[C_6H_{11}(CH_2)_3COO]_2AlOH$	THF	7.05	7.0	7.0	7.4	7.1
5	$[CH_3(CH_2)_3CH(C_2H_5)COO]_2AlOH$	THF	8.17	8.3	8.1	4.3	8.2
6	$(C_8H_4N_2)_4AlCl$	Conc. H_2SO_4	4.69	4.7	11.4	10.8	4.8
7	$[CH_3CH(OH)COO]_3Al$	H_2O	9.17	9.1	15.6	19.9	9.2
8	$Al(C_5H_7O_2)_3$	Acetylacetone	8.32	8.3†	11.3	15.8	8.4
9	$Al[OCH(CH_3)_2]_3$	Acetylacetone	13.21	27.7	21.1	9.40	27.2
10	$Al[OC(CH_3)_3]_3$	Acetylacetone	10.95	26.94	27.4	29.2	27.1
11	$Al(OC_4H_9)_3$	Acetylacetone	10.95	32.7	33.6	30.2	33.0

* Compound sources were as follows: Ref. No. 1, BDH; 2, Hopkin & Williams; 3, Hyde & Entwistle; 4–6, Eastman Kodak; 7, Fluka; 8, Lancaster Synthesis; and 9–11, Queen's University of Belfast.

† Parr bomb decomposition.

Results and Discussion

A series of 10-µl aliquots of solutions of the aluminium compounds in appropriate solvents, each containing 1 p.p.m. of aluminium, were ashed at 1400 °C and atomised at temperatures between 1900 and 2650 °C. All the compounds showed very similar atomisation profiles to give plateau values in absorbance above 2600 °C. Ash temperatures have to be below 1500 °C, as losses occur at temperatures above 1600 °C. At high concentration, above 10 p.p.m., highly fused double peaks were obtained, whereas at lower concentrations the effect was slight.

Results obtained using the finalised procedure are given in Table 1. The best accuracy of the results was obtained using pyrolytically coated graphite tubes, the results were marginally more precise (coefficients of variation: pyrolytically coated 1.75%, normal 2.17%, tantalum carbide-coated 4.20%, based on five results for compound 4). The confirmatory gravimetric analyses were carried out by oxidation of 0.1–0.2-g samples with 1 cm^3 of fuming nitric acid, evaporation to dryness, ignition at 1100 °C for 10 min and weighing as Al_2O_3. For compounds 1 and 3 a flow of oxygen was necessary to complete the removal of carbon. Compound 8, aluminium acetylacetonate, was too volatile for direct atomisation or for the gravimetric procedure and was pre-digested using fuming nitric acid in a closed bomb. Compounds 9–11 were clearly impure but gave satisfactory agreement between the gravimetric and direct atomisation procedure using pyrolytically coated tubes for aluminium contents.

The direct-tube atomisation is shown to be a satisfactory method of assay for a range of non-volatile oxygen-bonded organic aluminium compounds. The procedure also worked for aluminium phthalocyanine chloride (compound 6), which is a nitrogen–aluminium bonded ruby laser Q-switch dye. It is of interest that the pyrocoated tubes gave better results than tantalum-coated tubes, unlike our findings for organotin compounds.[5]

References

1. Eisch, J. J., *in* Wilkinson, G., Stone, F. G. A., and Abel, E. W., *Editors*, "Comprehensive Organometallic Chemistry," Volume I, Pergamon Press, Oxford, 1982, Chapter 6, p. 555.
2. Zietz, J. R., Jr., Robinson, G. C., and Lindsay, K. L., *in* Wilkinson, G., Stone, F. G. A., and Abel, E. W., *Editors*, "Comprehensive Organometallic Chemistry," Volume 7, Pergamon Press, Oxford, 1982, Chapter 46, p. 305.
3. Compton, T. R., "Chemical Analysis of Organometallic Compounds," Volume 5, Academic Press, London, 1977.
4. Belcher, R., Crossland, B., and Fennel, T. R. F. W., *Talanta*, 1970, **17**, 639.
5. Thorburn Burns, D., Dadgar, D., and Harriott, M., *Analyst*, 1984, **109**, 1099.
6. Aggett, J., and Sprott, A. J., *Anal. Chim. Acta*, 1974, **72**, 49.
7. Drowart, J., DeMaria, G., Burns, R. P., and Inghram, M. G., *J. Chem. Phys.*, 1960, **32**, 1366.
8. Burns, R. P., *J. Chem. Phys.*, 1966, **44**, 3307.
9. Sturgeon, R. E., Chakrabarti, C. L., and Langford, C. H., *Anal. Chem.*, 1976, **48**, 1792.
10. Persson, J., Frech, W., and Cedergren, A., *Anal. Chim. Acta*, 1977, **92**, 85.
11. Persson, J., Frech, W., and Cedergren, A., *Anal. Chim. Acta*, 1977, **92**, 95.
12. Sturgeon, R. E., and Chakrabarti, C. L., *Prog. Anal. At. Spectrosc.*, 1978, **1**, 5.
13. Frech, W., and Cedergren, A., *Anal. Chim. Acta*, 1976, **82**, 83.
14. Frech, W., and Cedergren, A., *Anal. Chim. Acta*, 1976, **82**, 93.
15. Muruta, T., Minegishi, K., and Sudoh, G., *Anal. Chim. Acta*, 1976, **81**, 313.
16. Manning, D. C., and Ediger, R. D., *At. Absorpt. Newsl.*, 1976, **15**, 42.
17. Hocquellett, P., and Labeyrie, N., *At. Absorpt. Newsl.*, 1977, **16**, 124.

Paper A4/175
Received May 10th, 1984
Accepted June 28th, 1984

Polarographic Behaviour of Yttrium

Tara C. Sharma,* Satish C. Sharma* and Kuldip S. Bhandari†
Chemistry Department, Gurukul Kangri University, Hardwar, U.P., India

Keywords: *Yttrium; polarography*

The polarographic study of rare-earth ions encounters certain difficulties, because of their negative reduction potentials and because of the possibility of a secondary reaction where the yttrium, for example, forms an electrode active complex with the medium. This complex may mask the primary wave, owing to the carrier wave obscuring their very negative $E_{\frac{1}{4}}$ values. Noddaek and Bruckel[1] employed 0.01 M yttrium sulphate solution without any supporting electrolyte. A double wave was formed with half-wave potentials of −1.76 and −1.84 V *versus* S.C.E. Noddaek and Bruckel concluded that the reduction proceeeded first to the +2 oxidation state and finally to the 0 state. It is much more probable that the first wave results from the reduction of hydrogen ions produced by the hydrolysis of the aquo Y^{3+} complex and the second wave corresponds to the three-electron reduction of Y^{3+} to Y^0. Kolthoff and Coetzee,[2] Wise and Cokal[3] and Almargo[4] noted that in non-aqueous solvents all trivalent rare earths are reduced at a dropping-mercury electrode in one step.

In this work we have tried to explain the polarographic behaviour of Y^{3+}. The kinetic parameters in each instance were determined by Koutecký's[5,6] method.

Experimental

A PL 55 Heyrovský polarograph was used with a drop size of mass (m) 1.34 mg and a drop time (t) of 4.5 s.

The aqueous saturated calomel electrode was used as a reference electrode. All measurements were made at 25 °C. The Y^{3+} solution was prepared by dissolving $YCl_3.H_2O$ in doubly distilled solvents. The *IR*-drop correction was made. Purified nitrogen was passed through the solution to remove dissolved oxygen.

Results and Discussion

Y^{3+} gave a single, well defined wave in aqueous formamide and dimethylformamide media, whereas, in an acetonitrile medium it gave two waves. The graphs of log ($i/i_d - i$) *versus* $E_{d.e.}$ for the first wave in each instance were linear. The slopes for these reductions indicated the irreversibility of the reduction, which is further confirmed by the plot of $E_{\frac{1}{4}}$ *versus* log t. The reduction of Y^{3+} at the dropping-mercury electrode takes place according to the over-all electrode reaction

$$Y^{3+} + e \rightleftharpoons Y^{2+}$$

The electronic configuration of the three states of yttrium are as follows: Y = (Kr)$4d^15s^2$; Y^{2+} = (Kr)$4d^1$; and Y^{3+} = (Kr). Thus yttrium attains a $4d^1$ configuration in the Y^{2+} state as the electron in Y^{3+} is added in the $4d$ orbital, although it has higher energy than the $5s$ orbital. The kinetic parameters have been calculated in each configuration by Hale *et al.*[7] by treatment of Koutecký's method for irreversible processes for the general reaction mechanism

$$Ox + ne \rightleftharpoons Red$$

and the equation for the wave is given by

$$\frac{i_l}{i_d} = f(x) - ZH_c(x) = f'(x) \quad \ldots \quad (1)$$

where

$$x = K_f \left(\frac{12t}{7D}\right)^{\frac{1}{2}}$$

and

$$Z = 504\, D^{\frac{1}{2}} m^{1/3} t^{1/6} \quad \ldots \quad (2)$$

where i_l is the maximum instantaneous current of the single drop at the potential $E_{d.e.}$; i_d is the current of the single drop in the limiting current region; Z is the charge on the ion; D is the diffusion coefficient; $H_c(x)$ is the correction factor introduced for the curvature of the drop; and $f(x)$ and $f'(x)$ are power series in the variable x. Their values have been taken from the papers by Koutecký. K_f is the rate constant for the forward reaction in the irreversible process, which varies with the electrode potential E according to the equation

$$K_f = K_f^0 \exp. \left(\frac{\alpha nFE}{RT}\right) \quad \ldots \quad (3)$$

where K_f^0 is the rate constant of the electron transfer at 0 V, α is the degree of ionisation and F is Faradays constant. The results are given in Table 1.

It can be seen from the results that the value of the half-wave potential in a formamide medium showed a negative shift, whereas in dimethylformamide and acetonitrile they showed a positive shift with respect to an aqueous medium. This change may be due either to some physical property of the solvents such as dielectric constant or viscosity or to the chemical action of the solvents. The Born[8] equation

Table 1. Polarographic behaviour of Y^{3+} in 0.1 M $NaClO_4$ in different solvents. $[Y^{3+}] = 1$ M; and $m = 1$

Solvent	i_d/ μA	$E_{\frac{1}{4}}$/V *vs.* S.C.E.	Slope*/ mV	$D^{\frac{1}{2}}$/ $cm^2 s^{-1}$	$n\alpha$	K_s'†/ $cm\ s^{-1}$	K_f^0/ $cm\ s^{-1}$
Water	5.05	1.45	70	4.9×10^{-3}	0.86	1.2×10^{-3}	1×10^{-17}
Formamide	2.75	1.50	80	2.9×10^{-3}	0.65	4.8×10^{-4}	3.16×10^{-15}
Dimethylformamide	7.5	1.35	145	8.6×10^{-3}	0.40	1.26×10^{-3}	3.2×10^{-10}
Acetonitrile	11.0	0.56	180	11.9×10^{-3}	0.28	2.1×10^{-2}	5.6×10^{-4}

* Slope of log ($i/i_d - i$) *versus* $E_{d.e.}$.
† K_s' is the rate constant of the electron transfer in the reaction at the limiting current region.

* Present address: College of Science, P.M.B. 27, Gombe (Bauchi State), Nigeria.
† Present address: Education Directorate, Delhi Administration, Delhi, India.

Table 2. Polarographic behaviour of Y^{3+} in 0.1 M $NaClO_4$ in different solvents after the addition of water. $[Y^{3+}] = 1$ M; $m = 1$

Solvent	i_d/ μA	$E_{\frac{1}{4}}$/V *vs.* S.C.E.	Slope*/ mV	$D^{\frac{1}{2}}$/ $cm^2 s^{-1}$	$n\alpha$	K'_s/ $cm\ s^{-1}$	K_f^0/ $cm\ s^{-1}$
Formamide	2.6	1.55	67	2.6×10^{-2}	0.85	3.16×10^{-4}	1.0×10^{-17}
Dimethylformamide ..	2.0	1.34	76	2.03×10^{-3}	0.75	2.4×10^{-4}	1.5×10^{-16}
Acetonitrile	4.9	1.25	88	4.8×10^{-3}	0.65	6.8×10^{-4}	8.0×10^{-14}

* Slope of log $(i/i_d - i)$ *versus* $E_{d.e.}$.
† K_s' is the rate constant of the electron transfer in the reaction at the limiting current region.

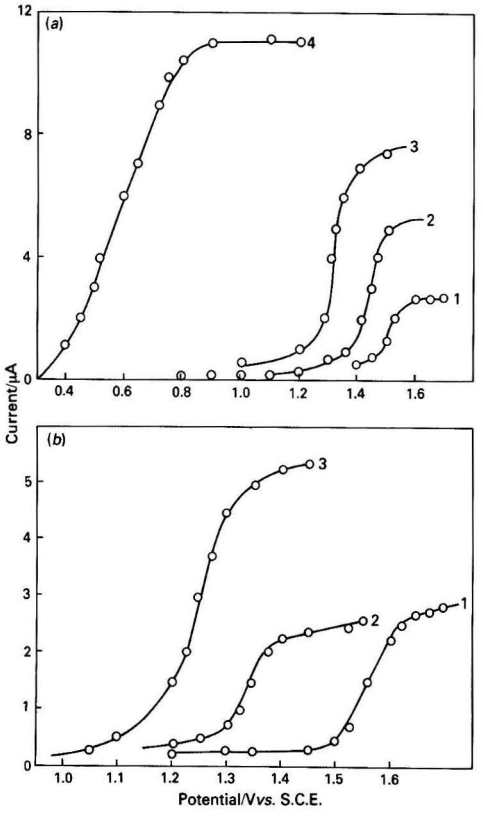

Fig. 1. (*a*) Polarograms of Y^{3+} in different solvents for a 1 M solution of Y^{3+} in 0.1 M $NaClO_4$. Solvents: 1, water; 2, formamide; 3, dimethylformamide; and 4, acetonitrile. (*b*) Polarograms of aquo complexes of Y^{3+} in different solvents for a 1 M solution of Y^{3+} in 0.1 M $NaClO_4$. Solvents: 1, formamide; 2, dimethylformamide; and 3, acetonitrile. $m = 1$ in both (*a*) and (*b*)

gives the following relationship for the half-wave potential and dielectric constant of the solvents:

$$(E_{\frac{1}{4}})_2 - (E_{\frac{1}{4}})_1 = \frac{Z}{2r_1}\left(\frac{1}{\varepsilon_1} - \frac{1}{\varepsilon_2}\right)$$

where $(E_{\frac{1}{4}})_2$ and $(E_{\frac{1}{4}})_1$ are the half-wave potentials in the two solvents with dielectric constants ε_1 and ε_2, respectively; and r_1 is the effective radius of the metal ion.

Our results do not show a direct relationship between $E_{\frac{1}{4}}$ and ε. This leads to the assumption that r_1 remains unchanged in a given solvent. The value of r_1 in different solvents is calculated by the equation

$$r_1 = \frac{r i_{d_1}^2 n_1}{i_{d_2}^2 n_2}$$

where r is the radius in aqueous medium, taken as 0.086 nm.

Effect of Water on Electrode Reaction

Shifts of the $E_{\frac{1}{4}}$ of the yttrium waves on addition of a small amount of water (0.5–10.0 ml of the test solution) to the non-aqueous solvents were studied. The magnitude and direction of the shifts of $E_{\frac{1}{4}}$ suggested the formation of an aquo complex ion prior to reduction. The results are shown in Fig. 1(*a*) and (*b*). If this shift in $E_{\frac{1}{4}}$ is due to adsorption, then shifts in $E_{\frac{1}{4}}$ must be on the positive side. Hence, there is every possibility that an aquo complex is formed, which is further supported by the decrease of the rate constant (Table 2).

References

1. Noddaek, W., and Bruckel, A., *Angew. Chem.*, 1937, **50**, 362.
2. Kolthoff, I. M., and Coetzee, J. F., *J. Am. Chem. Soc.*, 1957, **79**, 1852.
3. Wise, E. N., and Cokal, E. J., *J. Electroanal. Chem.*, 1966, **11**, 406.
4. Almargo, V., "Polarography," Macmillan, London, 1964, p. 667.
5. Koutecký, J., *Collect. Czech. Chem. Commun.*, 1953, **18**, 597.
6. Koutecký, J., *Collect. Czech. Chem. Commun.*, 1956, **21**, 836.
7. Hale, J. A. M., *et al.*, *Collect. Czech. Chem. Commun.*, 1962, **27**, 2444.
8. Born, M., *Z. Phys.*, 1920, **1**, 45.

Paper A3/454
Received December 29th, 1983
Accepted May 30th, 1984

Ebulliometric Study of Solubility and Ion-association Equilibria

Walace A. de Oliveira and Terezinha S. M. Omoto
Instituto de Química, Universidade Estadual de Campinas, C.P. 6154, Campinas, SP, Brazil

Keywords: *Ebulliometry; solubility product; ion pairs; calcium sulphate*

Precipitation equilibrium plays an important role in various fields of chemistry and the determination of solubility products is required for a quantitative description of species present in solution. The study of precipitation equilibria at elevated temperatures is more difficult because the experimental conditions are not favourable for the use of common methods. At the boiling temperature the determination of solubility products can be accomplished by means of recently described ebulliometric methods.[1] These procedures are based on the changes in the boiling temperature that accompany the precipitation equilibrium and permit the acquisition of data over a range of temperatures and for different types of compounds.

Equilibria involving ion association in solution are also important and the study of these systems has been an active area of chemical research. Frequently, both precipitation and dissociation equilibria are present and the complete assessment of all species in solution requires a knowledge of both the solubility product and the ion-pair formation constant.

This paper describes a method for the determination of both solubility products and ion-pair formation constants. The method is based on the changes in boiling temperatures that occur during an ebulliometric titration.[2] In order to test the procedure the constants for calcium sulphate were determined.

Theoretical

At the beginning of an ebulliometric titration, the amount of titrant added is not sufficient to cause precipitation and only the association equilibrium takes place. The data from this region of the titration curve were first used to calculate the ion-pair formation constant. The remainder of the data, up to the equivalence point, were then used for the calculation of the solubility product.

Equation for the Ion-pair Formation Constant

Considering the species present in the titration of a solution of calcium chloride with sodium sulphate and following procedures previously described,[3] it is possible to write

$$d\theta/K_b = dm_{Ca^{2+}} + dm_{Cl^-} + dm_{SO_4^{2-}} + dm_{Na^+} + dm_{CaSO_4} \quad (1)$$

where $d\theta$ is the change in the boiling temperature during the titration, K_b is the ideal ebullioscopic constant and m represents molality. It was assumed in the derivation of equation (1) that the activity coefficients do not vary during the titration. This assumption is based on the fact that titration is performed in a solution of high ionic strength and only small portions of titrant are added. Moreover, ion association decreases the ionic strength whereas addition of titrant favours an increase. Introducing in equation (1) the analytical molality of the titrant, $m_{Na_2SO_4}$, and remembering that m_{Cl^-} does not vary during titration, gives

$$d\theta/K_b = dm_{Ca^{2+}} + dm_{SO_4^{2-}} + 2dm_{Na_2SO_4} + dm_{CaSO_4} \quad (2)$$

Integration of equation (2) within the limits of the titration yields

$$\Delta\theta/K_b = m_{Ca^{2+}} - m_{i_{CaCl_2}} + m_{SO_4^{2-}} + 2m_{Na_2SO_4} + m_{CaSO_4} \quad (3)$$

where $m_{i_{CaCl_2}}$ is the initial molality of the titrand. Conservation of mass gives

$$m_{i_{CaCl_2}} = m_{Ca^{2+}} + m_{CaSO_4} \quad (4a)$$

and

$$m_{Na_2SO_4} = m_{SO_4^{2-}} + m_{CaSO_4} \quad (4b)$$

Solving equations (3) and (4) simultaneously and substituting the result in the expression for the molal ion-pair formation constant, $K_f' = m_{CaSO_4}/(m_{Ca^{2+}} m_{SO_4^{2-}})$, gives

$$K_f' = (3m_{Na_2SO_4} - \Delta\theta/K_b)/[(\Delta\theta/K_b - 2m_{Na_2SO_4})(\Delta\theta/K_b + m_{i_{CaCl_2}} - 3m_{Na_2SO_4})] \quad (5)$$

Calculation of Solubility Product

Following the arguments given above and considering the part of the titration where both equilibria exist, we obtain

$$\Delta\theta/K_b = 2m_{SO_4^{2-}} + m_{Na_2SO_4} + K_f' m_{SO_4^{2-}}(m_{i_{CaCl_2}} - m_{Na_2SO_4}) + K_f'(m_{SO_4^{2-}})^2 \quad (6)$$

Solving equation (6) and retaining only the root with physical meaning gives expressions for $m_{Ca^{2+}}$ and $m_{SO_4^{2-}}$, which are substituted in the equation for the molal solubility product $K_{so}' = m_{Ca^{2+}} m_{SO_4^{2-}}$, giving

$$K_{so}' = (a + b - 1/K_f')(a - b - 1/K_f') \quad (7)$$

where

$$a = [(K_f' m_{i_{CaCl_2}} - K_f' m_{Na_2SO_4} + 2)^2 + 4K_f'(\Delta\theta/K_b - m_{Na_2SO_4})]^{1/2}/(2K_f') \quad (8)$$

and

$$b = (m_{i_{CaCl_2}} - m_{Na_2SO_4})/2 \quad (9)$$

Experimental

An apparatus similar to that previously described[4] was used, consisting of a pair of identical ebulliometers assembled in such a way that one is used as a reference for the other. Boiling-temperature changes were measured with a pair of calibrated thermistors connected to a Wheatstone bridge. The imbalance voltage of the bridge was presented to a strip-chart recorder. The temperature uncertainty was about 6×10^{-5} °C.

The procedure used began by charging the ebulliometers with a solution of calcium chloride of various concentrations and ionic strength adjusted with sodium chloride. After the establishment of boiling-temperature equilibrium, pellets of sodium sulphate decahydrate were added through the condensers, alternately to each ebulliometer, while recording the changes in the boiling temperatures. Analytical-reagent grade chemicals were used throughout.

Results and Discussion

A typical ebulliometric titration curve is shown in Fig. 1. As can be seen, the slope of the curve decreases after the beginning of the titration and increases thereafter. This profile probably reflects the effects of the two equilibria in the boiling temperature of the solution, because the ion-pair formation

$$Ca^{2+}_{(aq.)} + SO_4^{2-}{}_{(aq.)} \rightleftharpoons CaSO_{4(aq.)} \quad (10)$$

represents a net increase of 2 mol of particles per mole of titrant (if the reaction is complete), whereas the precipitation

$$CaSO_{4(s)} \rightleftharpoons Ca^{2+}_{(aq.)} + SO_4^{2-}{}_{(aq.)} \quad (11)$$

causes an increase in solution of only 1 mol of particles per mole of titrant.

Extrapolation to Infinite Dilution

The data for each titration were used to calculate molal constants using equations (5) and (7). The average values of these constants are listed in Table 1. At each ionic strength four to six values were obtained and the standard deviation of the average was between 5 and 20%, with more uncertainty for the measurements of very small $\Delta\theta$, required to calculate K_f'.

The thermodynamic solubility product, K_{so}^0, defined in terms of the activity of the ions is related to the molal solubility product by the expression $K_{so}^0 = K_{so}' \gamma_\pm^2$, where $\gamma_\pm$ is the mean activity coefficient. Similarly, the thermodynamic ion-pair formation constant K_f^0 is given by $K_f^0 = K_f'/\gamma_\pm^2$, if the activity coefficient of the ion pair is regarded as unity. Using these expressions and the Debye - Hückel equation to represent $\gamma_\pm$, we obtain

$$\text{Log } K_{so}' = \log K_{so}^0 + 4.723\sqrt{I}/(1 + 0.3406a^0\sqrt{I}) \quad (12)$$

and

$$\text{Log } K_f' = \log K_f^0 - 4.723\sqrt{I}/(1 + 0.3406a^0\sqrt{I}) \quad (13)$$

where a^0 is the distance of closest approach, I is the ionic strength and the numerical constants[5] are for a temperature of 98.3 °C and the molal scale. The data in Table 1 were fitted to equations (12) and (13) with the help of a general multiparametric curve-fitting program[6] and the following results were obtained:

$$K_{so}^0 = 4.5 \pm 0.3 \times 10^{-6} \text{ mol}^2 \text{ kg}^{-2}; a^0 = 5.0 \text{ Å}$$

and

$$K_f^0 = 5.0 \pm 0.5 \times 10^2 \text{ mol}^{-1} \text{ kg}; a^0 = 7.6 \text{ Å}.$$

The precision of our results for K_f^0 and K_{so}^0 is around 10%. This seems to be satisfactory considering that the determination of these constants required the measurement of very small boiling-temperature changes. Evaluation of the accuracy of our results is impaired by the discrepancies found in the literature for the values of these constants. For instance, at 25 °C over 20 values for the ion-pair formation constant were found, which varied by as much as three orders of magnitude.[7,8] At about the temperature of our measurements the following values are given in the literature: Yeatts and Marshall[9] report $K_f^0 = 320$ mol^{-1} kg and $K_{so}^0 = 4.35 \times 10^{-6}$ mol^2 kg^{-2} and Gardner and Glueckauf[10] give $K_f^0 = 621$ mol^{-1} kg and $K_{so}^0 = 3.48 \times 10^{-6}$ mol^2 kg^{-2}. These values compare favourably with the results obtained in this work.

The value of a^0 for calcium sulphate has been considered[11] to be equal to 5 Å at 25 °C. Taking into account that the value of this parameter is little affected by changes in temperature,[1] it is expected that at the boiling temperature the value of a^0 should be around 5–6 Å. In the calculation of the solubility product the result for a^0 is in agreement with this prediction. However, for the calculation of K_f^0 the value of a^0 found (7.6 Å) is slightly higher. Although higher values of a^0 have been used by other workers,[12] this result could perhaps be caused by the assumption that the activity coefficient of the ion pair is equal to unity.

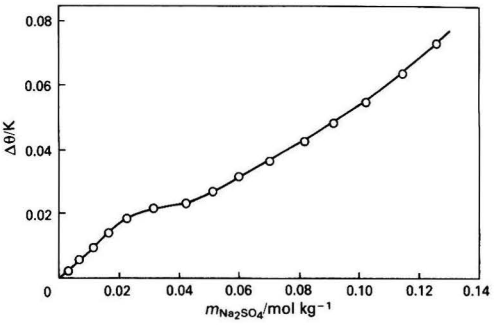

Fig. 1. Ebulliometric titration of a 0.1000 mol kg^{-1} solution of Ca^{2+}, of ionic strength 0.300 mol kg^{-1} with sodium sulphate solution

Table 1. Molal solubility product, K_{so}', and ion-pair formation constant, K_f', as functions of the ionic strength, I

I/mol kg^{-1}	K_f'/mol^{-1} kg	$10^5 K_{so}'$/mol^2 kg^{-1}
0.090	79.4	3.50
0.130	50.1	4.57
0.174	72.4	5.75
0.210	52.5	8.70
0.260	50.1	10.0
0.300	43.7	11.0
0.390	38.0	11.0
0.520	29.5	13.0

The ebulliometric method described here requires simple and inexpensive instrumentation and permits the acquisition of data over a range of temperatures, by varying the barometric pressure in the ebulliometer. The major requirement is that all solutes must be non-volatile at the boiling temperature of the solvent. An over-all evaluation of the proposed method led to the conclusion that ebulliometric measurements can be useful in the study of multiple equilibria in solution.

References

1. De Oliveira, W. A., *Anal. Chim. Acta*, 1982, **141**, 337.
2. De Oliveira, W. A., *Anal. Lett.*, 1981, **14**, 1391.
3. De Oliveira, W. A., *J. Coord. Chem.*, 1979, **9**, 7.
4. De Oliveira, W. A., and Meites, L., *Anal. Chim. Acta*, 1977, **93**, 3.
5. Robinson, R. A., and Stokes, R. H., "Electrolyte Solutions," Butterworths, London, 1955, p. 491.
6. Meites, L., "The General Multiparametric Curve-Fitting Program CFT4," Computing Laboratory, Department of Chemistry, Clarkson College of Technology, Potsdam, NY, 1976.
7. Yokoyama, H., and Yamatera, H., *Bull. Chem. Soc. Jpn.*, 1975, **48**, 2719.
8. Pitzer, K. S., *J. Chem. Soc., Faraday Trans. 2*, 1972, **68**, 101.
9. Yeatts, L. B., and Marshall, W. L., *J. Phys. Chem.*, 1969, **73**, 81.
10. Gardner, A. W., and Glueckauf, E., *Trans. Faraday Soc.*, 1970, **66**, 1081.
11. Meites, L., Pode, J. S. F., and Thomas, H. C., *J. Chem. Educ.*, 1966, **43**, 667.
12. Yokoyama, H., and Yamatera, H., *Bull. Chem. Soc. Jpn.*, 1975, **48**, 2708.

Paper A4/83
Received February 28th, 1984
Accepted July 12th, 1984

Spectrophotometric Method for the Determination of Cyanide and Its Application to Biological Fluids

Miss Sweta Upadhyay and V. K. Gupta*
Department of Chemistry, Ravishankar University, Raipur, 492 010 (M.P.), India

Keywords: *Cyanide determination; anthranilic acid; spectrophotometry; biological fluids*

Cyanides are used in various industries, *e.g.*, in the extraction of noble metals, the manufacture of organic chemicals, electroplating, hardening of steel, metal polishing and photography. In the gas industry, many atmospheres and effluents contain cyanides, *e.g.*, the effluents from coke ovens and other gas plants.[1] Hydrocyanic acid is used extensively for fumigation, particularly as a rapid and conveniently applied fumigant for food storage, orchards, buildings such as warehouses and holds of cargo ships.[2]

Cyanides are highly toxic, acting directly on the nervous system, and are also absorbed through the skin. Repeated exposure to small concentrations of cyanides over a long period causes weakness, nausea, muscle cramps, paralysis of the legs and arms, loss of appetite and psychoses. The recommended maximum allowable concentration of cyanide is 5 mg m^{-3} in air, calculated as CN^-.[1] The World Health Organization recommends that water containing more than 0.01 p.p.m. of cyanide (as CN^-) should be rejected as unfit for domestic supplies.[3]

For the determination of small amounts of cyanides, spectrophotometry is superior to other methods, including titrimetry, polarography and chromatography.[4] The standard methods for cyanide in trade wastes and effluents and for waters[5,6] are based on the colorimetric procedure developed by Alridge[7,8] and Epstein.[9] The best known methods for the spectrophotometric determination of cyanide are based on the formation of cyanogen bromide or chloride, which can react with pyridine to yield glutaconic aldehyde, which is subsequently condensed with benzidine,[10] *p*-phenylenediamine,[11] pyrazolone[9] or barbituric acid,[12] producing polymethine dyes. Benzidine and *p*-phenylenediamine are themselves toxic and carcinogenic hence their use is undesirable. Various indirect spectrophotometric methods[13–15] have been developed more recently, based on the discharge of the colour of metal complexes by removal of cyanide complexes, but these methods are very tedious.

In this paper, a method is proposed for the determination of cyanide by conversion into cyanogen bromide followed by reaction with pyridine. The glutaconic aldehyde so formed is condensed with anthranilic acid, a non-toxic compound, forming a yellow - orange dye, which is measured at 400 nm. The optimum reaction conditions and other analytical parameters have been studied.

Experimental

Apparatus

A Carl Zeiss Spekol and an ECIL Model GS-865 spectrophotometer with matched silica cells of 1 cm path length were used for all spectral measurements.

Reagents

All chemicals used were of analytical-reagent grade and solutions were prepared with distilled, de-ionised water.

Standard cyanide solution. Potassium cyanide (0.1 g) was dissolved in 100 ml of de-ionised water to give a solution of concentration 1 mg ml^{-1} in CN^-. Appropriate dilution gave a working standard solution of 10 μg ml^{-1}.

Pyridine reagent.[11] Concentrated HCl (3 ml) was mixed with 18 ml of freshly distilled pyridine and 12 ml of de-ionised water were added.

Sodium arsenite solution, 1.5% *m/V*.

Anthranilic acid solution, 0.1% *m/V*.

Bromine water, saturated.

Procedure

An aliquot of an aqueous sample containing 10–70 μg (1–7 p.p.m.) of cyanide was placed in a 10-ml calibrated flask, 0.3 ml of saturated bromine water was added and the mixture was allowed to stand for 1 min for complete bromination. The excess of bromine was decolorised by the dropwise addition of sodium arsenite solution, then 0.4 ml of pyridine reagent followed by 1 ml of anthranilic acid solution were added. The mixture was allowed to stand for 10 min for full colour development. The volume was then made up to the mark and the absorbance was measured at 400 nm using distilled water as reference. The same procedure was followed for the blank, which gave no colour under these conditions.

Results and Discussion

The absorption spectrum of the dye shows an absorption maximum at 400 nm.

Effect of Varying the Reaction Conditions

For bromination the amount of bromine water needed was checked by adding various amounts of saturated bromine water. A minimum 0.2 ml of bromine water was needed for complete bromination of the cyanide to cyanogen bromide. An excess of bromine caused no effect as the excess was decolorised with sodium arsenite solution.

Sodium arsenite solution was added dropwise until the bromine was decolorised. In the range 0.2–1 ml of 1.5% sodium arsenite solution no changes in the absorbance values were observed.

The amount of pyridine reagent needed for the conversion of cyanogen bromide into glutaconic aldehyde was also checked. A minimum of 0.2 ml of pyridine reagent was neeeded for the reaction. Addition of up to 1 ml of pyridine reagent had no noticeable effect on the absorbance but above 1 ml there was a decrease in absorbance.

It was found that constant absorbance values were obtained with the addition of volumes of 0.1% anthranilic acid solution from 1 to 5 ml.

* To whom correspondence should be addressed.

The effects of time and temperature on the colour development were studied. It was observed that 10 min were needed for full colour development and the colour remained stable for 15 min in the range 15–35 °C. At higher temperatures there was a decrease in absorbance.

Beer's Law, Sandell's Sensitivity and Reproducibility

Beer's law is obeyed in the range of 10–70 μg of cyanide. Sandell's sensitivity of the colour reaction was 0.0083 μg cm^{-2}. The reproducibility of the method was checked by seven replicate determinations. The standard deviation and relative standard deviation were 0.01 and 0.15%, respectively.

Effect of Foreign Species

Interferences from organic pollutants, *viz.*, benzene, phenol, ethanol, benzaldehyde, etc., and metal ions such as zinc, cadmium, lead, mercury and iron were not observed. Oxidising and reducing agents, if present in small amounts, are removed by the sodium arsenite and bromine water, respectively. The tolerance limits for diverse species are shown in Table 1.

Application of the Method

The method has been applied to the detection of cyanide in urine and whole blood. Several samples of urine and blood were tested and were found to be free of cyanide. Known amounts of cyanide were therefore added to these samples and they were analysed by the above procedure and Alridge's method[7] after deproteinisation with trichloroacetic acid.[7] The results in Table 2 show that the recoveries from urine and whole blood samples are about 95 and 98%, respectively, which is in agreement with the results of Alridge's method.

Table 1. Effect of foreign species. Concentration of cyanide, 4 p.p.m.

Foreign species	Tolerance limit,* p.p.m.
Benzene	2000
Phenol	1000
Benzaldehyde	800
Ethanol	1200
Aniline	500
Nitrobenzene	900
Zn^{2+}	100
Cd^{2+}	200
Pb^{2+}	150
Hg^{2+}	100
Fe^{2+}	250
Cu^{2+}	300
K^{+}	450
Na^{+}	500

* Amount of foreign species that causes a ±2% error.

Conclusion

The method is simple and sensitive, no use is made of carcinogenic compounds and it can be applied to the detection of cyanide in biological fluids. Further studies are being carried out on the determination of cyanide in effluent waters and other samples.

The authors are grateful to the Head, Department of Chemistry, Ravishankar University, Raipur, for providing laboratory facilities.

References

1. Jacobs, M. B. "The Analytical Toxicology of Industrial Inorganic Poisons," Volume 22, Interscience, New York, 1967, p. 721.
2. Patty, F. A., "Industrial Hygiene and Toxicology," Second Edition, Volume II, Interscience, New York, 1962, p. 1997.
3. World Health Organization, "International Standards for Drinking Water," WHO, Geneva, 1958.
4. Bark, L. S., *Ind. Chem.*, 1962, 525.
5. Jolly, S. C., *Editor*, "Official, Standardised and Recommended Methods of Analysis," Heffers, Cambridge, for Society for Analytical Chemistry, London, 1963, p. 253.
6. American Public Health Association, American Water Works Association and Water Pollution Control Federation, "Standard Methods for the Examination of Water and Waste Water," Eleventh Edition, American Public Health Association, Washington, DC, 1960, Parts III and IV.
7. Alridge, W. N., *Analyst*, 1944, **69**, 262.
8. Alridge, W. N., *Analyst*, 1945, **70**, 474.
9. Epstein, J., *Anal. Chem.*, 1947, **19**, 272.
10. Higson, H. G., and Bark, L. S., *Analyst*, 1964, **89**, 338.
11. Bark, L. S., and Higson, H. G., *Talanta*, 1964, **11**, 621.
12. Asmus, E., and Garschagen, H., *Fresenius Z. Anal. Chem.*, 1954, **138**, 414.
13. Dagnall, R. M., El-Gnamry, M. T., and West, T. S., *Talanta*, 1968, **15**, 167.
14. Wei, F.-S., Liu, Y.-Q., Yui, F., and Shen, N. K., *Talanta*, 1981, **28**, 694.
15. Zhu, Y., and Qi, W., *Fenxi Huaxue*, 1981, **9**, 692; *Chem. Abstr.*, 1983, **97**, 119677u.

Paper A4/203
Received June 14th, 1984
Accepted July 6th, 1984

Table 2. Recovery of cyanide from biological fluids. Volume of urine and blood samples, 1 ml

Sample	Sample No.	Cyanide added/ μg	Cyanide found by present method/ μg*	Recovery, %	Cyanide found by Aldridge's method/ μg*	Recovery, %
Urine	1	15	14.25	95.0	14.25	95.0
	2	30	28.45	94.8	28.55	95.2
	3	45	42.80	95.2	42.75	95.0
	4	60	56.15	93.6	56.10	93.5
Blood	1	15	14.78	97.9	14.70	98.0
	2	30	29.45	98.2	29.35	97.8
	3	45	44.10	98.0	44.20	98.2
	4	60	58.30	97.2	58.50	97.5

* Means of three replicate analyses.

High-performance Liquid Chromatographic Analysis of Urinary Hydroxylysyl Glycosides as Indicators of Collagen Turnover

Luigi Moro, Chiara Modricky, Nicola Stagni, Franco Vittur and Bernedetto de Bernard
Institute of Biological Chemistry, University of Trieste, 34127 Trieste, Italy

Keywords: *Collagen; hydroxylysyl glycosides; high-performance liquid chromatography*

Hydroxyproline is the urinary metabolite commonly measured to evaluate collagen turnover, but the assay for the component does not provide quantitative information on collagen breakdown. In fact, only 10–25% of collagen hydroxyproline is excreted in the urine[1] and further urinary hydroxyproline may derive from collagen of different tissues such as bone or soft tissues.

The glycosides of hydroxylysine (HLG), α-1,2-glucosylgalactosyl-*O*-hydroxylysine (GGH) and β-1-galactosyl-*O*-hydroxylysine (GH) appear to be better indicators of total collagen turnover than hydroxyproline.[2] Moreover, quantitative evaluation of urinary HLG indicates that collagen turnover is in fact 2–4-fold higher than that calculated from hydroxyproline measurements and accounts for 50–100% of degraded collagen.[3] HLG excretion is not significantly affected by diet[2] and by measuring GH and GGH in urine it is also possible to evaluate the metabolic turnover of different collagen, *e.g.*, from bone and skin. In fact, the ratio of the amounts of the two urinary metabolites is influenced by the type of collagen metabolised and by the age of the subject.[3]

Numerous methods for determining urinary HLG have been reported.[2] The procedure generally consists in HLG separation by ion-exchange chromatography, followed by their quantitation using the ninhydrin reaction or the orcinol-sulphuric acid assay for hexoses.[4] The amino acid analyser is so far the instrument of choice for separating and determining these metabolites in urine. In this paper, we describe a rapid and more sensitive method for measuring HLG in urine by converting the amino groups of hydroxylysine into fluorescent derivatives with dansyl chloride prior to their separation by reversed-phase high-performance liquid chromatography (HPLC).

Experimental

Chemicals

Reagents obtained from commercial suppliers were of analytical-reagent grade. Acetonitrile was purchased from BDH Chemicals (Poole, Dorset, UK) and 5-dimethylaminonaphthalene-1-sulphonyl chloride (dansyl chloride; Dns-Cl) from Sigma (St. Louis, MO, USA). Standards of GH and GGH were a generous gift from the Institute of Biological Chemistry of the University of Pavia (Italy), where they were prepared from sponges.[5]

Reagents

α-1,2-Glucosylgalactosyl-O-hydroxylysine solution, 116 nmol ml^{-1}.

β-1-Galactosyl-O-hydroxylysine solution, 74 nmol ml^{-1}.

Sodium carbonate solution, 0.3 M.

Dansyl chloride solution in dimethyl ketone, 10 mg ml^{-1}.

Buffer A. Sodium acetate (0.05 M, pH 6.3) + acetonitrile (12.5%) + propan-2-ol (5%).

Buffer B. Sodium acetate (0.05 M, pH 6.5) + acetonitrile (50%) + propan-2-ol (1%).

Procedure

Urine collection

The urine specimens (24 h) contained 0.1% of boric acid to prevent growth of bacteria.

Sample preparation

HLG standards and aliquots of urine were derivatised according to the method of Gray.[6] Briefly, 50 μl of an aqueous solution of HLG (5.8 nmol of GGH or 3.7 nmol of GH) or 50 μl of urine were added to a mixture of 50 μl of 0.3 M Na_2CO_3 solution and 100 μl of Dns-Cl in dimethyl ketone (10 mg ml^{-1}). The mixture was incubated at 60 °C for 30 min and 20 μl of the mixture were then injected into the column. The urine specimen did not require any hydrolytic pre-treatment, as already reported by Askenasi.[4]

HPLC procedure

HPLC separation was carried out with a Beckman Model 344 instrument, connected with a fluorimeter, using an excitation wavelength of 366 nm and an emission wavelength of 490 nm. The area of the peaks was calculated by an HP 3390 automatic integrator. Reversed-phase HPLC was performed using a 250 × 4.6 mm i.d. column of Ultrasphere-ODS (C_{18}) (5 μm); the two solvent systems used for the stepwise gradient were buffer A and buffer B. The flow-rate was maintained at 1 ml min^{-1}.

Results

In a series of preliminary experiments, the optimum stepwise gradient necessary for the full resolution of HLG was determined.

The elution patterns of the GGH and GH standards are shown in Fig. 1(*a*). The former standard (1.07 nmol injected) elutes as a double peak at 43.88 ± 0.37 and 44.19 ± 0.37 min [mean of ten experiments ± standard deviation (S.D.)]. The latter standard, GH (0.67 nmol injected), also elutes as a double peak at 49.04 ± 0.54 and 50.51 ± 0.33 (mean of ten experiments ± S.D.). Fig. 1(*b*) shows the elution profile of a 24-h urine sample from a boy aged 14. Many peaks can be seen, but under the experimental conditions reported, four peaks elute with the same profiles as the retention times of GGH and GH doublets. Addition of HLG standards (1.07 nmol of GGH and 0.67 nmol of GH) to the urine sample causes an increase of the profile peaks, as shown in Fig. 1(*c*).

The retention time and peak areas are reproducible for the standards, whereas the other chromatographic peaks are independent from those of the major derivatives. On the basis of the fluorescence intensity, there was 100% recovery of the injected standards.

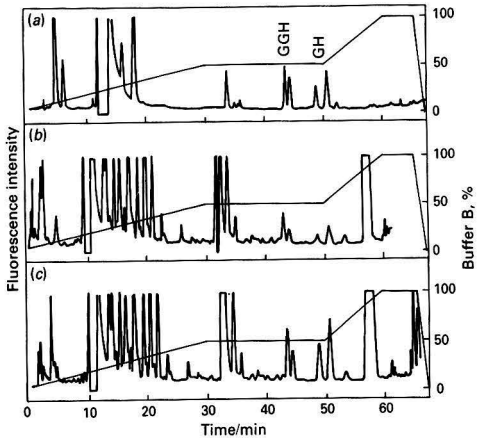

Fig. 1. HPLC elution profile of glycosides of hydroxylsine. (*a*) A mixture of 1.07 nmol of GGH and 0.7 nmol of GH was injected; (*b*) sample of 24-h urine; and (*c*) 1.07 nmol of GGH and 0.7 nmol of GH were added to the sample of urine before conversion into dansyl derivatives

By statistically evaluating the imprecision of the peak-area measurements and the batch imprecision of urine analysis, a coefficient of variation of 5% was obtained. Analysis of the correlation between peak areas and amounts of GGH and GH in the range 0–2 nmol provides the equations $y = 0.40x + 0.05$ and $y = 0.59x + 0.05$, respectively, with $r = 0.99$ in both instances.

Discussion

Under the experimental conditions reported, HLG standards are well separated. With a sample of urine, four peaks appear that are identical with the standards with respect to both retention time and peak shape and are identified as GGH and GH.

The fact that each collagen metabolite is marked by a double peak suggests the formation of mono- and di-dansyl derivatives of the compound. Based on the lipophilic properties of the two derivatives, it is suggested that the first peak of each pair is the mono-derivative and the second the di-derivative. As shown in the elution profile, the integrated area of the first peak of GGH is higher than that of the second, whereas the opposite applies to the GH peaks. This means that with the GGH doublet less of the molecule is di-dansylated in comparison with the GH doublet. This is not surprising if one considers that the glucidic moiety of GGH is larger than that of GH, leading to steric hindrance. Hence two different reaction rates for the formation of the dansyl derivatives could occur, which would explain the different slopes of the calibration graphs. The slope of the GH calibration graph is steeper than that of GGH, as there is more fluorescence per mole in the former than in the latter.

The sensitivity of the method is of the order of picomoles, as at 0.5 nmol of HLG the integrated peak areas are still high.

The determination of GGH and GH in urine is more rapid than with other procedures, as the sample preparation step[2] does not appear to be essential. Comparing the data obtained by other workers using conventional chromatographic techniques, the values we have obtained are of the same order of magnitude as those reported by Askenasi,[7] Segrest and Cunningham,[3] Kakimoto and Akazawa[8] and Cetta *et al.*[9]

Finally, HPLC equipment is much less expensive than an amino acid analyser and also offers a wider range of analytical applications to potential users.

In conclusion, the method described here appears to be reliable, simple and rapid and can be applied routinely to monitor the turnover rate of collagen in clinical conditions where this protein is involved.

The technical assistance of Mr. Niccolò Di Pietro is gratefully acknowledged.

References

1. Weiss, P. H., and Klein, L., *J. Clin. Invest.*, 1969, **48**, 1.
2. Segrest, J. P., *Methods Enzymol.*, 1982, **82**, 398.
3. Segrest, J. P., and Cunningham, L. W., *J. Clin. Invest.*, 1970, **49**, 1497.
4. Askenasi, R., *Biochim. Biophys. Acta*, 1973, **304**, 375.
5. Tenni, R., Rimoldi, P., Zanabuoni, G., Cetta, G., and Castellani, A. A., *Ital. J. Biochem.*, 1984, **33**, 117.
6. Gray, W. R., *Methods Enzymol.*, 1967, **11**, 139.
7. Askenasi, R., *in* Hall, D. A., *Editor*, "The Methodology of Connective Tissue Research," Joynson-Bruvvers, Oxford, 1976, p. 263.
8. Kakimoto, Y., and Akazawa, S., *J. Biol. Chem.*, 1970, **245**, 5751.
9. Cetta, G., De Luca, G., Tenni, R., Zanaboni, R., Lenzi, L., and Castellani, A. A., *Connect. Tissue Res.*, 1983, **11**, 103.

Paper A4/51
Received February 3rd, 1984
Accepted July 25th, 1984

Indirect Determination of Quinoline by Differential-pulse Polarography

Brian R. Kersten and Ali H. Bazzi
Department of Natural Sciences, University of Michigan - Dearborn, Dearborn, MI 48128, USA

Keywords: *Quinoline; indirect determination; differential-pulse polarography*

The polarographic reduction of quinoline has long been investigated. Kaye and Stonehill[1] found that quinoline gives a distorted wave unless the solution is made 50% ethanolic. It was observed that 2.35 electrons are transferred per molecule reduced. Anthione *et al.*[2] determined quinoline in anhydrous *N*,*N*-dimethylformamide at 25 °C in the presence of 0.1 M Et_4NI and Fujinaga *et al.*[3] studied the behaviour of quinoline in non-aqueous and mixed electrolytes and proposed a mechanism for the polarographic reduction of quinoline in solutions that were greater than 20% water, when perchloric acid was added.

Boltz and Simon[4] determined quinoline by indirect atomic-absorption spectrometry. The method was based on the formation of the molybdophosphate complex. The quinoline molybdophosphate was shown by Perrin[5] to be a 3 : 1 complex.

The compound formed between quinoline and molybdophosphoric acid has excellent thermal properties and also has been used for the thermogravimetric determination of phosphorus.[6]

As yet, no work has been described on the indirect determination of quinoline by differential-pulse polarography. The work described in this paper uses this technique for the determination of quinoline, based on the indirect measurement of the current due to the reduction of the equivalent molybdate at a dropping-mercury electrode.

Experimental

Apparatus

Differential-pulse polarograms were obtained using an EG & G PAR Model 174 polarographic analyser equipped with a Model 303 static mercury drop electrode and a Houston Model RE0089 *X* - *Y* recorder. A Servall Superspeed Centrifuge (Type SS-3) was utilised.

Reagents

Molybdosphosphoric acid solution. Dissolve 5 g of molybdosphosphoric acid in distilled water and dilute to 100 ml in a calibrated flask. Filter the solution through a sintered-glass crucible into a 250-ml filter flask. Transfer into a polyethylene bottle.

Sulphuric acid solution, 2.4 N. Add slowly 16.7 ml of concentrated sulphuric acid into 100 ml of distilled water; cool, stir and dilute to 250 ml in a calibrated flask. Transfer into a polyethylene bottle.

Sulphuric acid solution, 1.0 N. Add slowly 27.8 ml of concentrated sulphuric acid to 500 ml of distilled water; cool, stir and dilute to 1 l in a calibrated flask. Transfer into a polyethylene bottle.

Basic buffer solution. Dissolve 53.5 g of analytical-reagent grade ammonium chloride in about 500 ml of distilled water. Add 70 ml of ammonia solution and dilute to 1 l in a calibrated flask. Transfer into a polyethylene bottle.

Citric acid solution. Dissolve 37 g of citric acid in about 60 ml of distilled water; warm, stir and dilute to 100 ml in a calibrated flask. Transfer into a polyethylene bottle.

Standard quinoline solution. Weigh exactly 0.5 ml of analytical-reagent grade quinoline, dissolve it in approximately 2.5 ml of absolute ethanol, transfer into a 1-l calibrated flask and dilute to the mark. Store in a dark bottle. Calculate the concentration of this solution and dilute as necessary to prepare standard working solutions. Store in a dark bottle.

Procedure

Preparation of quinoline samples

Add to a 30-ml centrifuge tube between 200 and 1000 μg of quinoline. To each test-tube add 2.0 ml of 2.4 N sulphuric acid. Dilute each test-tube to a final volume of about 11 ml with distilled water. Next, add 5.0 ml of molybdophosphoric acid to each test-tube. Allow to stand for 5 min and then centrifuge for 10 min at between 16000 and 20000 rev min^{-1}. Carefully aspirate the yellow supernatant using a 10-cm^3 long-stemmed syringe. Wash down the sides of the tube once with 5 ml of 1.0 N sulphuric acid. Centrifuge again and carefully aspirate the wash solution.

Dissolve the precipitate in each test-tube with 10 ml of the basic buffer solution and shake until it is completely dissolved. Pour the dissolved precipitate into a 50-ml polyethylene beaker containing 10 ml of citric acid solution. Rinse the centrifuge tube with another 5-ml portion of the basic buffer solution and transfer into the polyethylene beaker. Transfer the contents of the polyethylene beaker into a 50-ml calibrated flask and wash the polyethylene beaker with a small amount of distilled water. Dilute to the mark.

Peak current measurement of equivalent molybdate

Transfer the contents of the calibrated flask into a polarographic cell and measure the current using the PAR 174 polarographic analyser. The differential-pulse polarograms are recorded using the PAR 174 polarographic analyser at the following settings: initial potential, −0.100 V; potential range, −1.500 V; modulation amplitude, 50 mV; scan rate, 2 mV s^{-1}, purge time, 4 min; drop time, 1 s; and drop size, medium. The peak current for molybdenum is measured at a potential of −0.578 V. The potentials were measured *versus* an Ag - AgCl reference electrode.

Results

A typical differential-pulse polarogram is shown in Fig. 1. The results for the two precision studies at the 10 and 14 p.p.m. levels and the calibration study are summarised in Tables 1 and 2 and Fig. 2, respectively.

Discussion

The method shows good linearity between 4 and 20 p.p.m. of quinoline. Below 4 p.p.m. of quinoline a negative deviation is observed owing to a slight solubility loss or incomplete formation of the complex. One disadvantage of the procedure is its inapplicability to quinoline concentrations below 4 p.p.m.

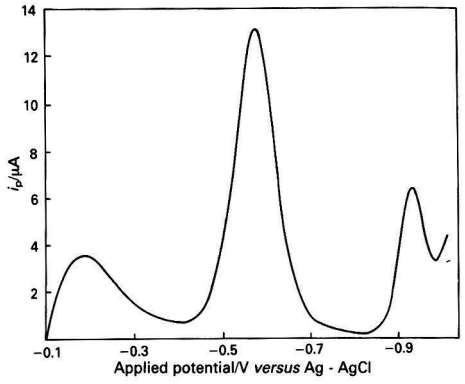

Fig. 1. Differential-pulse polarogram of 12 p.p.m. of quinoline at the optimum pH of 3.40

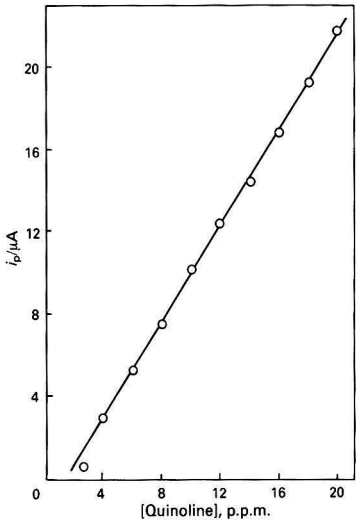

Fig. 2. Calibration graph for the indirect determination of quinoline. Concentration range, 4–20 p.p.m.

Table 1. Results obtained for the indirect determination of quinoline by differential-pulse polarography at the 10 p.p.m. level

Sample	i_p/μA*	E_p/V
1	10.14	−0.575
2	10.20	−0.578
3	10.16	−0.578
4	10.12	−0.578
5	10.12	−0.578
6	9.80	−0.578
7	10.06	−0.577

* Mean = 10.09 μA and relative standard deviation = 1.32% (n = 7).

Table 2. Results obtained for the indirect determination of quinoline by differential-pulse polarography at the 14 p.p.m. level

Sample	i_p/μA*	E_p/V
1	14.72	−0.578
2	14.72	−0.578
3	14.72	−0.578
4	14.70	−0.578
5	14.54	−0.577
6	14.52	−0.576
7	14.66	−0.574

* Mean = 14.65 μA and relative standard deviation = 0.60% (n = 7).

The effect of acidity was studied by changing the amount of citric acid added to the solution before the polarographic measurement. Between pH 3.30 and 3.59 the current remains virtually constant with the second peak of molybdenum symmetrical and well separated from the first peak. Above pH 4.21 the second peak becomes less symmetrical and the separation is not as adequate. At pH 5.95 the first peak disappears and the second peak becomes broader. Below pH 3.30 a reduction in peak height is obtained. The optimum pH range was chosen to be between 3.30 and 3.59 and the value of 3.40 was taken to keep the ionic strength constant. Within this range good sensitivity coupled with a very well defined molybdenum peak were obtained. However, pH values of less than 3.30 and also pH 5.95 could be used.

A typical differential-pulse polarogram at pH 3.40 is shown in Fig. 1 for a sample containing 12 p.p.m. of quinoline. A well defined molybdenum peak is obtained at −0.578 V with a maximum current of 12.44 μA. A smaller peak, which was not used for analysis, appears at a potential of −0.185 V. At a potential of −0.929 V a small peak is observed. When the solution was spiked with quinoline, this gave a higher current, which indicates that this peak is due to the reduction of quinoline itself.

The use of the Servall superspeed centrifuge at a higher speed was to ensure the formation of a tightly compacted precipitate at the base of the test-tube. Other centrifuges of slower speeds could be used but this might necessitate longer spinning times.

The reproducibility of the blank was studied by analysing five blank samples. An average current value of 0.0246 μA was obtained at −0.578 V. The standard deviation was 0.00702 μA. Two precision studies were made by analysing seven solutions, each containing 10 p.p.m. of quinoline and seven solutions each containing 14 p.p.m. of quinoline (see Tables 1 and 2). At the 10 p.p.m. level, the average current was 10.09 μA. The standard deviation was 0.133 current unit or a relative standard deviation of 1.32%. At the 14 p.p.m. level, the average current was 14.65 μA. The standard deviation was 0.0877 current unit or a relative standard deviation of 0.60%.

References

1. Kaye, R. C., and Stonehill, H. I., *J. Chem. Soc.*, 1952, 3240.
2. Anthione, G., Coppens, G., Nasielski, J., and Vander Ronckt, E., *Bull. Soc. Chim. Belg.*, 1964, **74**, 65.
3. Fujinaga, J., Izutsu, K., and Jakaska, K., *J. Electroanal. Chem.*, 1966, **12**, 203.
4. Boltz, D. F., and Simon, S. J., *Microchem. J.*, 1975, **20**, 468.
5. Perrin, C. H., *J. Assoc. Off. Agric. Chem.*, 1958, **41**, 758.
6. Hoffman, W. M., and Wendlandt, W. W., *Anal. Chem.*, 1960, **32**, 1011.

Paper A4/106
Received March 19th, 1984
Accepted June 25th, 1984

COMMUNICATION

Material for publication as a Communication must be on an urgent matter and be of obvious scientific importance. Rapidity of publication is enhanced if diagrams are omitted, but tables and formulae can be included. Communications should not be simple claims for priority: this facility for rapid publication is intended for brief descriptions of work that has progressed to a stage at which it is likely to be valuable to workers faced with similar problems. A fuller paper may be offered subsequently, if justified by later work.

Manuscripts are not subjected to the usual examination by referees and inclusion of a Communication is at the Editor's discretion

Improved Precision in Inductively Coupled Plasma Atomic-emission Spectrometry by a Parameter-related Internal Standard Method*

Michael H. Ramsey and Michael Thompson
Applied Geochemistry Research Group, Department of Geology, Imperial College, London SW7 2BP, UK

Keywords: *Chemometrics; simultaneous inductively coupled plasma atomic-emission spectrometry; parameter-related internal standard method; precision improvement; internal standard*

The "instrumental precision" of inductively coupled plasma atomic-emission spectrometry (ICP-AES) is estimated from the results of a few closely spaced integrations, observed during the continuous nebulisation of the test solution. When analytes are present at concentrations well above the detection limit, instrumental precisions fall typically in the coefficient of variation range 0.2–0.6%. A precision estimate more appropriate to conditions of routine analysis is derived from measurements repeated at intervals during the period between calibration adjustments (*i.e.*, up to several hours), and with the intercalation of blanks and other sample solutions. Typical values of this "routine precision" lie in the range 0.8–2.4% coefficient of variation. We present a simple chemometric correction procedure for simultaneous ICP-AES that reduces the routine precision to the same level as normal instrumental precision.

Correlated Variance in Simultaneous ICP-AES

When a multi-element test solution is repeatedly analysed by simultaneous ICP-AES under conditions closely resembling routine analysis, but with no calibration adjustments, individual analyte lines show both random and systematic variations within the range of their responses. When the data are examined in the multi-element domain it is clear that much of the variance is correlated between elements. For instance Na I 588.99 and Li I 670.78 nm are strongly correlated, as are Zn II 202.55 and Cd II 226.50 nm. This suggests the possibility of variance reduction by means of a ratioing technique. No simple internal standard technique will serve, however, as Li and Zn vary independently, but the majority of other lines correlate with both lines. This accounts for the difficulty that various workers have experienced in the attempt to identify useful internal standards for ICP-AES.[1–3]

Principle component analysis has been used to show that more than 90% of the variance in such a multi-element data set is correlated and therefore potentially correctable. However, the technique does not reveal or even suggest causal relationships that can be used to design a suitable correction procedure.

The variance in the multi-element data set is clearly the result of small uncontrolled variations in instrumental parameters. If all instrumental parameters are fixed absolutely invariant, only random uncorrelated noise could be apparent in the data, whereas correlated variation, both systematic and random, can be detected in the experimental data. Causal relationships were therefore investigated between experimental variations in individual parameters and the resulting variance in the multi-element domain. In addition, the co-variance between the dependent variables was exploited to provide correction terms to remove from the data the effects of the causal parameter variation.

At least ten separate instrumental parameters or environmental factors can be shown to cause variations in ICP-AES sensitivities, namely sample uptake rate, forward power, injector gas flow, primary spectrometer slit position, fume extract speed, primary lens opacity, air temperature around spray chamber, sample solution temperature, high salt nebulisation and ICP warm-up. Each of these gives rise to co-variance among the dependent variables (*i.e.*, the responses on the analyte lines). An elegant general solution to the problem of producing appropriate corrections has been devised by Lorbar and co-workers[4,5] and is called the generalised internal reference method (GIRM). This has been demonstrated to provide a remarkable improvement in precision in ICP-AES, although not as yet under conditions of routine analysis. In the GIRM procedure many internal standard lines are used to correct for a number of parameters by methods utilising numerical analysis.

Parameter-related Internal Standard Method (PRISM)

We have independently devised a system (PRISM) that is similar to GIRM but simpler to apply. If an instrumental

* Paper presented at BNASS, Leeds, July 10–13th, 1984; a fuller paper will be published in the forthcoming special issue of the *Analyst*.

parameter (such as forward power) is increased over a small range (say to 105% of its normal operational setting) element line sensitivities vary correspondingly. The relative change in response for the ith analyte line $(r_i - r_i^0)/r_i^0$ is related to the corresponding change $(r_s - r_s^0)/r_s^0$ for an internal standard line by the equation

$$\frac{(r_i - r_i^0)/r_i^0}{(r_s - r_s^0)/r_s^0} = \frac{r_i/r_i^0 - 1}{r_s/r_s^0 - 1} = k_{i,s} \quad \ldots \quad (1)$$

where r^0 and r are responses for normal and perturbed parameter conditions, respectively, and $k_{i,s}$ is a constant for a particular analyte (i) and internal standard (s) combination. The values of $k_{i,s}$ and all analogous constants are stable so long as instrumental conditions remain unchanged. Therefore the variance introduced into a routine analytical run due to uncontrolled power variations can be corrected by an equation of the form

$$R_i^{corr} = R_i/[1 + K_{i,s}\,(R_s/R_s^0 - 1)] \ldots \quad (2)$$

where R_i and R_s are the responses for the ith analyte and internal standard s at a particular time after calibration and R_s^0 is the response for s at the calibration time. R_i^{corr} is the response corrected back to the calibration time at which the power setting is standardised.

We have found that most of the variation encountered in routine simultaneous multi-element analysis can be accounted for by means of only two operational parameters, namely forward power and test solution uptake rate. The final PRISM equation for this double correction takes the form

$$R_i^{corr} = R_i/\{[1 + k_{i,A}\,(R_A/R^0{}_A - 1)][1 + k_{i,B}(R_B/R_B{}^0 - 1)]\} \quad (3)$$

where A and B are internal standards related to forward power and solution uptake rate, respectively.*

Effectiveness of the PRISM Correction Model

We have applied PRISM correction to simultaneous multi-element data sets produced by ICP-AES under conditions of routine analysis. Seventy-five measurements were made on a standard solution over a 4.4-h period, without re-calibration, on a total of 24 lines covering the wavelength range 178–766 nm. The lines used as internal standards were Zn II 202.55 nm and Li I 670.78 nm. As a result of the correction, "routine precision" (using all of the 75 measurements without excluding any data) was improved to the level of "instrumental precision" for each element, a median value of 0.52%.

The values of the $k_{i,s}$ factors were found to be stable for more than one year, so long as the operating conditions were kept nominally constant. Large changes in conditions such as those that might be brought about by the installation of a new nebuliser or plasma torch would warrant a redetermination of the k-values, but this is a task that can be accomplished within a few minutes.

Of the operating parameters investigated, three (injector gas flow, air temperature and primary lens opacity) gave multi-element parameter signatures (MPS) very similar to that of forward power. (The MPS is the vector of $k_{i,s}$ values over all of the analyte lines for internal standard s). Any variations in these other parameters would also be corrected by the forward power MPS. Likewise the MPSs of solution temperature and high salt nebulisation were similar to those of solution uptake rate and were similarly corrected. Drift due to "warm-up," which is detectable even after several hours of instrument running, was found to be largely a linear combination of the two main MPSs. Thus the eight parameters were corrected by only two internal standards and two MPSs.

It should be noted that while the variations in the routine analysis data could be "explained" by the MPSs for forward power and solution uptake, a causal relationship was not *demonstrated* as contributions from the other parameters would have a similar effect. Nevertheless, there is a strong presumption that the observed effects can be attributed to only one fundamental process, excitation efficiency in the plasma, which is itself affected by a number of operational parameters.

This is borne out by strong relationships between the MPS coefficients and the excitation and ionisation potentials of the analyte lines. The relationships make a choice of the two internal standard lines relatively simple. Normally, atom lines with low excitation potential (*e.g.*, Li I 670.78 nm; EP = 1.85 eV) are insensitive to forward power variations but highly susceptible to sample uptake rate. Likewise, the opposite properties are typical of ion lines of high combined ionisation and excitation potential (*e.g.*, Zn II 202.55 nm, EP + IP = 15.51 eV). These two types of lines tend to have extreme values in the MPS vectors and are, therefore, good internal standards for PRISM. No matching of the internal standards to individual analytes is at all necessary. Because of the complicated relationship between spatial variation in emissions and operating parameters,[6] these conclusions may apply only to plasma operating conditions typical of routine simultaneous analysis.

Conclusions

We have demonstrated that the PRISM method can be used to reduce variance due to both systematic and random effects in routine simultaneous multi-element analysis. Precision, measured over a 4.4 h run without calibration adjustment, is improved to a level equivalent to "instrumental precision." The two internal standard lines required are easy to select on the basis of total excitation potential. The coefficients for the correction equation can be determined in a few minutes, and are stable for as long as instrumental conditions are unchanged. The simple corrections can be applied in real time by means of the dedicated computer, and require only minor changes to the programme. A secondary benefit of PRISM is the potentially increased sample throughput, due to the greatly reduced requirement for calibration drift checks or adjustments.

References

1. Barrett, W. B., Fassel, V. A., and Knisely, R. N., *Spectrochim. Acta, Part B*, 1968, **23**, 642.
2. Barrett, W. B., Fassel, V. A., and Knisely, R. N., *Spectrochim. Acta, Part B*, 1970, **25**, 139.
3. Odegard, M., *J. Geochem. Expl.*, 1981, **14**, 119.
4. Lorber, A., and Goldbart, Z., *Anal. Chem.*, 1984, **56**, 37.
5. Lorber, A., Goldbart, Z., and Eldan, M., *Anal. Chem.*, 1984, **56**, 43.
6. Blades, M. W., and Horlick, G., *Spectrochim. Acta, Part B*, 1981, **36**, 861.

Paper A4/329
Received September 20th, 1984

* The corresponding equation for simple ratio internal standards in analogous form is as follows: $R_i^{corr} = R_i/[1 + (R_s/R_s^0 - 1)]$.

BOOK REVIEWS

Methods of Enzymatic Analysis. Third Edition. Volume IV. Enzymes 2: Esterases, Glycosidases, Lyases, Ligases
Edited by Hans Ulrich Bergmeyer. Pp. xxiv + 426. Verlag Chemie. 1984. Price DM230. ISBN 3 527 26044 7 (Verlag Chemie); 0 89573 234 3 (Verlag Chemie International).

This book follows the style adopted for the previous volume in this series. A total of 35 enzymes or classes of enzyme are covered under the general heading of esterases, glycosidases, C–N and anhydride splitting enzymes, lyases and ligases. For each enzyme information is provided about its source and distribution, effectors, the range of assay methods available and the availability of international reference standards and methods. The characteristic feature of the book is the detailed account of a selected method for each enzyme. This covers the method design, equipment, reagents and solutions, procedure and the validation of the method.

Several of the enzymes discussed are used routinely in clinical chemistry as an aid to diagnosis and management of disease, *e.g.*, alkaline phosphatase, cholinesterase, alpha-amylase, lipase, 5′-nucleotidase, acid phosphatase and lysozyme. Hence, this volume will be of particular interest to clinical chemists.

The depth of coverage is exemplified by the section on alkaline phosphatase (Bretaudiere and Spillman). This covers not only a routine method but also an IFCC Reference Method (provisional) and methods for determining alkaline phosphatase isoenzymes. Particular emphasis is given to the need to screen commercially available 2-amino-2-methylpropan-1-ol preparations for contaminating chelators that inactivate alkaline phosphatase.

In addition to conventional assays using soluble substrates, an account of various assays based on insoluble substrates is presented in the section on alpha-amylase (Wahlefeld). "Blue Starch Polymer" is an insoluble substrate prepared by reacting starch with Cibacron Blue F3G-A. Cleavage by alpha-amylase releases coloured soluble fragments, which can be separated from the insoluble substrate by centrifugation and then measured spectrophotometrically in solution. This represents a novel approach to enzyme analysis, which may perhaps be applicable to other enzyme assays.

This volume, together with the nine others in the series, will undoubtably find an established place on the bookshelves of libraries and laboratories as a source and reference text on enzymatic analysis.

Larry J. Kricka

Analysis of Food Contaminants
Edited by John Gilbert. Pp. xiv + 386. Elsevier. 1984. Price £40. ISBN 0 85334 255 5.

This is a multi-author volume that covers seven topics on the analysis of food contaminants. The topics selected are a mix of specific instrumental methods with broad application and of specialised analytical techniques for a specified contaminant.

Sample clean-up for contaminant analysis provides the applications platform for an in-depth theoretical treatment of size exclusion and gel chromatography. Factors that influence choice of solvent and matrix are discussed, together with the procedures for setting up instruments and optimisation of performance. Applications are not discussed in detail, this latter section being essentially a review of current literature to early 1982. Immunoassay techniques are discussed from the standpoint of the measurement of veterinary residues in meat; a much more concise account of the theoretical aspects of the subject is provided by Raymond V. Heitzman. The author concentrates on practical aspects of the application of the technique. He gives a clear discussion of checking and validation procedures necessary for successful assays together with some indication of the nature and performance of alternative methods.

The treatment afforded to developments in trace metal analysis, by V. Benton Jones, headspace gas chromatography, by Bruno Kolb, and analysis for mycotoxins by HPLC and other techniques, by Raymond D. Coker, follows much the same style as that given to immunoassays. The Editor himself presents a simplified outline of MS and selected ion monitoring methodology with appropriate examples to illustrate the practical problems in its application. A final chapter is devoted to chemiluminescent and other available techniques for the analysis of *N*-nitrosamines in foods. Performance of the chemiluminescent technique is considered against other available methods and in sufficient detail to indicate the relative merits of a number of analytical options.

Overall the book is up to date and well presented and edited. With the exception of the opening chapter, the style is reasonably uniform for a multi-author text. On the whole this is a useful volume, but at £40 it may be that the potential readership will consider the cost to be rather high and will attempt to find the book on the appropriate library shelves.

R. Sawyer

A History of Platinum and Its Allied Metals
Donald McDonald and Leslie B. Hunt. Pp. xii + 450. Johnson Matthey. 1982. Price £20; $37.50. ISBN 0 905118 83 9

This magnificant and scholarly review of the history of platinum and its allied metals should be of interest to present day practitioners and teachers of analytical chemistry. The commercial availability of platinum apparatus, due to Wollaston, was in its day a major advance and improved the speed and reliability of many analyses as well as permitting new methods to be introduced. Platinum crucibles are still essential in current practice although, mainly owing to cost, they are never seen by modern undergraduates.

The first platinum crucibles were prepared by F. K. Achard (1784), who melted arsenical platinum in a clay mould and then volatilised away the arsenic. After long and at times frustrating research Wollaston was, by 1805, able to produce marketable platinum in quantity, though details of the process were not revealed until just prior to his death in 1828. Among the first products were crucibles and lids, marketed through William Cary, a well known London instrument maker. These dishes and crucibles became world famous; the great chemist and analyst Berzelius wrote to Hisinger in October 1815, "I have just received from England a delicious platinum evaporating dish holding more than ½ stop. It is a jewel." (A stop was an old Swedish unit of capacity, equivalent to 654 ml.) It is pleasing to note that the subject still advances in the UK and the latest noble metal crucibles are the TRIM range, zirconia grain stabilised, platinum clad palladium, made by Johnson Matthey, publishers of this noble book on the noble metals The work was a delight and pleasure to read.

D. Thorburn Bur

Topics in Forensic and Analytical Toxicology. Proceedings of the Annual European Meeting of the International Association of Forensic Toxicologists, Munich, August 21–25, 1983
Edited by R. A. A. Maes. *Analytical Chemistry Symposia Series, Volume.* 20 Pp. x + 214. Elsevier. 1984. Price $57.75; DFl150. ISBN 0 444 42313 3 (Volume 20); 0 444 41786 9 (Series).

To misuse a somewhat hackneyed phrase, this is the book of the conference and consists of 23 papers on toxicological themes, 4 accounts of toxicology in developing countries, summaries of three round-table conferences on quality control, documentation and postgraduate education, and a subject index. The main group of contributions can then be subdivided into two large sections, which are either predominantly of forensic or of clinical toxicology in nature, two specialist papers on mass spectrometry and two that fall into the category of "what a marvellous machine my company is manufacturing."

As would be expected from such a *pot-pourri*, there is a considerable range of quality in the contributions. Some read like scripts of the corresponding lecture and desperately needed rewriting as prose. In others, the valiant efforts of authors, for whom English is not their native tongue, required extensive editing, as did the abundance of typographical errors. However, as the book is photoreproduced from the authors' typescripts, such editing would have been onerous.

Evaluation of the papers depends very much on the reader's interests. Some of the authors have succumbed to the temptation of writing a paper on a single fatal poisoning case; this may be of great interest to the few analysts who may have encountered a similar incident, but leaves the majority of readers relatively unmoved. Hence the following examples are very much a personal selection. That on the embryotoxicity of toxic oils and anilides by Repetto *et al.* has a very direct bearing on the Spanish cooking oil disaster. Arnold's paper on modern trends of chemical analysis in the drug scene gave an excellent summary of the present state of affairs. Two papers made valuable and cautionary contributions: that by Kimber and King showed that the use of subtilisin for the release of basic drugs from tissues was less efficient than had been claimed, and that by Minty and co-workers gave an indication of the level of errors when a drug-screening test was used by non-toxicology personnel. Some comments by Ludwig on the principles of the generation and application of toxicological data, with examples from research and practice, were also of considerable interest.

Although the book has been produced quickly after the conference, at a price of nearly £40 it cannot be strongly recommended except to the most dedicated of toxicologists.

R. L. Williams

The Practice of Ion Chromatography
Frank C. Smith, Jr., and Richard C. Chang. Pp. xiv + 218. Wiley-Interscience. 1983. Price £43.95. ISBN 0 471 05517 4.

This book, on the increasingly important and relatively new technique of ion chromatography (IC), is designed to "promote a thorough working knowledge of the practices of IC and provide a perspective of its analytical potential," the authors hoping that "scientists who have spent the effort to read it will have become familiar with the principles and practices of ion chromatography." There is no doubt that there is need of such a book and this book indeed should act as a useful reference for current methods and applications of this technique. The emphasis in the book is practical rather than theoretical, and indeed the reviewer would perhaps have liked to see a little more basic discussion, particularly with regard to the philosophy behind the various developments that have taken place.

The book deals initially with the development of IC and with existing instrumentation. There is a substantial chapter on methods based on suppressed IC with conductimetric detection, and much play is made of so-called "standard" operating conditions for cation and anion IC, ion exclusion and ion chromatography exclusion. Departures from such conditions, methods for improving and optimising performance and trouble-shooting are also covered. Non-suppressed IC with conductimetric detection is dealt with separately, as are resins and column packings. There is a substantial chapter on applications, as well as chapters on method development and future developments. An extensive set of tables in the Appendix summarises useful data relevant to IC.

The reviewer found the approach via "standard" conditions and modifications thereto a helpful one, and indeed the main value of the book would probably be to aid the establishment of routine IC methods. Again the wide range of applications described would be helpful. The section on future developments is bound to be speculative in a rapidly developing technique such as IC. Nevertheless, it is perhaps a pity that developments involving the use of a conventional UV detector for the detection of non-UV-absorbing ions were not emphasised more strongly, as this offers the possibility of IC being carried out on standard HPLC equipment without the purchase of a conductimetric detector.

The book itself is marred by a number of errors, particularly in Chapter 4 (non-suppressed IC), in which a number of the figures and tables contain inconsistencies with respect to the text. The index was also found to be inadequate on a number of occasions. Despite these reservations, however, the book is a timely and necessary addition to the chemical literature, even if its price does seem somewhat off-putting.

R. G. Anderson

ERRATA

Rapid Atomic-absorption Spectroscopic Analysis of Molybdenum in Plant Tissue with a Modified Carbon Rod Atomiser

John W. Steiner and Kevin M. Ryan
Analyst, 1984, **109**, 581–583

Page 582, Table 3, fourth column, Optical device: *for* the footnote mark ‡, *read* a plus sign (+).

Page 583, Table 5, third column, Amount of Mo added/μg: *for* the values 0.01, 0.02 and 0.03 *read* 0.1, 0.2 and 0.3.

Corrected
Au.

The companies appearing on this page are able to offer scientific support to users of laboratory instrumentation. THE ANALYST will regularly publish specific Application Notes provided by their applications chemists.

CUT HERE

FIRST FOLD HERE

THE ANALYST READER ENQUIRY SERVICE

For further information about any of the products featured in the advertisements in this issue, write the appropriate number on the postcard, detach and post.

FOLD HERE

THE ANALYST READER ENQUIRY SERVICE

DEC'84

For further information about any of the products featured in the advertisements in this issue, please write the appropriate number in one of the boxes below.
Postage paid if posted in the British Isles but overseas readers must affix a stamp.

PLEASE USE BLOCK CAPITALS LEAVING A SPACE BETWEEN WORDS *Valid 12 months*

1 NAME

2 COMPANY

PLEASE GIVE YOUR BUSINESS ADDRESS IF POSSIBLE. IF NOT, PLEASE TICK HERE ☐

3 STREET

4 TOWN

5 COUNTY
POST CODE

6 COUNTRY

7 DEPARTMENT/
DIVISION

8 YOUR JOB TITLE/
POSITION

9 TELEPHONE NO

OFFICE USE ONLY REC'D PROC'D

FOLD HERE

Postage will be paid by Licensee

Do not affix Postage Stamps if posted in Gt. Britain, Channel Islands, N. Ireland or the Isle of Man

BUSINESS REPLY SERVICE
Licence No. WD 106

Reader Enquiry Service
The Analyst
The Royal Society of Chemistry
Burlington House, Piccadilly
LONDON
W1E 6WF
England

A201 for further information. See page iv.

ANALAO 109(12) 1517–1628 (1984) December 1984

The Analyst

The Analytical Journal of The Royal Society of Chemistry

CONTENTS

Electronically typeset and printed by Heffers Printers Ltd, Cambridge, England